Technical Report

TR-98-04

Volume II

MAQARIN natural analogue study: Phase III

Edited by J A T Smellie

December 1998

Svensk Kärnbränslehantering AB
Swedish Nuclear Fuel
and Waste Management Co
Box 5864
SE-102 40 Stockholm Sweden
Tel 08-459 84 00
+46 8 459 84 00
Fax 08-661 57 19
+46 8 661 57 19

MAQARIN natural analogue study: Phase III

Edited by J.A.T. Smellie

December 1998

VOLUME I: Chapters 1–13

VOLUME II: Appendices A–R

CONTENTS

VOLUME II: Appendices A–R (this volume)

CONTENTS

VOLUME I: Chapters 1–13

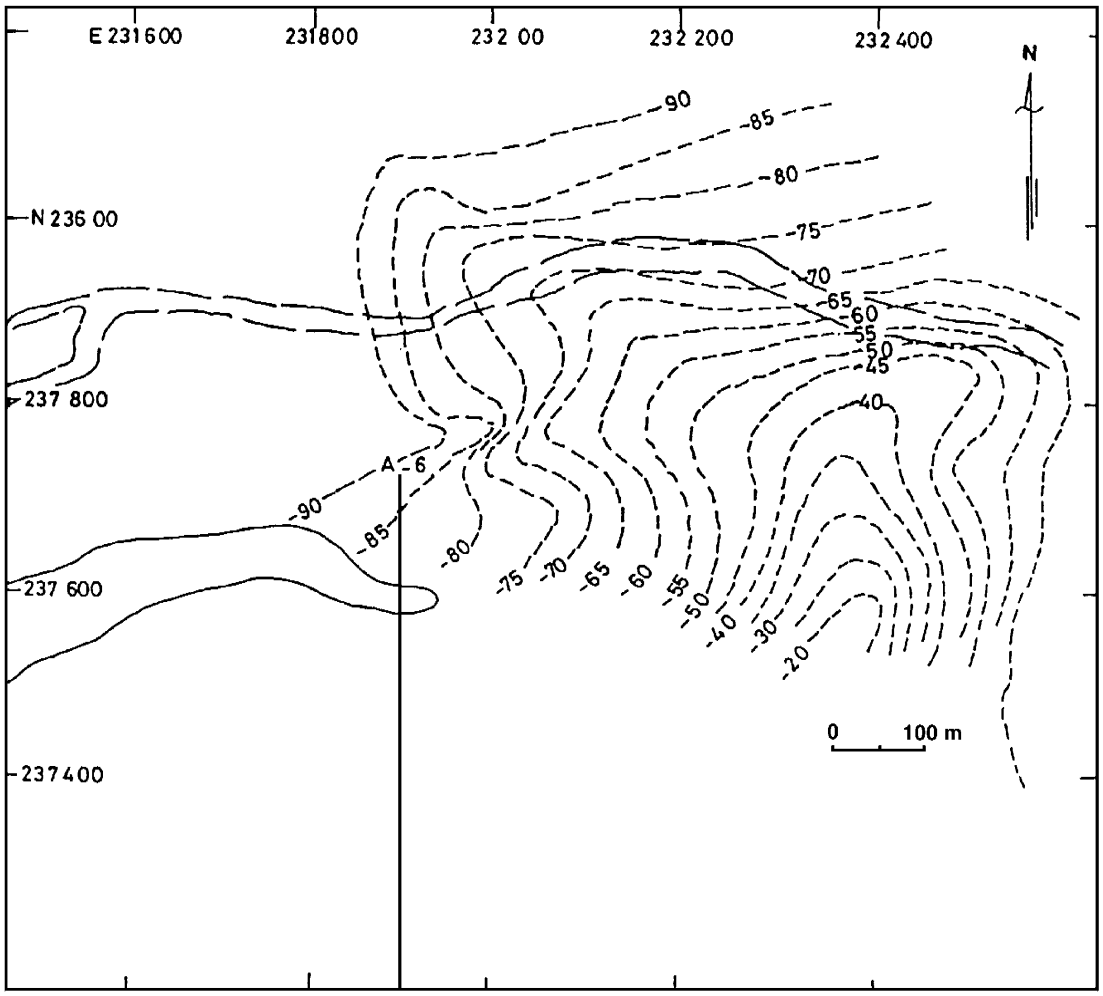

Figure A-1. *Contours showing the top of the Amman Formation (modified after Harza, 1982).*

APPENDIX A

Geology and Hydrogeology – Figures A-1 to A-14

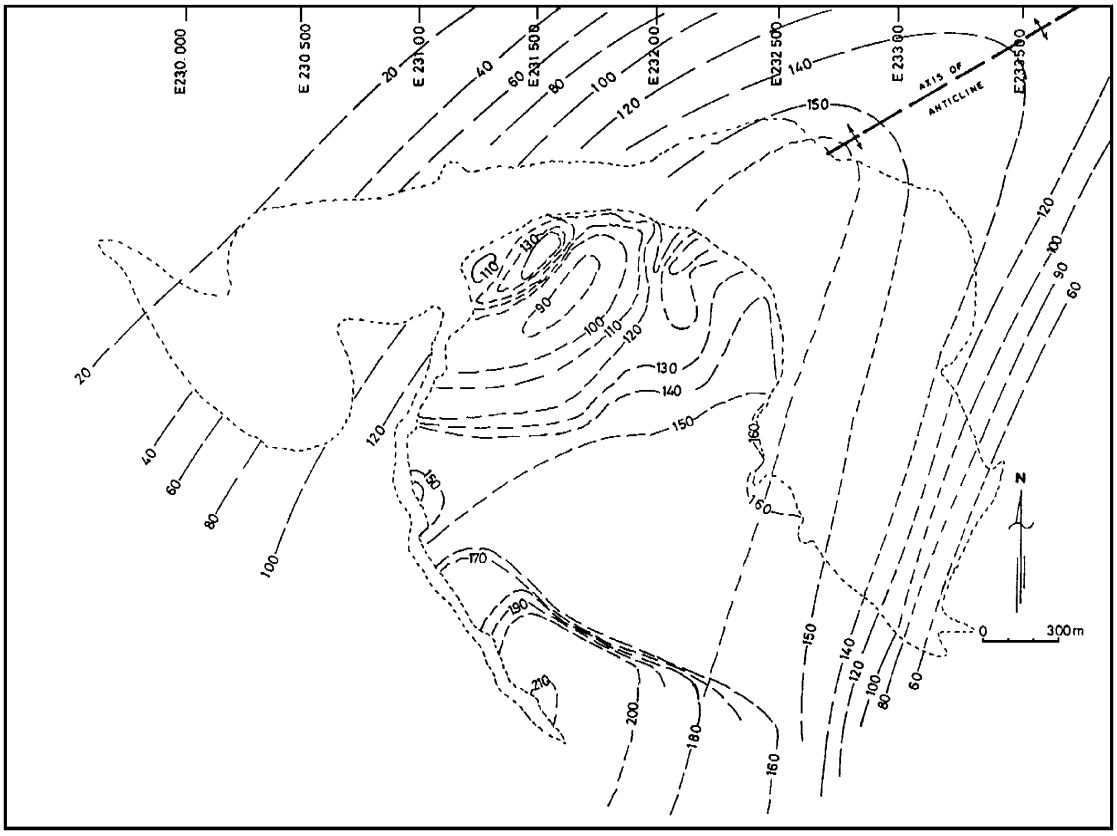

Figure A-2. *Projected top of the Bituminous Marl Formation (modified after Harza, 1982).*

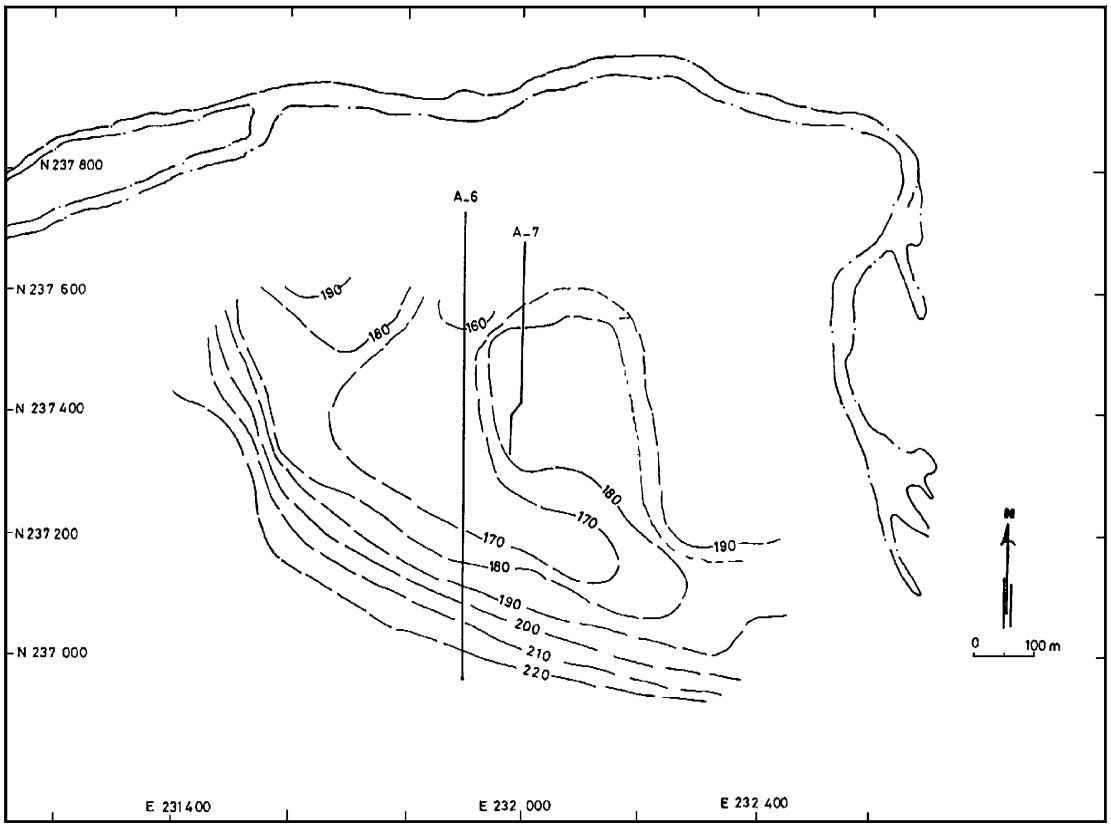

Figure A-3. *Contours showing the base of the Maqarin basalts (modified after Harza, 1982, and Jordan Valley Authorities, 1980).*

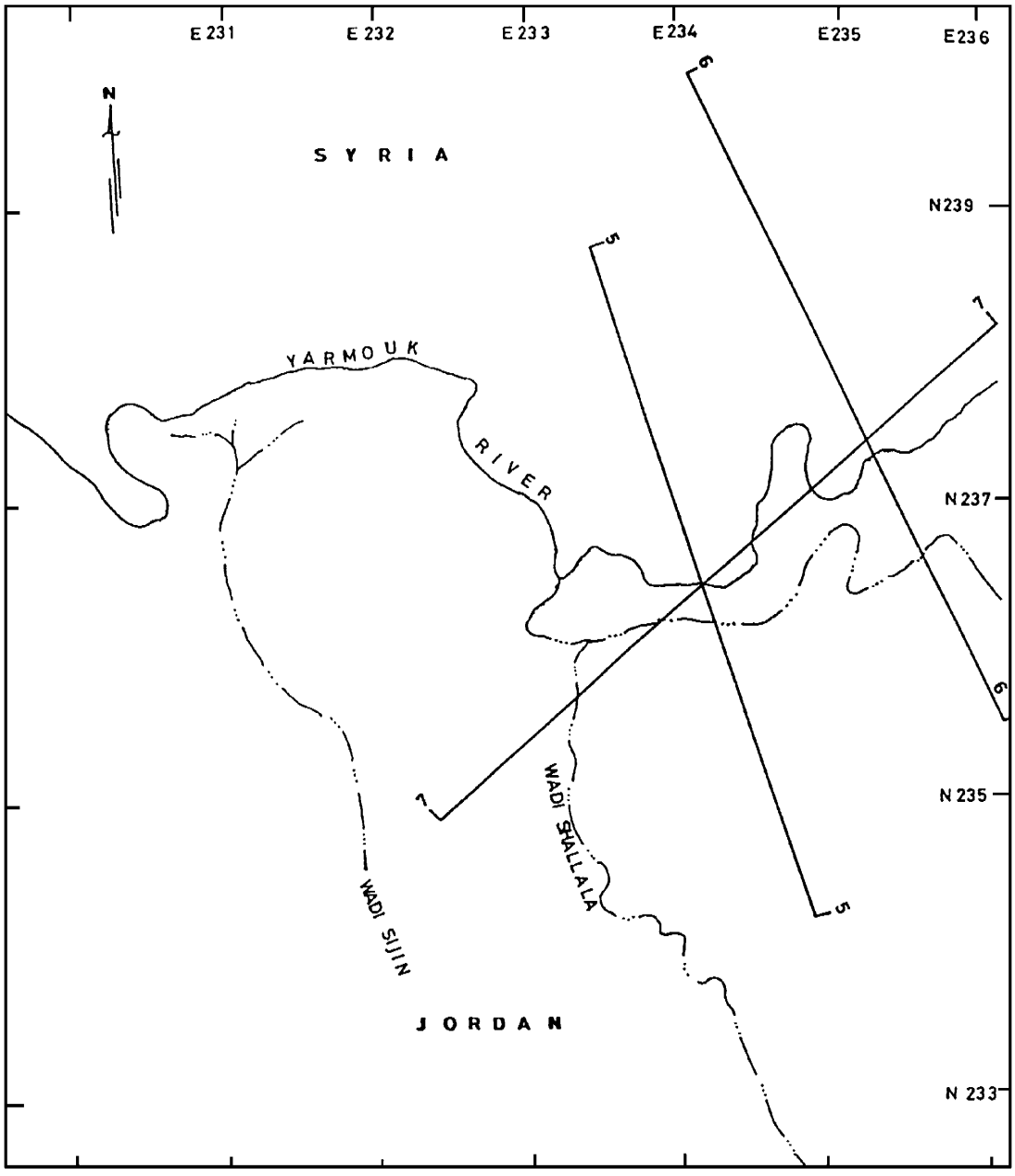

Figure A-4. *Location of cross-sectional profiles (5-7) from the Maqarin area.*

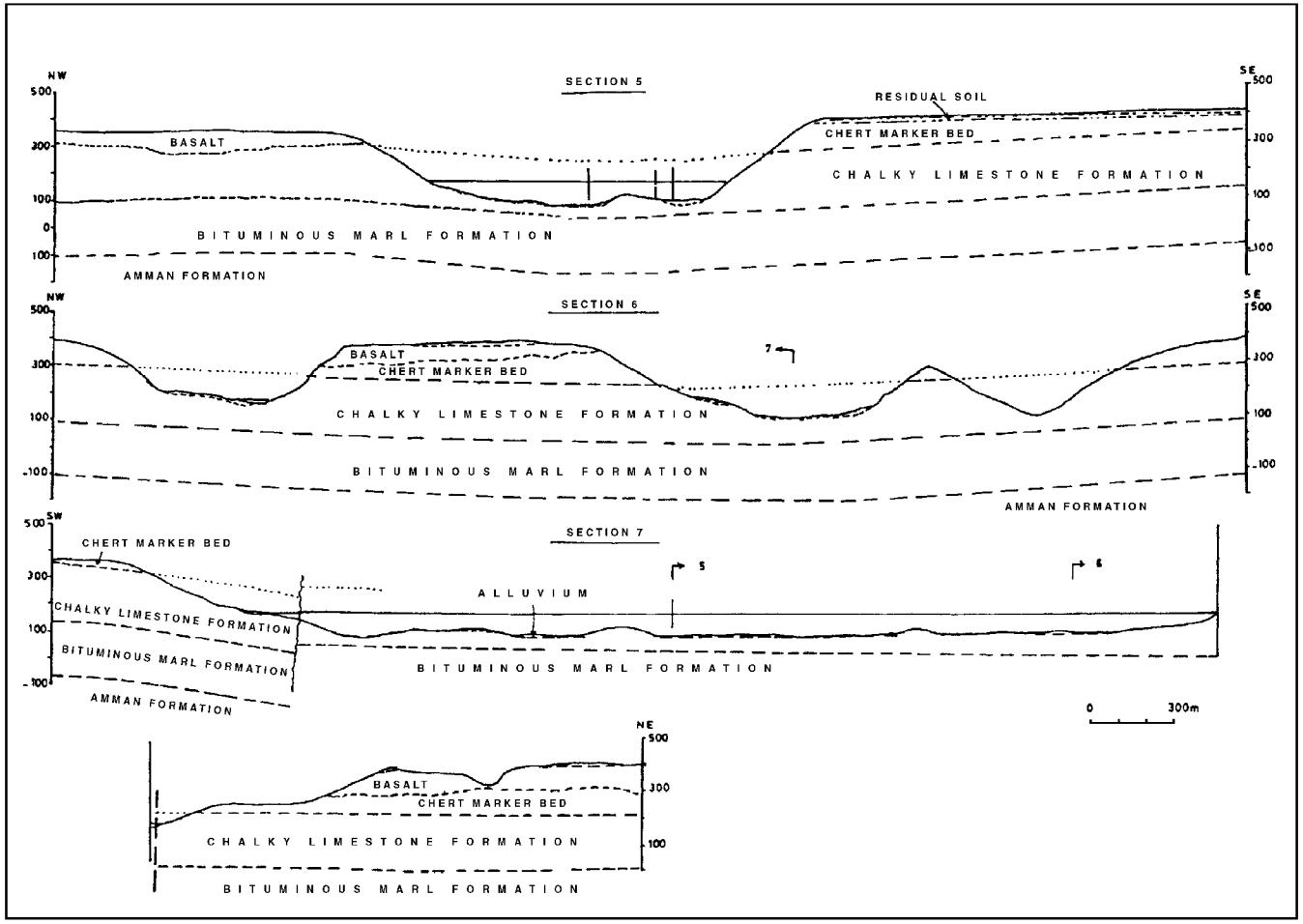

Figure A-5. *Cross-sectional profiles (5-7) from the Maqarin area (see Figure A-4).*

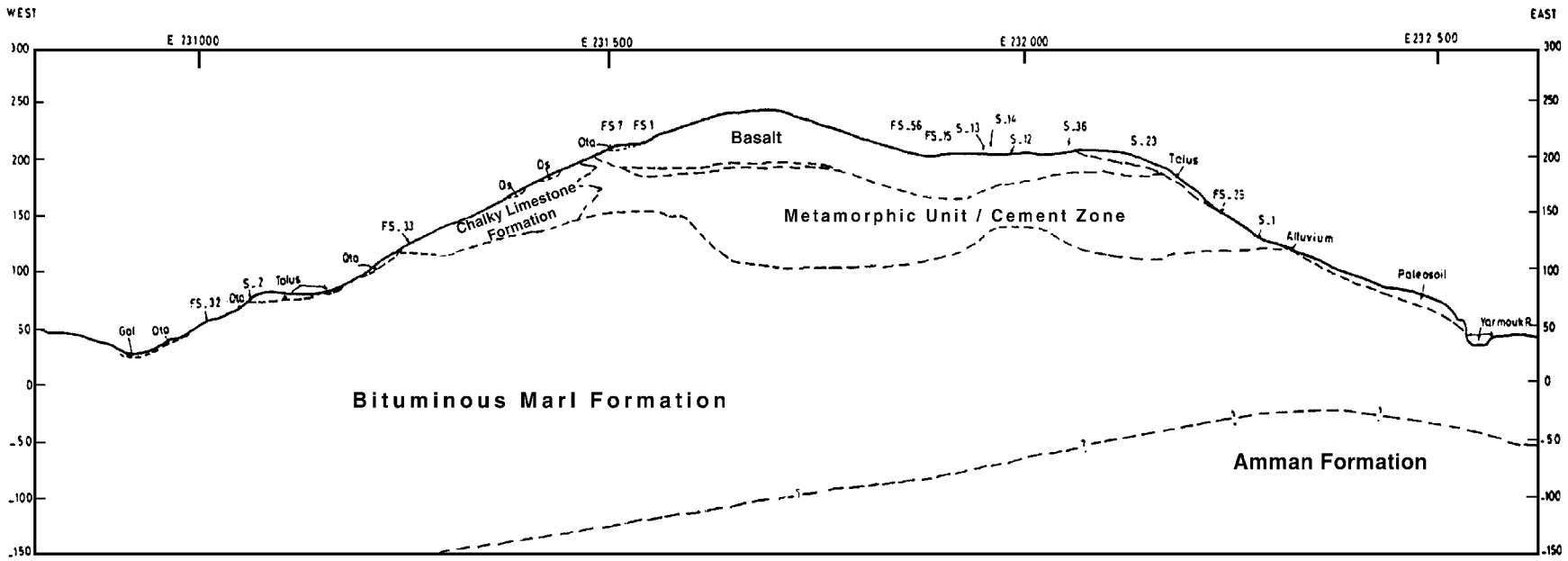

Figure A-6. *Integrated W-E cross-sectional profile through the Maqarin area (modified after Harza, 1982).*

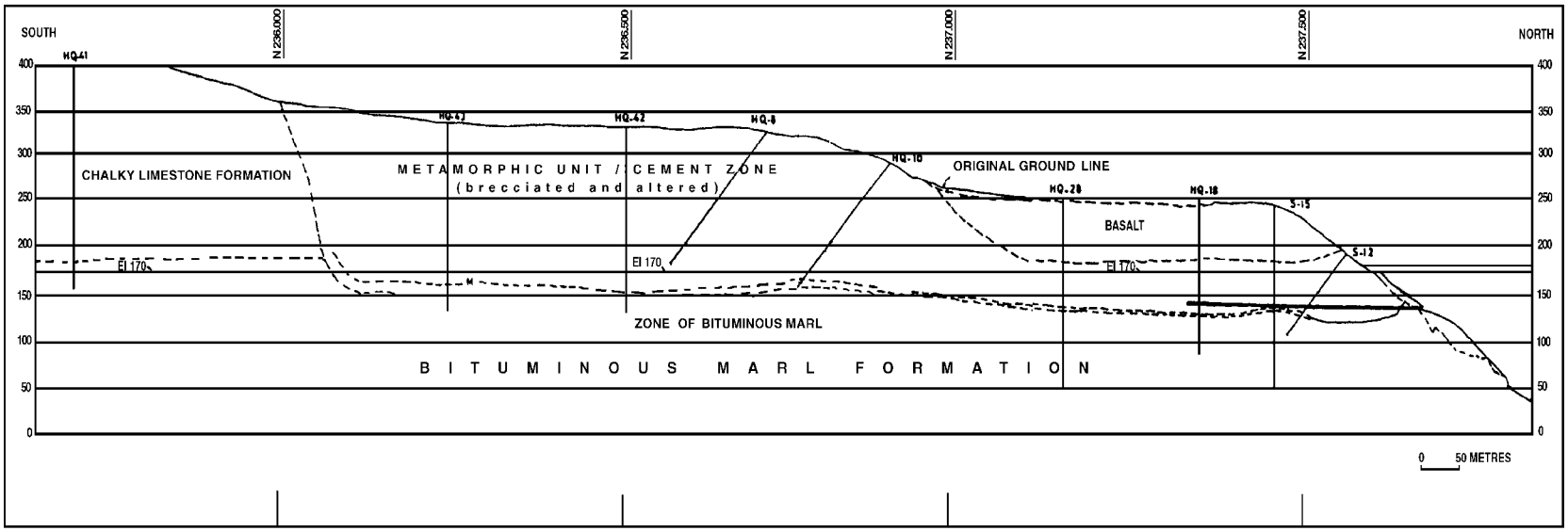

Figure A-7. *Integrated S-N cross-sectional profile through the Maqarin area (modified after Harza, 1982).*

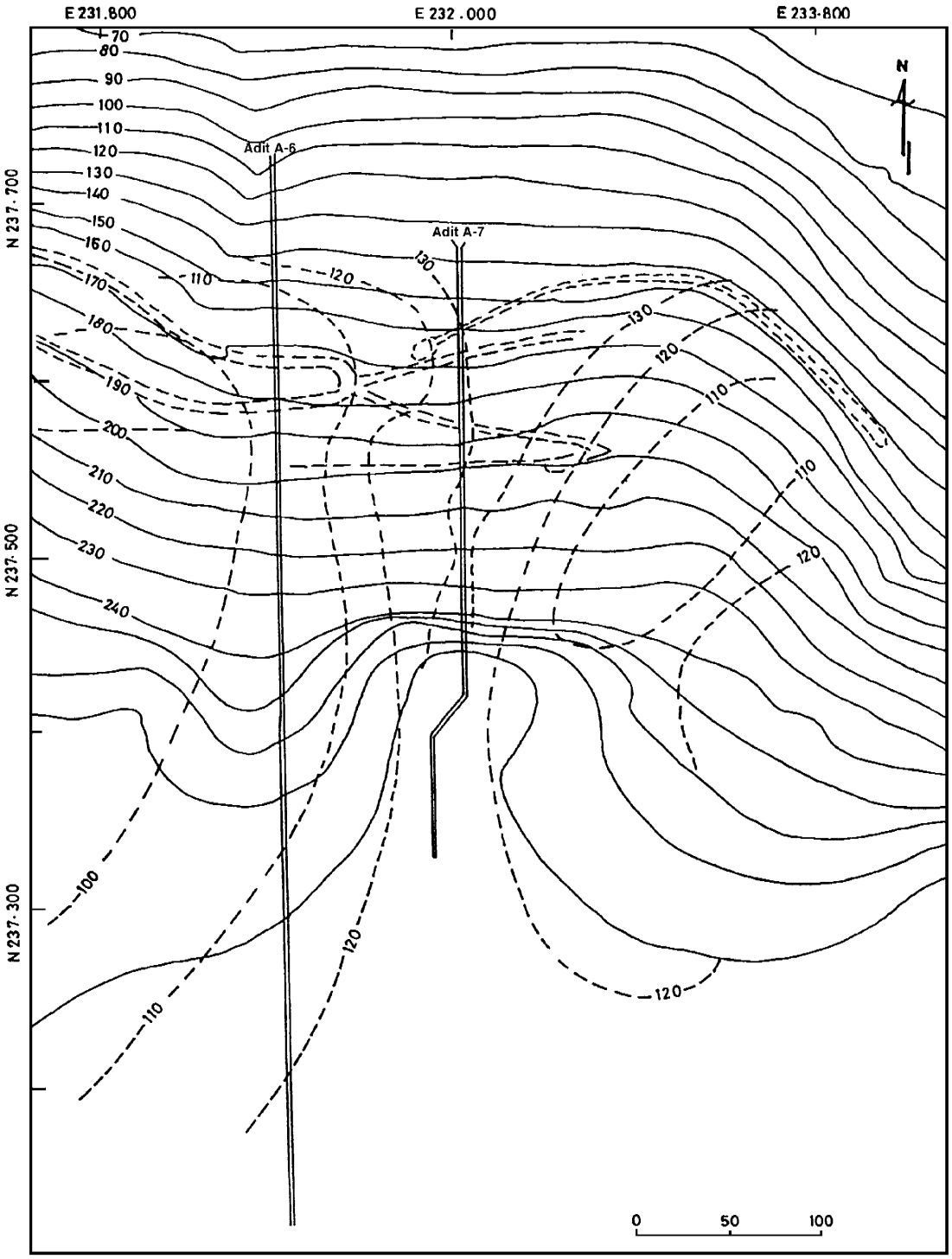

Figure A-8. *Contoured top of the unaltered Bituminous Marl Formation at Maqarin (modified after Harza, 1982, and Jordan Valley Authorities, 1980).*

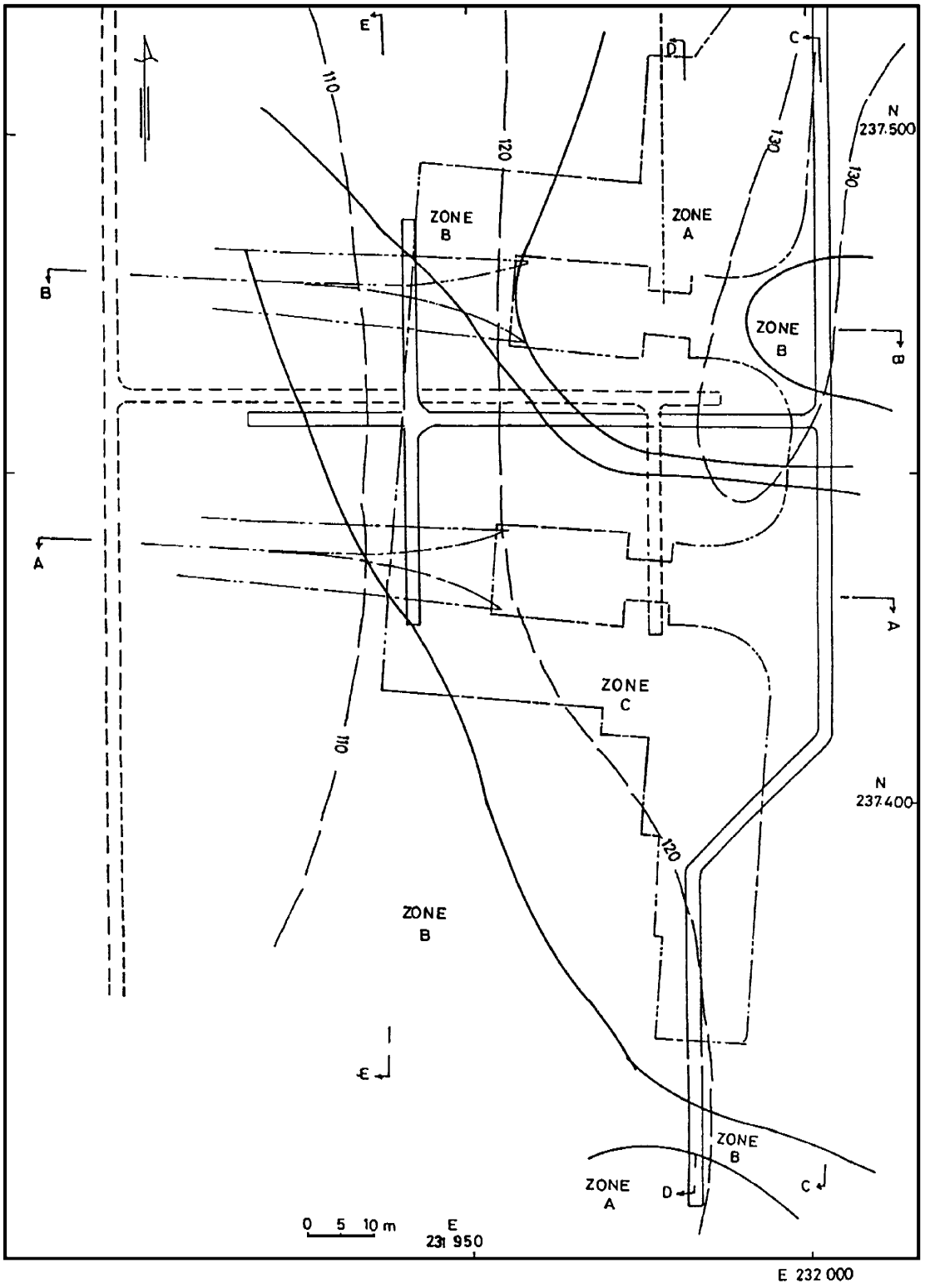

Figure A-9. *Location of cross-sectional profiles (A-E) illustrating the distribution of the Metamorphic Unit/Cement Zone (Zones A-C; see text) in the Maqarin area at elevation of Adit A-7 (after Harza, 1982).*

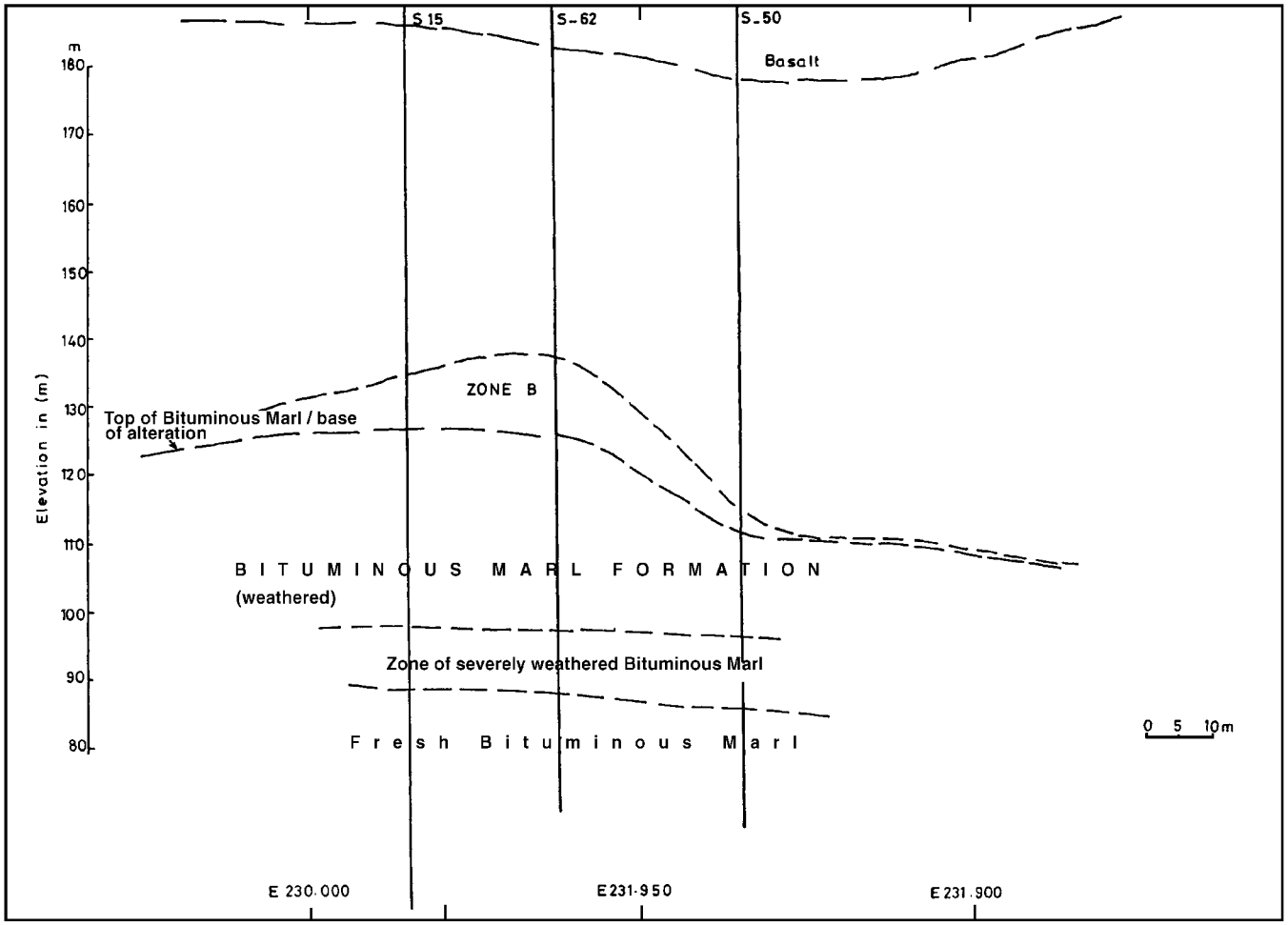

Figure A-10. *Cross-sectional profile A-A; see Figure A-9 for location (modified after Harza, 1982).*

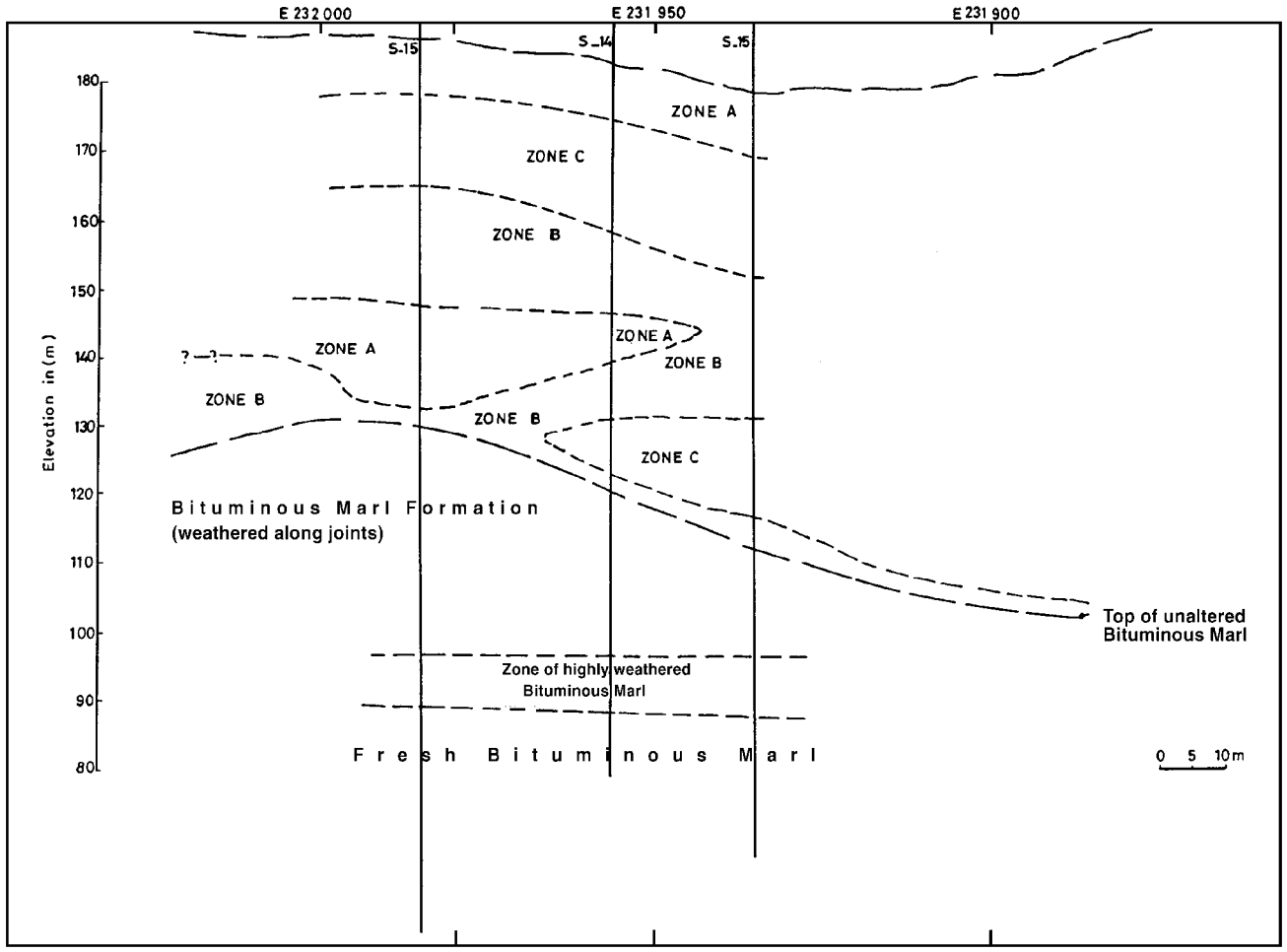

Figure A-11. *Cross-sectional profile B-B; see Figure A-9 for location (modified after Harza, 1982).*

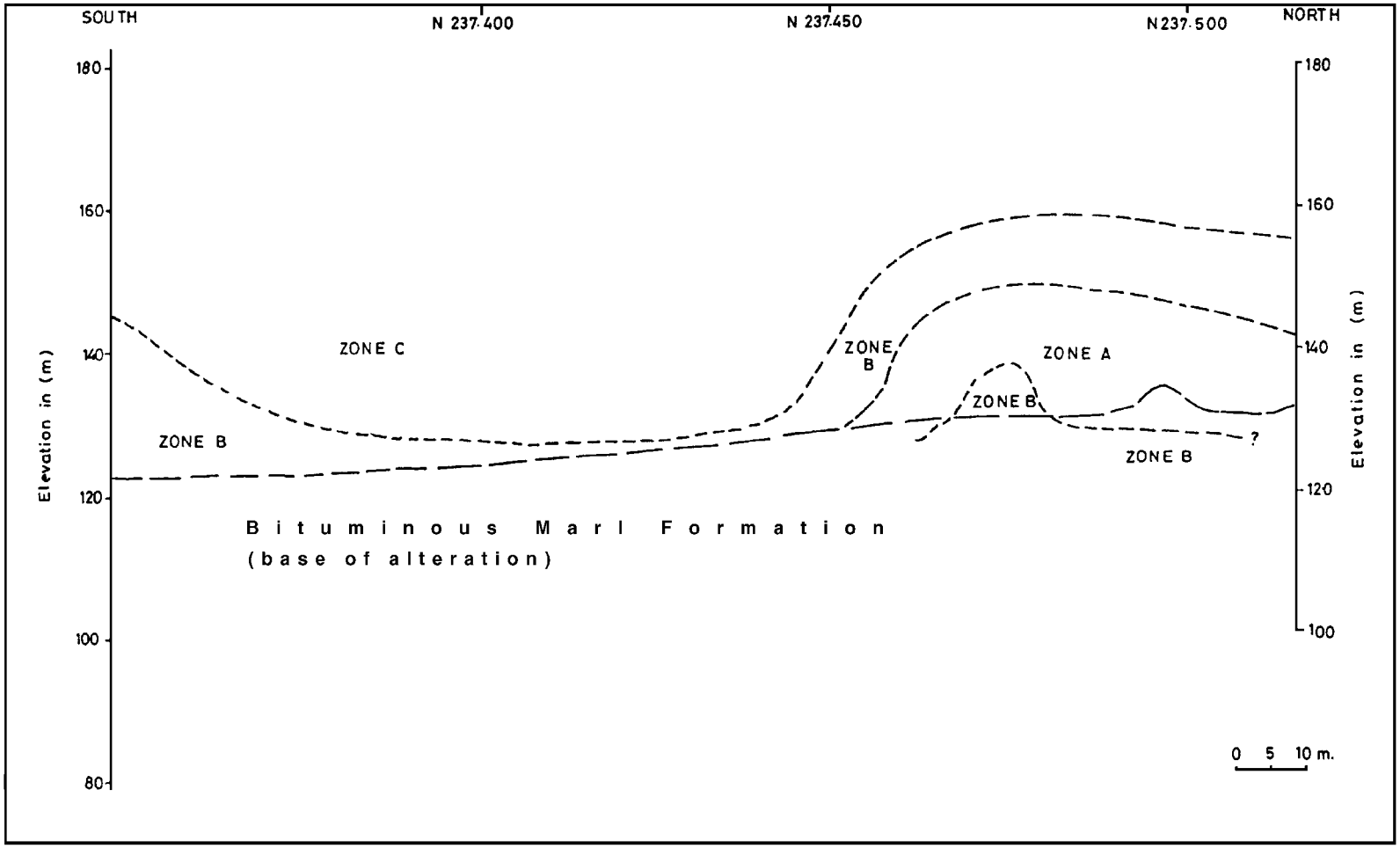

Figure A-12. *Cross-sectional profile C-C; see Figure A-9 for location (modified after Harza, 1982).*

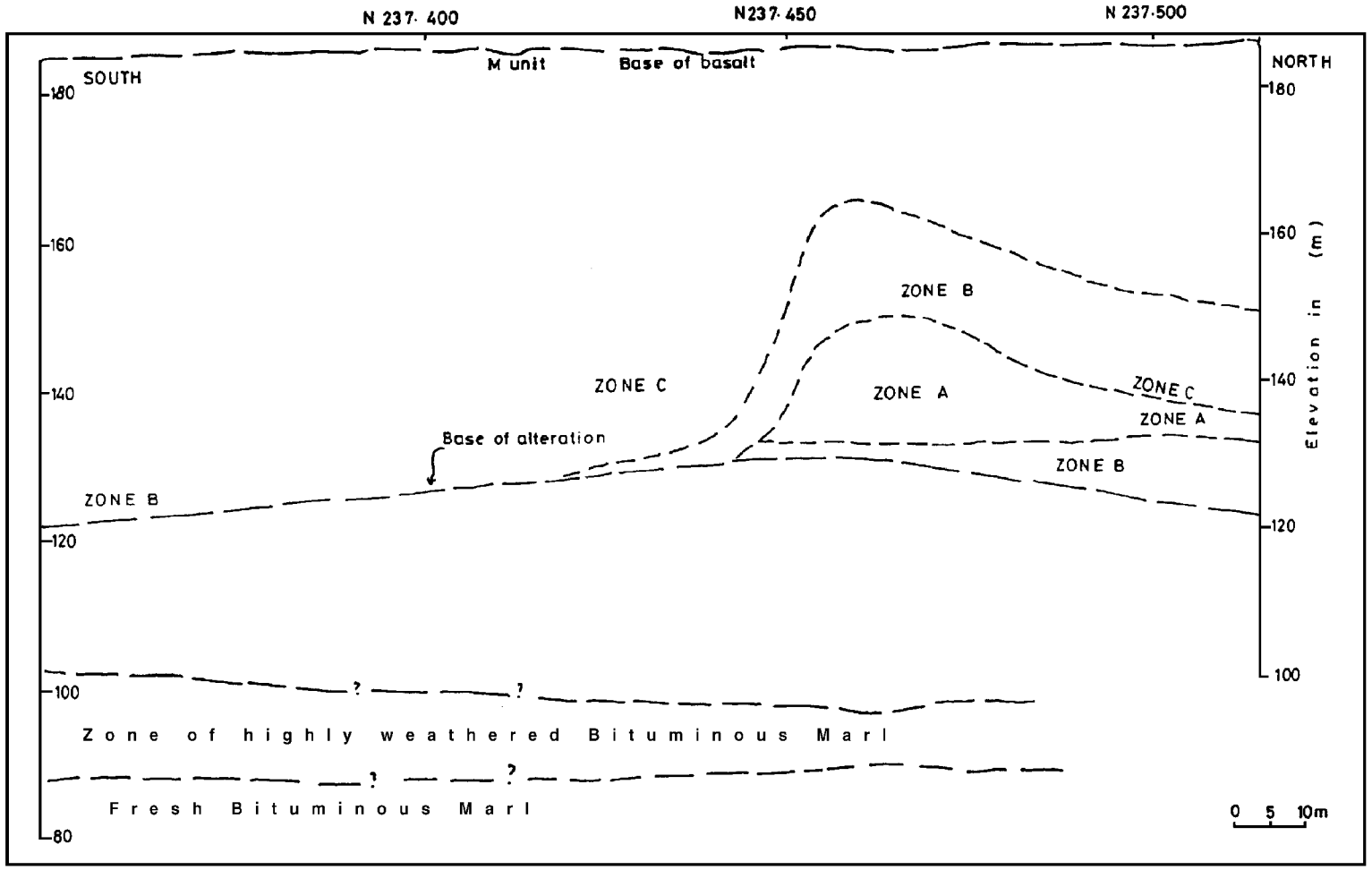

Figure A-13. *Cross-sectional profile D-D; see Figure A-9 for location (modified after Harza, 1982).*

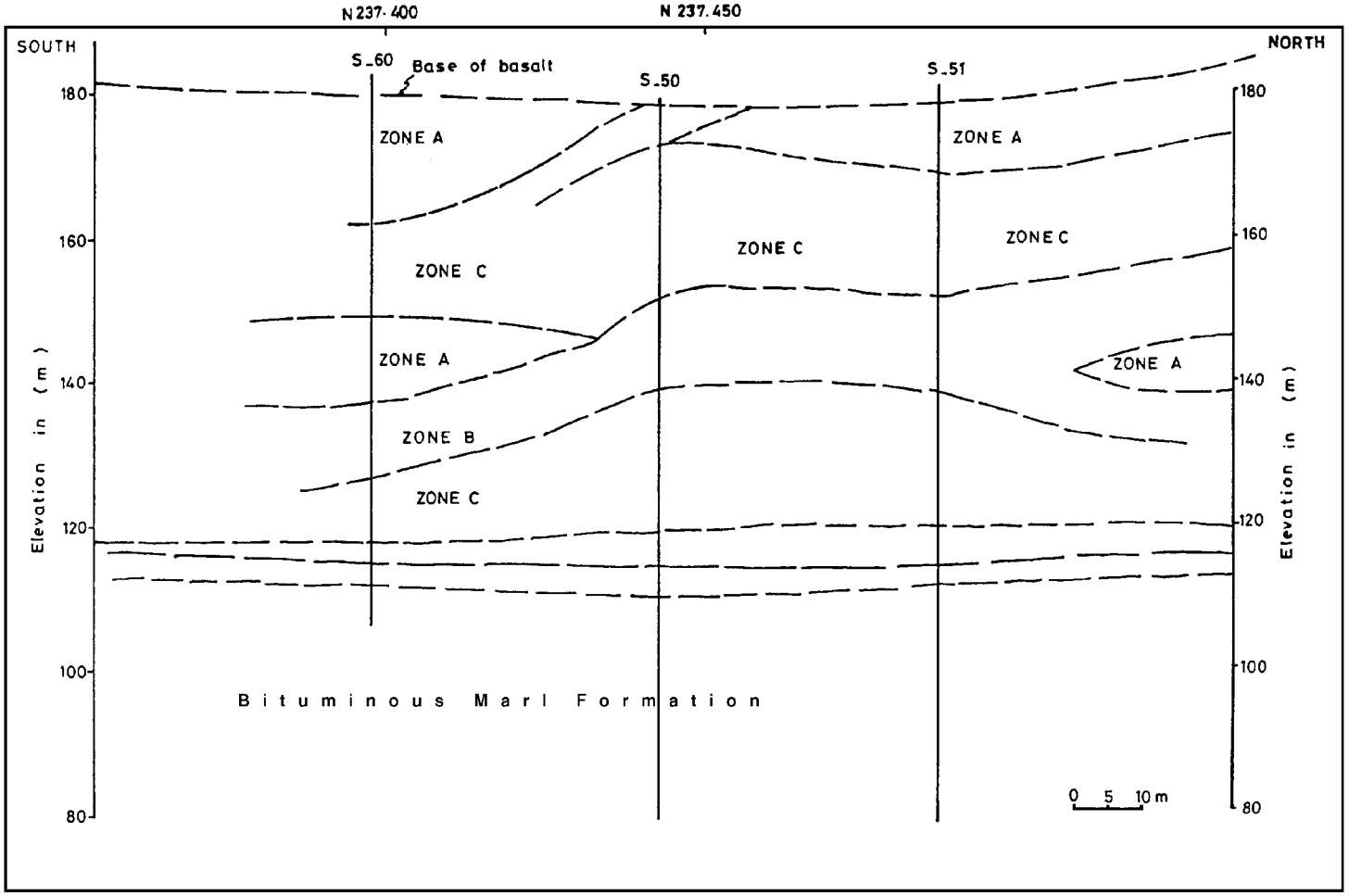

Figure A-14. *Cross-sectional profile E-E; see Figure A-9 for location (modified after Harza, 1982).*

APPENDIX B

Well Logs from the Maqarin Area

(Jordan Valley Authorities)

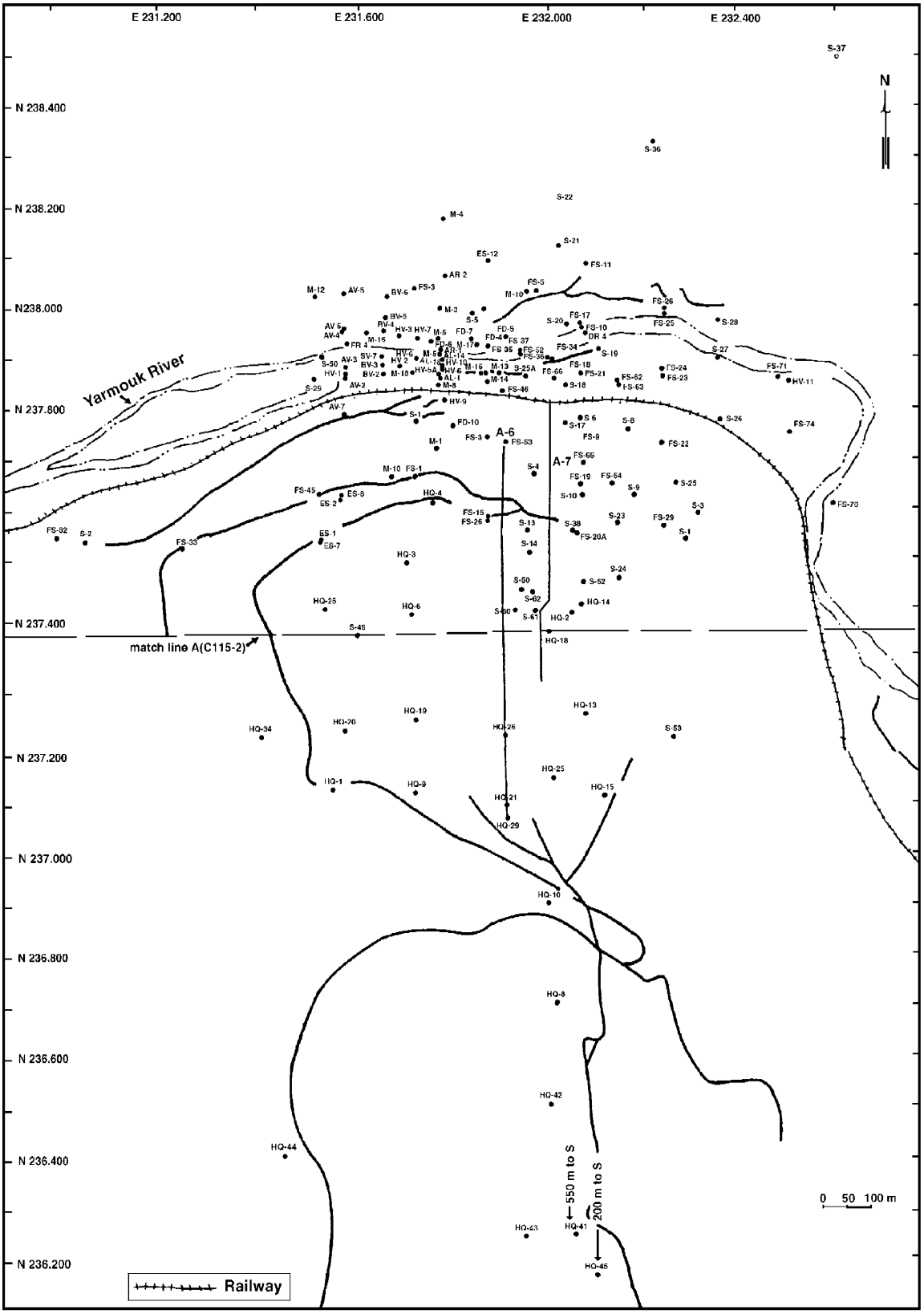

Figure B-1. *Locations and identification labels of existing boreholes in the Maqarin area. Also shown are the positions of Adits A-6 and A-7. After Harza (1982) and Jordan Valley Authorities (1980).*

Borehole/well log documentation

Some 142 borehole/well logs (location's shown in Fig. B-1) have been made available by the Jordan Valley Authorities. An example of Well Log AV-1 is reproduced in Figure B-2. The remainder have not been reproduced, but copies are available on request to:

The Swedish Nuclear Fuel and Waste Management Company
Box 5864
102 40 Stockholm
SWEDEN

Please refer to Technical Report (TR 98-04).

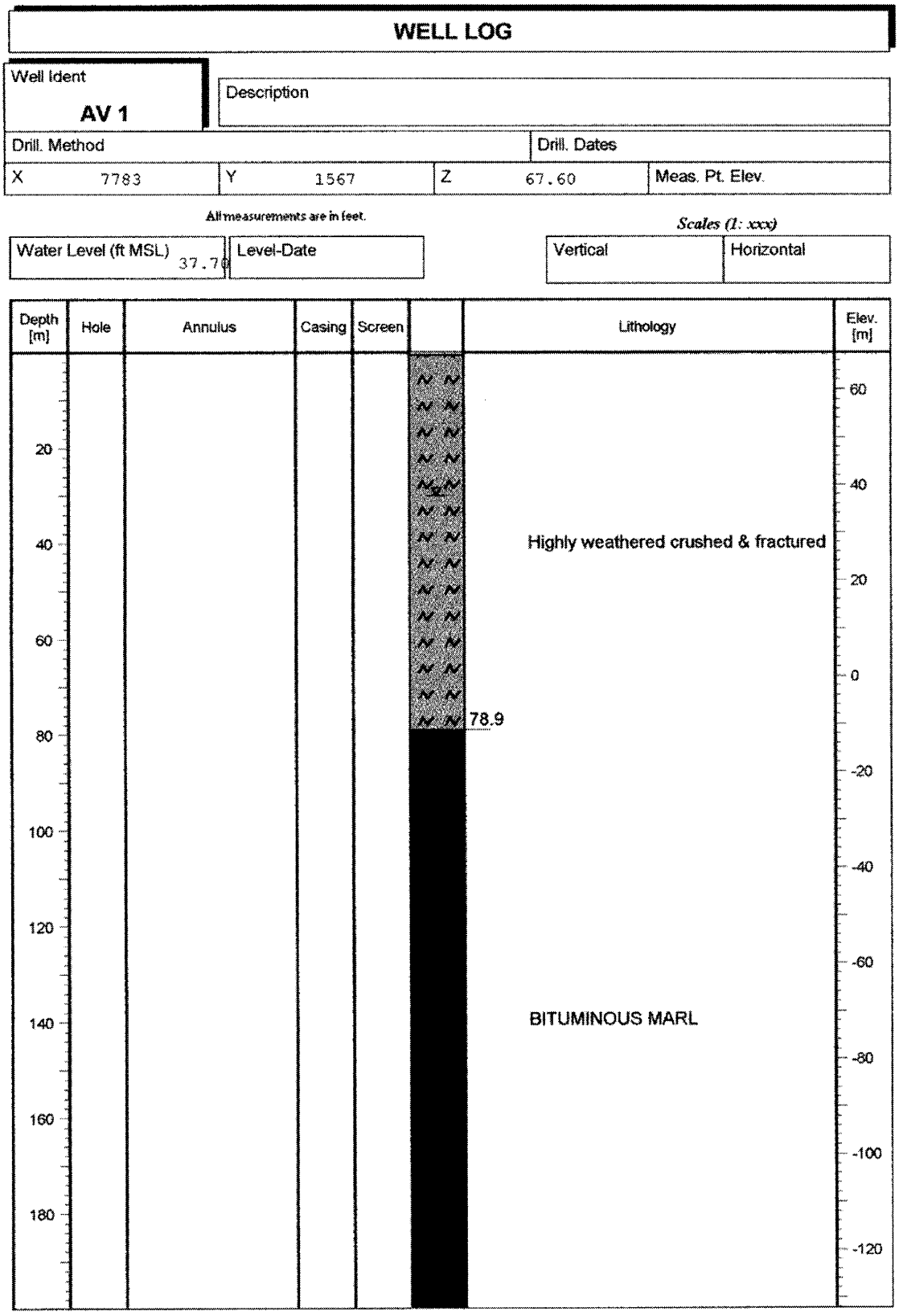

Figure B-2. *Example of available borehole/well logs made available by the Jordan Valley Authorities.*

APPENDIX C

Hydraulic Data from the Maqarin Area

(Jordan Valley Authorities)

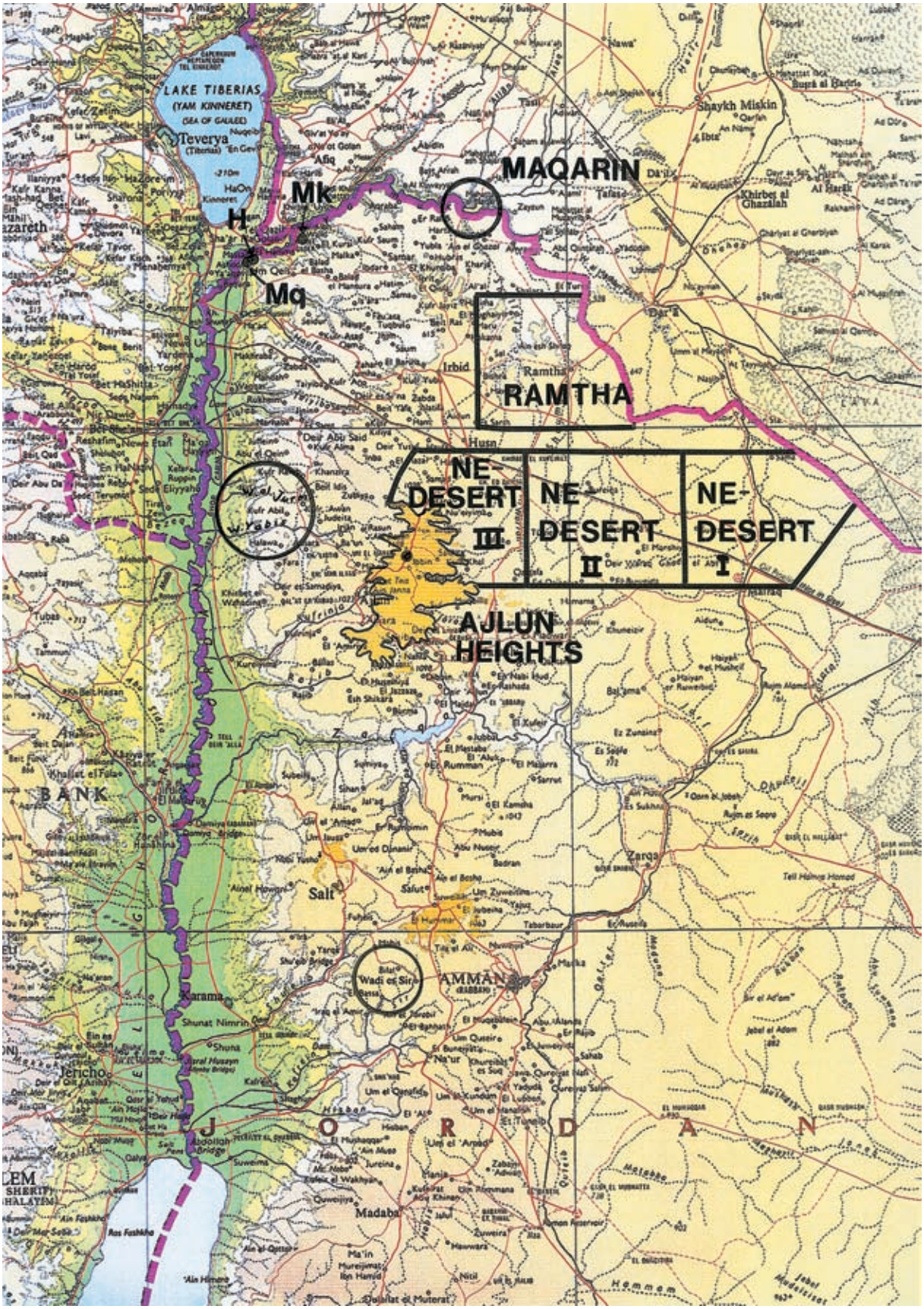

Figure C-1. *Regional topographic setting of the Maqarin Project area. Marked are key regions and some place names referred to in the text (H = El Hamma; Mq = Maqla; Mk = Mukheiba).*

(© Bartholomew 1995. Reproduced with kind permission).

Table C-1. Boreholes/wells in the study area: General hydrogeological information.

Location		Date of drilling	Co-ordinates N	Co-ordinates E	Elevation (m.)	Depth (m.)	Aquifer	Yield (m^3/h)
Recharge area								
1	Rafad Farhan		202.850	237.200		302	B_2/A_7	44
2	Nuaimeh Well 2		203.350	236.128	705	337	B_2/A_7	
3	Nuaimeh Well 1	1980	203.575	235.495	717	196	B_2/A_7	59
4	Hamad Farhan	1976	206.178	237.883	646	334	B_2/A_7	20
5	Yarmouk University 2	1983	206.000	237.240	668	280	B_2/A_7	25
6	Yamoon Well	1974	200.679	235.884	783	267	B_2/A_7	22
7	Kitm Well	1980	207.519	233.399	695	350	B_2/A_7	30
Mukheiba area								
8	Balsam Spr.		234.500	214.500	-50			1969
9	Maqla Spr.		234.500	214.500	-50			1969
10	JRV1	1981	234.500	214.700	-70	1 230	B_2-A_2	157
11	Mukheiba 1	1982	235.000	216.000	-80	350	B_2/A_7	6 000
12	Mukheiba 2	1982	235.100	215.950	-110	488	B_2	800
13	Mukheiba 3	1983	235.020	216.000	-80	333	B_2	2 822
14	Mukheiba 4	1983	235.100	215.980	-110	892	B_2/A_4	2 200
15	Mukheiba 5	1983	231.500	210.500	-118	900	B_2/A_7	200
16	Mukheiba 6	1983	235.150	215.750	-95	475	B_2	2 000
17	Mukheiba 7	1983	235.900	216.950	-115	500	B_2	2 100
Jordan River Valley (JRV)								
18	North Shuneh	1981	224.360	208.141	-178	967	B_2/A_7	900
19	Manshieh	1989	220.700	207.700	-175	1 150	B_2/A_7	200
21	Abu Ziad	1989	212.200	208.600	-120	1 126	B_2/A_7	90
22	Waqas		216.200	209.160	-90	1 300	B_2/A_7	60
Side Wadis								
25	Kufor Ubeh		215.550	224.300	475	287	A_7	41
26	Kufr Assad		225.750	217.025	100	263	B_2/A_7	81
27	Deir Yusef 3	1987	209.800	227.120	651	320	A_7	10
28	Juhfieh 1		210.650	226.800	628	300	A_7	92
29	Abu Said 2		213.000	215.600	180	284	B_2/A_7	176
30	Abu Said 1	1983	212.600	216.300	200	226	B_2/A_7	176
36	Jdeita Well		201.900	214.350	315	411	B_2/A_7	100
Wadi Arab								
35	Wadi Arab 5	1983	222.550	212.850	50	375	B_2	414
34	Wadi Arab 4	1982	226.500	213.300	27	750	B_2/A_7	702
33	Wadi Arab 3	1982	225.600	212.650	-20	257	B_2	1 486
32	Wadi Arab 2	1982	225.150	212.150	-26	407	B_2/A_7	1 571
31	Wadi Arab 1	1982	224.188	211.947	11	703	B_2/A_7	640
37	R. Elhazaimeh		221.375	220.245	357	341	B_2/A_7	55
38	Walid Khazar	1982	218.900	212.095	70	195	B_2	46
39	Moh. Adbelwali	1982	216.900	212.800	250	341	B_2	52

Table C-1 (contd.). Boreholes/wells in the study area: General hydrogeological information.

Location		Date of drilling	Co-ordinates N	Co-ordinates E	Elevation (m.)	Depth (m.)	Aquifer	Yield (m^3/h)
Ramtha area								
40	Rahub Spring		223.600	237.600	450	0		36
	Quelbeh		231.200	231.600	420			37
24	S-90	1968	211.326	248.790	566	2 190	B_2/A_7,k,z	
41	Ali Samara	1982	212.968	247.734	545	390	B_2/A_7	45
42	Kamel Tabah 2		211.620	249.820			B_2/A_7	
43	M.A. Haji	1983	218.866	242.092	534	490	B_2/A_7	50
44	Muhamad Samara		214.609	241.644	541	480	B_2/A_7	65
23	Mahasi No. 6	1988	221.580	243.750	481	702	B_2/A_7	100
45	Ahmad Fares	1971	224.115	242.723	462	70	B_4	30
46	Mahasi No. 4	1978	221.449	243.587	475	70	B_4	19
47	Nahlawi Well	1983	228.950	244.070	438	300	B_4	40
48	Kur Well	1983	229.585	243.669	435	250	B_4	32
49	Mahasi No. 1	1971	221.258	243.742	482	85	B_4	61
North Desert								
50	Yusef Hmeidi	1983	203.059	253.219	691	405	A_4	55
51	Taleb Masri	1982	212.150	261.960	582	213	B_2/A_7	82
52	Swelmeh Well	1983	211.765	258.860	631	385	B_2/A_7	59
53	Qraem Saket	1969	207.185	265.335	601	268	B_2/A_7	40
54	Qasem Awjan	1980	208.335	261.040	610	225	A_7	45
55	Muhamad S. Jalad	1981	202.170	274.725	678	293	B_2/A_7	52
56	M. Bechtian	1981	202.530	275.600	682	268	B_2/A_7	40
57	Ali Khasman	1980	206.675	273.900	657	323	B_2/A_7	40
58	Mohamad Arjani	1988	214.480	258.070	623	458	B_2/A_7	82
59	Muhamad Jahmani	1981	208.890	258.895	642	328	A_7	4
60	Ali Ajian	1970	207.95	265.160	599	160	A_7	73
61	Abdelhamid Zad 2	1979	205.365	272.120	653	310	B_2/A_7	5
62	Mousa Samara	1982	213.870	258.590	642	250	B_2/A_7	80
Adasiya area								
64	Adasiya 4		208.180	230.500	-209	80	Alluvium	162
65	Adasiya 5		207.720	229.900	-213	82	Alluvium	122
66	Adasiya 6		207.150	230.020	-215	80	Alluvium	151
69	Adasiya 8		207.550	228.860	-207	80	Alluvium	163
70	Adasiya 1B		207.560	230.900	-210	350	Alluvium	170
	Adasiya Sp		230.000	207.900	-210			

APPENDIX D

Geomorphology – Plates D-1 to D-7

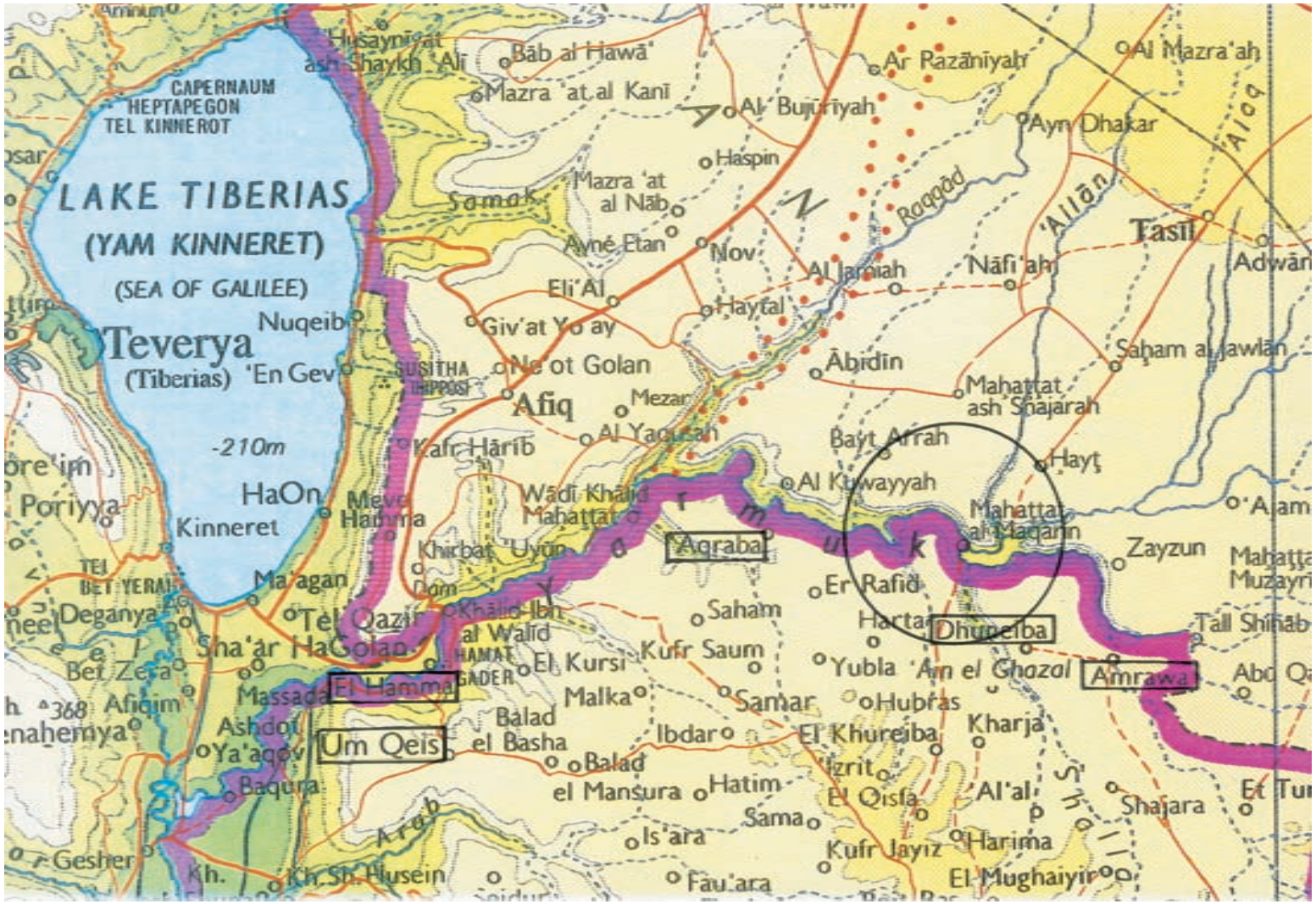

Figure D-1. *Enlarged map of the Maqarin / Yarmouk River Valley region showing locations of some of the place names (boxed) mentioned in the text.*

(© *Bartholomew 1995. Reproduced with kind permission*).

Plate D-1. *Maqarin Valley, looking north towards Qoussair, showing:*

– *the Syrian side, the staircase of basalt-capped levels on the upper valleyside, to the north.*

  Note the rockslide (centre) of a portion of the valley-fill basalt, down to a level only just above the river.

– *'nari' overed slope (foreground), contrasted with clear stratification (centre-left).*

Plate D-2. *The Zawe an Nasaytra 'terrace' looking northeast up the Maqarin Valley from Aqraba.*

Note the Yarmouk River channel, incised 10–20 m along the northern perimeter of the 'terrace' (old railway line (centre) shows the scale).

Plate D-3. *Limestone pavement 2 km east of Aqraba, looking west down the Wadi Aqraba, showing gentle regional dip to the north, joint pattern in the foreground, and 'nari'-covered valleyside slopes on the south side of the Wadi Aqraba.*

Plate D-4. *The ?Miocene Dhuneiba gravels beneath the Cover Basalt, showing the 0.2–0.4 m pink marly interlayer between the major chert/limestone gravel units, 'washed' below and 'encrusted' above (4 km southeast of Maqarin Station).*

Plate D-5. *The Al Arqub terrace, flood boulders and gravels of basalt, limestone, and chert, mantled by 0.5 m of colluvium, looking north (3.5 km WNW from Maqarin Station).*

The present valley floor of the Maqarin Valley is out of view, below the road, some 40 m lower than the terrace. A possible equivalent level may be recognised on the northern valleyside.

Note Cover Basalt on the skyline.

Plate D-6. *Typical 'gooseneck' valley meander of the upper Wadi Shallala, looking southwest from Ash Shajara (10.5 km SE of Maqarin Station).*

This phenomenon emphasises the importance of undercutting of lower valleyside slopes by lateral erosion of streams in the Maqarin area.

Episodic collapse of an undercut cliff, or even the severing of a 'gooseneck' itself, could be significant mechanisms in abruptly exposing Bituminous Marl bedrock to the atmosphere.

Plate D-7. *Superficial fault in the Upper Chalky Limestone Formation, induced by incipient landslipping (at Dhuneiba, 5 km SE of Maqarin Station).*

This mechanism may provide the abrupt entry of oxygenated water to Bituminous Marl substrata, needed for combustion.

APPENDIX E

Inventory of Rock and Mineral Samples

(Compiled by A.E. Milodowski and E.K. Hyslop)

Table E-1. Summary of rock and mineral sample information.

BGS code	Field code	Sample details
Eastern Springs, Maqarin, New Road Cutting		
Locality approx. 100 m W of Maqarin Station Railway Cutting. Active alkaline discharge over 40 m exposure of fresh, unaltered Bituminous Marl Formation. Excavated after December 1993		
C343	RC/1	Fresh unaltered bituminous clay biomicrite from east end of cutting. Dark brown, bituminous smelling.
C344	RC/2	Fresh Bituminous Marl with coating of portlandite + calcite precipitates on exposed fracture surfaces. Collected several metres below M8 seepage point.
C345	RC/3	Fracture fill from M8 active hyperalkaline groundwater seep. 8–9 cm thick infill of creamy-yellow, finely-laminated, calcareous tufa crust, with gel-like orange Fe-oxyhydroxide on upper active flowing surface.
C346	RC/4	Host rock from upper surface of M8 fracture. Wallrock bleached alteration zone up to 10 mm. Dark bituminous clay biomicrite altered to light orange-brown colour.
C347	RC/5	Samples of organic stain material on coated fracture surfaces.
C348	RC/6	Colluvial soil immediately overlying root cut.
C349	RC/7	Original colluvium matrix with calcareous pedogenic (calcrete) cement unrelated to hyperalkaline groundwater alteration.
C350	RC/8	Colluvium containing cobbles of marble and basalt showing reaction with hyperalkaline groundwater. Site has minor hyperalkaline groundwater seeps through colluvium, and along colluvium-bedrock interface.
C351	RC/9	Altered colluvium matrix material with basalt clasts showing palaeo-hyperalkaline groundwater interaction (now dry).
Eastern Springs, Adit A-6, Maqarin		
C352	A6 94/1	110 m from Adit A-6 entrance, approx. 20 m north of M1 site, approx. 2.5 m outside of cement zone. Complex vein with host rock extending approx.10 cm away from fracture. Series of intense subvertical veins, N163-trending, exposed over a 2 m interval in Adit A-6, and have typical spacings of 27–52 cm. Veins are typically 1–2 cm thick, with numerous sub-parallel braided network of hairline veinlets in wallrock.
C353	A6 94/2	108 m from adit entrance. Similar vein material to C352, showing thick (18–22 mm) alteration zone in wallrock.

Table E-1 (contd.). Summary of rock and mineral sample information.

BGS code	Field code	Sample details
Eastern Springs, Adit A-6, Maqarin (contd.)		
C354	A6 94/3	72 m from adit entrance. Relatively simple planar fracture system with approx.13–40 cm fracture spacing. Narrow zone (<10 mm) of carbonate precipitate around fractures indicates active flow. Host rocks relatively free of other fractures.
C355	A6 94/4	71 m from adit entrance. Large block containing several planar fractures similar to C354.
C356	A6 94/5	68 m from adit entrance. Single planar fracture showing active calcareous precipitates. Includes host rock and fracture fill.
C357	A6 94/6	53 m from adit entrance, corresponding to M2 site, west wall. Large block of clay biomicrite containing steep fracture with N136 trend. Contains complex vein of jennite + thaumasite-ettringite + calcite 1–2 mm thick.
C358	A6 94/7	53 m from adit entrance, corresponding to M2 site, east wall. Low-angle, north-dipping planar fractures (bedding sub-parallel), with generally 1 mm thick CSH + ettringite-thaumasite veining. Wallrock alteration zone is 15–17 mm wide.
C359	A6 94/8	53 m from adit entrance, fracture conducting main groundwater flow at M2 site. Thick jennite + ettringite-thaumasite vein with minor sub-parallel ettringite fractures in wallrock damage zone several cm's wide.
C360	A6 94/9	100 m from adit entrance. Large block of clay biomicrite containing a series of braided tobermorite veins.
C361	A6 94/10	Tobermorite vein fill from same locality as C360.
Eastern Springs, Bridge Corner Road Cut, Maqarin		
C376	BC1	Colluvium matrix.
C377	BC2	Basalt clasts with evidence of alkali alteration at margins.

Table E-1 (contd.). Summary of rock and mineral sample information.

BGS code	Field code	Sample details
Eastern Springs,Yarmouk River, Maqarin		
Freshly exposed area of cemented colluvium and tufa-encrusted bedrock, with active hyperalkaline groundwater seeps, revealed by recent flood surge. Exposure between 0-400 m downstream of Old Bridge (destroyed) corresponding to M9 and M10 groundwater sampling sites.		
C387	RY/1	Sample of colluvium matrix containing altered cobbles of clay biomicrite, chert and basalt.
Western Springs, Maqarin		
C362	M10/A	Site M10; various clasts lithologies from fluvial boulder gravels containing cobbles of clay biomicrite, limestone, chert, basalt and wood. Active hyperalkaline groundwater seepage with precipitation of calcite, aragonite, portlandite and ettringite.
C363	M10/B	Site M10; Altered sand matrix of fluvial boulder gravels. Saturated with hyperalkaline groundwater.
C364	M11/A	Site M11; Matrix to fluvial boulder gravels and small clasts from 40 cm downflow of hyperalkaline groundwater seepage point.
C365	M11/B	Site M11; Matrix of basal colluvium debris flow from approx. 2 m east of seepage point. Matrix distinct from C364, being less calcareous and brown in colour. Secondary (hyperalkaline) alteration along internal fractures.
C366	M11/C	Site M11; Recent colluvium from bank several metres above hyperalkaline seepage. Contains microfractures with calcareous (?calcrete) precipitation.
C367	M13/A	Site M13; Matrix to fluvial gravels + clasts immediately adjacent to active hyperalkaline groundwater seepage.
C368	M13/B	Site M13; Altered fluvial gravels from 2 m down flow of the hyperalkaline groundwater seepage. Active secondary mineral precipitation along internal fractures in matrix.
C369	M14/A	Site M14; Altered matrix of fluvial gravels within flow path of spring, 20 cm down flow of seepage point.
C370	M14/B	Site M14; Recent colluvium ("soil") from approx. 1 m above hyperalkaline seepage point. Unconsolidated material unaffected by alkaline groundwater.
C371	M16/A	Site M16; Fluvial gravels containing range of clast lithologies, including basaslt, chert, clay biomicrite and cement zone.
C372	M16B	Site M16; Altered matrix of fluvial gravels from point of spring discharge.

Table E-1 (contd.). Summary of rock and mineral sample information.

BGS code	Field code	Sample details
Western Springs, Maqarin (contd.)		
C373	M16/C	Site M16; Altered matrix of fluvial gravels + clasts from approx. 50 cm down flow of seepage point.
C374	M19/A	Site M19; Colluvium containing clasts of clay biomicrite, chert and cement zone, with evidence of past alkali-rock interaction.
C375	M19/B	Site M19; basalt-rich gravel sheet overlying altered sheet of clay biomicrite-rich colluvium.
New Sweileh Road cut, Amman, central Jordan		
C378	SW1	Green-coloured, highly altered "clay-rich" band within biomicrite/chalk from adjacent to fracture with evidence of palaeo-hyperalkaline groundwater activity.
C379	SW2/1	Upper 7 cm of pale green, poorly altered "clay-rich" chalk/biomicrite from adjacent to fracture with evidence of palaeo-hyperalkaline groundwater activity.
C380	SW2/2	Central 10 cm of dark red "clay-rich" chalk/biomicrite from adjacent to fracture with evidence of palaeo-hyperalkaline groundwater activity.
C381	SW2/3	5 cm thick band of green altered "clay-rich" chalk/biomicrite from adjacent to fracture with evidence of palaeo-hyperalkaline groundwater activity.
C382	SW2/4	12 cm thick band of orange, poorly altered "clay-rich" chalk/biomicrite from adjacent to fracture with evidence of palaeo-hyperalkaline groundwater activity.
C383	SW3	Weakly altered "clay-rich" chalk/biomicrite, from same horizon as SW2/1-4, taken approx. 25 m distant from fracture with evidence of palaeo-hyperalkaline groundwater activity.
C384	SW4	Subvertical fracture above SW1 site. Limestone band adjacent to this shows fine, green secondary precipitate on steep fracture surfaces.
C385	SW5	Black bituminous phorphorite band from top bed of exposed sequence.
C386	SW6	Travertine deposit from fault at south-western end of exposure.

Table E-1 (contd.). Summary of rock and mineral sample information.

BGS code	Field code	Sample details
Other background lithologies		
C768	n/a	Silicified Limestone Formation (part of the Amman Formation) sampled where exposed in the Irbid area.
C779	n/a	Chert Chalky Limestone Member, Maqarin, sampled from outcrop.
C782	n/a	Quaternary basalt; massive basalt, Maqarin, sampled *in situ* from outcrop.
C783	n/a	Quaternary basalt; vesicular basalt, Maqarin, sampled *in situ* from outcrop.

APPENDIX F

Groundwater Sampling and Analytical Protocols

F GROUNDWATER SAMPLING AND ANALYTICAL PROTOCOLS

F.1 Groundwater Sampling Protocol

Groundwater samples were taken and preserved in the field as follows:

Major and Trace Cations

60 mL samples for the analysis of major cations (Ca, Mg, Na, K), trace cations (Si, Ba, Sr, Mn, Fe, Al, Co, Ni, Cu, Zn, Cr, Mo, Cd, Pb, V, Li, U and Th), total S and Si were sampled on-site, directly at the sampling point, by using a plastic syringe to minimise atmospheric contact, and filtered "on-line" through 0.45 mm pore diameter Acrodisc nylon filter disks directly into Nalgene bottles. The samples were preserved by acidification to 1% with respect to AristaR HNO_3. A blank sample using double-distilled water (supplied by BGS) and processed on-site in the same manner was also prepared.

Major and Trace Anions

60 mL samples for major and trace anions (Cl, SO_4, NO_3, NO_2 and Br), and for Total Organic Carbon (TOC) and Total Inorganic Carbon (TIC) were taken in a similar manner as for major and trace cations, except the samples remained unacidified. A blank sample using double-distilled water (supplied by BGS) and processed on-site in the same manner was also prepared.

Reduced Sulphur

60 mL samples for the determination of reduced sulphur were taken by plastic syringe directly at the sampling points. The samples were not filtered but were preserved 1% with respect to NaOH. A blank sample using double-distilled water (supplied by BGS) and processed on-site in the same manner was also prepared.

Selenium and Arsenic

60 mL samples for the determination of Se and As were taken and filtered as for major and trace cations but were preserved by acidification to 1% with respect to AristaR HCl. A blank sample using double-distilled water (supplied by BGS) and processed on-site in the same manner was also prepared.

Ferrous Iron

Samples for the determination of ferrous iron were sampled directly using a plastic syringe and filtered through "on-line" 0.45 mm pore diameter Acrodisc nylon filters directly into Sterylin plastic tubes to which 1 mL of 1% 2,2-bipyridyl solution (HCl acidified) had been added. The volume was made up to 10 mL total with the sample. The 2,2-bipyridyl forms a stable red complex with ferrous iron in solution. A blank sample using double-distilled water (supplied by BGS) and processed on-site in the same manner was also prepared.

Ammonium

60 mL samples for the analysis of ammonium were sampled on-site, directly at the sampling point, by using a plastic syringe to minimise atmospheric contact, and filtered "on-line" through 0.45 mm pore diameter Acrodisc nylon filter disks directly into Nalgene bottles. The samples were preserved by acidification to 1% with respect to AristaR H_2SO_4. A blank sample using double-distilled water (supplied by BGS) and processed on-site in the same manner was also prepared.

F.1.1 Field Measurements

Hydrochemical parameters measured in the field at the sampling points include temperature, pH, Eh, electrical conductivity and dissolved oxygen. Bicarbonate was also determined for normal bicarbonate groundwater types. The field measurements are summarised with other groundwater analyses in Chapter 4, Tables 4-2 and 4-3.

Two Orion portable meters (ORION RESEARCH Model SA250) and specific ion electrodes were used to measure temperature (±0.1°C), pH (±0.01 pH unit) and Eh (±0.1 mV). pH and temperature were determined using a Ross combination glass electrode. This type of electrode has proved reliable at high pH during previous studies (Milodowski et al., 1998a). The pH electrodes were calibrated with commercially-available buffer solutions at pH 4, 7 and 10, and 13 depending on the pH range of the sample being measured.

Eh was measured with a standard Pt-Ag/AgCl electrode verified with Zobell's solution (standard solution Eh = 200–250 mV) and corrected (corrected Eh = uncorrected Eh +(244-T), where T is the temperature in degrees Celcius). As was the case in Phase I and Phase II, the flow from the hyperalkaline seeps was generally too low to enable Eh to be measured within a sealed flow-through cell. Therefore at most sites Eh, pH, temperature and conductivity were measured by immersing the electrodes/probe directly in the discharging groundwater, or in standing pools of water, from which samples were taken for analysis. In the case of the borehole WS1 (sample M17) and borehole RW2 (sample M18), a sealed perspex flow-through cell (Ball and Milodowski, 1989) was used to measure pH, Eh and temperature. During measurement, Eh readings typically drifted slowly downwards and never achieved stable readings.

Conductivity was measured using a hand-held Bibby Conductivity SMC-1 conductivity probe. The conductivity probe was calibrated using a standard conductivity KCl solution.

Dissolved oxygen was determined in the field using commercially-available small portable colorimetric dissolved oxygen test kits (CHEMetrics CHEMets(R) kits: Model K-7512 and Model K-7501). These kits contained pre-prepared vials of colorimetric reagent, sealed under vacuum, into which a fixed volume of groundwater was taken up when the seal of the vial was broken. The colour developed was assessed visually by comparison with a set of vials of standard concentrations for a range of dissolved oxygen contents. The kits used were prepared for two ranges of dissolved oxygen (0–1 ppm; 1–12 ppm dissolved O_2), and measurements reported are considered to be accurate to within ±1 ppm.

Bicarbonate was determined by titration on normal bicarbonate-type groundwater using a portable mechanical autotitrator kit. The water sample was titrated with standard sulphuric acid using Bromocresol Green indicator. Titrations were checked against 200 ppm bicarbonate standard solutions pre-prepared at BGS.

F.2 Laboratory Analysis of Groundwater Samples

F.2.1 General

Groundwater samples were flown to the U.K. and on receipt were stored at 4°C prior to analysis. The groundwater chemical data for the Maqarin groundwaters are summarised in Chapter 4, Tables 4-2 and 4-3. Table 4-2 also includes the field data (Eh, Field pH, T, Field bicarbonate, Conductivity and Dissolved O_2) for comparison and completeness. However, the user should be aware of the caveats described in Chapter 4, Subsection 4.3.5 when considering the field data.

The analytical methods used here are similar to those used in Phase II, described in detail by Milodowski et al. (1998b). For the sake of brevity the analytical methods are only briefly summarised in this report.

F.2.2 pH and Total Alkalinity

Laboratory measurements of pH and Total Alkalinity were determined as soon as possible after delivery to the laboratory, with effort made to ensure minimal contact and reaction with the atmosphere. pH and Total Alkalinity were determined using a Radiometer VIT90 Titrator Controller module with an ABU93 autoburette and a SAM90 sample station. Sample pH was determined with Radiometer G2040B glass pH and K4040 calomel reference electrodes. The pH electrode was calibrated using pH7 and 9.2, or 7 and 13 buffers, depending on the sample pH. To check the accuracy of the field measurement, the pH buffer solution used in the field was measured against the laboratory pH 13 standard and gave a value of 12.92 at 22°C.

Theoretically, total alkalinity is a measure of the hydroxide, carbonate (x2) and bicarbonate contents, as well as any contributions from other anions that take part in hydrolysis, e.g. organic bases, silicates, borates, sulphides and phosphates. For these solutions, samples which were pH 12.0 have been characterised in terms of hydroxide and carbonate concentration. The concentration of bicarbonate in these solutions is

assumed to be negligible (<5% [CO_3^-] for the purposes of this calculation). For samples with pH <9.0 the concentration of hydroxide is assumed to be negligible (<10 mg/L [OH^-]) and the results calculated as carbonate and bicarbonate concentration. Using these assumptions as the basis for the identification of end-points obtained during the titration, the concentrations are determined by direct calculation.

Because of the highly alkaline nature of some of the samples, contamination by adsorption of atmospheric CO_2 is a major potential problem. Every effort was made to fill the bottles to the brim in the field so that no air space existed on sampling, and that the samples were analysed quickly when returned to the laboratory. Nevertheless, some CO_2 adsorption will have occurred and the results for the hyperalkaline groundwater samples (M5, M8, M10-M15 and M18) should be regarded as maximum values.

F.2.3 Major Cations and Trace Elements

Major cations (Ca, Mg, Na, K including Sr), and trace cations (Si, Ba, Mn, Fe, Al, Co, Ni, Cu, Zn, Cr, Zr, Mo, Cd, Pb, V, Li, U and Th), total S and Si were determined by a combination inductively coupled plasma-atomic emission spectroscopy (ICP-AES) and inductively coupled plasma-mass spectrometry (ICP-MS) techniques.

F.2.4 Major and Trace Anions

Major and trace anions (Cl, SO_4, NO_3, NO_2 and Br) were determined by ion chromatography. Most anions are stable in solution for an appreciable length of time and certainly with the delay between sampling and analysis during this project. Nitrate and nitrite will, however, be modified by microbial activity. Therefore, ion chromatography analysis was carried out as soon as possible after receipt of the samples from Jordan. NO_2/NO_3 change very rapidly in normal groundwaters and although the microbial activity in the Maqarin alkaline groundwaters is low, this factor must be considered in using the NO_2/NO_3 data for redox modelling. The highly alkaline nature of the samples altered the column retention characteristics to shorter retention times compared to the standards. Consequently, the results for each sample had to be calculated manually as the integrator did not correctly identify each peak. This had no effect on the peak areas and hence did not affect the accuracy of the measurement.

F.2.5 Fluoride

Fluoride (F^-) was determined by ion-selective electrode (Orion Model 90/01 single junction reference electrode used in conjunction with an Orion Model 94/09 Fluoride electrode) using filtered unpreserved samples were used. Total Ionic Strength Adjustment Buffer was added to the samples at a ratio of 1:1. This functions to maintain sample pH between 5–5.5 and prevents interference from complexation of F^- by H^+ or OH^-, and also preferentially complexes interfering metal complexes (in particular, Fe and Al complexes).

F.2.6 Total Organic and Inorganic Carbon

Total organic carbon (TOC) and total inorganic carbon (TIC) were determined on filtered unpreserved samples, using Shimadzu TOC-5000 non-dispersive infrared total organic carbon analyser. Inorganic (IC) carbon content represents the sum of the carbonate and bicarbonate present in solution. The method is essentially interference free as long as the IC or TOC is converted to CO_2 during the two different oxidation procedures, which is verified by external check standards. The error in the analysis of the organic carbon is slightly greater than that for the inorganic carbon as it is calculated by difference. The inorganic carbon values in the hyperalkaline groundwater samples must be regarded as maximum values as small amounts of atmospheric carbon will probably have been adsorbed.

F.2.7 Reduced Sulphur

Reduced sulphur was determined by hydride generation ICP-AES using the method described by Cave and Green (1988). Sulphide is stabilised under alkaline conditions but it is still likely that some loss will be incurred within a relatively short timescale. For this reason, reduced sulphur content is determined as soon as possible after collection of the samples. The reduced sulphur content is determined on an unfiltered sample, as it is likely that degassing of the H_2S would occur on filtration. Particulate sulphide may therefore contribute to the reported total. The reported value may also include a contribution from any organic sulphur released from solution as gaseous organic sulphur species or sulphide gas on acidification.

F.2.8 Arsenic and Selenium

As and Se were determined by hydride generation ICP-AES following the method published by Cave and Green (1989). Analyses were performed on samples preserved by acidification to 1% with respect to AristaR® HCl.

F.2.9 Reduced Iron

Reduced iron (Fe^{2+}) was determined by colorimetric method using the chromogenic reagent 2,2-bipyridyl. Ferrous iron is rapidly oxidised in air to ferric iron, so the sampling methods used must ensure that air is excluded during sampling and filtration. For this reason, the samples were filtered out of contact with air by using plastic syringes with on-line Acrodisc nylon filter disks fitted to the ends of the syringes. The water was filtered directly into a sample tube into which 2,2-bipyridyl solution colorimetric reagent had been added previously, thereby ensuring that the reduced iron is stabilised immediately. The complex stabilises the ferrous iron in solution and deterioration is considered negligible over the timescale between collection and analysis.

The validity of the data can also be checked by comparing the results for the colorimetric method with the ICP-AES results for total Fe. The value for the reduced iron should never be higher than the total Fe (within the error of the analytical measurements).

F.2.10 Ammonium

Ammonium was determined colorimetrically using a flow-injection analysis method. The sample type and method of sampling are important in this determination. The amount of free ammonia present varies with pH. Above pH 12, the ammonium/ammonia equilibrium in solution is such that over 90% exists as free ammonia. For the samples with high pH there would, undoubtedly, have been losses of ammonia (i.e. during collection and filtration) during the sampling although they were acidified in the field. It is not possible to give accurate estimates of these losses and this should be taken into consideration when interpreting the data and the NH_4 values should be regarded as minimum values.

F.2.11 Orthophosphate

Orthophosphate was determined colorimetrically using a flow injection technique based on the method published by Osburn et al. (1974).

F.3 References

Ball, T.K. and Milodowski, A.E., 1989. The geological, geochemical, topographical and hydrogeological characteristics of the Broubster natural analogue site, Caithness. Brit. Geol. Surv. Tech. Rep., Fluid Proc. Res. Gr., (WE/89/37), Keyworth, UK.

Cave, M.R. and Green, K.A., 1988. Determination of reduced sulphur content of groundwaters by hydrogen sulphide generation-inductively coupled plasma optical emission spectroscopy. At. Spect., 9, 149–152.

Cave, M.R. and Green, K.A., 1989. Feasibility study of the determination of iodide, tin, arsenic, selenium, and hydrogen carbonate in groundwaters by inductively coupled plasma atomic emission spectroscopy using a membrane gas-liquid separator. J. Anal. Spect., 4, 223–225.

Osburn, Q.W., Lemmel, D.E. and Downey, R.L., 1974. Automated method for ortho, ortho plus hydrolysable and total phosphate in surface and waste waters. Environ. Sci. Technol., 8, 363–366.

Linklater, C.M. (Ed.), 1998. A natural analogue study of cement-buffered, hyperalkaline groundwaters and their interaction with a repository host rock: Phase II. Nirex Science Report, S/98/003, Nirex, Harwell, U.K.

Milodowski, A.E., Hyslop, E.K., Khoury, H.N. and Salameh, E., 1998a. Site description and field sampling programme. In: C.M. Linklater (Ed.), A natural analogue study of cement-buffered, hyperalkaline groundwaters and their interaction with a repository host rock: Phase II. Nirex Science Report, S/98/003, Nirex, Harwell, U.K., p. 10–47.

Milodowski, A.E., Cave, M.R., Reeder, S., Smith, B., Chenery, S.R.N. and Cook, J.M., 1988b. Aqueous geochemistry at Maqarin. In: C.M. Linklater (Ed.), A natural analogue study of cement-buffered, hyperalkaline groundwaters and their interaction with a repository host rock: Phase II. Nirex Science Report, S/98/003, Nirex, Harwell, U.K., p. 48–63.

APPENDIX G

Mineralogy and Geochemistry – Analytical Methods

G MINERALOGY AND GEOCHEMISTRY – ANALYTICAL METHODS

G.1 General

A comprehensive suite of mineralogical and petrological techniques was used in the characterisation of materials from Maqarin and central Jordan. Details of the samples collected during Phase III are summarised in Appendix E. Bulk mineralogical composition and separated clay-fractions were determined by X-ray diffraction analysis (XRD). Petrographic analysis was undertaken using optical microscopy, backscattered scanning electron microscopy (BSEM) and analytical transmission electron microscopy (ATEM). Mineral compositions were determined by electron microprobe analysis (EMPA) and ATEM, with trace element compositions of selected mineral samples determined by laser-ablation microprobe – inductively-coupled plasma – mass spectrometry (LAMP-ICP-MS). Uranium distribution was characterised by quantitative fission track registration analysis (FTR). Whole-rock chemistry was determined by a combination of X-ray fluorescence analysis (XRF) and inductivelycoupled plasma – mass spectrometry (ICP-MS).

Many of the analytical techniques used have been described in detail in earlier (Phase I and Phase II) reports (Clark et al., 1992 and Milodowski et al., 1998) and consequently, only outline descriptions are given here. Detailed description of methodology is only given here where it is specific to the work undertaken during Phase III.

G.2 Bulk Mineralogical Analysis

Bulk mineralogical analysis of a total of nineteen samples from the Western Springs, central Jordan and Sweileh road cut sites were studied by X-ray diffraction (XRD) techniques. Table G-1 provides a listing of sample number, location and the method of analysis employed.

G.2.1 Standard Whole-rock Sample Preparation

A representative, approx. 20 g subsample from the central Jordan and Sweileh road cut samples was ground to pass a 250 μm sieve using an automatic pestle and mortar.

Approx. 3 g portions of these <250 μm samples together with tema-milled material or acid-leached material (see below) from the Western Springs samples were micronised under acetone for 10 minutes and dried at 55°C. The resulting material was disaggregated in a pestle and mortar and back-loaded into a standard aluminium sample holder for whole-rock XRD analysis.

G.2.2 Acid Leaching

In order to more closely examine the non-carbonate mineralogy of the Western Springs samples, the samples were treated with a buffered acetic acid-sodium acetate reagent at pH 5.3 following the method of Jackson (1969).

Approx. 20 g of tema-milled sample was treated with 200 mL of the buffered reagent, treated with ultrasound for 2–3 minutes and then placed in a water bath maintained at 40–50°C for 5–6 hours. After standing overnight, the supernatant was discarded and the leaching procedure repeated until no further reaction was observed. The leached material was then washed three times with distilled water and dried at 55°C.

G.2.3 Clay Fraction (<2 μm) Mineralogy

Approximately 10 g of <2 mm crushed material (central Jordan and Sweileh road cut samples) or approximately 3 g of acid leached material (Western Springs) was placed in distilled water and treated with ultrasound for approx. 5 minutes to disaggregate the material and disperse any clay minerals present. The suspensions were then sieved on 63 μm and the <63 μm material placed in a 250 mL measuring cylinder and allowed to stand. After a period dictated by Stokes' Law, a nominal <2 μm fraction was removed and dried at 55°C. 80 mg of the <2 μm material was then re-suspended in a minimum of distilled water and pipetted onto a ceramic tile in a vacuum apparatus to produce an oriented mount.

G.2.4 XRD Analysis

XRD analysis was carried out using a Philips PW1700 series diffractometer equipped with a cobalt-target tube and operating at 45 kV and 40 mA. Whole-rock samples were scanned over the range 2–50 °2θ at a speed of 0.48 °2θ/minute. Oriented <2 μm mounts were scanned from analysed using Philips APD1700 software coupled to a JCPDS database running on a DEC 1.5–32 °2θ at 0.9 °2θ/minute in the air-dry and glycol-solvated states. Diffraction data were MicroVax 2000 micro-computer system.

G.3 Petrographic Analysis

Optical Petrography

Representative samples from Maqarin and central Jordan were examined by optical petrographic microscope. The samples were prepared as polished thin sections to facilitate optical petrographic analysis and also, backscattered scanning electron microscopy, electron microprobe analysis, laser-ablation microprobe – inductively coupled plasma massspectrometry, and fission-track registration analysis. Polished thin sections were prepared following injection of samples with a ultraviolet (UV) light fluorescent epoxy-resin. This was to enable porosity fabrics to be observed under UV epifluorescence microscopy observation. The thin sections were examined under normal transmitted light and under UV illumination, using a Zeiss Universal petrological

microscope fitted with UV-transparent (fluorite) lenses and a mercury vapour UV light source. Photomicrographs of the samples were taken using a Nikon Autoflex camera system. Photomicrographs of areas of interest were recorded with 1000 ASA 35 mm colour film. Although this film has a high grain size, a fast film speed was necessary to enable photography at low-levels obtained under UV illumination.

G.3.1 Backscattered Scanning Electron Microscopy

After optical examination, the polished thin sections were studied by backscattered scanning electron microscopy (BSEM). BSEM observations were made using a Cambridge Instruments Stereoscan S250 Mark I SEM instrument equipped with a KE Developments 4element solid-state backscattered electron detector. Mineral identification was made by qualitative examination of the characteristic energy-dispersive X-ray spectra (EDXA) recorded during observation of a given phase, with a Link Systems 860 Mark I energy-dispersive X-ray spectrometer fitted to the electron microscope. Observations were made at 20 kV electron beam excitation. The EDXA system has a detection limit of approx. 0.2% (weight) for most common elements but this is probably of the order of 0.5% (weight) for uranium, thorium and lanthanides. The polished sections were coated with a thin layer of carbon (approx. 250 Å thick) prior to examination in the SEM in order to make the surface electrically conductive.

In BSEM mode, the image obtained from polished sections is related to the composition of the material being examined. Image brightness is proportional to a combination of the average atomic number of the material and its density, thus allowing the distribution of different minerals or phases to be determined on the basis of their chemical composition. Further details of this method are given in Milodowski et al. (1998).

G.3.2 Electron Microprobe Analysis

Electron microprobe analysis (EMPA) was performed on selected samples using a computer controlled Cameca SX50 electron microprobe fitted with three wavelength-dispersive spectrometers. An accelerating voltage of 15 kV and 30 nA current was used for all analyses. Profiles of up to 700 analyses were made across polished thin sections to establish variations in major element chemistry and resin content. A 50 µm beam diameter was used to ensure that each area analysed was representative of the mineralogy at that distance from the fracture.

In addition, X-ray elemental maps were produced of selected areas adjacent to the EMPA profiles to help identify what changes in mineralogy had occurred and therefore explain the variations in porosity determined. A 1 µm beam diameter was used with a 10 msec dwell time at 10 kV and 60 nA current, with a step size of 2 µm between points to create 256 x 256 pixel maps equivalent to 120 μm^2.

G.3.3 Analytical Transmission Electron Microscopy

Analytical transmission electron microscopy (ATEM) analyses were carried out at the University of Manchester, using a Philips 400T transmission electron microscope (TEM) fitted with a Philips EDAX energy-dispersive X-ray microanalysis system.

X-ray emission spectra were processed according to the thin-film method of Cliff and Lorimer (1975). The ATEM system at Manchester University has been calibrated for the analysis of phyllosilicates by determining proportionality constants relative to silicon from ultra-thin sections of standard micas.

Ultra-thin sections of the samples were prepared for TEM examination following the ion-etching technique of Phakey et al. (1972). This method of analysis does not facilitate the rapid acquisition of representative chemical data as readily as from dispersed mounts but does allow the crystallographic, ultra-micropetrographic and textural relationships of different phases to be examined (Hughes, 1989)

Limitations of ATEM

X-ray counting statistics impose a fundamental limit in ATEM. The excitation volume is very small, often <0.05 μm^3, hence sensitivity is low. The procedure used in Manchester usually gives a precision of better than 5% for major detectable elements, falling to about 11% for minor components. Data for elements present in concentrations <5% by weight are of qualitative value only and values <0.5% are considered ambiguous. Thermolabile elements, specially Na and K, are not readily quantified in ATEM unless some account is made of the mobility under the operating conditions used (a cryogenic stage offers currently the best solution to this problem; for discussion see references above). During the analysis of clay phases, especially smectites, additional problems with the quantification of Na and K occur because of the common presence of ultra-fine salts admixed with clay laths. Indeed, even in the TEM smectite laths cannot always be sufficiently isolated to negate this sort of contamination. As a consequence, concentrations of Na and K in smectites are rarely given with confidence.

G.3.4 Laser-Ablation Microprobe – Inductively Coupled Plasma – Mass Spectrometry

A small number of samples from Adit A-6 were analysed by laser-ablation microprobe – inductively coupled plasma – mass spectrometry (LAMP-ICP-MS) to determine trace element compositions of selected phases at lower levels than is possible by conventional EMPA techniques. The LAMP-ICP-MS system used was a purpose-built, Nd YAG ultra-violet laser, laser ablation microprobe system designed and built for BGS by the Department of Chemistry, Birkbeck College, University of London. The method works on the principle that the test material is placed in an ablation cell and a small amount of sample is removed by ablation with a laser. The ablated material is then introduced by an argon carrier gas stream into the ICP-MS and elemental ratios determined. LAMP-ICP-MS data are determined in terms of elemental ratios. Data, for a common major element, determined from EMPA from the same areas of the sample were used to convert these values to absolute concentrations. Alternatively, compositions were calculated assuming ideal major element compositions for known mineral phases. The method and system used is described in detail in Milodowski et al. (1998).

G.3.5 Image Analysis

Automated image analysis (IA) of ultra violet (UV) fluorescence petrography photomicrographs was used to quantify pore fabrics in samples from Maqarin. Representative UV fluorescence photomicrographs from each specimen were processed using a Kontron IBAS image analysis system using a purpose written macro built from standard image processing operations. This allowed batch processing of images with the minimum of operator intervention. Measurements made by the IBAS system were calibrated using a scanned (same scale) photomicrograph of a National Physics Laboratory-certified scale graticule.

UV images were scanned as full colour images, at a resolution of 200 dots per inch, using an Epson GT8000 flatbed scanner controlled by an IBM type personal computer (PC). Resulting images were 768 x 512 pixels, equivalent to approximately 80% of the photographed area. Images were then converted to composite red, green and blue (RGB) format using Conversion Artist 2.0 software and colour channels from the composites saved as separate TIFF5.0 image files. These were then converted to Kontron IMG format using the IMFAD software utility. Preliminary processing of the RGB composites showed porosity features identified by microscopy to be the brightest phases within the images. Inspection of the RGB colour channels in the composite images showed the red channel to accurately represent pores as the highest grey level value objects. Pores were segmented by fixed threshold grey level discrimination from the total image using the red component. The threshold value was determined by inspection of the grey level data in images obtained from several samples. Segmented areas were then converted to binary objects and measured automatically by the IBAS system. All measurements were automatically archived by the macro for further analysis. Processed images of identified porosity were superimposed on to the original RGB colour images to confirm accurate identification of the pores by the system.

G.3.6 Fission Track Registration Analysis

The uranium distribution along alteration profiles away from fractured wallrock in Adit A-6 was examined in polished thin sections by fission track registration analysis (FTR). Individual uranium-bearing phases located by FTR were identified by optical and backscattered scanning electron microscopy. The FTR technique records fission fragments derived from uranium under neutron irradiation in a reactor [(n,f) reaction]. Interference from thorium was avoided by selecting a highly thermalised neutron flux in which only ^{235}U undergoes appreciable fission. Irradiations were carried out at the Scottish Universities Research and Reactor Centre, East Kilbride.

The method employed was based on that of Kleeman and Lovering (1967). "Lexan" polycarbonate plastic was used as a detector and tracks of the induced fission fragments revealed by etching for 5–10 minutes at 60°C in 6 molar NaOH solution. The technique yields accurate spatial information on the location of uranium in the sample in the form of micromaps. Quantitative estimation of the uranium content of different host mineral phases was achieved by the irradiation of uranium-doped standard glasses along with the sample batches and consequent track counting on an equal area basis using an optical microscope. Neutron fluence was chosen to yield discrete tracks with minimum overlap to ensure reasonable counting accuracy (typically 2 x 1015 t.n.cm^{-2} is used).

G.4 Porosimetry Determination

G.4.1 Liquid Resaturation Porosimetry

Samples to be tested were oven dried at 60°C for a minimum of 24 hours before testing. The samples were weighed and then placed in a resaturation desiccator. The desiccator was evacuated for at least 24 hours before being flooded with propanol. The samples were then saturated for at least 24 hours. The saturated samples were then weighed, first below the propanol and then, still saturated with propanol, in air. The dry weight, saturated weight under propanol and its propanol saturated weight in air were recorded; in addition the density of the propanol was noted. From these values sample dry bulk density, grain density and effective porosity was calculated as follows (after API RP 40 1960):

$$\rho_b = \frac{(w\rho_f)}{(S_1 - S_2)} \ gcm^{-3} \qquad \textit{Equation 1}$$

$$\rho_g = \frac{(w\rho_f)}{(w - S_2)} \ gcm^{-3} \qquad \textit{Equation 2}$$

$$\Phi = 100 \frac{(S_1 - w)}{(w - S_2)} \ gcm^{-3} \qquad \textit{Equation 3}$$

where

w = dry sample weight (g)

S_1 = saturated sample weight in air (g)

S_2 = saturated sample weight under propanol (g)

ρ_b = dry bulk density (gcm^{-3})

ρ_g = grain density (gcm^{-3})

Φ = effective porosity (%)

ρ_f = density of propanol (gcm^{-3})

The aim of standard core laboratory liquid resaturation porosimetry was to determine a reproducible value of sample porosity under normal laboratory conditions. A suite of tests performed following the same procedures and under the same conditions with identical experimental errors will then be internally consistent. The absolute accuracy of individual observations and of the internally consistent data set is a function of experimental configuration and experimental errors. The experimental errors involved in liquid resaturation porosimetry can be evaluated from Equation 3. Measurement errors can be shown to be a function of absolute sample porosity. For example, measurement errors range from an error of ± 0.4% for samples with a porosity of approx. 24%, to an error of ± 20.5% for samples with a porosity of approx. 0.4%. However, in addition the liquid resaturation technique contains several unquantifiable errors. The non-quantifiable errors involved in liquid resaturation porosimetry arise due to uncertainties in the experimental procedure. First, samples may not be fully saturated with propanol, with consequent underestimation of pore volume. A second source of unquantifiable error is the "skin" of propanol on the outside of the sample, present while weighing the saturated sample in air. This error has the contrary effect of

overestimating sample porosity. Consequently, effective errors, as suggested by correlations with porosity measurements obtained from helium gas expansion tests, are taken to be ± 0.5 porosity percent.

G.4.2 Pore Size Distribution Measurement

Pore size distribution was determined, by mercury injection capillary pressure (MICP) measurement, for two samples of fracture wallrock associated with active hyperalkaline seepage from Adit A-6 (samples C353 and C359). For each sample, two slices were taken; one slice adjacent to the fracture (C353-0–15 mm; C359 0–10 mm) and one representing more background material (C353; 45–60 mm; C359; 48–63 mm). MICP specifically characterises the distribution of pore throat diameters within a sample by describing the relationship between an applied hydrostatic pressure and the volume of mercury intrusion into a sample. The MICP test used here follows a similar procedure to that developed by Ritter and Drake (1945).

Samples were oven dried at 60°C for a minimum of 24 hours, then placed in a penetrometer which is in turn sealed in a bell jar containing mercury. With the penetrometer stem above the mercury, the bell jar was evacuated. Once vacuum was achieved, the stem of the penetrometer was placed under the mercury. Sufficient air was slowly admitted into the bell jar to prime the penetrometer with mercury, after which the penetrometer stem was removed from the mercury. Air was then admitted into the bell jar and the pressure slowly raised to atmospheric pressure. The penetrometer was then removed from the bell jar and sealed into a high pressure cell. The cell was slowly pressurised to a maximum pressure of approximately 50 000 psi. After this, the cell was depressurised to atmospheric pressure.

During each pressurisation cycle, from vacuum to atmospheric pressure, and from atmospheric pressure to 50 000 psi, intrusion of mercury into the sample in the penetrometer may occur. Before each pressurisation cycle the sample weight was recorded. During the test, pressure increase and concomitant mercury intrusion are logged by computer. The volume of mercury intruded into the plug in the penetrometer is proportional to the change in length of the mercury column in the penetrometer stem, which is measured by a change in the capacitance of a sensing system. In addition to the automated records, atmospheric pressure was recorded and any intrusion that occurs during transfer of the penetrometer from the low pressure filling apparatus to the high pressure cell was also noted. The intrusion volume measurements are used to calculate percentage mercury intrusion. From a consideration of capillary rise (or depression) of a free liquid surface in a capillary, Ritter and Drake (1945) showed that capillary size (or pore throat size) could be related to intrusion pressure as follows:

$$d = \frac{(4\sigma\cos\theta)}{P} \qquad \textit{Equation 4}$$

where

d = diameter of capillary (m)

σ = interfacial tension between liquid and capillary wall (N/m)

θ = contact angle made by liquid

P = intrusion pressure (N/m^2)

If Equation 4 is evaluated using q = 130° and s = -68 Nm^{-1}, i.e. typical values of contact angle and interfacial tension for a wide range of rock types, then the following expression is obtained:

Pore throat diameter (μm) = 175/Intrusion pressure (psi) ***Equation 5***

Pore size distribution curves are plotted as "*log pore diameter*" versus "*percentage intrusion*". Percentage, not absolute, intrusion is used as this effectively normalises the intrusion volumes, so that samples of different absolute porosity may be compared on the same figure.

The error in pressure measurement associated with the MICP tests is ± 0.5%. Any error in the pressure measurement will cause the MICP curves to move parallel to the x-axis of an MICP plot. The error may alter the form of the curve if the error is consistent throughout the course of the test. However, a 0.5% error is negligible, causing insignificant changes to the position and form of the curve. The error in measured intruded mercury volume cannot be quantified (observed variation in apparent "intrusion volumes" during blank runs show that evaluation of errors in intruded volumes is not possible). However, an upper limit of ± 0.02 cm^3 of mercury is suggested. This error reflects the degree of agreement between MICP intrusion volumes and helium gas expansion determined porosities. The error estimate represents an approx. 50% error in measured intruded volume of a sample with a porosity of approx. 1%. Consequently, samples where the intruded volume of mercury is less than 0.02 cm^3 are considered to show no intrusion. Samples with intruded volumes of mercury between 0.02 cm^3 and 0.05 cm^3 are giving results at the limit of the MICP equipment and their pore size distribution plots should be interpreted with caution.

G.5 Chemical Analysis

Major and trace element analyses were determined by X-ray fluorescence analysis (XRF). XRF was undertaken using two sequential, fully-automated, wavelength-dispersive XRF spectrometers (Philips PW2400 and Philips PW1480/10 XRF spectrometers) fitted with a 60 kV generator and 3 kW rhodium ("Super Sharp") end-window X-ray tube, and a 100 kV generator and 3 kW tungsten side-window X-ray tube, respectively.

Major element analysis of whole-rock samples by XRF was carried out to determine SiO_2, TiO_2, Al_2O_3, Fe_2O_3, MnO, MgO, CaO, Na_2O, K_2O and P_2O_5 contents. Samples were Temamilled and finely powdered, then prepared as fused glass beads with di-lithium tetraborate flux at approximately 1200°C. Loss on ignition (LOI) was also determined by heating the samples to 1050°C, prior to glass bead preparation. Analyte angles were calibrated from international and in-house standard reference materials. All standards and unknowns were prepared as fused glass beads. Drift correction was catered for by an external ratio monitor, and background corrections applied where necessary. It should be noted that Fe_2O_3 determined represents the total Fe in the samples.

Trace elements were determined by XRF using pressed powder pellets. Pellets were prepared by grinding powdered samples with Elvacite 2013 binder (Dupont n-butyl methacrylate copolymer) in an agate planetary ball mill, followed by pressing at 25 tons load into 40 mm diameter pellets.

G.6 Strontium Isotope Analysis

A limited number of strontium isotopic rations ($^{87}Sr/^{86}Sr$) were measured on groundwaters and whole rocks from the Maqarin area with the specific aim of trying to further pin-down the origin/flow-path of the high-pH groundwaters discharging at the Western Springs. Four whole rock samples were selected to represent the principal potential groundwater source lithologies:

(i) Amman Formation (Silicified Limestone);

(ii) Chalky Limestone Formation;

(iii) Calcite-ellestadite-spurrite-browmillerite marble, taken from core sampled during Phase I (Alexander, 1992). Corresponds to the cement zone within the Bituminous Marl Formation;

(iv) Quaternary basalt.

Three groundwater samples were also analysed from Maqarin and included:

(i) bicarbonate-type groundwater from the deep Amman Formation aquifer (sampled from site M9);

(ii) water sampled from borehole WS1 (site M17) at the Western Springs, i.e. samples bicarbonate-type groundwater from the Bituminous Marl Formation (part from the Chalky Limestone Formation);

(iii) high pH groundwater from site M5, Western Springs.

G.7 Uranium Disequilibrium Studies

Uranium series disequilibrium (USD) measurements were made along alteration profiles from four samples of fractured clay biomicrite from Adit A-6 which had previously been examined by fission track registration (FTR). A detailed profile of measurements was made for two samples (C353 and C359) by preparing a series of 5–15 mm thick parallel slices of wallrock, cut parallel to the fracture surface. Measurements for the other two samples (C357 and C358) were restricted to a 10–15 mm slice taken adjacent to the fracture wall, and a slice prepared from background rock >40 mm distant from the fracture surface.

G.8 References

Clark, I.D., Fritz, P., Milodowski, A.E. and Khoury, H.N., 1992. Sampling and analytical methods. In: W.R. Alexander (Ed.), A natural analogue study of the Maqarin hyperalkaline groundwaters. I: Source term description and thermodynamic database testing. Nagra Tech. Rep. (NTB 91-10), Nagra, Wettingen, Switzerland, p. 19–40.

Cliff, G. and Lorimer, G.W., 1975. The quantitative analysis of thin specimens. J. Micro., 103, 203–207.

Hughes, C.R., 1989. The application of analytical transmission electron microscopy to the study of oolitic ironstones: a preliminary study. In: (Eds.) T.P. Young and W.E.G. Taylor, Phanerozoic Ironstones. Spec. Publ. Geol. Soc., London, 46, 121–131.

Jackson, M.L., 1969. Soil Chemical Analysis-Advanced Course: 2nd Edition., Published by the author, Madison, Wisconsin. 895 pp.

Kleeman, J.D. and Lovering, J.F., 1967. Uranium distribution in rocks by fission track registration in Lexan plastic prints. Atomic Energy of Australia, 10, 3–8.

Milodowski, A.E., Hughes, C.R., Ingelthorpe, S.D.J., MacKenzie, A.B., Pearce, J.M., Chenery, S.R.N., Strong, G.E. and Wheal, N., 1998. Mineralogical and petrological methods. In: C.M. Linklater (Ed.), A natural analogue study of cement-buffered, hyperalkaline groundwaters and their interaction with a repository host rock: Phase II. Nirex Science Report, S/98/003, Nirex, Harwell, U.K., Appendix B.

Phakey, P.P., Curtis, C.D. and Oertel, G., 1972. Transmission electron microscopy of fine-grained phyllosilicates in ultra-thin rock sections. Clays and Clay Min, 20, 193–197.

Ritter, H.L. and Drake, L.C., 1945. Pore size distribution in porous media: Pressure porosimeter and determination of complete macro-pore distributions. Ind. Eng. Chem. Anal. Ed., 17, 782–786.

TABLE

Table G-1. Summary of sample numbers, localities and method of XRD analysis.

Sample No.	Locality	Method of XRD analysis			
		Whole-rock	Acid leach Whole-rock	<2 μm oriented	Acid leach <2 μm oriented
C364	Western Springs	√	√	–	√
C365	Western Springs	√	√	–	√
C369	Western Springs	√	√	–	√
C370	Western Springs	√	√	–	√
C372	Western Springs	√	√	–	√
C390	Central Jordan S3	√	–	–	–
C391	Central Jordan S3	√	–	√	–
C392	Central Jordan S3	√	–	–	–
C393	Central Jordan S3	√	–	√	–
C394	Central Jordan S3	√	–	–	–
C711	Central Jordan S3	√	–	–	–
C395	Central Jordan S3	√	–	√	–
C396	Central Jordan S3	√	–	√	–
C378	Sweileh road cut	√		√	–
C379	Sweileh road cut	√		√	–
C380	Sweileh road cut	√		√	–
C381	Sweileh road cut	√		√	–
C382	Sweileh road cut	√		√	–
C383	Sweileh road cut	√		√	–

APPENDIX H

A: ANALYSIS OF INDIVIDUAL ROCK AND MINERAL COMPONENTS USING:

- Analytical Transmission Electron Microscopy (ATEM)
- Electron Microprobe Analysis (EMPA)
- Laser Ablation Microprobe (LAMP)

B: MOLAR PLOTS OF THE DATA

A: Analysis of Individual Rock and Mineral Components

Table H-1. Sample C362 (ATEM results).

Wt% oxide	feldspar	feldspar	feldspar	feldspar	fibres	fibres	gel	gel	gel	gel	gel	gel	gel	gel	gel	gel	gel	gel
Na_2O	7.24	4.39	6.01	6.39	0.00	2.14	5.20	5.82	7.04	6.59	6.86	7.55	3.57	2.97	3.17	0.00	2.16	0.00	2.20
MgO	1.15	1.03	1.08	1.18	5.15	5.79	1.94	2.49	1.38	1.63	1.58	4.66	1.60	1.61	0.00	2.80	9.14	1.40	1.69
Al_2O_3	18.85	19.54	24.83	25.43	16.54	16.67	12.08	11.61	11.43	12.08	11.82	10.17	12.31	12.76	12.50	8.28	8.28	14.34	13.98
SiO_2	62.70	63.69	53.52	54.08	52.29	50.56	57.84	57.13	54.25	60.21	58.49	49.60	60.65	57.85	63.92	57.34	52.79	67.17	63.09
P_2O_5	0.00	0.00	0.00	0.00	0.00	0.00	0.00	0.00	0.00	0.00	0.00	0.00	0.75	0.00	0.00	0.00	0.00	0.00	0.00
SO_3	0.00	0.00	0.00	0.00	0.00	0.00	0.00	0.00	0.00	0.00	0.00	0.00	0.00	0.00	0.00	0.00	0.00	0.00	0.00
Cl	0.00	0.00	0.00	0.00	0.00	0.00	20.5	1.83	2.88	2.89	2.56	0.00	2.00	1.57	1.70	2.25	1.34	1.02	0.64
K_2O	4.97	7.09	0.85	0.58	6.62	4.75	2.81	3.11	1.96	1.85	1.87	2.88	3.83	3.01	4.03	9.05	5.63	4.62	2.73
CaO	2.72	1.95	9.14	9.46	3.15	3.64	9.39	7.97	7.33	8.39	8.69	4.02	8.80	10.18	8.57	10.87	6.56	7.84	9.06
TiO_2	0.00	0.00	0.70	0.00	0.69	1.81	1.11	1.18	1.29	0.71	1.01	1.11	1.03	2.23	1.11	1.03	1.09	0.00	0.83
MnO	0.00	0.00	0.00	0.00	0.00	0.00	0.00	0.00	0.00	0.00	0.00	0.00	0.00	0.00	0.00	0.00	0.00	0.00	0.00
FeO	0.00	0.00	0.00	0.00	0.00	0.00	0.00	0.00	0.00	0.00	0.00	0.00	0.00	0.00	0.00	0.00	0.00	0.00	0.00
Fe_2O_3	2.37	2.31	3.86	2.88	15.56	14.63	7.57	8.86	12.44	5.64	7.12	20.01	5.46	7.82	5.00	8.39	13.01	3.60	5.78
Total	100.00	100.00	100.00	100.00	100.00	100.00	100.00	100.00	100.00	100.00	100.00	100.00	100.00	100.00	100.00	100.00	100.00	100.00	100.00
Ca^{2+}	0.93	0.76	1.64	1.69	1.51	1.79	1.70	1.69	1.54	1.52	1.60	1.92	1.46	1.63	1.13	1.96	2.67	1.07	1.35
Al^{3+}	2.13	2.17	3.28	3.33	2.24	2.33	1.48	1.44	1.49	1.42	1.43	1.45	1.44	1.56	1.38	1.02	1.11	1.51	1.57
$(SO_4)^{2-}$	0.00	0.00	0.00	0.00	0.00	0.00	0.00	0.00	0.00	0.00	0.00	0.00	0.00	0.00	0.00	0.00	0.00	0.00	0.00
Si^{4+}	6.00	6.00	6.00	6.00	6.00	6.00	6.00	6.00	6.00	6.00	6.00	6.00	6.00	6.00	6.00	6.00	6.00	6.00	6.00
Ca:Si	0.16	0.13	0.27	0.28	0.25	0.30	0.28	0.28	0.26	0.25	0.27	0.32	0.24	0.27	0.19	0.33	0.45	0.18	0.22

Table H-2. Sample C362AP1 (EMPA results).

Wt% oxide	C362AP1/ acicular phase	C362AP1/ acicular phase	C362AP1/ acicular phase	C362AP1/ acicular phase	C362AP1/ acicular phase	C362AP1/ acicular phase	C362AP1/ acicular phase	C362AP1/ acicular phase	C362AP1/ acicular phase	C362AP1/ acicular phase	C362AP1/ acicular phase	C362AP1/ acicular phase	C362AP1/ acicular phase	C362AP1/ acicular phase	C362AP1/ acicular phase	C362AP1/ acicular phase	C362AP1/ acicular phase	C362AP1/ acicular phase	C362AP1/ acicular phase	C362AP1/ acicular phase
Na_2O	0.10	0.17	0.11	0.09	0.08	0.11	0.15	0.14	0.13	0.10	0.28	0.20	0.28	0.29	0.24	0.19	0.16	0.31	0.17	0.10
SeO_2	–	–	–	–	–	–	–	0.04	–	–	–	–	–	–	–	–	–	–	–	–
MgO	0.06	0.07	0.05	0.06	0.06	0.07	0.06	0.07	0.07	0.08	0.14	0.08	0.12	0.22	0.10	0.08	0.05	0.07	0.10	0.06
Al_2O_3	8.28	7.71	7.53	8.76	8.13	7.23	8.97	8.43	7.58	8.89	8.35	10.24	13.35	7.71	7.92	8.13	5.98	6.34	6.64	6.55
SiO_2	26.10	24.87	23.63	27.75	25.32	22.75	27.62	25.97	23.01	26.73	21.63	26.25	33.12	23.85	24.97	25.14	19.75	20.63	22.71	21.89
SO_3	0.06	0.10	–	–	0.10	0.10	0.11	–	0.15	0.25	0.38	0.07	0.14	0.41	0.14	0.24	0.12	0.23	0.13	–
Cl^-	1.08	1.02	1.07	0.78	0.92	1.02	0.80	0.90	0.90	0.98	0.83	0.87	0.68	0.94	1.18	1.06	1.16	0.58	1.14	1.14
K_2O	1.07	1.22	1.10	1.10	0.92	0.97	1.11	1.17	0.97	1.01	1.11	1.21	1.62	1.24	1.15	1.20	0.86	1.21	1.40	0.87
CaO	3.67	3.39	3.44	3.88	3.74	3.25	3.76	3.87	3.28	4.01	8.08	4.70	6.31	3.70	3.44	3.69	2.56	10.35	3.30	2.74
TiO_2	–	–	–	–	–	–	–	–	–	–	–	–	0.04	0.04	–	–	0.03	–	–	–
Cr_2O_3	0.06	0.06	–	–	–	–	–	0.06	–	–	–	–	–	–	–	–	–	–	–	–
MnO	–	–	–	–	–	–	–	–	–	0.04	–	–	–	–	–	–	–	–	–	–
FeO	0.09	0.06	0.06	0.11	0.09	0.06	0.08	0.06	0.09	0.07	0.94	0.12	0.21	0.48	0.21	0.22	–	0.11	0.17	0.06
CoO	–	–	–	–	–	–	0.11	–	–	0.06	–	–	–	–	–	–	–	–	–	–
NiO	–	–	–	–	0.07	0.07	–	–	–	–	–	–	–	–	–	–	–	–	–	–
CuO	0.09	0.12	–	–	–	–	–	–	–	–	–	–	–	–	0.10	–	–	–	–	–
Total	40.66	38.79	36.99	42.53	39.43	35.62	42.77	40.71	36.16	42.21	41.75	43.74	55.86	38.86	39.44	39.94	30.65	39.83	35.76	33.39
Ca^{2+}	1.08	1.10	1.14	1.07	1.11	1.11	1.06	1.16	1.11	1.13	2.67	1.37	1.46	1.27	1.12	1.17	1.04	3.54	1.21	0.98
Al^{3+}	2.24	2.19	2.25	2.23	2.27	2.25	2.30	2.30	2.33	2.35	2.73	2.76	2.85	2.29	2.24	2.29	2.14	2.17	2.07	2.11
$(SO_4)^{2-}$	0.01	0.02	0.00	0.00	0.02	0.02	0.02	0.00	0.03	0.04	0.08	0.01	0.02	0.08	0.03	0.04	0.03	0.05	0.03	0.00
Si^{4+}	6.00	6.00	6.00	6.00	6.00	6.00	6.00	6.00	6.00	6.00	6.00	6.00	6.00	6.00	6.00	6.00	6.00	6.00	6.00	6.00
Ca:Si	0.18	0.18	0.19	0.18	0.18	0.18	0.18	0.19	0.19	0.19	0.45	0.23	0.24	0.21	0.19	0.19	0.17	0.59	0.20	0.16

Table H-3. Sample C364 (ATEM results).

Wt% oxide	cellular framework	cellular framework	cellular framework	cellular framework	cellular framework	cellular framework	cellular framework	cellular framework
Na_2O	25.46	27.43	33.57	15.56	6.82	8.92	0.00	7.85
MgO	0.00	9.26	5.43	5.64	3.16	3.74	3.28	10.99
Al_2O_3	3.41	7.91	8.04	6.10	7.85	4.15	6.66	8.62
SiO_2	6.32	26.41	22.94	19.91	22.82	46.74	29.55	23.74
P_2O_5	0.00	0.00	0.00	0.00	0.00	0.00	3.00	0.00
SO_3	0.00	0.00	0.00	4.23	0.00	0.00	3.14	0.00
Cl	0.00	0.00	2.22	0.00	0.00	0.00	0.00	0.00
K_2O	3.28	0.00	0.00	0.00	0.00	0.00	0.00	0.00
CaO	61.53	28.99	27.81	48.56	59.35	36.45	52.90	48.81
TiO_2	0.00	0.00	0.00	0.00	0.00	0.00	0.00	0.00
FeO	0.00	0.00	0.00	0.00	0.00	0.00	0.00	0.00
Fe_2O_3	0.00	0.00	0.00	0.00	0.00	0.00	1.46	0.00
CuO	0.00	0.00	0.00	0.00	0.00	0.00	0.00	0.00
Total	100.00	100.00	100.00	100.00	100.00	100.00	100.00	100.00
Ca^{2+}	75.39	13.23	14.18	20.51	18.85	6.29	12.52	18.34
Al^{3+}	3.82	2.12	2.48	2.17	2.43	0.63	1.59	2.57
$(SO_4)^{2-}$	0.00	0.00	0.00	0.96	0.00	0.00	0.48	0.00
Si^{4+}	6.00	6.00	6.00	6.00	6.00	6.00	6.00	6.00
Ca:Si	12.57	2.20	2.36	3.42	3.14	1.05	2.09	3.06

Table H-4a. Sample C365 (ATEM results).

Wt% oxide	late precipitates	late precipitates	late precipitates	late precipitates	late precipitates	late precipitates	late precipitates	late precipitates	late precipitates	late precipitates	late precipitates	late precipitates	late precipitates	late precipitates	late precipitates	late precipitates
Na_2O	0.00	0.00	0.00	0.00	0.00	0.00	0.00	0.00	0.00	0.00	0.00	0.00	0.00	0.00	0.00	0.00
MgO	0.00	0.00	0.00	0.00	0.00	0.00	0.00	0.00	0.00	0.00	0.00	0.00	0.00	0.00	4.27	0.00
Al_2O_3	9.05	0.00	0.00	9.44	8.78	8.16	8.51	8.98	9.14	9.54	9.69	9.23	10.46	10.00	13.77	10.13
SiO_2	59.53	54.68	58.20	63.00	61.68	58.07	58.96	62.58	61.81	63.07	61.71	55.70	62.96	61.42	51.05	59.02
P_2O_5	0.00	0.00	0.00	0.00	0.00	0.00	0.00	0.00	0.00	0.00	0.00	0.00	0.00	0.00	0.00	0.00
SO_3	0.00	0.00	0.00	0.00	0.00	0.00	0.00	0.00	0.00	0.00	0.00	0.00	0.00	0.00	1.56	0.00
Cl	0.00	0.00	0.00	0.00	0.00	1.66	0.97	0.00	0.00	0.00	0.00	0.00	0.00	0.00	0.00	0.00
K_2O	2.54	5.16	0.00	4.95	6.08	10.21	8.85	6.31	6.99	6.54	7.46	7.31	6.83	6.53	10.09	9.24
CaO	27.27	33.10	33.88	21.81	22.57	20.97	21.80	21.33	21.22	20.85	20.04	26.04	18.86	21.16	9.21	20.37
TiO_2	0.00	0.00	0.00	0.00	0.00	0.00	0.00	0.00	0.00	0.00	0.00	0.00	0.00	0.00	0.00	0.00
MnO	0.00	0.00	0.00	0.00	0.00	0.00	0.00	0.00	0.00	0.00	0.00	0.00	0.00	0.00	0.00	0.00
FeO	0.00	0.00	0.00	0.00	0.00	0.00	0.00	0.00	0.00	0.00	0.00	0.00	0.00	0.00	0.00	0.00
Fe_2O_3	1.62	7.06	7.93	0.79	0.89	0.91	0.92	0.81	0.84	0.00	1.09	1.72	0.90	0.88	10.07	1.24
Total	100.00	100.00	100.00	100.00	100.00	100.00	100.00	100.00	100.00	100.00	100.00	100.00	100.00	100.00	100.00	100.00
Ca^{2+}	3.03	4.08	3.75	2.38	2.54	2.66	2.67	2.39	2.43	2.33	2.32	3.26	2.14	2.42	2.29	2.52
Al^{3+}	1.08	0.00	0.00	1.06	1.01	0.99	1.02	1.02	1.05	1.07	1.11	1.17	1.18	1.15	1.91	1.21
$(SO_4)^{2-}$	0.00	0.00	0.00	0.00	0.00	0.00	0.00	0.00	0.00	0.00	0.00	0.00	0.00	0.00	0.14	0
Si^{4+}	6.00	6.00	6.00	6.00	6.00	6.00	6.00	6.00	6.00	6.00	6.00	6.00	6.00	6.00	6.00	6.00
Ca:Si	0.51	0.68	0.62	0.40	0.42	0.44	0.44	0.40	0.40	0.39	0.39	0.54	0.36	0.40	0.38	0.42

Table H-4b. Sample C365 (ATEM results).

Wt% oxide	late precipitates	late precipitates	prismatic	prismatic	prismatic	prismatic	prismatic	prismatic	fibres	fibres	fibres	fibres	fibres	fibres	plates	plates	plates	gel	gel	gel	gel	gel
Na_2O	0.00	0.00	2.97	0.00	5.88	1.70	4.35	1.77	0.00	0.00	0.00	0.00	0.00	0.00	0.00	0.00	0.00	9.11	0.00	8.78	0.00	0.00
MgO	0.00	0.00	1.36	0.00	1.43	1.45	0.00	0.00	0.00	0.00	0.00	0.00	0.00	0.00	0.00	0.00	0.00	0.00	0.00	0.00	2.15	0.00
Al_2O_3	8.55	10.97	18.95	5.59	14.86	13.96	9.58	8.98	5.78	9.82	8.78	11.40	4.37	7.75	9.38	8.91	6.11	9.94	0.00	11.31	18.70	4.32
SiO_2	52.77	65.67	43.43	22.26	43.73	52.15	50.19	52.64	24.76	39.67	43.13	44.98	19.83	25.62	30.51	55.72	28.33	37.58	34.57	42.47	49.69	22.28
P_2O_5	0.00	0.00	0.00	0.00	0.00	0.00	0.00	0.00	0.00	0.00	0.00	0.00	0.00	1.46	0.00	0.00	0.00	0.00	0.00	0.00	0.00	0.00
SO_3	1.81	0.00	1.99	3.12	1.20	0.00	0.00	0.00	4.12	2.65	3.53	2.61	2.66	2.92	3.23	0.00	9.31	2.66	0.00	0.00	0.00	0.00
Cl	0.00	0.00	0.63	1.00	0.55	0.00	0.00	0.00	0.00	0.00	0.00	0.00	0.00	1.09	0.00	0.00	0.00	0.00	0.00	0.00	0.00	0.00
K_2O	14.98	4.94	10.75	5.62	3.78	11.41	7.36	5.47	3.72	3.99	4.88	4.29	6.37	3.86	3.84	5.64	5.86	6.99	8.25	7.85	7.90	0.00
CaO	20.40	17.45	18.22	48.53	25.35	15.36	27.17	29.98	55.06	38.44	34.69	32.47	56.73	46.90	50.08	27.05	40.61	31.57	57.18	27.55	7.90	42.32
TiO_2	0.00	0.00	0.00	0.00	0.00	0.00	0.00	0.00	0.00	0.00	0.00	0.00	0.00	0.00	0.00	0.00	0.00	0.00	0.00	0.00	0.00	0.00
MnO	0.00	0.00	0.00	0.00	0.00	0.00	0.00	0.00	0.00	0.00	0.00	0.00	0.00	0.00	0.00	0.00	0.00	0.00	0.00	0.00	0.00	0.00
FeO	0.00	0.00	0.00	0.00	0.00	0.00	0.00	0.00	0.00	0.00	0.00	0.00	0.00	0.00	0.00	0.00	0.00	0.00	0.00	0.00	0.00	0.00
Fe_2O_3	1.49	0.96	1.70	13.88	3.22	3.97	1.35	1.17	6.57	5.42	4.98	4.25	10.04	10.39	2.96	2.67	9.78	2.15	0.00	2.03	13.67	31.08
Total	100.00	100.00	100.00	100.00	100.00	100.00	100.00	100.00	100.00	100.00	100.00	100.00	100.00	100.00	100.00	100.00	100.00	100.00	100.00	100.00	100.00	100.00
Ca^{2+}	3.03	1.85	3.65	14.52	4.58	2.66	4.02	3.96	14.60	6.43	5.39	4.83	19.03	12.07	10.81	3.32	9.62	6.47	11.10	5.13	1.72	12.23
Al^{3+}	1.15	1.18	3.09	1.78	2.40	1.89	1.35	1.21	1.65	1.75	1.44	1.79	1.56	2.14	2.18	1.13	1.53	1.87	0.00	1.88	2.66	1.37
$(SO_4)^{2-}$	0.15	0.00	0.21	0.63	0.12	0.00	0.00	0.00	0.75	0.30	0.37	0.26	0.60	0.51	0.48	0.00	1.48	0.32	0.00	0.00	0.00	0.00
Si^{4+}	6.00	6.00	6.00	6.00	6.00	6.00	6.00	6.00	6.00	6.00	6.00	6.00	6.00	6.00	6.00	6.00	6.00	6.00	6.00	6.00	6.00	6.00
Ca:Si	0.51	0.31	0.61	2.42	0.76	0.44	0.67	0.66	2.43	1.07	0.90	0.80	3.17	2.01	1.80	0.55	1.60	1.08	1.85	0.86	0.29	2.04

Table H-5a. Sample C365AP1 (EMPA results).

Analysis	C365AP1/ phase A	C365AP1/ phase A	C365AP1/ phase A	C365AP1/ phase A	C365AP1/ phase A	C365AP1/ phase A	C365AP1/ phase A	C365AP1/ phase A	C365AP1/ phase A	C365AP1/ phase A	C365AP1/ phase A	C365AP1/ phase A	C365AP1/ phase A	C365AP1/ phase A	C365AP1/ phase A	C365AP1/ phase A
	Low BSE fibro-radiating	Low BSE fibro-radiating	Low BSE fibro-radiating	Low BSE fibro-radiating	Low BSE fibro-radiating	Low BSE fibro-radiating	Low BSE fibro-radiating	Low BSE fibro-radiating	Low BSE fibro-radiating	Low BSE fibro-radiating	Low BSE fibro-radiating	Low BSE fibro-radiating	Low BSE fibro-radiating	Low BSE fibro-radiating	Low BSE fibro-radiating	Low BSE fibro-radiating
Na	0.26	0.31	0.28	0.15	0.28	0.23	0.34	0.29	0.31	0.33	0.30	0.31	0.30	0.20	0.28	0.35
Sc	0.03	0.00	0.00	0.02	0.04	0.00	0.00	0.00	0.02	0.00	0.00	0.00	0.00	0.00	0.00	0.00
Mg	0.04	0.06	0.01	0.02	0.01	0.01	0.04	0.02	0.01	0.03	0.01	0.02	0.03	0.04	0.01	0.01
Al	2.94	3.33	2.73	2.54	3.48	3.10	3.24	3.11	3.39	2.98	3.30	3.53	3.64	2.33	3.02	6.00
Si	7.98	8.53	7.39	11.06	12.29	8.43	10.80	9.18	10.58	13.78	17.47	8.69	10.00	6.38	14.84	16.99
S	0.24	0.26	0.14	0.08	0.04	0.10	0.23	0.18	0.12	0.14	0.06	0.16	0.14	0.22	0.09	0.02
Cl	1.10	1.14	1.31	0.75	0.68	0.98	0.97	1.02	0.93	0.69	0.57	1.09	0.94	1.12	0.65	0.63
K	1.27	1.39	1.31	1.08	1.79	1.02	1.58	1.13	1.47	1.70	1.82	1.26	1.76	1.03	1.63	2.69
Ca	2.23	2.08	1.78	9.11	8.36	2.77	4.36	2.98	3.55	7.33	9.98	2.12	3.01	1.88	7.04	2.60
Ti	0.01	0.00	0.00	0.02	0.01	0.00	0.00	0.00	0.00	0.00	0.00	0.00	0.00	0.00	0.00	0.00
Cr	0.00	0.00	0.03	0.01	0.01	0.00	0.00	0.00	0.00	0.00	0.00	0.00	0.00	0.00	0.00	0.00
Mn	0.03	0.02	0.00	0.00	0.02	0.00	0.05	0.00	0.00	0.00	0.00	0.00	0.00	0.00	0.00	0.00
Fe	0.19	0.24	0.11	0.13	0.24	0.06	0.17	0.15	0.24	0.26	0.17	0.12	0.23	0.19	0.31	0.05
Co	0.07	0.00	0.00	0.02	0.00	0.00	0.04	0.00	0.00	0.00	0.00	0.00	0.00	0.00	0.00	0.00
Ni	0.05	0.00	0.02	0.07	0.00	0.00	0.00	0.07	0.00	0.00	0.06	0.00	0.00	0.00	0.00	0.00
Cu	0.03	0.04	0.00	0.01	0.00	0.00	0.00	0.00	0.00	0.00	0.00	0.00	0.00	0.00	0.00	0.00
O	13.09	14.02	11.82	18.78	20.89	13.93	17.81	15.09	17.15	22.03	27.45	14.53	16.59	10.78	23.06	26.44
Total	29.55	31.42	29.94	43.85	48.13	30.64	39.64	33.23	37.78	49.25	61.19	31.83	36.63	24.17	50.94	55.79
Ca^{2+}	1.64	1.51	1.53	3.72	3.26	1.74	2.13	1.74	1.82	2.59	2.69	1.47	1.75	1.70	2.30	1.06
Al^{3+}	2.30	2.43	2.31	1.43	1.77	2.30	1.87	2.11	2.00	1.35	1.18	2.54	2.27	2.28	1.27	2.21
$(SO_4)^{2-}$	0.16	0.16	0.10	0.04	0.02	0.06	0.11	0.10	0.06	0.05	0.02	0.10	0.08	0.18	0.03	0.01
Si^{4+}	6.00	6.00	6.00	6.00	6.00	6.00	6.00	6.00	6.00	6.00	6.00	6.00	6.00	6.00	6.00	6.00
Ca:Si	0.27	0.25	0.26	0.62	0.54	0.29	0.35	0.29	0.30	0.43	0.45	0.24	0.29	0.28	0.38	0.18

Table H-5b. Sample C365AP1 (EMPA results).

Analysis	C365AP1/ phase A	C365AP1/ phase A	C365AP1/ phase A	C365AP1/ phase A	C365AP1/ phase A	C365AP1/ phase A	C365AP1/ phase A	C365AP1/ phase A	C365AP1/ phase A	C365AP1/ phase A	C365AP1/ phase A	C365AP1/ phase A	C365AP1/ phase A	C365AP1/ phase A	C365AP1/ phase A	C365AP1/ phase A
	Low BSE fibro-radiating	Low BSE fibro-radiating	Low BSE fibro-radiating	Low BSE fibro-radiating	Low BSE fibro-radiating	Low BSE fibro-radiating	Low BSE fibro-radiating	Low BSE fibro-radiating	Low BSE fibro-radiating	Low BSE fibro-radiating	Low BSE fibro-radiating	Low BSE fibro-radiating	Low BSE fibro-radiating	Low BSE fibro-radiating	Low BSE fibro-radiating	Low BSE fibro-radiating
Na	0.32	0.39	0.28	0.41	0.24	0.26	0.21	0.20	0.21	0.15	0.20	0.19	0.22	0.21	0.26	0.49
Se	0.00	0.00	0.00	0.04	0.00	0.00	0.00	0.00	0.00	0.00	0.04	0.00	0.00	0.00	0.00	0.00
Mg	0.00	0.01	0.00	0.00	0.02	0.01	0.01	0.00	0.01	0.00	0.01	0.00	0.02	0.01	0.00	0.00
Al	5.49	6.84	5.87	7.02	5.68	6.73	4.89	5.81	5.69	5.79	6.44	4.24	4.81	4.91	4.84	7.53
Si	16.03	18.84	16.41	19.24	13.59	15.42	11.27	12.78	12.37	14.10	15.46	12.48	10.85	11.00	13.45	20.77
S	0.03	0.04	0.05	0.07	0.06	0.07	0.05	0.07	0.04	0.09	0.08	0.04	0.07	0.04	0.06	0.05
Cl	0.82	0.59	0.71	0.49	0.79	0.77	0.99	0.94	0.96	0.60	0.58	0.91	1.04	1.08	0.88	0.45
K	2.49	2.75	2.21	3.08	2.15	2.49	1.91	1.97	2.02	1.78	2.34	1.85	1.76	1.84	2.05	3.44
Ca	2.43	2.96	2.53	3.85	3.09	3.54	2.53	2.74	2.83	5.41	3.88	3.87	2.32	2.53	2.11	3.22
Ti	0.00	0.00	0.00	0.00	0.00	0.00	0.00	0.00	0.00	0.00	0.02	0.00	0.00	0.00	0.00	0.00
Cr	0.00	0.00	0.00	0.00	0.00	0.00	0.05	0.00	0.04	0.00	0.00	0.00	0.00	0.00	0.00	0.00
Mn	0.00	0.00	0.00	0.00	0.04	0.00	0.00	0.00	0.00	0.00	0.00	0.00	0.04	0.00	0.00	0.00
Fe	0.00	0.05	0.05	0.11	0.59	0.62	0.20	0.08	0.10	0.74	1.97	0.49	0.08	0.05	0.00	0.10
Co	0.00	0.00	0.00	0.00	0.00	0.00	0.00	0.00	0.00	0.00	0.00	0.00	0.06	0.00	0.06	0.00
Ni	0.00	0.00	0.00	0.00	0.00	0.05	0.00	0.00	0.00	0.00	0.00	0.00	0.00	0.00	0.05	0.00
Cu	0.00	0.00	0.00	0.00	0.00	0.00	0.00	0.00	0.00	0.00	0.00	0.00	0.00	0.00	0.00	0.00
O	24.77	29.52	25.55	30.62	22.57	25.87	18.82	21.42	20.88	24.13	26.15	20.18	18.16	18.42	21.10	32.62
Total	52.37	62.00	53.65	64.94	48.82	55.84	40.91	46.03	45.16	52.80	57.17	44.25	39.42	40.07	44.88	68.69
Ca^{2-}	1.05	1.05	1.00	1.26	1.36	1.37	1.37	1.29	1.38	1.93	1.43	1.68	1.32	1.40	1.06	1.10
Al^{3+}	2.14	2.27	2.23	2.28	2.61	2.73	2.71	2.84	2.87	2.56	2.60	2.12	2.77	2.79	2.25	2.26
$(SO_4)^{2-}$	0.01	0.01	0.02	0.02	0.02	0.02	0.02	0.03	0.02	0.03	0.03	0.02	0.03	0.02	0.03	0.01
Si^{4+}	6.00	6.00	6.00	6.00	6.00	6.00	6.00	6.00	6.00	6.00	6.00	6.00	6.00	6.00	6.00	6.00
Ca:Si	0.17	0.18	0.17	0.21	0.23	0.23	0.23	0.22	0.23	0.32	0.24	0.28	0.22	0.23	0.18	0.18

Table H-5c. Sample C365AP1 (EMPA results).

Analysis	C365AP1/ phase A	C365AP1/ phase B	C365AP1/ phase B	C365AP1/ phase B	C365AP1/ phase B	C365AP1/ phase B	C365AP1/ phase B	C365AP1/ phase B	C365AP1/ phase B	C365AP1/ phase B	C365AP1/ phase B	C365AP1/ phase B	C365AP1/ phase B	C365AP1/ phase B	C365AP1/ phase B	C365AP1/ phase B
	Low BSE fibro-radiating	mod BSE colloform band	mod BSE colloform band	mod BSE colloform band	mod BSE colloform band	mod BSE colloform band	mod BSE colloform band	mod BSE colloform band	mod BSE colloform band	mod BSE colloform band	mod BSE colloform band	mod BSE colloform band	mod BSE colloform band	mod BSE colloform band	mod BSE colloform band	mod BSE colloform band
Na	0.36	0.22	0.32	0.24	0.22	0.26	0.22	0.26	0.24	0.24	0.25	0.25	0.26	0.29	0.25	0.25
Se	0.00	0.03	0.00	0.01	0.02	0.00	0.00	0.00	0.00	0.04	0.00	0.04	0.00	0.00	0.00	0.00
Mg	0.00	0.00	0.00	0.00	0.00	0.00	0.00	0.00	0.01	0.00	0.00	0.00	0.01	0.00	0.00	0.00
Al	5.34	2.25	2.60	2.66	2.27	2.50	2.56	2.58	2.39	2.44	2.55	2.69	2.30	2.54	2.47	2.64
Si	15.38	16.45	19.06	17.99	16.35	17.64	19.08	19.16	18.10	18.21	19.00	20.16	17.55	18.77	18.56	19.42
S	0.00	0.05	0.00	0.03	0.01	0.03	0.02	0.03	0.00	0.02	0.04	0.04	0.00	0.04	0.03	0.04
Cl	0.77	0.50	0.43	0.50	0.42	0.50	0.48	0.48	0.50	0.56	0.52	0.37	0.46	0.52	0.49	0.48
K	2.70	1.46	1.88	1.48	1.62	1.66	1.65	1.63	1.62	1.48	1.61	1.84	1.76	1.86	1.63	1.57
Ca	2.42	11.21	12.33	12.35	11.52	11.29	11.43	11.43	11.24	11.22	11.83	12.21	11.43	11.39	12.02	12.18
Ti	0.00	0.00	0.00	0.00	0.01	0.01	0.00	0.00	0.02	0.00	0.00	0.00	0.00	0.00	0.00	0.00
Cr	0.00	0.01	0.00	0.01	0.00	0.02	0.00	0.00	0.00	0.00	0.00	0.00	0.00	0.00	0.00	0.00
Mn	0.00	0.01	0.00	0.02	0.00	0.02	0.00	0.00	0.04	0.00	0.00	0.00	0.00	0.00	0.00	0.00
Fe	0.07	0.03	0.04	0.05	0.13	0.06	0.09	0.00	0.00	0.07	0.08	0.12	0.11	0.07	0.05	0.05
Co	0.00	0.00	0.01	0.02	0.01	0.01	0.00	0.00	0.00	0.00	0.05	0.00	0.05	0.00	0.00	0.00
Ni	0.00	0.00	0.00	0.01	0.04	0.00	0.00	0.00	0.00	0.00	0.00	0.00	0.05	0.00	0.00	0.00
Cu	0.00	0.01	0.00	0.08	0.00	0.01	0.00	0.00	0.00	0.00	0.00	0.00	0.00	0.00	0.00	0.08
O	23.93	25.56	29.36	28.15	25.64	27.22	29.03	29.15	27.68	27.84	29.14	30.80	27.11	28.76	28.60	29.84
Total	50.97	57.79	66.02	63.60	58.27	61.23	64.56	64.72	61.84	62.11	65.08	68.53	61.10	64.25	64.09	66.56
Ca^{2+}	1.12	3.11	2.99	3.11	3.23	2.95	2.75	2.74	2.85	2.81	2.85	2.79	3.01	2.82	2.96	2.86
Al^{3+}	2.17	0.85	0.85	0.92	0.87	0.88	0.84	0.84	0.82	0.84	0.84	0.83	0.82	0.85	0.83	0.85
$(SO_4)^{2-}$	0.00	0.02	0.00	0.01	0.00	0.01	0.01	0.01	0.00	0.01	0.01	0.01	0.00	0.01	0.01	0.01
Si^{4+}	6.00	6.00	6.00	6.00	6.00	6.00	6.00	6.00	6.00	6.00	6.00	6.00	6.00	6.00	6.00	6.00
Ca:Si	0.19	0.52	0.50	0.52	0.54	0.49	0.46	0.46	0.48	0.47	0.47	0.46	0.50	0.47	0.49	0.48

Table H-5d. Sample C365AP1 (EMPA results).

Analysis	C365AP1/ phase B	C365AP1/ phase B	C365AP1/ phase B	C365AP1/ phase B	C365AP1/ phase B	C365AP1/ phase B	C365AP1/ phase B	C365AP1/ phase B	C365AP1/ phase B	C365AP1/ phase B	C365AP1/ phase B	C365AP1/ phase B	C365AP1/ phase B	C365AP1/ phase B	C365AP1/ phase B	C365AP1/ phase B
	mod BSE colloform band	mod BSE colloform band	mod BSE colloform band	mod BSE colloform band	mod BSE colloform band	mod BSE colloform band	mod BSE colloform band	mod BSE colloform band	mod BSE colloform band	mod BSE colloform band	mod BSE colloform band	mod BSE colloform band	mod BSE colloform band	mod BSE colloform band	mod BSE colloform band	mod BSE colloform band
Na	0.18	0.17	0.19	0.16	0.17	0.20	0.20	0.15	0.16	0.18	0.27	0.28	0.26	0.26	0.19	0.22
Se	0.00	0.00	0.00	0.00	0.00	0.02	0.00	0.00	0.00	0.00	0.04	0.00	0.00	0.00	0.00	0.04
Mg	0.02	0.00	0.00	0.00	0.00	0.00	0.00	0.00	0.00	0.00	0.00	0.00	0.00	0.01	0.00	0.00
Al	2.29	2.27	2.12	2.16	2.17	2.11	2.03	2.06	1.98	1.97	2.79	2.79	2.83	2.92	2.80	2.75
Si	16.37	16.10	15.20	14.81	15.34	14.99	14.47	14.80	13.84	12.76	19.27	19.28	19.18	19.99	19.49	19.44
S	0.04	0.04	0.04	0.03	0.06	0.03	0.06	0.05	0.04	0.05	0.00	0.02	0.03	0.03	0.02	0.00
Cl	0.62	0.68	0.66	0.73	0.69	0.74	0.73	0.72	0.78	0.92	0.36	0.39	0.43	0.31	0.37	0.41
K	1.50	1.29	1.17	1.28	1.16	1.22	1.25	1.27	1.16	1.35	2.68	2.94	2.39	2.19	1.84	1.91
Ca	10.23	10.24	9.75	9.55	9.99	9.67	9.40	10.02	9.00	7.33	13.63	13.50	13.55	14.28	14.03	13.95
Ti	0.00	0.00	0.01	0.00	0.00	0.00	0.00	0.00	0.00	0.00	0.00	0.02	0.00	0.00	0.00	0.00
Cr	0.00	0.00	0.00	0.00	0.00	0.00	0.00	0.00	0.00	0.00	0.04	0.00	0.04	0.00	0.00	0.00
Mn	0.00	0.00	0.00	0.00	0.00	0.05	0.00	0.00	0.00	0.00	0.00	0.06	0.00	0.00	0.00	0.00
Fe	0.00	0.00	0.00	0.00	0.05	0.06	0.05	0.05	0.00	0.00	0.06	0.07	0.00	0.00	0.06	0.05
Co	0.00	0.00	0.00	0.00	0.00	0.00	0.00	0.00	0.00	0.00	0.00	0.00	0.00	0.00	0.00	0.00
Ni	0.00	0.00	0.00	0.00	0.00	0.00	0.00	0.00	0.00	0.00	0.00	0.00	0.00	0.00	0.00	0.00
Cu	0.00	0.00	0.00	0.00	0.00	0.00	0.00	0.00	0.08	0.00	0.00	0.00	0.00	0.00	0.00	0.00
O	25.20	24.84	23.47	22.97	23.78	23.21	22.48	23.09	21.48	19.61	30.56	30.61	30.42	31.66	30.79	30.66
Total	56.45	55.64	52.63	51.69	53.40	52.30	50.68	52.21	48.51	44.15	69.72	69.97	69.14	71.65	69.60	69.44
Ca^{2+}	2.87	2.88	2.91	2.94	2.94	2.93	2.97	3.07	2.96	2.69	3.33	3.32	3.29	3.29	3.27	3.27
Al^{3+}	0.87	0.88	0.87	0.91	0.88	0.88	0.88	0.87	0.89	0.96	0.90	0.90	0.92	0.91	0.90	0.88
$(SO_4)^{2-}$	0.01	0.01	0.01	0.01	0.02	0.01	0.02	0.02	0.01	0.02	0.00	0.01	0.01	0.01	0.01	0.00
Si^{4+}	6.00	6.00	6.00	6.00	6.00	6.00	6.00	6.00	6.00	6.00	6.00	6.00	6.00	6.00	6.00	6.00
Ca:Si	0.48	0.48	0.48	0.49	0.49	0.49	0.49	0.51	0.49	0.45	0.55	0.55	0.55	0.55	0.54	0.54

Table H-5e. Sample C365AP1 (EMPA results).

Analysis	C365AP1/ phase B	C365AP1/ phase B	C365AP1/ phase B	C365AP1/ phase B	C365AP1/ phase B	C365AP1/ phase C	C365AP1/ phase C	C365AP1/ phase C	C365AP1/ phase C	C365AP1/ phase C	C365AP1/ phase C	C365AP1/ phase C	C365AP1/ phase C	C365AP1/ phase C	C365AP1/ phase C	C365AP1/ phase C
	mod BSE colloform band	mod BSE colloform band	mod BSE colloform band	mod BSE colloform band	mod BSE colloform band	low BSE colloform band	low BSE colloform band	low BSE colloform band	low BSE colloform band	low BSE colloform band	low BSE colloform band	low BSE colloform band	low BSE colloform band	low BSE colloform band	low BSE colloform band	low BSE colloform band
Na	0.18	0.18	0.16	0.16	0.16	0.34	0.35	0.15	0.14	0.22	0.40	0.46	0.34	0.35	0.32	0.45
Se	0.00	0.00	0.00	0.00	0.00	0.01	0.01	0.02	0.00	0.00	0.00	0.00	0.03	0.00	0.00	0.00
Mg	0.00	0.00	0.00	0.00	0.00	0.00	0.00	0.00	0.00	0.00	0.00	0.02	0.00	0.00	0.00	0.02
Al	2.64	2.66	2.44	2.37	2.16	3.33	3.32	2.90	3.46	3.23	2.92	3.51	3.14	3.33	3.59	3.62
Si	18.78	18.99	17.40	16.78	15.75	19.38	22.70	18.37	23.11	20.21	18.73	23.83	21.10	22.80	24.66	23.23
S	0.00	0.00	0.02	0.00	0.00	0.09	0.07	0.11	0.02	0.03	0.05	0.10	0.02	0.06	0.06	0.04
Cl	0.45	0.41	0.56	0.52	0.58	0.11	0.07	0.08	0.03	0.04	0.29	0.13	0.03	0.04	0.03	0.16
K	1.62	1.66	1.41	1.46	1.20	1.75	2.01	1.16	1.16	1.73	2.52	2.64	2.24	2.41	2.43	2.71
Ca	13.67	13.62	12.68	12.65	12.18	23.56	22.47	24.96	24.37	23.41	8.86	13.24	20.07	22.44	19.53	11.48
Ti	0.00	0.00	0.00	0.00	0.00	0.00	0.00	0.02	0.00	0.02	0.00	0.00	0.00	0.00	0.02	0.00
Cr	0.00	0.00	0.04	0.00	0.00	0.00	0.00	0.02	0.05	0.03	0.00	0.00	0.00	0.00	0.00	0.00
Mn	0.00	0.00	0.00	0.00	0.00	0.02	0.00	0.00	0.01	0.03	0.00	0.00	0.00	0.00	0.00	0.00
Fe	0.06	0.00	0.00	0.06	0.08	0.07	0.04	0.06	0.10	0.02	0.04	0.00	0.00	0.07	0.05	0.07
Co	0.00	0.00	0.00	0.00	0.00	0.00	0.02	0.01	0.00	0.04	0.00	0.00	0.00	0.00	0.06	0.00
Ni	0.00	0.00	0.08	0.00	0.00	0.00	0.02	0.11	0.01	0.00	0.00	0.00	0.00	0.00	0.00	0.00
Cu	0.00	0.00	0.00	0.00	0.00	0.01	0.02	0.04	0.01	0.00	0.00	0.00	0.00	0.00	0.00	0.09
O	29.61	29.84	27.46	26.65	25.04	35.02	38.40	33.94	39.49	35.75	28.21	36.40	35.46	38.60	39.81	35.09
Total	67.03	67.37	62.25	60.66	57.15	83.69	89.49	81.94	91.96	84.76	62.03	80.33	82.42	90.09	90.56	76.95
Ca^{2+}	3.28	3.24	3.27	3.39	3.45	5.37	4.41	5.88	4.56	5.09	2.36	2.65	4.29	4.42	3.59	2.40
Al^{3+}	0.88	0.88	0.88	0.88	0.86	1.07	0.91	0.99	0.94	1.00	0.97	0.92	0.93	0.91	0.91	0.97
$(SO_4)^{2-}$	0.00	0.00	0.01	0.00	0.00	0.02	0.02	0.03	0.00	0.01	0.02	0.02	0.01	0.01	0.01	0.01
Si^{4+}	6.00	6.00	6.00	6.00	6.00	6.00	6.00	6.00	6.00	6.00	6.00	6.00	6.00	6.00	6.00	6.00
Ca:Si	0.55	0.54	0.55	0.57	0.58	0.89	0.73	0.98	0.76	0.85	0.39	0.44	0.71	0.74	0.60	0.40

Table H-5f. Sample C365AP1 (EMPA results).

Analysis	C365AP1/ phase C	C365AP1/ phase C	C365AP1/ phase C	C365AP1/ phase C	C365AP1/ phase C	C365AP1/ phase C	C365AP1/ phase C	C365AP1/ phase C	C365AP1/ phase C	C365AP1/ phase C	C365AP1/ phase C	C365AP1/ phase C	C365AP1/ phase C	C365AP1/ phase C	C365AP1/ phase C	C365AP1/ phase C
	low BSE colloform band	low BSE colloform band	low BSE colloform band	low BSE colloform band	low BSE colloform band	low BSE colloform band	low BSE colloform band	low BSE colloform band	low BSE colloform band	low BSE colloform band	low BSE colloform band	low BSE colloform band	low BSE colloform band	low BSE colloform band	low BSE colloform band	low BSE colloform band
Na	0.42	0.26	0.21	0.29	0.12	0.18	0.10	0.22	0.16	0.22	0.18	0.17	0.19	0.14	0.16	0.18
Se	0.00	0.00	0.03	0.00	0.00	0.00	0.00	0.00	0.00	0.00	0.00	0.00	0.00	0.00	0.00	0.06
Mg	0.00	0.00	0.00	0.00	0.00	0.00	0.00	0.02	0.00	0.00	0.00	0.00	0.01	0.00	0.00	0.00
Al	3.75	3.30	3.25	3.44	3.15	3.34	3.49	3.71	3.44	3.15	3.29	3.42	3.69	3.80	3.91	3.74
Si	25.90	22.38	22.62	24.05	20.60	22.21	22.44	23.09	22.11	18.84	21.55	22.36	23.70	24.53	25.05	24.25
S	0.05	0.03	0.04	0.04	0.03	0.03	0.07	0.00	0.03	0.07	0.04	0.04	0.05	0.03	0.00	0.00
Cl	0.03	0.00	0.03	0.03	0.05	0.07	0.03	0.07	0.05	0.15	0.06	0.02	0.06	0.00	0.00	0.01
K	2.61	2.02	2.02	2.30	1.53	1.59	1.17	1.60	1.51	1.74	1.73	1.72	1.59	1.69	1.87	2.19
Ca	16.50	22.03	22.12	20.42	22.47	20.47	24.50	23.05	25.64	19.42	24.34	22.36	23.38	22.28	21.11	20.74
Ti	0.00	0.00	0.00	0.02	0.01	0.00	0.00	0.00	0.00	0.00	0.02	0.00	0.00	0.00	0.00	0.00
Cr	0.00	0.00	0.04	0.00	0.00	0.00	0.00	0.00	0.00	0.00	0.00	0.00	0.00	0.00	0.00	0.00
Mn	0.00	0.04	0.00	0.00	0.00	0.00	0.06	0.00	0.00	0.06	0.00	0.00	0.05	0.00	0.00	0.00
Fe	0.00	0.00	0.00	0.00	0.00	0.08	0.06	0.07	0.23	0.11	0.00	0.08	0.08	0.07	0.00	0.00
Co	0.00	0.00	0.00	0.00	0.00	0.00	0.00	0.00	0.00	0.00	0.00	0.00	0.00	0.00	0.00	0.00
Ni	0.00	0.00	0.07	0.00	0.09	0.00	0.00	0.00	0.00	0.00	0.00	0.00	0.00	0.07	0.00	0.00
Cu	0.00	0.00	0.09	0.00	0.00	0.00	0.00	0.10	0.00	0.00	0.00	0.00	0.00	0.00	0.00	0.00
O	40.19	37.78	38.10	39.22	35.67	36.89	38.85	39.26	38.96	32.58	37.67	37.92	40.11	40.68	40.87	39.76
Total	89.46	87.85	88.62	89.79	83.72	84.86	90.78	91.19	92.14	76.33	88.87	88.09	92.90	93.29	92.98	90.94
Ca^{2+}	2.96	4.38	4.34	3.82	4.77	4.06	4.72	4.38	5.05	4.57	4.95	4.40	4.32	3.99	3.73	3.82
Al^{3+}	0.90	0.92	0.90	0.89	0.96	0.94	0.97	1.00	0.97	1.05	0.95	0.95	0.97	0.97	0.98	0.96
$(SO_4)^{2-}$	0.01	0.01	0.01	0.01	0.01	0.01	0.02	0.00	0.01	0.02	0.01	0.01	0.01	0.01	0.00	0.00
Si^{4+}	6.00	6.00	6.00	6.00	6.00	6.00	6.00	6.00	6.00	6.00	6.00	6.00	6.00	6.00	6.00	6.00
Ca:Si	0.49	0.73	0.72	0.64	0.79	0.68	0.79	0.73	0.84	0.76	0.83	0.73	0.72	0.66	0.62	0.64

Table H-5g. Sample C365AP1 (EMPA results).

Analysis	C365AP1/ phase C	C365AP1/ phase C	C365AP1/ phase C	C365AP1/ phase C	C365AP1/ phase C	C365AP1/ phase C	C365AP1/ phase C	C365AP1/ phase E	C365AP1/ phase E	C365AP1/ phase E	C365AP1/ phase E	C365AP1/ phase E	C365AP1/ phase E	C365AP1/ phase E	C365AP1/ phase E	C365AP1/ phase E
	low BSE colloform band	low BSE colloform band	low BSE colloform band	low BSE colloform band	low BSE colloform band	low BSE colloform band	low BSE colloform band	high BSE acicular	high BSE acicular	high BSE acicular	high BSE acicular	high BSE acicular	high BSE acicular	high BSE acicular	high BSE acicular	high BSE acicular
Na	0.25	0.15	0.16	0.13	0.16	0.20	0.17	0.26	0.27	0.21	0.18	0.37	0.26	0.31	0.20	0.23
Se	0.04	0.00	0.00	0.00	0.04	0.00	0.00	0.00	0.06	0.00	0.00	0.00	0.00	0.04	0.00	0.00
Mg	0.03	0.00	0.00	0.00	0.00	0.00	0.00	0.02	0.01	0.01	0.00	0.02	0.00	0.00	0.00	0.02
Al	3.92	3.45	3.43	3.61	3.60	3.77	3.68	3.04	2.85	2.12	2.19	3.77	2.75	2.86	2.33	2.37
Si	25.33	23.07	22.24	22.61	22.51	23.46	23.25	17.39	16.09	13.38	13.49	21.87	15.73	16.18	13.87	14.30
S	0.03	0.03	0.00	0.03	0.00	0.02	0.00	0.06	0.03	0.06	0.03	0.10	0.00	0.05	0.06	0.06
Cl	0.00	0.03	0.06	0.04	0.04	0.03	0.02	0.64	0.69	0.83	0.46	0.34	0.73	0.72	0.64	0.80
K	2.41	1.64	1.74	1.43	1.86	2.20	1.90	2.24	2.16	1.57	2.09	2.65	1.89	2.07	1.77	1.77
Ca	19.42	25.02	26.10	25.71	25.13	22.31	22.64	7.00	6.48	7.23	7.43	8.89	6.46	6.41	7.67	6.88
Ti	0.02	0.00	0.00	0.00	0.00	0.00	0.02	0.00	0.00	0.00	0.00	0.00	0.00	0.00	0.00	0.00
Cr	0.00	0.00	0.00	0.00	0.00	0.00	0.00	0.00	0.00	0.04	0.04	0.00	0.00	0.03	0.00	0.00
Mn	0.00	0.04	0.00	0.00	0.00	0.00	0.00	0.00	0.00	0.00	0.00	0.00	0.00	0.00	0.00	0.00
Fe	0.13	0.08	0.00	0.00	0.00	0.00	0.00	0.00	0.00	0.06	0.05	0.07	0.05	0.05	0.08	0.00
Co	0.00	0.00	0.00	0.00	0.00	0.00	0.00	0.00	0.00	0.00	0.00	0.00	0.00	0.00	0.00	0.06
Ni	0.00	0.00	0.00	0.00	0.00	0.00	0.00	0.00	0.00	0.00	0.00	0.00	0.00	0.00	0.05	0.00
Cu	0.00	0.00	0.00	0.00	0.00	0.10	0.00	0.07	0.00	0.00	0.08	0.00	0.00	0.00	0.00	0.00
O	40.79	39.79	39.20	39.60	39.31	39.55	39.24	25.98	24.06	20.54	20.87	32.66	23.44	24.18	21.48	21.70
Total	92.36	93.30	92.93	93.16	92.64	91.64	90.91	56.70	52.71	46.05	46.92	70.73	51.31	52.92	48.14	48.17
Ca^{2+}	3.46	4.74	5.13	4.94	4.90	4.23	4.30	2.02	2.05	2.58	2.70	2.03	2.05	2.01	2.65	2.35
Al^{3+}	0.97	0.93	0.96	1.00	1.00	1.00	0.99	1.09	1.11	0.99	1.01	1.08	1.09	1.11	1.05	1.03
$(SO_4)^{2-}$	0.01	0.01	0.00	0.01	0.00	0.01	0.00	0.02	0.01	0.02	0.01	0.02	0.00	0.01	0.02	0.02
Si^{4+}	6.00	6.00	6.00	6.00	6.00	6.00	6.00	6.00	6.00	6.00	6.00	6.00	6.00	6.00	6.00	6.00
Ca:Si	0.58	0.79	0.86	0.82	0.82	0.71	0.72	0.34	0.34	0.43	0.45	0.34	0.34	0.34	0.44	0.39

Table H-5h. Sample C365AP1 (EMPA results).

Analysis	C365AP1/ phase E	C365AP1/ phase E	C365AP1/ phase E	C365AP1/ phase E	C365AP1/ phase E	C365AP1/ phase E	C365AP1/ phase E	C365AP1/ phase E	C365AP1/ phase E	C365AP1/ phase E
	high BSE acicular	high BSE acicular	high BSE acicular	high BSE acicular	high BSE acicular	high BSE acicular	high BSE acicular	high BSE acicular	high BSE acicular	high BSE acicular
Na	0.16	0.18	0.16	0.20	0.18	0.25	0.19	0.20	0.20	0.17
Se	0.00	0.00	0.00	0.02	0.04	0.00	0.00	0.00	0.00	0.00
Mg	0.00	0.00	0.01	0.00	0.01	0.00	0.00	0.01	0.00	0.00
Al	1.95	2.03	1.97	2.08	2.27	2.17	2.12	2.14	2.18	2.10
Si	12.62	12.94	12.14	12.84	14.58	13.57	13.14	13.89	13.74	13.19
S	0.05	0.05	0.04	0.02	0.03	0.08	0.00	0.06	0.04	0.08
Cl	0.87	0.87	0.93	0.92	0.75	0.86	0.82	0.94	0.83	0.94
K	1.42	1.43	1.21	1.50	1.55	1.57	1.67	1.54	1.55	1.52
Ca	7.29	6.81	6.61	6.34	8.25	6.43	6.62	6.99	6.90	6.53
Ti	0.00	0.00	0.00	0.00	0.00	0.00	0.01	0.00	0.00	0.00
Cr	0.00	0.00	0.00	0.00	0.04	0.00	0.00	0.00	0.00	0.00
Mn	0.00	0.00	0.00	0.00	0.00	0.04	0.00	0.00	0.00	0.00
Fe	0.00	0.05	0.00	0.00	0.00	0.00	0.05	0.10	0.04	0.05
Co	0.07	0.00	0.00	0.00	0.04	0.00	0.00	0.00	0.00	0.00
Ni	0.00	0.00	0.00	0.00	0.00	0.00	0.00	0.00	0.06	0.00
Cu	0.00	0.00	0.00	0.00	0.00	0.00	0.00	0.00	0.00	0.00
O	19.46	19.71	18.58	19.41	22.41	20.50	19.92	21.02	20.81	20.00
Total	43.90	44.05	41.64	43.32	50.17	45.48	44.53	46.89	46.35	44.58
Ca^{2+}	2.72	2.50	2.55	2.38	2.66	2.31	2.44	2.41	2.41	2.38
Al^{3+}	0.97	0.98	1.01	1.01	0.97	1.00	1.01	0.96	0.99	0.99
$(SO_4)^{2-}$	0.02	0.02	0.02	0.00	0.01	0.03	0.00	0.02	0.02	0.03
Si^{4+}	6.00	6.00	6.00	6.00	6.00	6.00	6.00	6.00	6.00	6.00
Ca:Si	0.45	0.42	0.43	0.40	0.44	0.39	0.41	0.40	0.40	0.40

Table H-6a. Sample C368 (ATEM results).

Wt% oxide	ettring-ite	ettring-ite	ettring-ite	ettring-ite	ettring-ite	ettring-ite	ettring-ite	ettring-ite	ettring-ite	ettring-ite	ettring-ite	ettring-ite	ettring-ite	ettring-ite	ettring-ite	ettring-ite	gel	gel
Na_2O	0.00	0.00	0.00	0.00	0.00	0.00	0.00	0.00	0.00	0.00	0.00	0.00	0.00	0.00	0.00	0.00	0.00	0.00
MgO	0.00	0.00	0.00	0.00	0.00	0.00	0.00	0.00	0.00	0.00	0.00	0.00	0.00	0.00	0.00	0.00	4.39	3.75
Al_2O_3	12.90	14.50	12.76	12.30	11.43	4.92	10.41	9.87	13.13	11.50	0.00	10.57	11.95	15.04	14.90	14.58	13.40	11.58
SiO_2	0.00	0.00	4.88	0.00	6.69	11.70	8.85	9.48	5.61	8.58	18.94	10.00	4.71	4.44	3.33	5.25	46.13	45.73
P_2O_5	0.00	0.00	0.00	0.00	0.00	0.00	0.00	0.00	0.00	0.00	0.00	0.00	0.00	0.00	0.00	0.00	0.00	0.00
SO_3	33.20	32.61	28.27	32.36	29.68	34.69	26.65	25.79	26.52	21.55	24.27	19.20	23.70	28.33	29.60	26.95	0.00	0.00
Cl	9.43	0.00	0.00	9.72	4.45	16.90	0.00	0.00	0.00	0.00	0.00	12.58	0.00	0.00	0.00	0.00	0.00	0.00
K_2O	0.00	0.00	0.00	0.00	0.00	0.00	0.00	0.00	0.00	0.00	0.00	0.00	0.00	0.00	0.00	0.00	4.39	3.51
CaO	44.47	52.89	54.09	45.63	47.75	31.79	54.10	54.86	54.75	58.36	56.79	47.65	58.53	52.18	51.33	52.47	20.10	26.20
TiO_2	0.00	0.00	0.00	0.00	0.00	0.00	0.00	0.00	0.00	0.00	0.00	0.00	0.00	0.00	0.00	0.00	0.00	0.00
MnO	0.00	0.00	0.00	0.00	0.00	0.00	0.00	0.00	0.00	0.00	0.00	0.00	0.00	0.00	0.00	0.00	0.00	0.00
FeO	0.00	0.00	0.00	0.00	0.00	0.00	0.00	0.00	0.00	0.00	0.00	0.00	0.00	0.00	0.00	0.00	0.00	0.00
Fe_2O_3	0.00	0.00	0.00	0.00	0.00	0.00	0.00	0.00	0.00	0.00	0.00	0.00	1.11	0.00	0.85	0.76	11.59	9.23
Total	100.00	100.00	100.00	100.00	100.00	100.00	100.00	100.00	100.00	100.00	100.00	100.00	100.00	100.00	100.00	100.00	100.00	100.00
Ca^{2+}	6.00	6.00	6.00	6.00	6.00	6.00	6.00	6.00	6.00	6.00	6.00	6.00	6.00	6.00	6.00	6.00	3.84	4.57
Al^{3+}	1.91	1.81	1.56	1.78	1.58	1.02	1.27	1.19	1.58	1.30	0.00	1.46	1.35	1.90	1.91	1.83	2.06	1.79
$(SO_4)^{2-}$	3.13	2.59	2.19	2.98	2.61	4.58	2.07	1.97	2.03	1.55	1.79	1.69	1.70	2.28	2.42	2.16	0.00	0.00
Si^{4+}	0.00	0.00	0.50	0.00	0.78	2.06	0.91	0.97	0.57	0.82	1.87	1.17	0.45	0.48	0.36	0.56	6.00	6.00
Ca:Si	–	–	–	–	–	–	–	–	–	–	–	–	–	–	–	–	0.64	0.76

Table H-6b. Sample C368 (ATEM results).

Wt% oxide	gel	gel	gel	gel	gel	gel	gel	gel	gel	gel	gel	gel	gel	gel	gel	gel	gel	gel	gel	gel	gel
Na_2O	0.00	0.00	0.00	0.00	0.00	0.00	0.00	0.00	0.00	0.00	0.00	0.00	0.00	0.00	0.00	0.00	0.00	0.00	0.00	0.00	0.00
MgO	3.87	2.50	2.79	3.89	3.49	3.07	2.67	0.00	0.00	0.00	12.55	0.00	10.06	6.72	11.60	5.08	0.00	5.31	3.57	0.00	0.00	0.00
Al_2O_3	12.69	9.85	10.61	11.74	12.05	12.23	16.83	17.05	11.25	6.19	10.25	5.78	10.06	9.12	11.00	12.60	6.04	13.25	12.26	6.96	6.48	6.25
SiO_2	46.23	44.82	46.18	47.00	46.95	49.15	42.72	44.03	45.40	44.47	42.63	43.18	39.94	42.01	39.13	44.44	47.41	45.07	40.72	44.40	44.08	43.08
P_2O_5	0.00	0.00	0.00	0.00	0.00	0.00	0.00	0.00	0.00	0.00	0.00	0.00	0.00	0.00	0.00	0.00	0.00	0.00	0.00	0.00	0.00	0.00
SO_3	0.00	0.00	0.00	0.00	0.00	0.00	0.00	0.00	0.00	0.00	0.00	0.00	0.00	0.00	0.00	0.00	0.00	0.00	0.00	0.00	0.00	0.00
Cl	0.00	0.00	0.00	0.00	0.00	0.00	0.00	0.00	0.00	0.00	0.00	0.00	0.00	0.00	0.00	0.00	0.00	0.00	0.00	0.00	0.00	0.00
K_2O	4.84	3.12	3.67	4.13	4.14	5.00	7.10	7.40	5.77	2.55	2.32	2.22	1.69	2.23	2.09	4.81	0.00	5.66	6.67	0.00	0.00	0.00
CaO	21.69	29.90	27.62	23.74	24.03	22.54	18.89	19.05	27.49	41.10	14.11	42.78	18.97	24.38	17.10	19.53	42.68	17.56	20.28	46.74	47.33	48.73
TiO_2	0.00	0.00	0.00	0.00	0.00	0.00	0.00	0.00	0.00	0.00	0.00	0.00	0.00	0.00	0.00	0.00	0.00	0.00	1.26	0.00	0.00	0.00
MnO	0.00	0.00	0.00	0.00	0.00	0.00	0.00	0.00	0.00	0.00	0.00	0.00	0.00	0.00	0.00	0.00	0.00	0.00	0.00	0.00	0.00	0.00
FeO	0.00	0.00	0.00	0.00	0.00	0.00	0.00	0.00	0.00	0.00	0.00	0.00	0.00	0.00	0.00	0.00	0.00	0.00	0.00	0.00	0.00	0.00
Fe_2O_3	10.68	9.82	9.15	9.50	9.35	8.01	11.79	12.46	10.09	5.69	18.14	6.04	19.29	15.53	19.09	13.54	3.87	13.15	15.24	1.91	2.11	1.94
Total	100.00	100.00	100.00	100.00	100.00	100.00	100.00	100.00	100.00	100.00	100.00	100.00	100.00	100.00	100.00	100.00	100.00	100.00	100.00	100.00	100.00	100.00
Ca^{2+}	3.97	4.93	4.54	4.16	4.13	3.71	3.72	3.11	4.14	6.06	4.87	6.48	5.39	5.27	5.57	4.06	5.80	3.80	4.30	6.78	6.91	7.28
Al^{3+}	1.94	1.55	1.63	1.77	1.82	1.76	2.79	2.74	1.75	0.98	1.70	0.95	1.78	1.54	1.99	2.01	0.90	2.08	2.13	1.11	1.04	1.03
$(SO_4)^{2-}$	0.00	0.00	0.00	0.00	0.00	0.00	0.00	0.00	0.00	0.00	0.00	0.00	0.00	0.00	0.00	0.00	0.00	0.00	0.00	0.00	0.00	0.00
Si^{4+}	6.00	6.00	6.00	6.00	6.00	6.00	6.00	6.00	6.00	6.00	6.00	6.00	6.00	6.00	6.00	6.00	6.00	6.00	6.00	6.00	6.00	6.00
Ca:Si	0.66	0.82	0.76	0.69	0.69	0.62	0.62	0.52	0.69	1.01	0.81	1.08	0.90	0.88	0.93	0.68	0.97	0.63	0.72	1.13	1.15	1.21

Table H-7. Sample C369 (ATEM results).

Wt% oxide	ettring-ite	ettring-ite	ettring-ite	ettring-ite	fibres/ laths	fibres/ laths	fibres/ laths	fibres/ laths	fibres/ laths	fibres/ laths	fibres/ laths	fibres/ laths	gel	gel	gel	sheet
Na_2O	0.00	0.00	0.00	0.00	0.00	0.00	0.00	0.00	0.00	0.00	0.00	1.69	0.00	0.00	2.05	0.00
MgO	1.04	1.15	0.00	0.00	2.88	8.93	1.74	1.71	0.00	0.00	0.00	42.68	27.00	21.00	42.39	0.00
Al_2O_3	13.27	13.74	13.53	12.52	1.44	5.37	4.40	7.63	11.82	2.89	3.27	7.42	3.60	2.82	5.89	0.00
SiO_2	3.52	3.25	2.69	2.89	47.30	41.97	41.80	32.40	7.12	46.02	46.14	35.16	50.79	50.00	34.09	46.18
P_2O_5	2.04	2.22	1.96	1.94	0.00	0.00	0.00	0.00	1.68	0.00	0.00	0.00	0.00	0.00	0.00	0.00
SO_3	29.33	31.17	31.49	31.95	1.54	1.39	0.00	10.48	26.98	2.48	2.57	0.00	0.00	0.00	2.04	0.00
Cl	0.00	0.00	0.00	0.00	1.44	0.99	1.15	0.00	0.00	1.27	1.14	1.07	0.70	1.46	1.19	3.03
K_2O	0.46	0.00	0.00	0.00	0.00	2.40	0.00	0.00	0.00	0.00	0.00	0.00	0.00	0.00	0.00	0.00
CaO	50.34	48.47	49.54	50.69	43.59	35.22	49.23	46.42	52.40	45.96	45.51	6.73	13.94	21.17	7.55	49.28
TiO_2	0.00	0.00	0.00	0.00	0.00	0.00	0.00	0.00	0.00	0.00	0.00	0.00	0.00	0.00	0.00	0.00
MnO	0.00	0.00	0.00	0.00	0.00	0.00	0.00	0.00	0.00	0.00	0.00	0.00	0.00	0.00	0.00	0.00
FeO	0.00	0.00	0.00	0.00	0.00	0.00	0.00	0.00	0.00	0.00	0.00	0.00	0.00	0.00	0.00	0.00
Fe_2O_3	0.00	0.00	0.78	0.00	1.81	3.72	1.67	1.36	0.00	1.37	1.37	5.26	3.97	3.54	4.79	1.52
Total	100.00	100.00	100.00	100.00	100.00	100.00	100.00	100.00	100.00	100.00	100.00	100.00	100.00	100.00	100.00	100.00
Ca^{2+}	6.19	6.20	6.00	6.00	6.48	7.42	7.95	9.70	47.38	6.43	6.35	12.24	6.53	6.49	12.73	6.87
Al^{3+}	1.74	1.87	1.80	1.63	0.22	0.91	0.74	1.67	11.75	0.44	0.50	1.49	0.50	0.40	1.22	0.00
$(SO_4)^{2-}$	2.44	2.70	2.67	2.64	0.15	0.15	0.00	1.46	17.06	0.24	0.25	0.00	0.00	0.00	0.27	0.00
Si^{4+}	0.39	0.37	0.30	0.32	6.00	6.00	6.00	6.00	6.00	6.00	6.00	6.00	6.00	6.00	6.00	6.00
Ca:Si	–	–	–	–	1.08	1.24	1.33	1.62	7.90	1.07	1.06	2.04	1.09	1.08	2.12	1.14

Table H-8a. Sample C369AP1 silico-sulphate phases (EMPA results).

Wt% oxide	C369AP1/ silico-sulphates	C369AP1/ silico-sulphates	C369AP1/ silico-sulphates	C369AP1/ silico-sulphates	C369AP1/ silico-sulphates	C369AP1/ silico-sulphates	C369AP1/ silico-sulphates	C369AP1/ silico-sulphates	C369AP1/ silico-sulpåhates	C369AP1/ silico-sulphates	C369AP1/ silico-sulphates	C369AP1/ silico-sulphates	C369AP1/ silico-sulphates
Na_2O	0.02	0.04	0.00	0.04	0.00	0.00	0.02	0.00	0.03	0.00	0.00	0.00	0.00
SeO_2	1.62	0.15	0.74	0.00	1.98	1.22	0.57	0.48	0.15	0.39	0.24	0.43	0.14
MgO	0.00	0.00	0.14	0.33	0.00	0.00	0.00	0.00	0.05	0.00	0.00	0.00	0.00
Al_2O_3	6.26	1.70	7.32	3.32	5.44	6.27	5.79	7.27	3.54	7.15	5.03	2.33	0.59
SiO_2	4.19	5.28	4.39	5.60	4.40	3.03	2.43	2.14	2.10	2.03	1.83	2.03	2.08
SO_3	10.38	2.85	12.43	5.96	10.99	9.71	10.84	13.07	6.07	10.37	10.70	6.99	1.28
Cl^-	0.54	1.13	0.32	0.85	0.62	0.75	0.69	0.23	0.91	0.70	0.70	1.48	1.42
K_2O	0.00	0.11	0.05	0.16	0.00	0.00	0.02	0.00	0.02	0.00	0.03	0.02	0.03
CaO	35.30	12.66	39.53	20.52	34.59	31.16	31.67	38.89	18.34	30.32	30.78	17.70	5.43
TiO_2	0.00	0.00	0.00	0.00	0.00	0.00	0.00	0.00	0.00	0.00	0.00	0.00	0.00
Cr_2O_3	2.39	0.68	3.39	1.30	2.41	1.94	3.07	4.08	1.48	1.91	4.77	2.58	0.17
MnO	0.00	0.00	0.00	0.00	0.00	0.00	0.00	0.00	0.00	0.00	0.00	0.00	0.00
FeO	0.07	0.06	0.18	0.31	0.10	0.09	0.00	0.12	0.09	0.07	0.00	0.00	0.06
CoO	0.00	0.00	0.06	0.00	0.00	0.00	0.00	0.00	0.00	0.00	0.00	0.00	0.05
NiO	0.00	0.00	0.00	0.00	0.09	0.00	0.00	0.00	0.00	0.00	0.12	0.00	0.00
CuO	0.00	0.00	0.00	0.00	0.00	0.00	0.00	0.00	0.00	0.11	0.11	0.00	0.00
Total	60.77	24.68	68.55	38.39	60.61	54.16	55.10	66.28	32.77	53.02	54.31	33.56	11.24
Ca^{2+}	6.00	6.00	6.00	6.00	6.00	6.00	6.00	6.00	6.00	6.00	6.00	6.00	6.00
Al^{3+}	1.47	1.12	1.60	1.34	1.35	1.60	1.63	1.70	1.63	1.83	1.76	1.51	0.85
$(SO_4)^{2-}$	1.24	0.94	1.32	1.21	1.34	1.31	1.44	1.41	1.39	1.44	1.46	1.66	0.99
Si^{4+}	0.66	2.32	0.62	1.52	0.71	0.54	0.43	0.31	0.64	0.37	0.33	0.64	2.14
Ca:Si	9.03	2.59	9.65	3.95	8.42	11.01	13.98	19.51	9.39	16.02	18.00	9.36	2.80

Table H-8b. Sample C369AP1 silico-sulphate phases (EMPA results).

Wt% oxide	C369AP1/ silico-sulphates	C369AP1/ silico-sulphates	C369AP1/ silico-sulphates	C369AP1/ silico-sulphates	C369AP1/ silico-sulphates	C369AP1/ silico-sulphates	C369AP1/ silico-sulphates	C369AP1/ silico-sulphates	C369AP1/ silico-sulphates	C369AP1/ silico-sulphates	C369AP1/ silico-sulphates	C369AP1/ silico-sulphates
Na_2O	0.09	0.00	0.00	0.03	0.02	0.04	0.02	0.07	0.05	0.08	0.07	0.06
SeO_2	0.00	1.08	0.82	0.06	0.21	0.32	0.51	0.08	0.07	0.07	0.08	0.14
MgO	0.46	0.00	0.00	0.28	0.02	0.05	0.00	0.00	0.00	0.21	0.00	0.00
Al_2O_3	0.27	0.83	0.66	2.65	1.52	2.08	5.48	5.29	5.59	2.96	4.00	5.52
SiO_2	2.20	8.27	5.94	13.64	8.56	3.44	1.83	8.48	8.94	13.18	11.13	6.36
SO_3	0.58	10.21	10.98	4.92	3.90	5.97	9.65	10.66	12.55	7.45	8.49	11.56
Cl^-	0.50	0.82	0.80	0.46	1.76	0.71	1.01	0.74	0.40	0.57	0.71	0.71
K_2O	0.07	0.00	0.00	0.38	0.14	0.04	0.00	0.15	0.16	0.30	0.21	0.12
CaO	36.33	32.52	29.42	31.38	15.01	41.10	25.13	30.13	35.25	28.30	28.22	30.27
TiO_2	0.00	0.00	0.00	0.04	0.00	0.00	0.00	0.00	0.00	0.19	0.00	0.00
Cr_2O_3	0.16	2.29	4.20	0.16	0.78	1.40	0.95	0.00	0.17	0.38	0.14	0.00
MnO	0.00	0.00	0.00	0.00	0.00	0.07	0.00	0.09	0.07	0.00	0.08	0.00
FeO	0.10	0.06	0.00	0.59	0.06	0.18	0.00	0.27	0.22	0.47	0.20	0.20
CoO	0.09	0.00	0.00	0.00	0.00	0.00	0.00	0.00	0.07	0.00	0.00	0.00
NiO	0.00	0.00	0.00	0.12	0.00	0.00	0.00	0.10	0.00	0.00	0.00	0.00
CuO	0.00	0.00	0.00	0.00	0.00	0.00	0.00	0.00	0.00	0.00	0.00	0.00
Total	40.84	56.08	52.81	54.68	31.97	55.39	44.58	56.05	63.55	54.16	53.34	54.93
Ca^{2+}	6.00	6.00	6.00	6.00	6.00	6.00	6.00	6.00	6.00	6.00	6.00	6.00
Al^{3+}	0.07	0.48	0.78	0.58	0.89	0.48	1.61	1.15	1.06	0.74	0.95	1.20
$(SO_4)^{2-}$	0.07	1.32	1.57	0.65	1.08	0.61	1.61	1.48	1.49	1.10	1.26	1.60
Si^{4+}	0.34	1.42	1.13	2.41	3.17	0.47	0.41	1.57	1.41	2.58	2.19	1.17
Ca:Si	17.77	4.21	5.31	2.48	1.89	12.82	14.73	3.83	4.24	2.32	2.73	5.12

Table H-9a. Sample C369AP1 CSH phases (EMPA results).

Wt% oxide	amorphous gel	amorphous gel	amorphous gel	amorphous gel	amorphous gel	amorphous gel	amorphous gel	amorphous gel	amorphous gel	amorphous gel	amorphous gel	amorphous gel	amorphous gel
Na_2O	0.05	0.00	0.05	0.04	0.05	0.08	0.05	0.04	0.04	0.03	0.03	0.03	0.05
SeO_2	0.00	0.08	0.00	0.06	0.00	0.00	0.04	0.11	0.07	0.04	0.00	0.03	0.00
MgO	0.00	0.02	0.00	0.00	0.00	0.00	0.00	0.05	0.00	0.02	0.00	0.02	0.08
Al_2O_3	0.38	0.66	0.28	0.32	0.20	0.28	0.22	0.72	0.49	0.54	0.54	0.66	0.46
SiO_2	11.04	10.28	13.28	8.51	10.44	11.34	11.10	11.10	7.51	6.99	15.01	16.63	13.91
SO_3	1.07	1.68	0.42	1.01	0.60	0.66	0.37	0.71	1.41	1.10	0.22	0.25	0.17
Cl^-	1.17	1.35	1.14	1.29	1.26	1.14	1.22	1.10	1.25	1.20	1.00	0.97	0.84
K_2O	0.19	0.20	0.26	0.18	0.22	0.22	0.21	0.11	0.11	0.14	0.33	0.36	0.25
CaO	13.25	13.00	12.85	10.51	10.08	11.23	11.06	11.91	9.10	8.76	13.77	14.67	19.69
TiO_2	0.00	0.00	0.00	0.00	0.00	0.00	0.00	0.00	0.00	0.00	0.00	0.00	0.03
Cr_2O_3	0.17	0.27	0.00	0.21	0.13	0.13	0.04	0.51	0.44	0.39	0.05	0.00	0.00
MnO	0.00	0.00	0.05	0.00	0.00	0.00	0.00	0.00	0.00	0.00	0.00	0.00	0.00
FeO	0.00	0.05	0.00	0.00	0.06	0.06	0.00	0.08	0.00	0.08	0.06	0.05	0.10
CoO	0.00	0.00	0.00	0.00	0.00	0.00	0.00	0.05	0.00	0.00	0.00	0.00	0.00
NiO	0.00	0.00	0.00	0.09	0.00	0.00	0.00	0.00	0.00	0.00	0.00	0.00	0.00
CuO	0.00	0.00	0.00	0.00	0.00	0.00	0.00	0.00	0.00	0.00	0.00	0.00	0.00
Total	27.32	27.56	28.33	22.21	23.04	25.14	24.33	26.49	20.41	19.28	31.01	33.68	35.57
Ca^{2+}	7.81	8.20	6.32	8.05	6.31	6.48	6.50	6.96	7.88	8.16	5.99	5.77	9.19
Al^{3+}	0.24	0.45	0.15	0.27	0.13	0.17	0.14	0.46	0.46	0.55	0.25	0.28	0.24
$(SO_4)^{2-}$	0.44	0.73	0.14	0.53	0.26	0.26	0.15	0.29	0.84	0.71	0.07	0.07	0.05
Si^{4+}	6.00	6.00	6.00	6.00	6.00	6.00	6.00	6.00	6.00	6.00	6.00	6.00	6.00
Ca:Si	1.30	1.37	1.05	1.34	1.05	1.08	1.08	1.16	1.31	1.36	1.00	0.96	1.53

Table H-9b. Sample C369AP1 CSH phases (EMPA results).

Wt% oxide	amorphous gel	amorphous gel	amorphous gel	amorphous gel	amorphous gel	amorphous gel	amorphous gel
Na_2O	0.02	0.05	0.04	0.06	0.00	0.03	0.05
SeO_2	0.00	0.00	0.00	0.00	0.00	0.00	0.00
MgO	0.20	0.09	0.00	0.00	0.03	0.00	0.19
Al_2O_3	0.60	0.42	0.56	0.52	0.34	0.45	0.64
SiO_2	13.97	12.17	13.03	14.64	9.54	13.01	14.39
SO_3	0.20	0.17	0.35	0.13	0.20	0.24	0.32
Cl^-	0.96	1.00	1.31	1.09	1.22	1.16	0.62
K_2O	0.24	0.22	0.31	0.33	0.24	0.28	0.29
CaO	12.95	13.09	12.30	13.25	9.07	11.74	21.34
TiO_2	0.02	0.00	0.00	0.00	0.00	0.00	0.00
Cr_2O_3	0.05	0.00	0.00	0.00	0.00	0.00	0.05
MnO	0.00	0.00	0.00	0.00	0.00	0.00	0.00
FeO	0.10	0.10	0.05	0.08	0.00	0.06	0.24
CoO	0.00	0.00	0.00	0.00	0.00	0.00	0.00
NiO	0.07	0.00	0.00	0.00	0.00	0.00	0.00
CuO	0.00	0.00	0.08	0.00	0.00	0.00	0.00
Total	29.39	27.30	28.01	30.10	20.64	26.96	38.12
Ca^{2+}	6.03	7.01	6.18	5.93	6.20	5.90	9.63
Al^{3+}	0.30	0.24	0.30	0.25	0.25	0.24	0.32
$(SO_4)^{2-}$	0.07	0.06	0.12	0.04	0.10	0.08	0.10
Si^{4+}	6.00	6.00	6.00	6.00	6.00	6.00	6.00
Ca:Si	1.01	1.17	1.03	0.99	1.03	0.98	1.60

Table H-10. Sample C374(1) (ATEM results).

Wt% oxide	gel	gel	gel	gel	gel	gel	gel	gel	gel	gel
Na_2O	0.00	0.00	0.00	0.00	0.00	0.00	0.00	0.00	0.00	0.00
MgO	0.00	0.00	0.00	0.00	0.00	0.00	0.00	0.00	0.00	0.00
Al_2O_3	1.70	2.27	1.86	2.10	1.98	2.50	3.44	0.00	2.70	2.19
SiO_2	59.97	59.67	52.57	48.10	58.48	60.10	57.67	59.14	56.93	59.69
P_2O_5	0.00	0.00	0.00	0.00	0.00	0.00	0.00	0.00	0.00	0.00
SO_3	0.00	0.00	0.00	0.00	0.00	0.00	0.00	0.00	0.00	0.00
Cl	0.00	0.00	0.00	0.00	0.00	0.00	0.00	0.00	0.00	0.00
K_2O	1.48	1.21	2.49	1.28	2.28	1.70	2.27	1.01	1.05	1.07
CaO	36.85	36.85	43.08	48.52	37.26	35.70	35.19	39.85	39.32	37.04
TiO_2	0.00	0.00	0.00	0.00	0.00	0.00	0.00	0.00	0.00	0.00
MnO	0.00	0.00	0.00	0.00	0.00	0.00	0.00	0.00	0.00	0.00
FeO	0.00	0.00	0.00	0.00	0.00	0.00	0.00	0.00	0.00	0.00
Fe_2O_3	0.00	0.00	0.00	0.00	0.00	0.00	1.44	0.00	0.00	0.00
Total	100.00	100.00	100.00	100.00	100.00	100.00	100.01	100.00	100.00	99.99
Ca^{2+}	4.00	4.01	5.37	6.54	4.18	3.88	4.00	4.37	4.48	4.03
Al^{3+}	0.20	0.27	0.25	0.31	0.24	0.29	0.42	0.00	0.34	0.26
$(SO_4)^{2-}$	0.00	0.00	0.00	0.00	0.00	0.00	0.00	0.00	0.00	0.00
Si^{4+}	6.00	6.00	6.00	6.00	6.00	6.00	6.00	6.00	6.00	6.00
Ca:Si	0.67	0.67	0.89	1.09	0.70	0.65	0.67	0.73	0.75	0.67

Table H-11a. Sample C374(2) (ATEM results).

Wt% oxide	chert	chert	chert	chert	chert	chert	gel replacement	gel replacement	gel replacement	gel replacement	gel replacement	gel replacement	gel replacement	gel replacement
Na_2O	1.81	2.90	2.10	2.67	2.21	0.00	2.72	2.78	2.11	2.28	2.15	2.30	2.28	2.05
MgO	13.17	17.34	17.02	16.59	20.56	20.35	7.43	13.15	9.44	9.97	11.43	12.22	8.51	10.10
Al_2O_3	3.35	5.79	5.44	5.02	5.84	5.72	7.27	5.80	5.58	5.72	6.39	6.25	6.98	6.47
SiO_2	32.10	56.40	55.56	49.36	59.83	64.42	59.87	54.46	51.44	48.96	56.96	55.71	60.16	56.18
P_2O_5	0.00	0.00	0.00	0.00	0.00	0.00	0.00	0.00	0.00	0.00	0.00	0.00	0.00	0.00
SO_3	0.00	0.00	0.00	0.00	0.00	0.00	0.00	0.00	0.00	0.00	0.00	0.00	0.00	0.00
Cl	0.00	0.00	0.00	0.00	0.00	0.00	0.00	0.00	0.00	0.00	0.00	0.00	0.00	0.00
K_2O	0.00	1.17	0.57	0.96	0.00	0.00	0.87	0.95	0.00	0.79	0.00	0.67	0.76	0.80
CaO	49.56	15.64	18.58	24.68	10.29	7.98	21.83	21.89	30.46	31.43	22.15	21.95	20.63	23.45
TiO_2	0.00	0.00	0.00	0.00	0.00	0.00	0.00	0.00	0.00	0.00	0.00	0.00	0.00	0.00
MnO	0.00	0.00	0.00	0.00	0.00	0.00	0.00	0.00	0.00	0.00	0.00	0.00	0.00	0.00
FeO	0.00	0.00	0.00	0.00	0.00	0.00	0.00	0.00	0.00	0.00	0.00	0.00	0.00	0.00
Fe_2O_3	0.00	0.76	0.73	0.72	1.26	1.53	0.00	0.97	0.97	0.85	0.92	0.89	0.68	0.94
Total	100.00	100.00	100.00	100.00	100.00	100.00	100.00	100.00	100.00	100.00	100.00	100.00	100.00	100.00
Ca^{2+}	13.78	4.73	5.02	6.42	4.29	3.63	3.62	4.93	5.57	6.12	4.41	4.64	3.61	4.43
Al^{3+}	0.74	0.73	0.69	0.72	0.69	0.63	0.86	0.75	0.77	0.83	0.79	0.79	0.82	0.81
$(SO_4)^{2-}$	0.00	0.00	0.00	0.00	0.00	0.00	0.00	0.00	0.00	0.00	0.00	0.00	0.00	0.00
Si^{4+}	6.00	6.00	6.00	6.00	6.00	6.00	6.00	6.00	6.00	6.00	6.00	6.00	6.00	6.00
Ca:Si	2.30	0.79	0.84	1.07	0.72	0.60	0.60	0.82	0.93	1.02	0.73	0.77	0.60	0.74

Table H-11b. Sample C374(2) (ATEM results).

Wt% oxide	gel replacement	gel replacement	gel replacement	gel replacement	gel replacement	gel replacement	gel replacement	gel replacement	gel replacement	gel replacement	gel replacement	gel replacement
Na_2O	2.32	2.55	0.00	0.00	0.00	0.00	0.00	0.00	0.00	0.00	0.00	2.25
MgO	12.06	10.26	12.44	12.18	11.65	11.20	12.85	11.02	30.02	28.97	28.43	27.57
Al_2O_3	5.87	6.25	5.61	5.97	6.72	6.43	6.39	5.83	2.96	3.20	3.18	3.56
SiO_2	52.31	56.23	56.34	59.89	63.33	61.59	61.95	54.49	59.52	62.81	62.94	61.67
P_2O_5	0.00	0.00	0.00	0.00	0.00	0.00	0.00	0.00	0.00	0.00	0.00	0.00
SO_3	0.00	0.00	0.00	0.00	0.00	0.00	0.00	0.00	0.00	0.00	0.00	0.00
Cl	0.00	0.00	0.00	0.00	0.00	0.00	0.00	0.00	0.00	0.00	0.00	0.00
K_2O	0.71	0.72	0.00	0.00	0.00	0.63	0.65	0.72	0.92	0.57	0.64	0.67
CaO	25.61	23.22	24.61	21.00	17.39	19.11	17.13	26.95	6.58	4.45	4.81	3.86
TiO_2	0.00	0.00	0.00	0.00	0.00	0.00	0.00	0.00	0.00	0.00	0.00	0.00
MnO	0.00	0.00	0.00	0.00	0.00	0.00	0.00	0.00	0.00	0.00	0.00	0.00
FeO	0.00	0.00	0.00	0.00	0.00	0.00	0.00	0.00	0.00	0.00	0.00	0.00
Fe_2O_3	1.11	0.77	1.00	0.96	0.92	1.04	1.03	0.99	0.00	0.00	0.00	0.42
Total	100.00	100.00	100.00	100.00	100.00	100.00	100.00	100.00	100.00	100.00	100.00	100.00
Ca^{2+}	5.37	4.45	4.79	4.08	3.41	3.64	3.66	5.02	5.26	4.60	4.56	4.53
Al^{3+}	0.79	0.79	0.70	0.71	0.75	0.74	0.73	0.76	0.35	0.36	0.36	0.41
$(SO_4)^{2-}$	0.00	0.00	0.00	0.00	0.00	0.00	0.00	0.00	0.00	0.00	0.00	0.00
Si^{4+}	6.00	6.00	6.00	6.00	6.00	6.00	6.00	6.00	6.00	6.00	6.00	6.00
Ca:Si	0.90	0.74	0.80	0.68	0.57	0.61	0.61	0.84	0.88	0.77	0.76	0.76

Table H-11c. Sample C374(2) (ATEM results).

Wt% oxide	gel replacement	gel replacement	gel replacement	fine C-A-S-H	fine C-A-S-H	fine C-A-S-H	fine C-A-S-H	fine C-A-S-H	fine C-A-S-H	fine C-A-S-H	fine C-A-S-H	fine C-A-S-H
Na_2O	0.00	0.00	0.00	0.00	0.00	0.00	0.00	0.00	0.00	0.00	0.00	0.00
MgO	29.02	28.75	28.13	0.00	0.00	0.00	0.00	3.20	6.23	3.17	3.26	4.68
Al_2O_3	3.13	3.22	3.32	28.43	28.75	29.01	28.63	25.41	17.09	14.90	28.42	17.11
SiO_2	62.08	62.44	59.56	5.47	4.28	2.70	7.85	26.13	20.91	23.18	21.42	23.63
P_2O_5	0.00	0.00	0.00	0.00	0.00	0.00	0.00	0.00	0.00	0.00	0.00	0.00
SO_3	0.00	0.00	0.00	0.00	0.00	0.00	0.00	0.00	0.00	0.00	3.36	0.00
Cl	0.00	0.00	0.00	0.00	0.00	0.00	0.00	0.00	0.00	0.00	0.00	0.00
K_2O	0.91	0.79	0.69	0.00	0.00	0.00	0.00	0.00	0.00	0.00	0.00	0.00
CaO	4.86	4.80	7.94	66.10	66.96	68.29	63.52	44.25	55.76	58.75	43.53	54.58
TiO_2	0.00	0.00	0.00	0.00	0.00	0.00	0.00	0.00	0.00	0.00	0.00	0.00
MnO	0.00	0.00	0.00	0.00	0.00	0.00	0.00	0.00	0.00	0.00	0.00	0.00
FeO	0.00	0.00	0.00	0.00	0.00	0.00	0.00	0.00	0.00	0.00	0.00	0.00
Fe_2O_3	0.00	0.00	0.37	0.00	0.00	0.00	0.00	1.01	0.00	0.00	0.00	0.00
Total	100.00	100.00	100.00	100.00	100.00	100.00	100.00	100.00	100.00	100.00	100.00	100.00
Ca^{2+}	4.72	4.64	5.11	77.79	100.71	162.82	52.09	12.00	19.83	17.54	14.44	16.64
Al^{3+}	0.36	0.36	0.39	36.77	47.53	76.02	25.80	6.88	5.78	4.55	9.39	5.12
$(SO_4)^{2-}$	0.00	0.00	0.00	0.00	0.00	0.00	0.00	0.00	0.00	0.00	0.71	0.00
Si^{4+}	6.00	6.00	6.00	6.00	6.00	6.00	6.00	6.00	6.00	6.00	6.00	6.00
Ca:Si	0.79	0.77	0.85	12.96	16.79	27.14	8.68	2.00	3.31	2.92	2.41	2.77

Table H-12. Sample C375 (ATEM results).

Wt% oxide	albite	albite	gel	gel	gel	gel	gel	fibres	fibres	fibres	fibres	fibres	fibres
Na_2O	5.16	3.11	6.03	0.00	0.00	0.00	0.00	7.44	7.14	6.12	7.27	10.54	6.79
MgO	0.00	1.13	2.38	2.87	2.71	4.07	5.24	1.67	1.48	1.57	1.76	0.00	1.85
Al_2O_3	19.10	17.91	5.18	8.82	10.00	8.33	8.88	10.96	10.75	9.66	10.78	9.25	10.15
SiO_2	63.84	61.17	29.16	27.34	38.49	40.43	47.14	54.02	57.22	53.33	57.84	51.08	54.80
P_2O_5	0.00	0.00	0.00	0.00	0.00	0.00	0.00	0.00	0.00	0.00	0.00	0.00	0.00
SO_3	0.00	0.00	0.00	0.00	0.00	0.00	0.00	1.11	0.00	0.00	0.00	1.63	0.00
Cl	0.00	0.00	0.00	0.00	0.00	0.00	0.00	0.00	0.00	0.00	0.00	0.00	0.00
K_2O	7.74	7.81	11.26	3.86	5.85	0.00	0.00	8.48	8.50	7.23	6.38	8.04	6.05
CaO	2.11	4.98	37.09	50.83	36.20	33.42	28.17	11.96	11.26	16.74	11.35	14.81	15.43
TiO_2	0.00	0.60	0.00	0.00	0.00	1.17	0.00	0.00	0.00	0.00	0.00	0.00	0.00
Cr_2O_3	0.00	0.00	0.00	0.00	0.00	0.00	0.00	0.00	0.00	0.00	0.00	0.00	0.00
FeO	0.00	0.00	0.00	0.00	0.00	0.00	0.00	0.00	0.00	0.00	0.00	0.00	0.00
Fe_2O_3	2.05	3.29	8.90	6.28	6.74	12.58	10.56	4.37	3.65	5.35	4.62	4.64	4.93
Total	100.00	100.00	100.00	100.00	100.00	100.00	100.00	100.00	100.00	100.00	100.00	100.00	100.00
Ca^{2+}	0.68	1.08	10.26	13.18	6.98	6.22	4.84	2.40	2.15	2.88	2.11	2.77	2.69
Al^{3+}	2.12	2.07	1.26	2.28	1.84	1.46	1.33	1.44	1.33	1.28	1.32	1.28	1.31
$(SO_4)^{2-}$	0.00	0.00	0.00	0.00	0.00	0.00	0.00	0.09	0.00	0.00	0.00	0.14	0.00
Si^{4+}	6.00	6.00	6.00	6.00	6.00	6.00	6.00	6.00	6.00	6.00	6.00	6.00	6.00
Ca:Si	0.11	0.18	1.71	2.20	1.16	1.04	0.81	0.40	0.36	0.48	0.35	0.46	0.45

Table H-13. Colluvium sample C365; trace element data from LAMP analysis.

Sample Name	Chromium ^{53}Cr	Cobalt ^{59}Co	Selenium ^{78}Se	Selenium ^{82}Se	Strontium ^{86}Sr	Zirconium ^{90}Zr	Molybdenum ^{98}Mo	Caesium ^{133}Cs	Barium ^{138}Ba	Lead ^{208}Pb	Thorium ^{232}Th	Uranium ^{238}U
Zeolite gel												
C365/4A	43	3.8	660	222	4 614	2.5	2.7	46	763	10	0.3	0.5
C365/4B	42	2.6	660	222	4 428	2.8	1.1	49	834	10	0.3	0.5
C365/4C	18	2.5	495	166	2 200	1.9	1.1	39	506	5	0.2	0.5
C365/1A	51	4.9	123	41	1 050	35	0.9	8.0	88	5.0	0.9	1.0
C365/1B	59	1.4	518	174	3 895	10	0.6	27	206	12	0.4	1.0
C365/1C	33	3.1	62	21	491	15	0.4	2.8	93	2.1	0.7	1.0
C365/1D	37	1.5	309	104	2 793	10	1.5	10	233	7.2	0.4	1.0
CSH gel												
C365/4D	61	2.1	115	39	1 098	5.7	0.3	8.8	1.857	24	0.3	0.5
C365/4E	62	2.5	317	106	4 982	3.7	1.3	14	6 992	7.6	0.1	0.5
Basalt (overall)												
C365/4G	184	37	749	251	1 368	393	4.2	2.7	410	13	4.9	2.9
C365/4H	56	10	159	53	1 003	305	2.2	2.0	355	12	9.4	2.9
C365/1J	178	115	417	140	3 634	250	3.2	7.3	3 435	17	7.4	2.0
C365/1K	265	158	394	132	1 625	340	1.2	10	486	22	4.7	2.0
Colluvium carbonate matrix												
C365/4I	87	5	106	45	1 363	30	2.2	3.7	693	2.8	1.4	2.9
C365/4J	149	13	216	73	2 035	47	2.2	12.4	417	7.7	2.2	2.9
C365/4K	151	20	91	53	1 326	71	1.2	6.9	226	7.4	3.4	2.9
C365/4L	183	12	107	36	1 208	83	2.0	6.8	175	9.2	4.2	2.9
C365/1E	171	15	208	70	2 146	77	2.1	10	353	21	3.9	2.5
C365/1F	95	7.3	100	33	1 254	51	1.9	4.2	131	6.3	2.6	2.5
C365/3C	68	12	69	23	1 234	31	0.7	4.0	340	4.2	1.5	1.0
C365/3D	88	6.4	158	53	2 795	36	0.7	6.7	808	3.9	1.6	1.0

Table H-13 (contd.). Sample C365; trace element data from LAMP analysis.

Sample Name	Chromium ^{53}Cr	Cobalt ^{59}Co	Selenium ^{78}Se	Selenium ^{82}Se	Strontium ^{86}Sr	Zirconium ^{90}Zr	Molybdenum ^{98}Mo	Caesium ^{133}Cs	Barium ^{138}Ba	Lead ^{208}Pb	Thorium ^{232}Th	Uranium ^{238}U
Fibrous vein phase												
C365/1G	41	7.1	668	224	9 619	8	1.9	28	9 546	33	0.3	1.0
C365/1H	42	1.4	291	385	2 891	3	0.6	5.9	200	6.0	0.1	1.0
Fe oxide fragment												
C365/1I	38	462	110	43	1 461	97	39.7	1.9	1 267	23	3.2	1.0
Biomicrite clast												
C365/3A	228	2.5	110	37	2 771	8.3	2.9	2.9	235	2.0	1.8	9
C365/3B	181	1.8	58	27	1 095	9.4	4.5	1.5	128	1.4	0.6	11
Carbonate and siliceous clasts												
C365/3E	465	43	313	105	1 960	1 650	3.6	0.8	251	14	3.7	2.0
C365/3I	47	12	331	111	913	31	0.5	1.3	172	6.3	0.9	2.0
C365/3J	211	16	728	245	3 124	60	1.5	6.3	643	14	3.8	2.0
Microfossils (calcite)												
C365/3G	382	6.8	744	250	6 215	16	1.9	7.1	486	4.9	0.5	2.0
C365/3H	37	5.2	251	84	2 160	3.1	0.1	1.1	96	5.8	0.1	2.0

Note: Data not subjected to full correction procedure (semi-quantitative only).
Uranium data derived from fission track analysis.

Table H-14. Colluvium sample C369; trace element data from LAMP analysis.

Sample Name	Chromium ^{53}Cr	Cobalt ^{59}Co	Selenium ^{78}Se	Selenium ^{82}Se	Strontium ^{86}Sr	Zirconium ^{90}Zr	Molybdenum ^{98}Mo	Caesium ^{133}Cs	Barium ^{138}Ba	Lead ^{208}Pb	Thorium ^{232}Th	Uranium ^{238}U
Marl clast												
C369/1A	917	2.5	106	37	1 202	12	1.4	0.6	224	3.6	0.9	20
C369/1B	671	2.8	37	17	964	12	1.0	0.5	208	1.5	0.8	20
C369/1C	728	3.2	41	50	1 103	12	0.8	0.6	226	2.2	0.8	20
Altered biomicrite												
C369/1D	634	2.4	60	30	1 124	10	1.2	0.8	285	2.9	0.7	19
C369/1E	1 961	18	141	49	1 687	38	8.2	10.3	652	8.3	2.6	19
C369/1F	591	1.3	46	16	876	7.3	2.8	0.7	242	1.9	0.5	19
Ettringite												
C369/1G	45 411	7.9	12 288	12 904	4 672	2.9	3.0	1.1	19	12	0.4	1.0
C369/1H	4 699	2.8	2 136	2 330	1 962	1.6	1.0	0.4	37	6	0.1	1.0
C369/1I	13 557	0.6	1 512	1 628	429	0.9	0.1	0.1	19	1	0.1	1.0
C369/1BA	207	0.3	49	44	73	0.3	0.1	0.1	6	0.8	0.01	1.0
C369/1BB	31	0.2	38	34	67	0.3	0.1	0.1	7	1.0	0.01	1.0
C369/1BC	100	1.8	27	9.5	85	0.5	0.2	0.2	10	0.9	0.01	1.0
C369/7D	13 258	4.1	5 197	4 377	534	4.4	2.3	0.7	62	7.8	0.2	4.0
C369/7E	965	3.4	579	513	454	4.9	3.8	0.4	86	4.8	0.2	4.0
Altered colluvium carbonate matrix												
C369/7A	1 844	2.4	150	157	532	15	2.1	3.4	130	2.1	1.1	7.0
C369/7B	1 050	3.3	75	66	637	16	3.7	3.8	165	3.5	0.9	7.0
C369/7C	1 357	3.1	161	95	1 446	16	3.0	4.8	100	3.9	1.0	7.0

Note: Data not subjected to full correction procedure (semi-quantitative only).
Uranium data derived from fission track analysis.

Table H-15. Colluvium sample C374; trace element data from LAMP analysis.

Sample	Chromium	Iron	Cobalt	Nickel	Selenium	Selenium	Strontium	Zirconium	Molyb-denum	Caesium	Barium	Lead	Thorium	Uranium
Name	^{53}Cr	^{57}Fe	^{59}Co	^{60}Ni	^{78}Se	^{82}Se	^{86}Sr	^{90}Zr	^{98}Mo	^{133}Cs	^{138}Ba	^{208}Pb	^{232}Th	^{238}U
Collophane fragment														
C374/1A	69	1 264	0.1	9	49	33	366	8.5	1.5	0.2	14	1.2	0.6	74
C374/1B	63	1 481	0.3	13	107	71	605	8.8	1.3	0.4	24	0.9	0.8	67
C374/1C	714	52 686	0.9	198	395	264	424	79	1.3	1.3	36	26	0.2	10
C374/2A	54	2 101	1.3	14	238	159	1 154	11	3.4	0.8	187	6	0.3	132
C374/2B	131	23 087	0.3	70	39	26	75	33	1.1	0.1	14	39	0.1	3
C374/4A	17	829	0.5	7.1	78	52	642	6	0.8	0.3	22	0.9	0.5	60
Barite														
C374/5A	188	2 224	1.2	11	241	161	247	36	0.6	0.8	12 702	3.6	0.2	1
C374/5B	208	2 512	2.8	22	146	98	1 723	6	0.4	0.5	34 574	5.6	0.1	3
C374/5C	124	10 132	5.3	80	617	412	3 547	19	2.6	2.1	171	31	0.4	3
Opaque ?organic phase														
C374/3A	95	3 134	7 691	5 028	101	68	1 338	28	193	1.0	17 974	5 872	0.5	32
C374/3B	85	4 893	14 487	8 849	166	111	2 333	64	253	0.6	30 813	9 911	0.6	32
C374/3C	113	1 983	5 613	2 390	38	26	218	20	27	0.1	1 807	543	0.6	70
Colluvium carbonate matrix														
C374/4B	352	4 288	2.7	66	48	32	349	14	0.8	0.3	59	4.4	0.8	7
C374/4C	261	5 147	1.6	63	125	83	696	9	1.4	0.4	20	3.8	2.2	7
C374/2D	505	9 783	1.7	88	120	80	1 543	20	1.0	0.4	33	5.2	0.8	7
C374/1D	613	8 973	1.4	101	112	48	517	23	0.8	0.2	18	2.9	4.9	10
Vein calcite														
C374/4D	23	6 330	2.4	35	205	137	313	8	0.6	0.7	23	4.1	0.1	2
C374/4E	31	8 535	2.6	29	284	190	404	2	0.7	1.0	132	3.0	0.2	2
C374/2C	11	552	0.2	5	86	57	62	1.0	0.2	0.3	4	0.7	0.1	3
Biomicrite fragment														
C374/6A	522	8 563	2.0	93	171	114	1 889	18	1.4	0.6	36	3.5	1.0	7
C374/6B	539	7 716	1.5	87	61	41	963	26	0.8	0.3	23	3.1	0.7	7

Note: Data not subjected to full correction procedure (semi-quantitative only).
Uranium data derived from fission track analysis.

Table H-16. Colluvium sample C375; trace element data from LAMP analysis.

Sample Name	Chromium ^{53}Cr	Cobalt ^{59}Co	Selenium ^{78}Se	Selenium ^{82}Se	Strontium ^{86}Sr	Zirconium ^{90}Zr	Molybdenum ^{98}Mo	Caesium ^{133}Cs	Barium ^{138}Ba	Lead ^{208}Pb	Thorium ^{232}Th	Uranium ^{238}U
Carbonate-replaced siliceous clast												
C3751B	49	0.7	361	126	60	0.9	0.7	0.4	12	1.3	0.1	50
C3751C	15	0.6	301	105	74	0.8	0.4	0.3	15	1.4	0.1	50
C3752A	97	2.5	1 211	422	166	5.1	1.8	1.2	3 083	2.4	0.4	50
C3752B	20	0.9	440	153	49	2.5	0.5	0.4	1 829	0.9	0.2	13
C3752C	1	0.3	167	58	24	1.2	0.4	0.2	6	0.7	0.1	13
C3751A	4	0.2	88	31	24	0.6	0.1	0.1	3	0.5	0.03	13
Carbonate clast												
C375/CA	346	5.5	177	75	4 006	35	22	0.7	953	6	1.4	81
C375/CB	3 869	377	5 653	1 968	97 971	564	77	116	8 424	216	24	81
C375/CC	2 988	365	5 368	1 869	111 790	620	64	108	9 556	180	26	81
C375/DA	3.5	0.1	12	4.0	273	0.8	0.1	0.2	254	0.1	0.02	2.5
C375DB	2.5	0.1	7.9	3.3	221	0.8	0.1	0.1	65	0.1	0.02	2.5
C375/DC	18	1.1	57	32	1 114	3.0	0.5	1.5	1 103	1.5	0.05	2.5
C375/MA	62	1.9	138	48	1 490	5.3	4	0.7	1 344	19	0.2	2.1
C375//MB	27	1.0	33	11	330	3.0	23	0.3	193	3.5	0.1	2.1
C375/MC	71	2.2	152	53	1 197	7.4	3	1.3	951	13	0.1	2.1
Basalt clast												
C375/KA	35	54	795	280	884	210	1.9	1.6	400	6.8	6.0	2.0
C375/KB	41	17	908	316	1 159	228	2.7	2.4	695	8.4	6.3	2.0
C375/KC	50	23	617	215	1 568	135	2.4	8.7	755	11	3.7	2.0
Ettringite												
C375/HA	6.7	10	151	55	168	40	0.4	0.3	76	1.3	1.1	0.4
C375/HB	7.7	3.3	172	60	220	43	0.5	0.5	132	1.6	1.2	0.4
C375/HC	10	4.3	117	41	298	26	0.4	1.6	143	2.2	0.7	0.4

Table H-16 (contd.). Colluvium sample C375; trace element data from LAMP analysis.

Sample Name	Chromium ^{53}Cr	Cobalt ^{59}Co	Selenium ^{78}Se	Selenium ^{82}Se	Strontium ^{86}Sr	Zirconium ^{90}Zr	Molybdenum ^{98}Mo	Caesium ^{133}Cs	Barium ^{138}Ba	Lead ^{208}Pb	Thorium ^{232}Th	Uranium ^{238}U
Phosphatic marl clast												
C375/IC	2.7	0.2	8.7	4.8	169	0.5	0.1	0.2	168	0.2	0.01	0.4
C375/FA	903	7.7	339	118	3 805	33	13	2.3	303	4.8	1.8	55
C375/FB	762	5.5	352	123	3 682	32	12	1.4	383	6.0	1.5	55
C375/FC	876	7.4	358	125	4 155	32	15	1.0	374	5.4	1.8	55
Biomicrite clast												
C375/FD	206	2	60	21	978	8	3.6	0.5	89	1.0	0.6	16
C375/FE	233	2	97	34	1 243	9	4.3	0.5	92	1.3	0.5	16
C375/FF	216	2	67	23	1 120	9	4.4	0.4	96	1.6	0.5	16
Colluvium carbonate matrix												
C375/JD	175	10	356	124	5 914	23	1.6	4	700	22	1.1	4.5
C375/JE	122	5.2	115	40	1 918	12	3.0	3.4	309	7.6	0.7	4.5
C375/JF	112	5.6	448	156	9 323	17	2.2	1.4	464	20	0.2	4.5
Chert clast												
C375/LA	13	0.6	294	102	12	6.3	0.4	0.3	126	0.6	0.1	1.0
C375/LB	21	0.7	327	114	1 976	4.5	2.1	0.3	18 557	0.7	0.1	1.0
CaSiAlFe cavity lining phase												
C375/IA	0.5	0.02	1.8	0.6	42	0.1	0.01	0.03	39	0.02	0.002	0.4
C375/IB	0.4	0.02	1.2	0.5	34	0.1	0.02	0.02	10	0.02	0.002	0.4
C375/JA	294	31	188	66	1 256	191	6.8	18	381	32	8.9	4.5
C375/JB	285	27	312	109	4 516	145	5.5	15	538	39	6.9	4.5
C375/JC	468	27	222	77	618	167	6.3	17	1 048	32	8.7	4.5

Note: Data not subjected to full correction procedure (semi-quantitative only).
Uranium data derived from fission track analysis.

Table H-17. Colluvium sample C391; trace element data from LAMP analysis.

Sample Name	Chromium ^{53}Cr	Cobalt ^{59}Co	Selenium ^{78}Se	Selenium ^{82}Se	Strontium ^{86}Sr	Zirconium ^{90}Zr	Molybdenum ^{98}Mo	Caesium ^{133}Cs	Barium ^{138}Ba	Lead ^{208}Pb	Thorium ^{232}Th	Uranium ^{238}U
Colluvium carbonate matrix												
C391/1A	695	4.5	119	41	1 269	58	1.9	9.3	71	8.4	2.4	16
C391/1B	825	3.9	95	33	1 074	64	1.8	10.3	73	5.6	1.8	16
C391/8B	391	2.8	67	23	403	19	1.2	3.8	57	5.5	0.9	9.0
C391/8C	322	1.6	38	13	596	14	1.5	3.4	31	2.3	0.9	9.0
C391/8D	399	1.8	60	21	677	14	1.3	6.0	55	5.8	1.2	9.0
Collophane fragment												
C391/1C	38	0.7	131	46	1 527	4.4	1.8	0.1	61	1.9	0.3	62
C391/1D	57	1.5	189	66	2 645	6.8	2.0	0.2	106	3.6	0.2	120
C391/4A	52	0.3	56	20	802	3.9	1.6	0.3	34	1.1	0.6	90
C391/8A	40	0.5	150	52	2 171	5.1	1.8	0.1	119	1.6	0.7	80
Fe-Ti fragment												
C391/4B	58	3.9	146	51	130	155	0.6	1.5	12	4.4	0.4	2.0
C391/4C	167	10.4	628	219	95	64	20.2	0.6	112	119	34	2.0
Carbonate/silica replaced plant root												
C391/5A	21	1.8	482	168	390	1.4	1.0	0.5	27	1.3	0.2	0.9
C391/5B	22	0.4	183	64	457	0.3	0.2	0.9	29	1.1	0.1	1.4
C391/5C	31	0.3	137	48	556	0.3	0.2	0.2	60	0.6	0.1	1.4
C391/5D	79	0.5	36	30	993	1.2	1.2	0.1	19	0.8	0.02	0.7
C391/5E	93	0.5	50	28	966	1.1	1.5	0.1	22	0.7	0.04	0.7
C391/5F	4 149	5.3	471	164	10 613	25	34	2.3	288	19	0.7	11
C391/5G	7 821	5.3	552	192	12 341	24	30	1.9	222	15	0.6	11
C391/6A	89	0.4	60	21	587	1.4	0.3	0.3	24	1.0	0.02	1.0
C391/6B	177	0.3	47	17	668	2.1	0.8	0.2	19	1.4	0.04	1.0
C391/7A	35	0.1	50	17	207	0.6	0.1	0.1	1.6	0.2	0.02	1.0
C391/7B	27	0.1	39	15	168	0.3	0.0	0.1	1.3	0.2	0.01	1.0
C391/7C	647	0.7	128	44	1 502	0.6	3.9	0.1	31	1.8	0.05	1.0
Carbonate halo around root in colluvium carbonate matrix												
C391/5H	267	0.9	21	7.5	401	4.7	1.0	1.3	20	5.5	0.5	9.0
C391/5I	526	1.7	65	23	1 149	15	2.2	4.2	50	3.6	0.9	9.0
C391/5J	312	1.2	50	17	896	12	1.6	2.9	38	3.5	0.7	9.0
C391/5K	296	1.5	52	18	751	12	1.4	4.1	36	3.3	0.7	9.0
C391/5L	516	2.4	47	16	632	18	1.3	1.9	24	2.8	1.2	9.0
C391/5M	624	2.9	52	18	782	21	1.6	2.8	28	7.1	1.2	9.0

Note: Data not subjected to full correction procedure (semi-quantitative only).
Uranium data derived from fission track analysis.

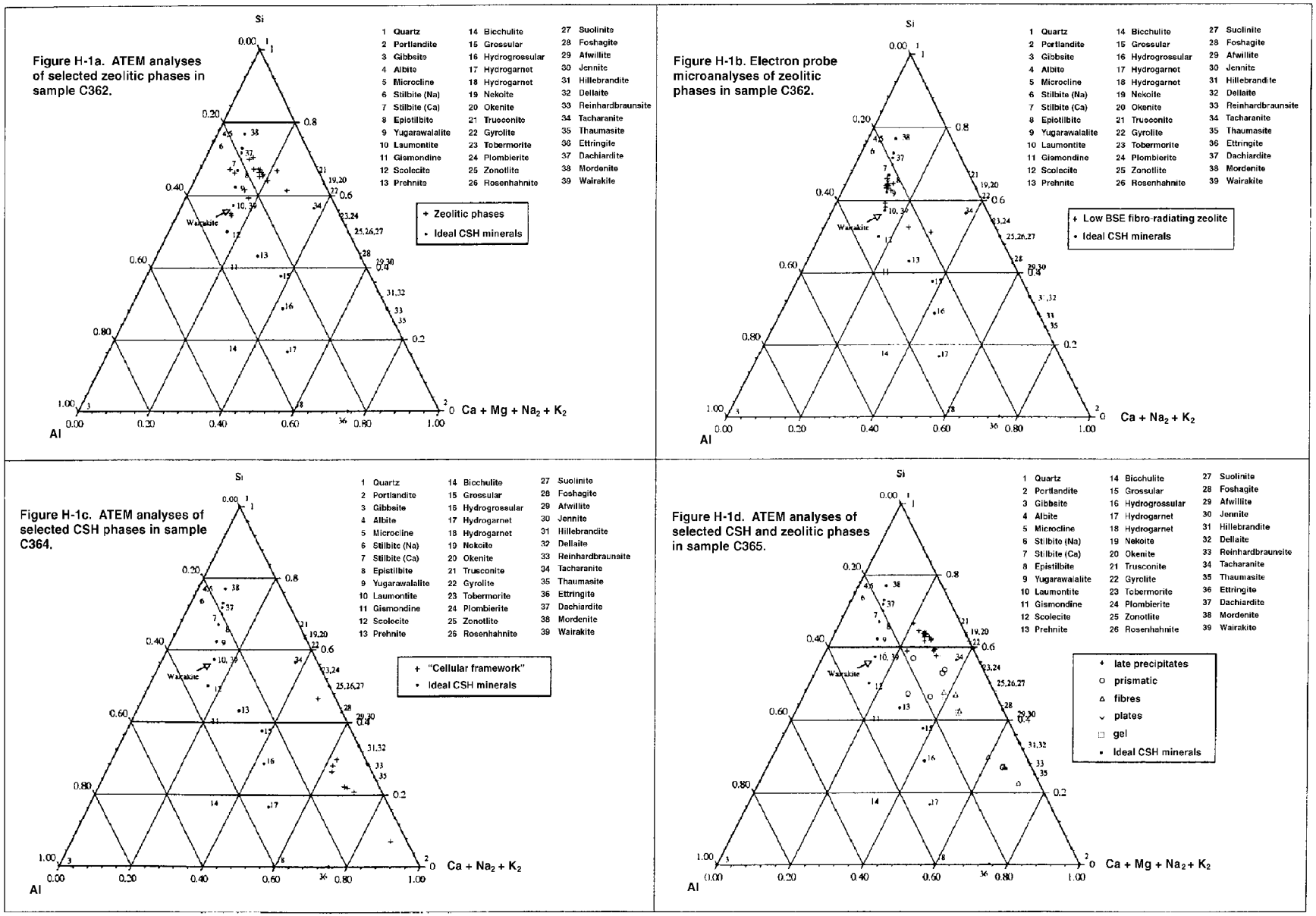
Figure H-1a. ATEM analyses of selected zeolitic phases in sample C362.
Si
Al
Ca + Mg + Na2 + K2
1 Quartz
2 Portlandite
3 Gibbsite
4 Albite
5 Microcline
6 Stilbite (Na)
7 Stilbite (Ca)
8 Epistilbite
9 Yugarawalalite
10 Laumontite
11 Gismondine
12 Scolecite
13 Prehnite
14 Bicchulite
15 Grossular
16 Hydrogrossular
17 Hydrogarnet
18 Hydrogarnet
19 Nekoite
20 Okenite
21 Trusconite
22 Gyrolite
23 Tobermorite
24 Plombierite
25 Zonotlite
26 Rosenhahnite
27 Suolinite
28 Foshagite
29 Afwillite
30 Jennite
31 Hillebrandite
32 Dellaite
33 Reinhardbraunsite
34 Tacharanite
35 Thaumasite
36 Ettringite
37 Dachiardite
38 Mordenite
39 Wairakite
+ Zeolitic phases
• Ideal CSH minerals
Figure H-1b. Electron probe microanalyses of zeolitic phases in sample C362.
Si
Al
Ca + Na2 + K2
+ Low BSE fibro-radiating zeolite
• Ideal CSH minerals
Figure H-1c. ATEM analyses of selected CSH phases in sample C364.
Si
Al
Ca + Na2 + K2
+ "Cellular framework"
• Ideal CSH minerals
Figure H-1d. ATEM analyses of selected CSH and zeolitic phases in sample C365.
Si
Al
Ca + Mg + Na2 + K2
+ late precipitates
o prismatic
△ fibres
⌄ plates
□ gel
▪ Ideal CSH minerals

Figure H-1

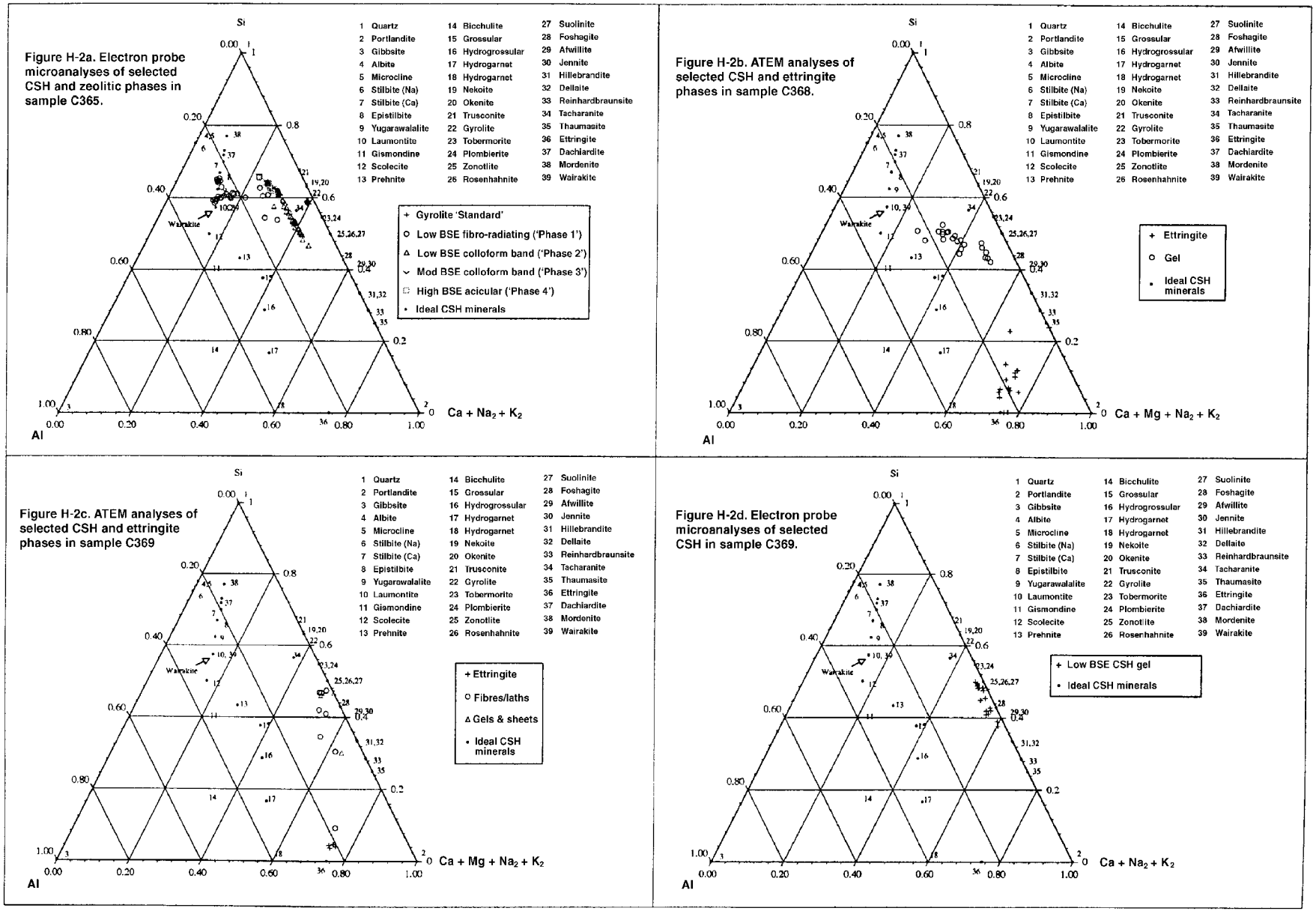
Figure H-2a. Electron probe microanalyses of selected CSH and zeolitic phases in sample C365.
Figure H-2b. ATEM analyses of selected CSH and ettringite phases in sample C368.
Figure H-2c. ATEM analyses of selected CSH and ettringite phases in sample C369
Figure H-2d. Electron probe microanalyses of selected CSH in sample C369.
Si
Al
Ca + Na2 + K2
Ca + Mg + Na2 + K2
1 Quartz
2 Portlandite
3 Gibbsite
4 Albite
5 Microcline
6 Stilbite (Na)
7 Stilbite (Ca)
8 Epistilbite
9 Yugarawalalite
10 Laumontite
11 Gismondine
12 Scolecite
13 Prehnite
14 Bicchulite
15 Grossular
16 Hydrogrossular
17 Hydrogarnet
18 Hydrogarnet
19 Nekoite
20 Okenite
21 Trusconite
22 Gyrolite
23 Tobermorite
24 Plombierite
25 Zonotlite
26 Rosenhahnite
27 Suolinite
28 Foshagite
29 Afwillite
30 Jennite
31 Hillebrandite
32 Dellaite
33 Reinhardbraunsite
34 Tacharanite
35 Thaumasite
36 Ettringite
37 Dachiardite
38 Mordenite
39 Wairakite
Wairakite
+ Gyrolite 'Standard'
o Low BSE fibro-radiating ('Phase 1')
Δ Low BSE colloform band ('Phase 2')
Mod BSE colloform band ('Phase 3')
High BSE acicular ('Phase 4')
• Ideal CSH minerals
+ Ettringite
o Gel
• Ideal CSH minerals
+ Ettringite
o Fibres/laths
Δ Gels & sheets
• Ideal CSH minerals
+ Low BSE CSH gel
• Ideal CSH minerals

Figure H-2

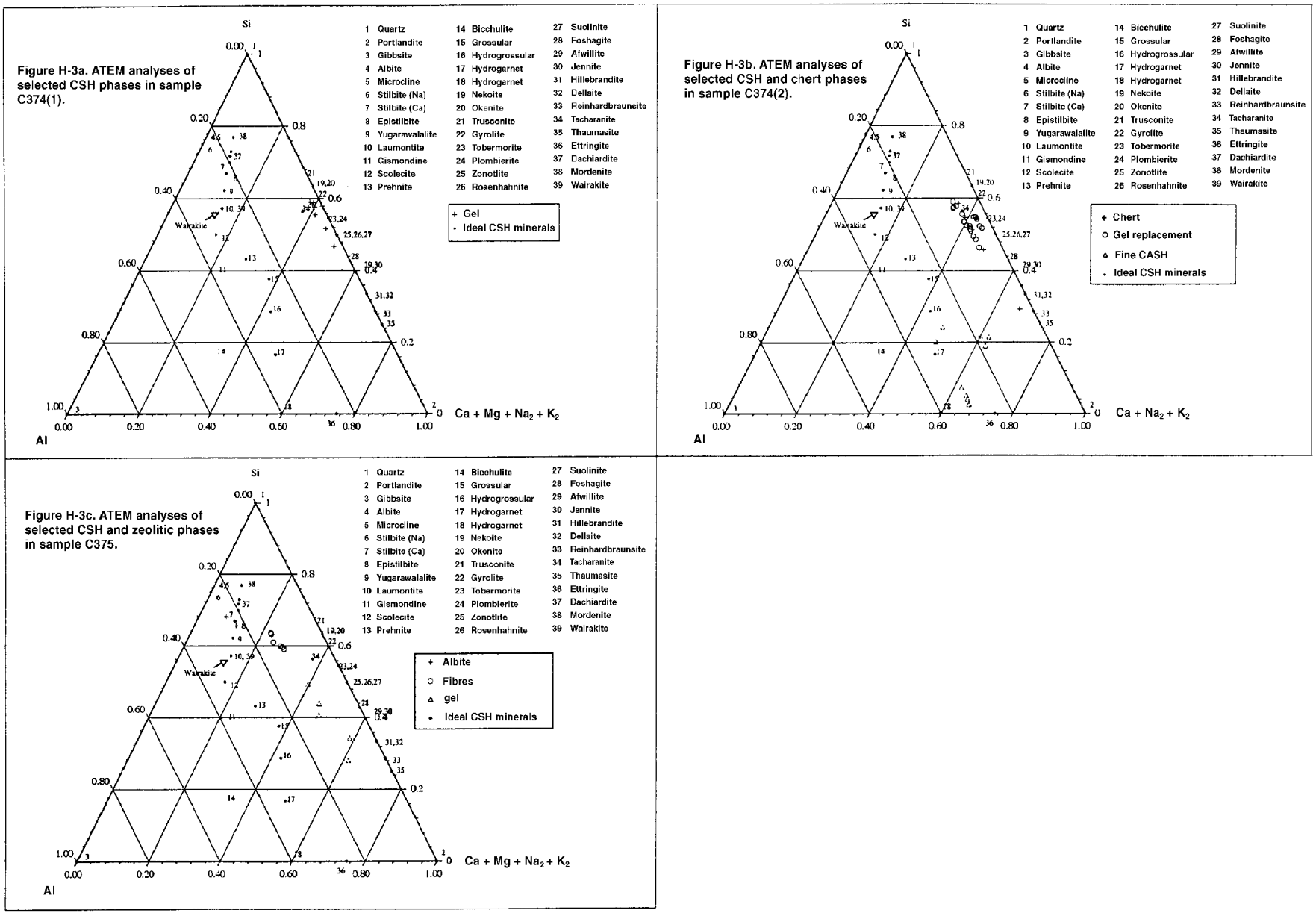
Figure H-3a. ATEM analyses of selected CSH phases in sample C374(1).
Figure H-3b. ATEM analyses of selected CSH and chert phases in sample C374(2).
Figure H-3c. ATEM analyses of selected CSH and zeolitic phases in sample C375.
Si
Al
Ca + Mg + Na2 + K2
Ca + Na2 + K2
1 Quartz
2 Portlandite
3 Gibbsite
4 Albite
5 Microcline
6 Stilbite (Na)
7 Stilbite (Ca)
8 Epistilbite
9 Yugarawalalite
10 Laumontite
11 Gismondine
12 Scolecite
13 Prehnite
14 Bicchulite
15 Grossular
16 Hydrogrossular
17 Hydrogarnet
18 Hydrogarnet
19 Nekoite
20 Okenite
21 Trusconite
22 Gyrolite
23 Tobermorite
24 Plombierite
25 Zonotlite
26 Rosenhahnite
27 Suolinite
28 Foshagite
29 Afwillite
30 Jennite
31 Hillebrandite
32 Dellaite
33 Reinhardbraunsite
34 Tacharanite
35 Thaumasite
36 Ettringite
37 Dachiardite
38 Mordenite
39 Wairakite
Wairakite
+ Gel
· Ideal CSH minerals
+ Chert
○ Gel replacement
△ Fine CASH
· Ideal CSH minerals
+ Albite
○ Fibres
△ gel
· Ideal CSH minerals

Figure H-3

APPENDIX I

Mineralogy and Geochemistry – Plates I-1 to I-24

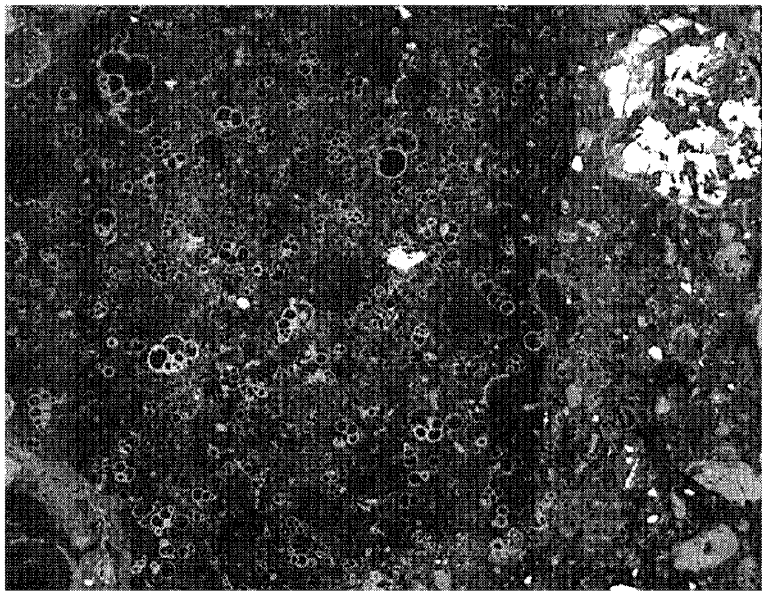

Plate I-1. *BSEM photomicrograph of altered dolomitic biomicrite clast in colluvium deposit. Fine-grained dolomite in the matrix of the clast has been leached and the dissolution porosity infilled by amorphous secondary Ca-Si-S-Al-rich alteration products (dark-grey). Alteration occurs largely around the margins of the clast. Calcitic foraminiferal tests are largely unaffected by dissolution but test chambers are infilled by secondary Ca-Si-S-Al-rich reaction products. Sample C365, Basal Colluvium Layer, Western Springs, Maqarin.*

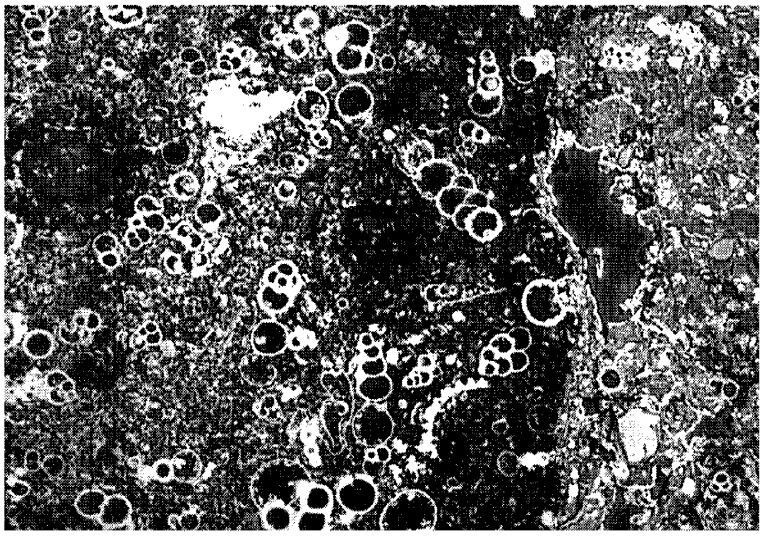

Plate I-2. *BSEM photomicrograph showing detail of alteration at the edge of the dolomitic biomicrite clast in Plate I-1. Alteration (dark-grey region) of the matrix occurs mainly within the outer 100-250 m of the clast. Note that the calcitic foraminiferal tests show little evidence of dissolution, even within the intensely altered margin of the clast. Sample C365, Basal Colluvium Layer, Western Springs, Maqarin.*

Plate I-3. *BSEM photomicrograph showing margin of chert clast which has reacted with hyperalkaline groundwater. The chert clast (dark-grey clast labelled `ch') has been replaced along its margin by a rim of fine-grained cryptocrystalline calcite (light-grey). Sample C362, Fluvial Boulder Gravel, Western Springs, Maqarin.*

Plate I-4. *BSEM photomicrograph of alteration around vesicular cavity in a basalt clast. The vessicle porosity connects with the matrix porosity of the gravel. The glassy matrix and lath-like crystals of plagioclase of the basalt have dissolved, producing secondary porosity (black areas) around the margins of the vesicular cavity (large black area) to a depth of about 1 mm. A secondary, zeolitic composition CASH mineral (z) lines the vesicular cavity in the basalt, and also occurs within the dissolution porosity in the clast matrix. Sample C362, Fluvial Boulder Gravel, Western Springs, Maqarin.*

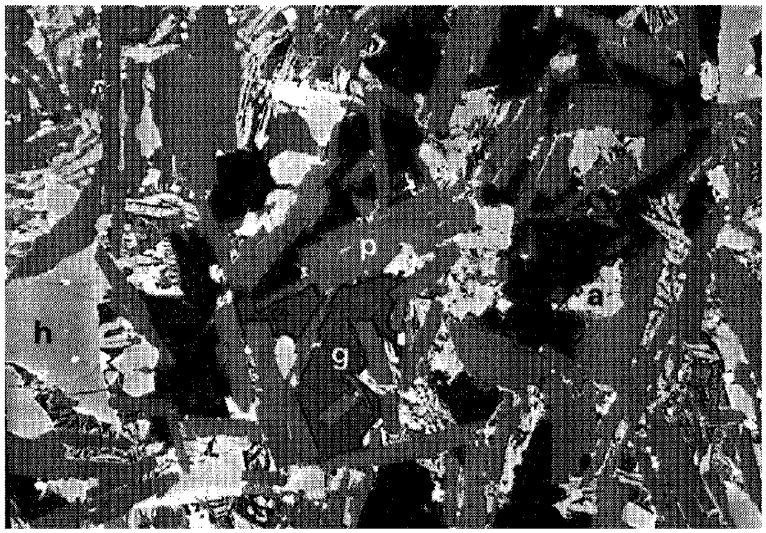

Plate I-5. *BSEM photomicrograph showing alteration in the margin of a basalt clast as a result of reaction with hyperalkaline groundwater. The interstitial glass matrix of the basalt (g) is particularly reactive, and has largely dissolved with very fine-grained secondary amorphous secondary CASH alteration products filling the dissolution porosity (dark areas). Primary augite (a), hypersthene (h) and plagioclase show little or no alteration in this clast. Sample C368, Fluvial Boulder Gravel, Western Springs, Maqarin.*

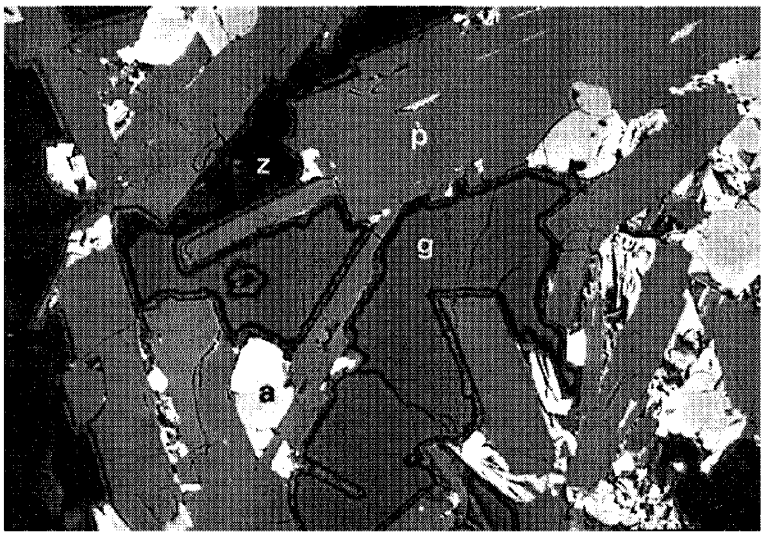

Plate I-6. *BSEM photomicrograph showing detail of alteration in basalt clast. Interstitial glass is largely dissolved and replaced by secondary CASH material (z). Residual areas of glassy matrix (g), where preserved, display secondary alteration around their margins to fibrous CASH. Plagioclase (p) shows only very slight corrosion and augite (a) shows no evidence of alteration. Sample C368, Fluvial Boulder Gravel, Western Springs, Maqarin.*

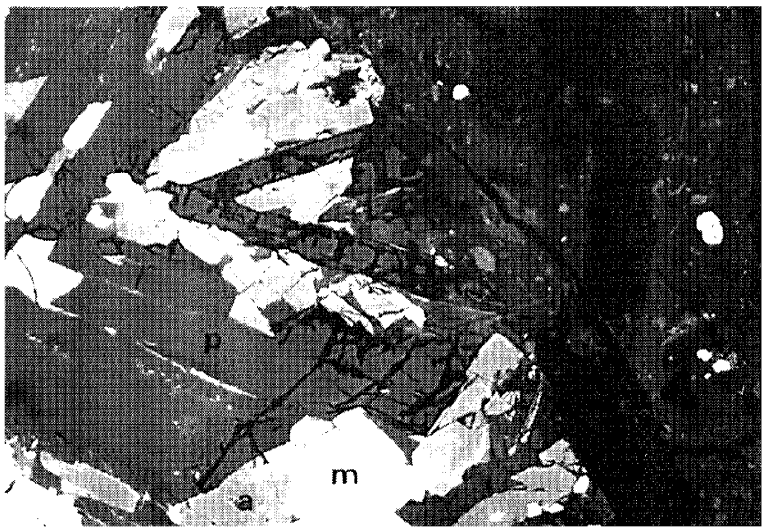

Plate I-7. *BSEM photomicrograph showing alteration at the margin of basalt clast. Plagioclase laths (p) show severe corrosion where they are exposed in the margins of the clast with dissolution occuring to a depth of up to 200 m. Augite (a) and magnetite (m) show little alteration. Sample C368, Fluvial Boulder Gravel, Western Springs, Maqarin.*

Plate I-8. *BSEM photomicrograph showing highly altered plagioclase (p) at the margin of a basalt clast which is largely altered to secondary amorphous or gel-like CASH (z). Sample C362, Fluvial Boulder Gravel, Western Springs, Maqarin.*

Plate I-9. *BSEM photomicrograph showing sand-grade fragment of olivine (o) and plagioclase (p) within colluvium which has reacted with hyperalkaline groundwater. The olivine shows virtually no alteration whilst the plagioclase is highly corroded and altered to a fibrous or gel-like mass of fine-grained secondary CASH material. Sample C365, Basal Colluvium Layer, Western Springs, Maqarin.*

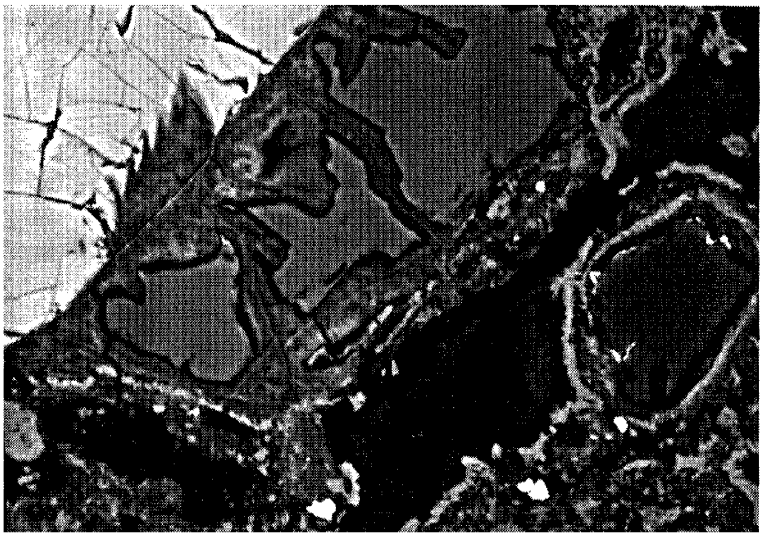

Plate I-10. *BSEM photomicrograph showing detail of alteration of plagioclase seen in Plate I-9. Fine-grained secondary CASH reaction product completely fills the porosity formed by feldspar dissolution and effectively replaces the plagioclase. Sample C365, Basal Colluvium Layer, Western Springs, Maqarin.*

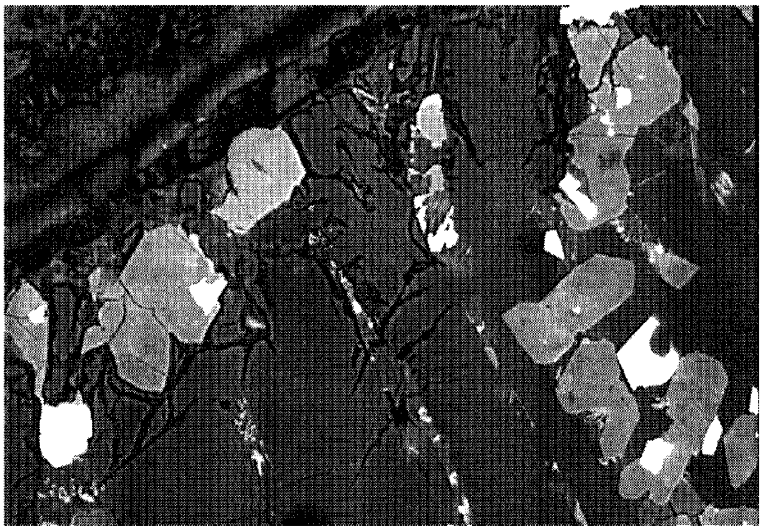

Plate I-11. *BSEM photomicrograph showing alteration, pitting and corrosion of plagioclase (dull-grey) at the margins of a basalt clast that has reacted with hyperalkaline groundwater. Augite (light-grey) and magnetite (white) show little evidence of reaction. Sample C368, Fluvial Boulder Gravel, Western Springs, Maqarin.*

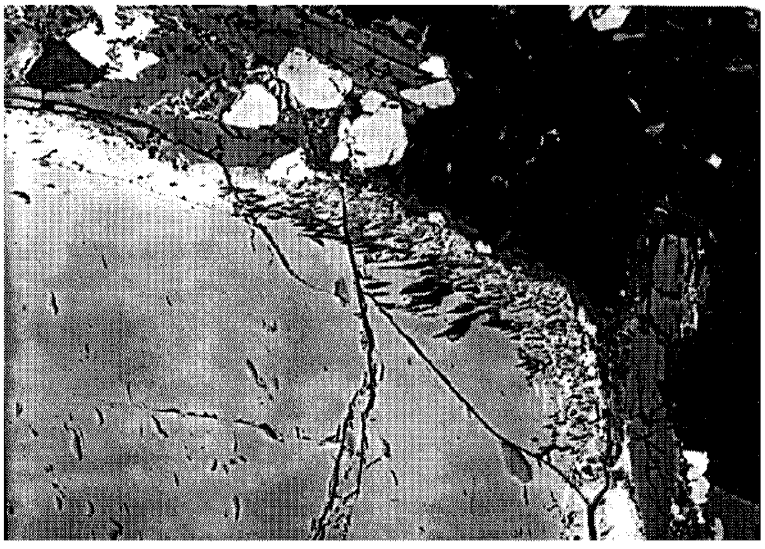

Plate I-12. *BSEM photomicrograph showing very limited corrosion of hypersthene (light-grey) at the very margins of basalt clasts reacted with hyperalkaline groundwater. A fine colloform rim of CASH alteration products (dull-grey) lines the clast surfaces exposed in the intergranular porosity (black area) Sample C362, Fluvial Boulder Gravel, Western Springs, Maqarin.*

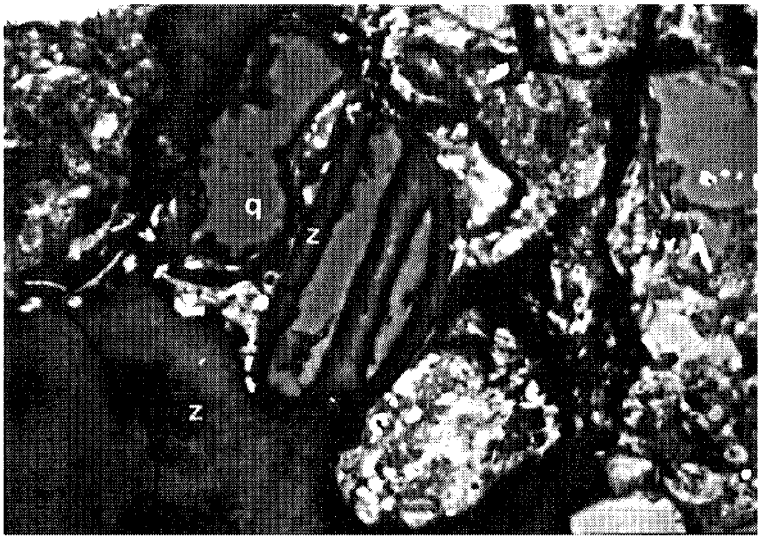

Plate I-13. *BSEM photomicrograph showing highly altered quartz sand grain within the colluvium matrix. The quartz (q) is fractured and corroded with fine-grained gel-like secondary CSH alteration products (z) filling the fractures and cementing the sandy matrix. Bright areas are calcitic material. Sample C365, Basal Colluvium Layer, Western Springs, Maqarin.*

Plate I-14. *BSEM photomicrograph showing dark organic material (plant material) with cellular cavities infilled by calcite (light-grey). Sample C364, Fluvial Boulder Gravel, Western Springs, Maqarin.*

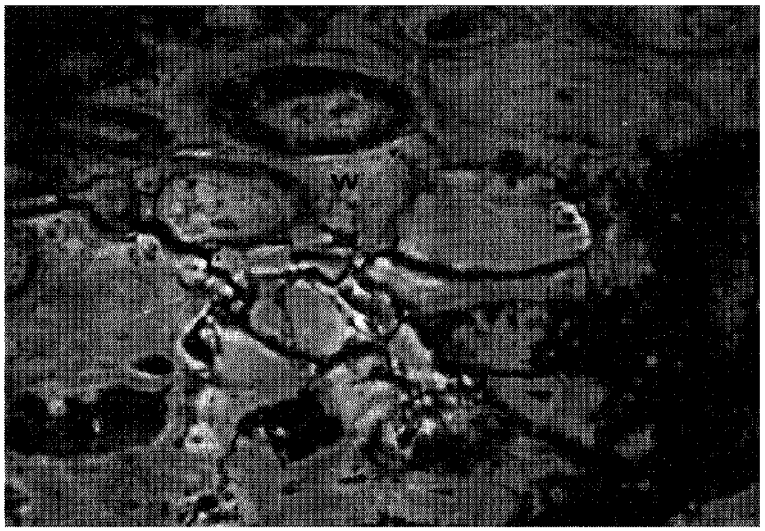

Plate I-15. *BSEM photomicrograph of section through woody plant material which has reacted with hyperalkaline groundwater. The cell walls of plant material (w) have been completely replaced and mineralised by calcite, whilst preserving the original cellular structure of the plant material. Sample C364, Fluvial Boulder Gravel, Western Springs, Maqarin.*

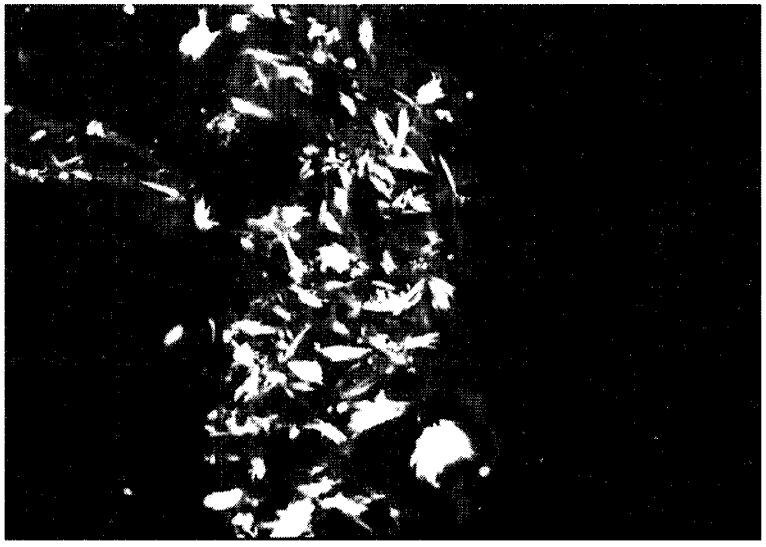

Plate I-16. *BSEM photomicrograph showing fine-grained fibrous chromium ettringite (bright) replacing part of the cellular fabric of woody plant material reacted with hyperalkaline groundwater. Sample C364, Fluvial Boulder Gravel, Western Springs, Maqarin.*

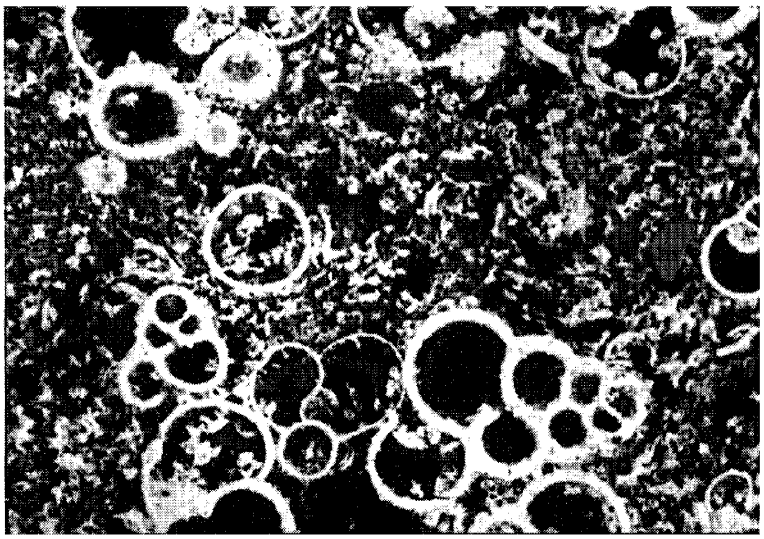

Plate I-17. *BSEM photomicrograph showing unaltered calcitic microfossils in micritic limestone clasts in colluvium reacted with hyperalkaline groundwater. The microfossil tests are infilled with secondary CSH gel (dull-grey). Sample C365, Basal Colluvium Layer, Western Springs, Maqarin.*

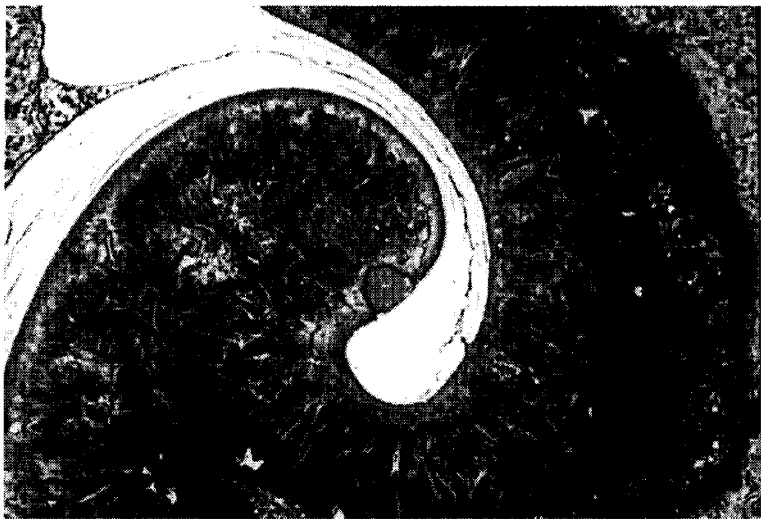

Plate I-18. *BSEM photomicrograph showing microfibrous CSH mineralisation lining calcite walls (bright) of microfossil test in colluvium reacted with hyperalkaline groundwater. Sample C365, Basal Colluvium Layer, Western Springs, Maqarin.*

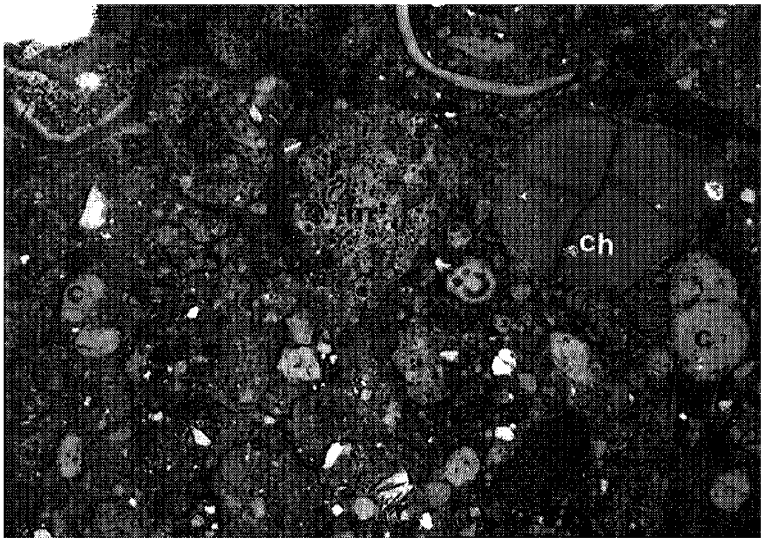

Plate I-19. *BSEM photomicrograph showing typical poorly-sorted fabric of the colluvium matrix. It comprises granule-grade fragments of mainly micritic (m), dolomicritic limestone and minor chert (ch), and sand-grade calcite micofossils and fragments of contemporary land-snail shells (c), 'floating' in a matrix of fine sand- to silt-grade calcite (micritic limestone) detritus with minor quartz silt. The chert grain (ch) exhibits alteration along microfractures as a result of reaction with hyperalkaline groundwater. Shrinkage cracks are seen in the matrix and are mineralised by secondary CSH and CASH alteration products. Sample C365, Basal Colluvium Layer, Western Springs, Maqarin.*

Plate I-20. *UV optical photomicrograph of thin-section of colluvium impregnated with UV-fluorescent-dyed epoxy-resin. The poorly-sorted sediment comprises angular clasts of micritic limestone and chert floating in a calcareous silty-sand to clay-grade matrix. The bright yellow regions indicate areas with higher porosity (i.e. areas impregnated with epoxy-resin). Higher porosity exists in the rims of clasts where reaction with hyperalkaline groundwater has produced a very porous altered microfabric. Width of field of view = approximately 4 mm. Sample C365, Basal Colluvium Layer, Western Springs, Maqarin.*

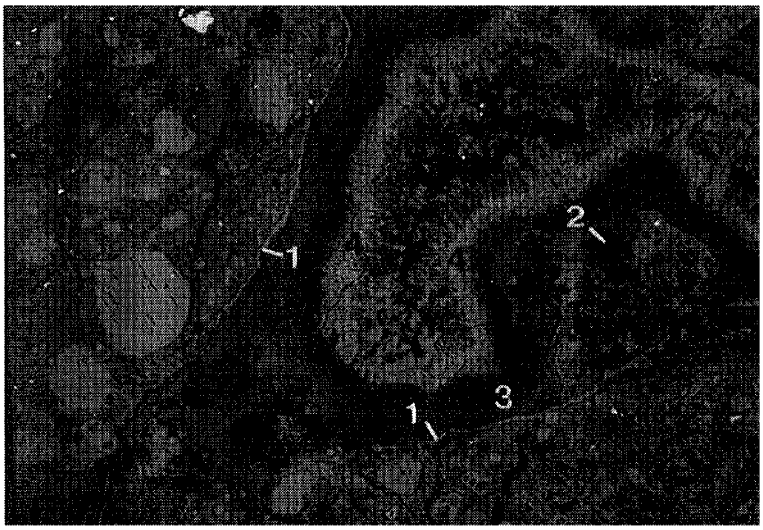

Plate I-21. *BSEM photomicrograph of irregular fissures or shrinkage cracks within the matrix of the colluvium mineralised and filled by complex fibrous and gel-like CSH/CASH alteration products. The early fissure-lining consists of a thin film of bright iron oxide (1). Relicts of a very hydrous fibrous CASH alteration product (2) are preserved locally within major gel-like CSH(I) to CHS(II) (or their Al-substituted equivalent compounds) forming the main fissure fill (3). Fibrous CSH (4) encrusts the gel-like CSH phase and is partially replaced by blocky aragonite or calcite. Sample C365, Basal Colluvium Layer, Western Springs, Maqarin.*

Plate I-22. *BSEM photomicrograph showing detail of hyperalkaline alteration products seen in Plate I-21: relicts of a very hydrous fibrous CASH alteration product (1) are preserved locally within major gel-like CSH(I) to CHS(II) (or their Al-substituted equivalent compounds) forming the main fissure fill (2); with fibrous CSH (3) encrusting the gel-like CSH phase and partially replaced by blocky aragonite or calcite. Sample C365, Basal Colluvium Layer, Western Springs, Maqarin.*

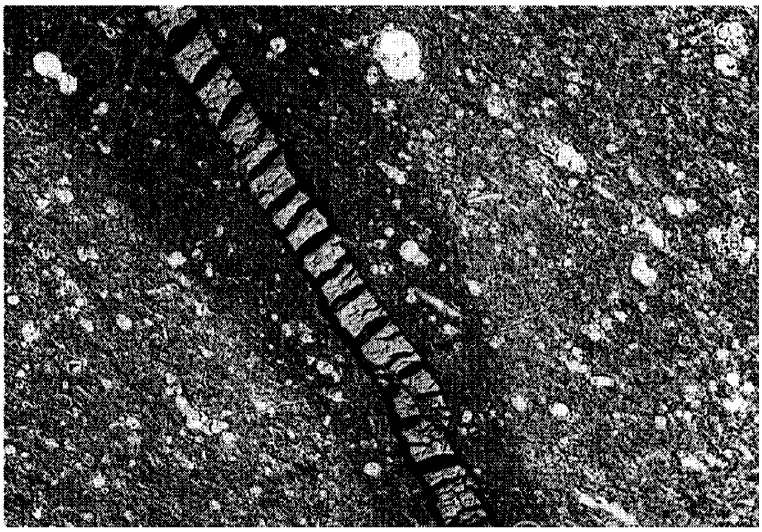

Plate I-23. *BSEM photomicrograph showing zone of enhanced microporosity in the biomicrite wallrock to a thin vein of ettringite formed by reaction of the biomicrite with hyperalkaline groundwater. Sample C359, Adit A-6, Maqarin.*

Plate I-24. *UV optical photomicrograph showing zone of enhanced microporosity (yellow fluorescent areas) in biomicrite wallrock to a thin veinlets of ettringite formed in highly microfractured biomicrite. Ettringite veins are formed as a result of reaction of the biomicrite with hyperalkaline groundwater. Field of view = 4 mm. Sample C359, Adit A-6, Maqarin.*

APPENDIX J

Matrix Diffusion Studies in Fractured Clay Biomicrite

PROFILE C353

Figure J-1. *Profile C353. Photograph showing sample vein and wallrock.*

Figure J-2. *Contact print of polished thin section of sample C353 showing complex vein structure (upper half) and relatively uniform biomicrite host rock (lower half). Note presence of microveining in host rock. Length of polished section is 35 mm.*

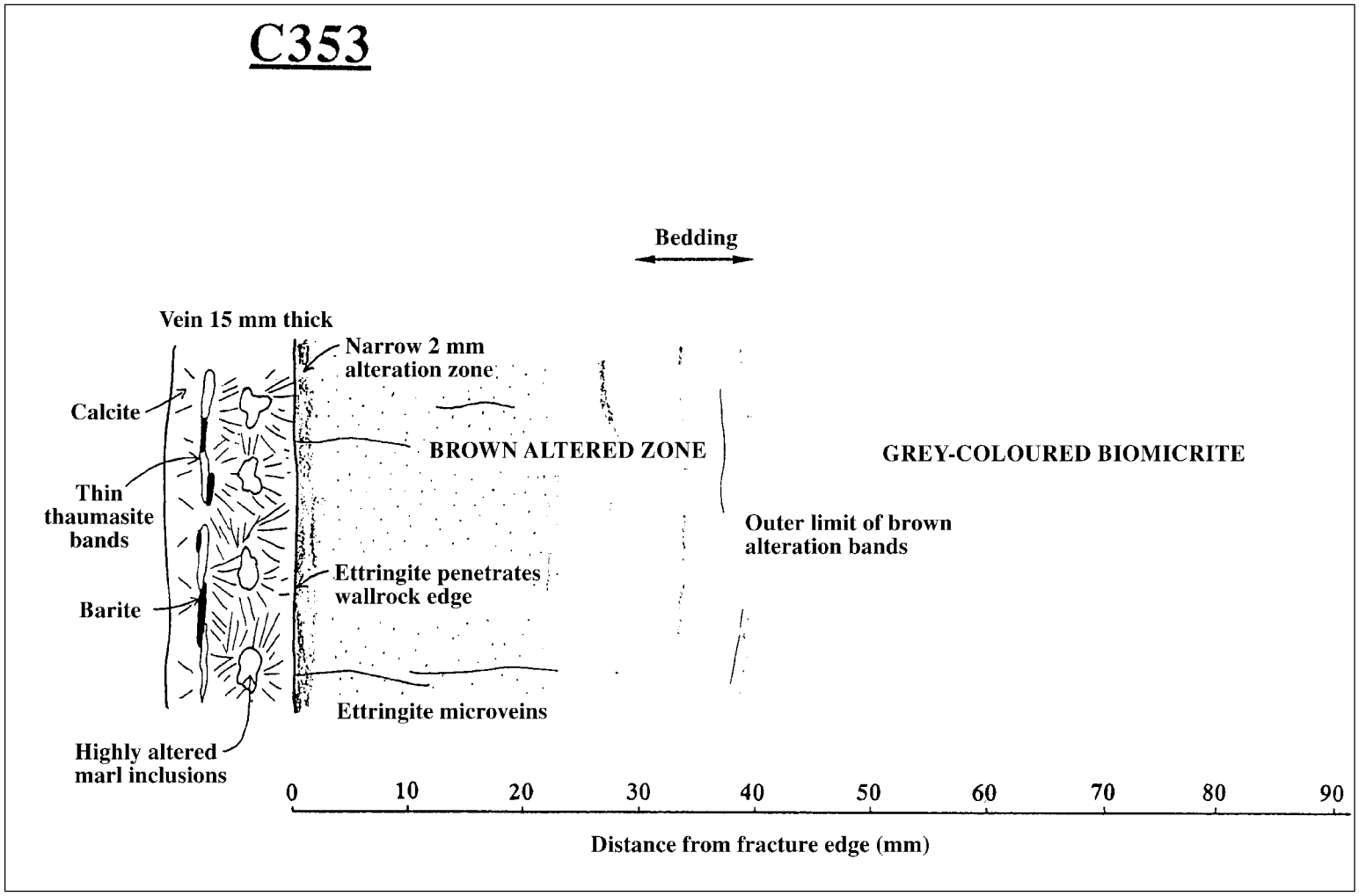

Figure J-3. *Profile C353. Diagrammatic sketch of vein and wallrock profile in sample C353.*

Table J-1. Profile C353. Geochemical profiles across biomicrite wallrock with increasing distance from fracture edge in sample C353. [Major elements are expressed as oxide weight per cent; trace elements as parts per million. LOI = Loss On Ignition; Total = total major element oxides including LOI. Total iron is expressed as Fe_2O_3].

Sample	SiO_2 %	TiO_2 %	Al_2O_3 %	Fe_2O_3t %	MnO %	MgO %	CaO %	Na_2O %	K_2O %	P_2O_5 %	LOI %	SO_3 %	Cr_2O_3 %	SrO %	Total %
C353 0–15	9.91	0.17	4.38	2.59	0	0.31	46.28	0.09	0.05	2.23	32.36	0.7	0.09	0.51	99.67
C353 15–30	9.57	0.16	4.51	2.05	0.01	0.27	46.88	0.07	0.06	2.17	32.73	0.6	0.09	0.59	99.76
C353 30–45	9.49	0.16	4.5	1.88	0.01	0.29	46.76	0.07	0.05	2.14	33.08	0.4	0.09	0.58	99.5
C353 45–60	9.64	0.17	4.62	2.03	0.01	0.29	46.78	0.07	0.04	2.16	32.99	0.3	0.08	0.64	99.82
C353 60–75	9.54	0.17	4.58	1.97	0	0.28	46.73	0.08	0.04	2.15	33.2	0.2	0.08	0.7	99.72
C353 75–90	9.29	0.16	4.37	1.92	0.01	0.27	46.81	0.07	0.07	2.12	33.43	0.3	0.08	0.76	99.66
C357 0–10	7.76	0.06	1.89	0.9	0	0.18	43	0.08	0.13	1.65	40.23	3.3	0.04	0.2	99.42
C357 50–75	4.88	0.07	2.01	1.04	0	0.22	42.54	0.11	0.1	1.83	43.33	3.1	0.05	0.26	99.54
C358 0–15	9.02	0.06	3.29	0.95	0	0.2	42.47	0.09	0.12	1.35	40.02	1.8	0.04	0.21	99.62
C358 40–55	5.28	0.07	1.79	1.05	0	0.24	42.52	0.1	0.12	1.51	43.69	2.9	0.05	0.21	99.53
C359 0–10	4.68	0.06	2.17	0.72	0	0.2	46.6	0.06	0.02	1.64	41.03	2.6	0.04	0.17	99.99
C359 10–17	5.48	0.06	2.22	0.67	0	0.18	46.59	0.07	0.02	1.61	40.31	2.4	0.03	0.18	99.82
C359 17–32	4.21	0.06	1.29	0.69	0	0.2	46.94	0.06	0.01	1.74	42.04	2.3	0.04	0.18	99.76
C359 32–48	5.04	0.06	1.15	0.67	0	0.19	46.67	0.07	0.02	1.7	41.17	2.7	0.04	0.18	99.66
C359 48–63	4.64	0.05	1.2	0.65	0	0.19	46.69	0.07	0.02	1.69	41.68	2.6	0.03	0.18	99.7
C359 63–77	3.85	0.06	1.13	0.68	0	0.2	46.88	0.06	0.01	1.72	42.17	2.6	0.04	0.17	99.57

Table J-1 (contd.). Profile C353. Geochemical profiles across biomicrite wallrock with increasing distance from fracture edge in sample C353. [Major elements are expressed as oxide weight per cent; trace elements as parts per million].

Sample	Chromium ppm	Cobalt ppm	Nickel ppm	Selenium ppm	Strontium ppm	Zirconium ppm	Molybdenum ppm	Caesium ppm	Barium ppm	Lead ppm	Thorium ppm	Uranium ppm
C353 (0–15)	564	4.0	264	50	4644	33.5	17.2	1.40	102	<5	2.82	23.4
C353 (15–30)	480	6.7	224	49	5309	27.0	5.4	1.83	118	<5	2.65	23.8
C353 (30–45)	408	7.5	208	42	5516	26.3	5.2	2.10	113	<5	2.51	22.7
C353 (45–60)	437	6.7	194	42	5646	26.2	4.9	2.23	102	<5	2.57	23.0
C353 (60–75)	454	6.7	196	45	6296	28.0	4.8	2.44	95	<5	2.52	22.4
C353 (75–90)	471	6.7	203	43	7208	27.4	5.4	3.00	93	<5	2.48	22.3
C357 (0–10)	318	4.7	162	63	1907	16.3	15.2	1.61	396	<5	1.12	20.1
C357 (50–75)	329	4.5	170	33	2256	16.1	13.8	1.11	106	<5	1.30	22.5
C358 (0–15)	289	2.6	90	33	1794	13.8	10.4	1.33	521	<5	1.03	16.3
C358 (40–55)	325	3.9	151	30	1855	15	13.1	1.17	135	<5	1.17	19.9
C359 (0–10)	250	3.6	127	53	1475	13.1	10.2	0.74	87	<5	0.93	13.0
C359 (10–17)	246	4.0	126	51	1515	13.7	10.5	1.05	109	<5	0.93	13.1
C359 (17–32)	268	3.9	137	49	1532	13.4	9.4	0.95	92	<5	0.95	13.7
C359 (32–48)	253	3.7	138	50	1628	13.2	8.7	1.27	121	<5	0.99	13.5
C359 (48–65)	254	3.9	139	41	1630	13.2	9.2	1.13	122	<5	0.96	13.4
C359 (63–77)	270	4.1	142	47	1529	13.6	10.1	0.89	97	<5	1.07	13.7

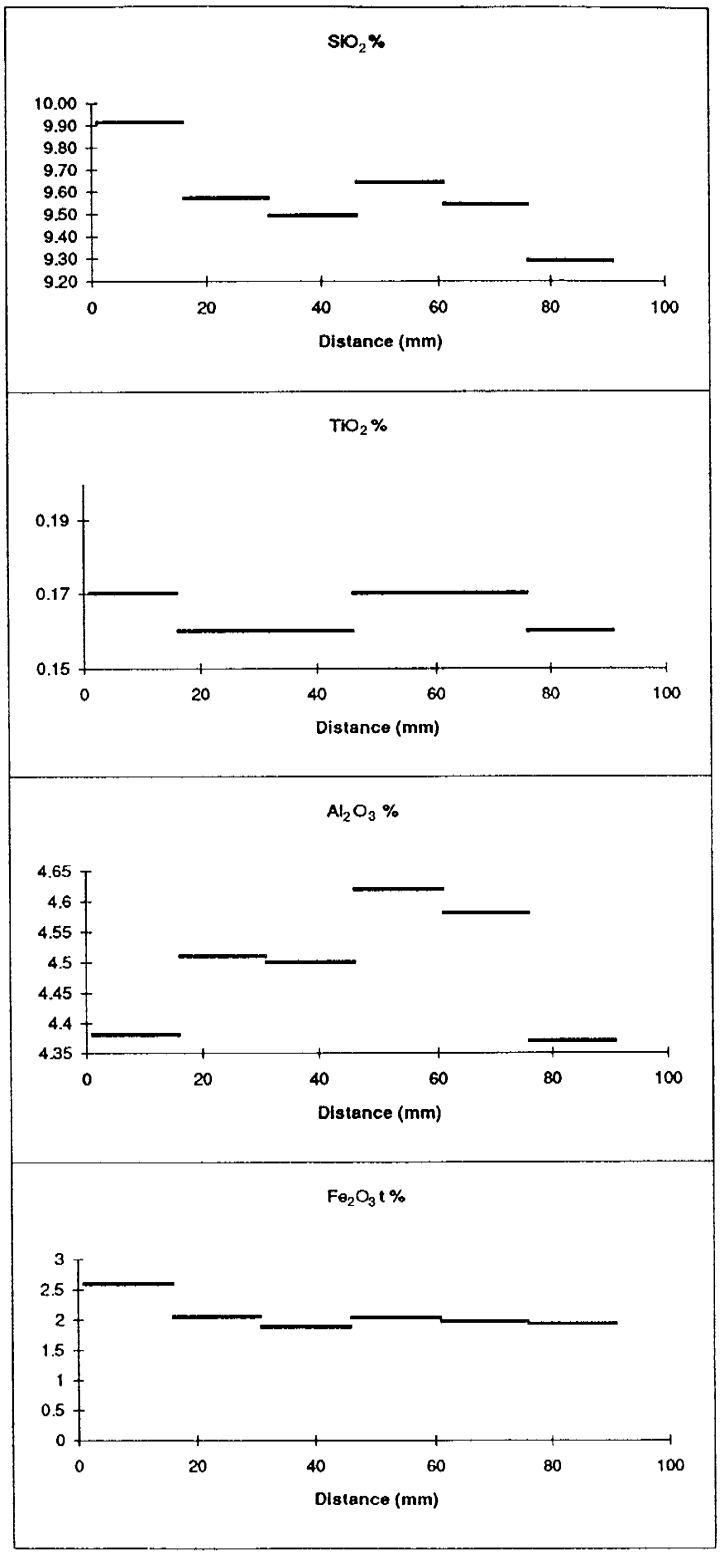
SiO2 %
10.00
9.90
9.80
9.70
9.60
9.50
9.40
9.30
9.20
0
20
40
60
80
100
Distance (mm)
TiO2 %
0.19
0.17
0.15
0
20
40
60
80
100
Distance (mm)
Al2O3 %
4.65
4.6
4.55
4.5
4.45
4.4
4.35
0
20
40
60
80
100
Distance (mm)
Fe2O3 t %
3
2.5
2
1.5
1
0.5
0
0
20
40
60
80
100
Distance (mm)

Figure J-4

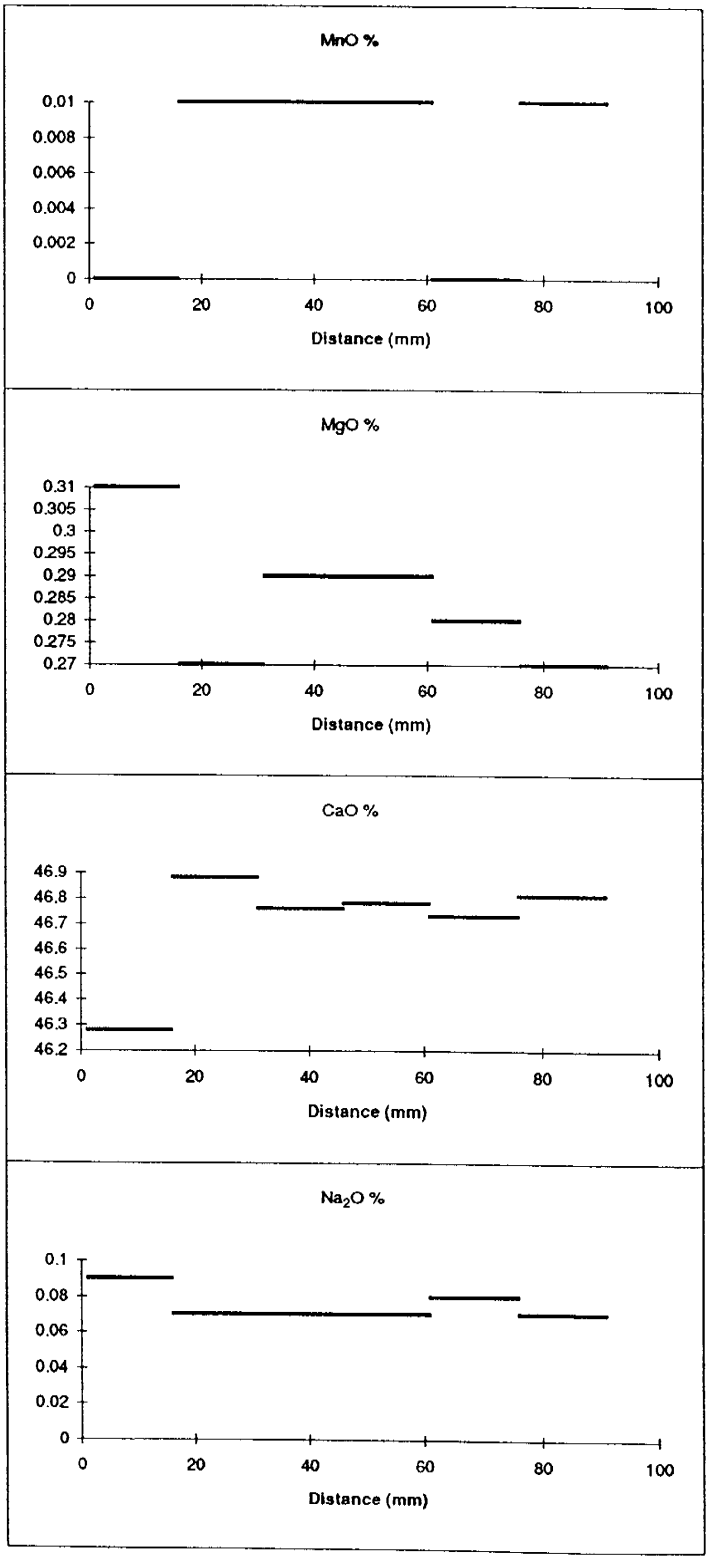
MnO %
0.01
0.008
0.006
0.004
0.002
0
0
20
40
60
80
100
Distance (mm)
MgO %
0.31
0.305
0.3
0.295
0.29
0.285
0.28
0.275
0.27
0
20
40
60
80
100
Distance (mm)
CaO %
46.9
46.8
46.7
46.6
46.5
46.4
46.3
46.2
0
20
40
60
80
100
Distance (mm)
Na2O %
0.1
0.08
0.06
0.04
0.02
0
0
20
40
60
80
100
Distance (mm)

Figure J-5

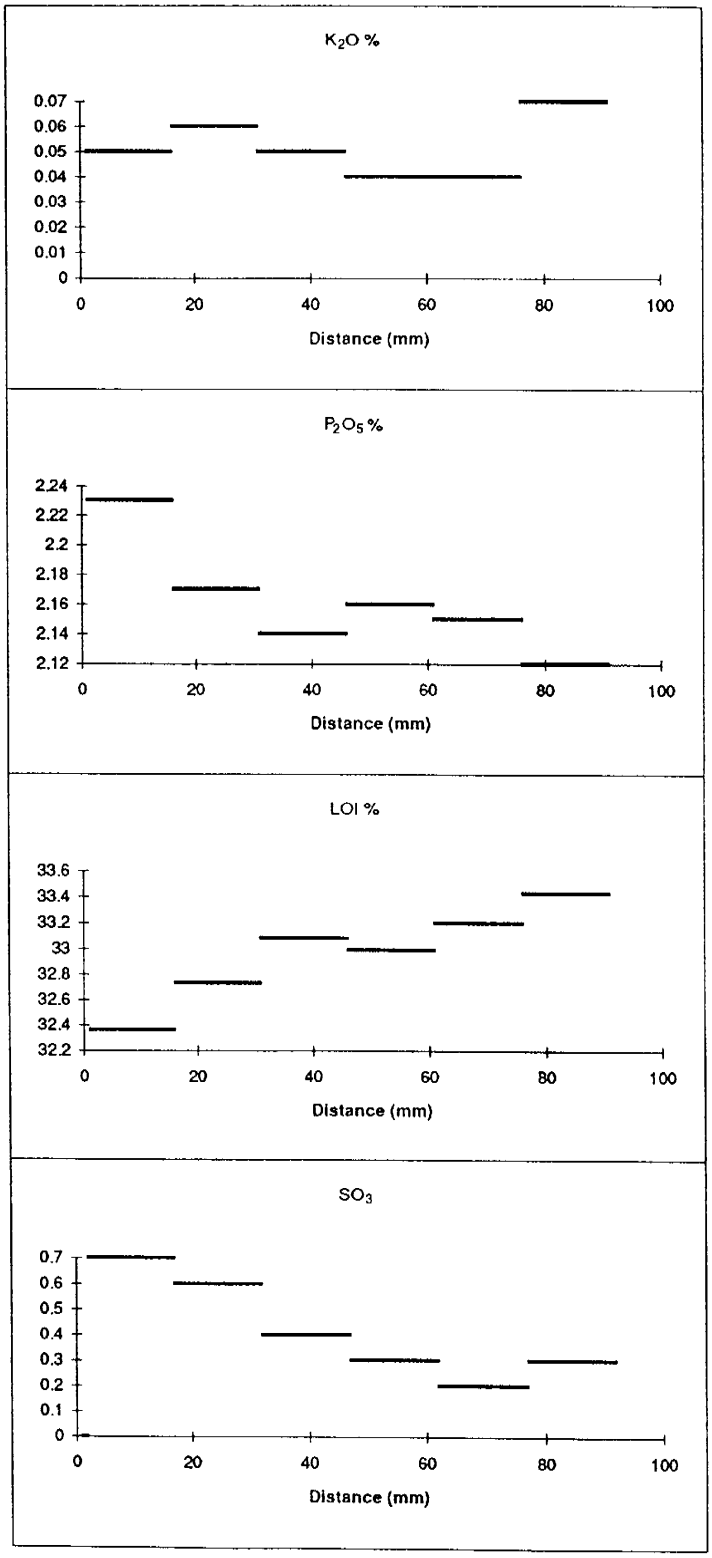
K2O %
0.07
0.06
0.05
0.04
0.03
0.02
0.01
0
0
20
40
60
80
100
Distance (mm)
P2O5 %
2.24
2.22
2.2
2.18
2.16
2.14
2.12
0
20
40
60
80
100
Distance (mm)
LOI %
33.6
33.4
33.2
33
32.8
32.6
32.4
32.2
0
20
40
60
80
100
Distance (mm)
SO3
0.7
0.6
0.5
0.4
0.3
0.2
0.1
0
0
20
40
60
80
100
Distance (mm)

Figure J-6

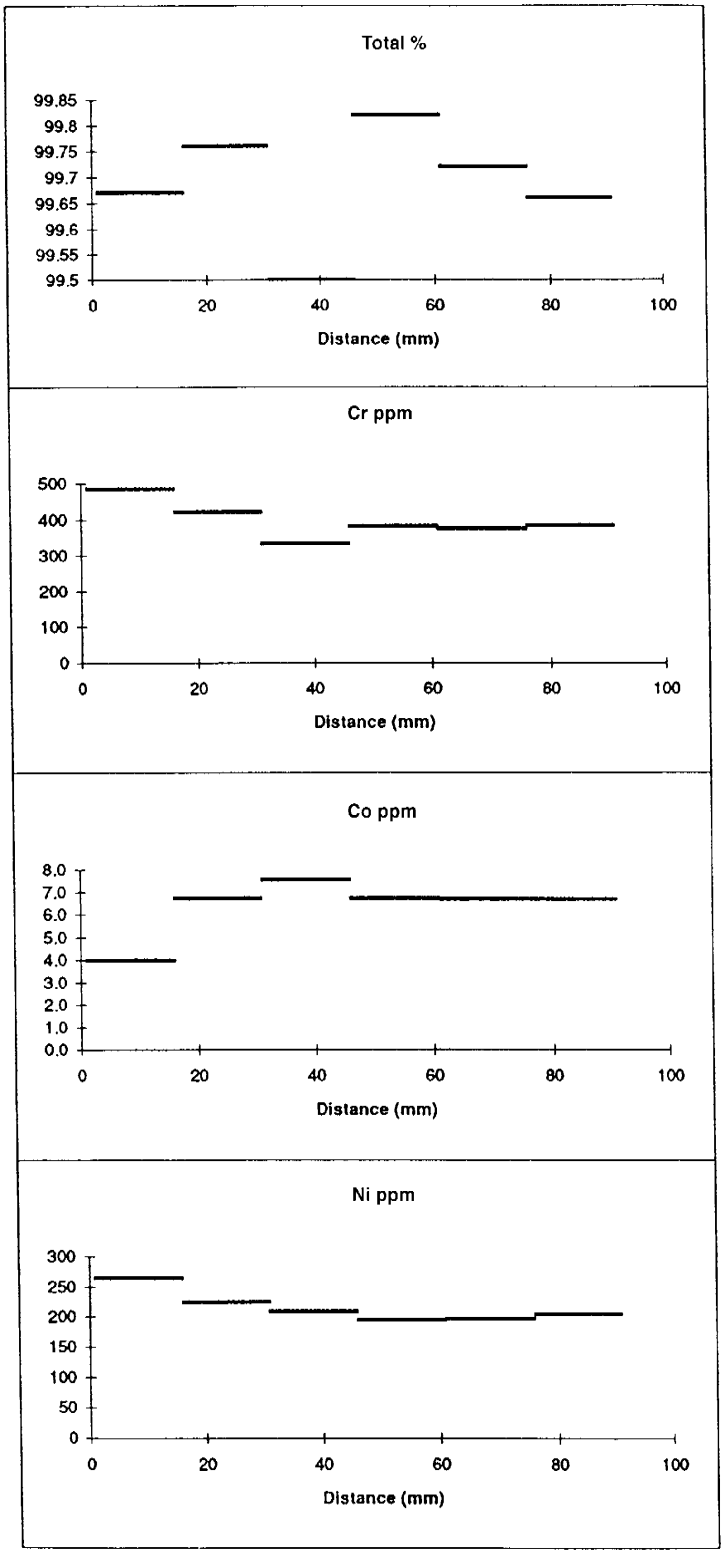
Total %
99.85
99.8
99.75
99.7
99.65
99.6
99.55
99.5
0
20
40
60
80
100
Distance (mm)
Cr ppm
500
400
300
200
100
0
0
20
40
60
80
100
Distance (mm)
Co ppm
8.0
7.0
6.0
5.0
4.0
3.0
2.0
1.0
0.0
0
20
40
60
80
100
Distance (mm)
Ni ppm
300
250
200
150
100
50
0
0
20
40
60
80
100
Distance (mm)

Figure J-7

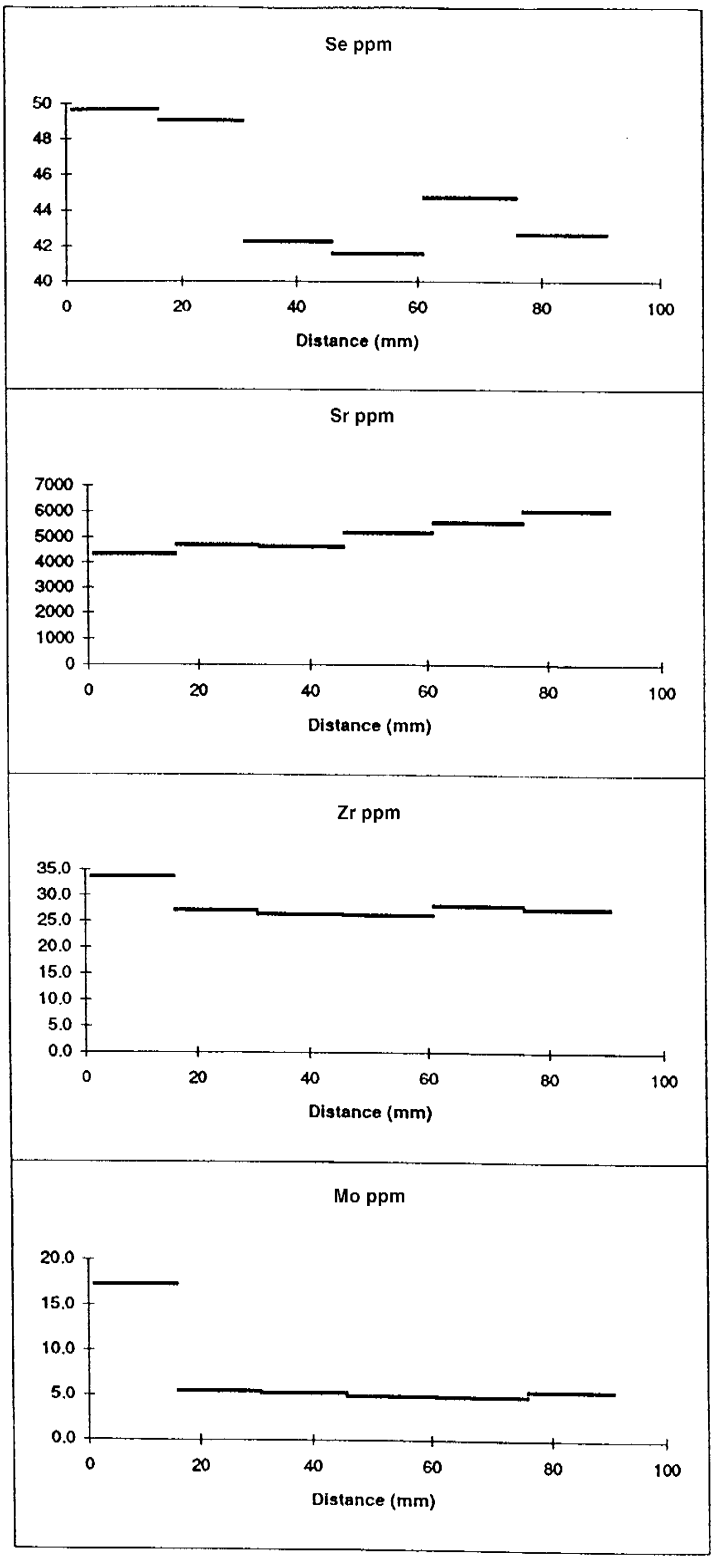
Se ppm
50
48
46
44
42
40
0
20
40
60
80
100
Distance (mm)
Sr ppm
7000
6000
5000
4000
3000
2000
1000
0
0
20
40
60
80
100
Distance (mm)
Zr ppm
35.0
30.0
25.0
20.0
15.0
10.0
5.0
0.0
0
20
40
60
80
100
Distance (mm)
Mo ppm
20.0
15.0
10.0
5.0
0.0
0
20
40
60
80
100
Distance (mm)

Figure J-8

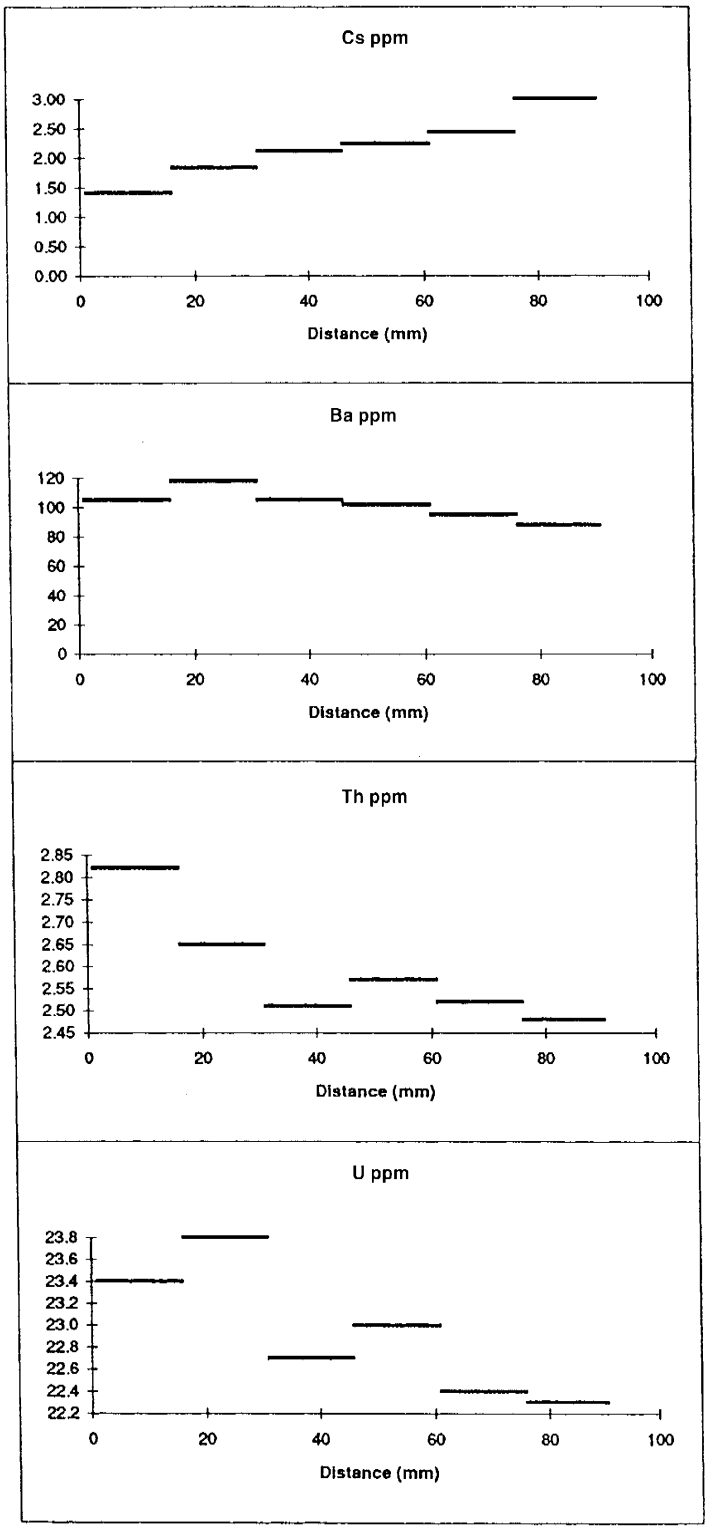
Cs ppm
3.00
2.50
2.00
1.50
1.00
0.50
0.00
0
20
40
60
80
100
Distance (mm)
Ba ppm
120
100
80
60
40
20
0
0
20
40
60
80
100
Distance (mm)
Th ppm
2.85
2.80
2.75
2.70
2.65
2.60
2.55
2.50
2.45
0
20
40
60
80
100
Distance (mm)
U ppm
23.8
23.6
23.4
23.2
23.0
22.8
22.6
22.4
22.2
0
20
40
60
80
100
Distance (mm)

Figure J-9

Table J-2. Profile C353. In situ Laser Ablation Microprobe – Inductively Coupled Plasma – Mass Spectrometry (LAMP-ICP-MS) element profiles across the biomicrite wallrock with increasing distance from fracture edge in sample C353.

Distance from vein (mm)	Sample	Aluminium ^{27}Al	Calcium ^{44}Ca	Chromium ^{53}Cr	Iron ^{57}Fe	Cobalt ^{59}Co	Nickel ^{60}Ni	Selenium ^{78}Se	Selenium ^{82}Se	Strontium ^{86}Sr	Zirconium ^{90}Zr	Molybdenum ^{98}Mo	Caesium ^{133}Cs	Barium ^{138}Ba	Lead ^{208}Pb	Thorium ^{232}Th	Uranium ^{238}U
0.1	C353/8A	35715	334286	2506	5362	10.0	464	584	483	2086	13	18.0	1.0	183	7.2	1.1	13
0.1	C353/8B	41563	334286	3929	5159	18.2	821	3850	3287	2291	14	19.3	1.2	314	5.8	1.0	17
0.25	C353/8D	40117	334286	1567	6532	7.2	194	91	54	7330	28	8.4	3.0	265	3.7	3.2	35
0.5	C353/BE	30008	334286	1112	6291	4.2	163	87	53	5755	25	6.2	2.1	200	4.0	2.5	29
1	C353/8F	28025	334286	1037	7656	2.7	172	84	51	5435	24	9.1	1.9	183	4.6	3.7	38
1.5	C353/8G	31011	334286	1222	10517	2.7	218	90	55	6120	23	9.5	2.0	232	4.3	3.1	30
2	C353/8H	28790	334286	1122	15401	2.9	321	77	47	5384	26	10.2	1.8	182	4.9	4.2	32
3	C353/8I	25733	334286	994	11912	3.1	408	68	42	4369	21	7.3	1.7	180	3.7	1.8	22
4	C35378J	25706	334286	932	12670	2.9	246	65	40	4520	23	8.0	2.1	174	4.0	2.4	22
5	C353/8K	21556	334286	722	7444	2.4	155	74	45	4326	24	6.5	1.5	167	3.0	2.4	27
6	C353/8L	21844	334286	717	6732	2.0	142	70	43	4172	25	5.9	1.6	140	2.8	1.7	20
7	C353/8M	24487	334286	837	15431	2.8	227	68	41	4599	21	15.3	1.9	182	4.0	2.0	21
8	C353/8N	20007	334286	720	10789	2.3	160	61	37	3662	15	10.3	1.4	134	3.6	1.6	17
9	C353/8O	22469	334286	706	8710	2.3	166	60	37	3835	23	5.8	1.5	147	3.0	2.1	27
10	C353/8P	22744	334286	667	7554	2.3	152	69	42	4107	28	4.4	1.7	148	3.7	1.9	21
12	C353/8Q	25721	334286	816	6654	2.1	140	60	37	4577	26	4.2	1.8	170	2.6	2.3	24
13.5	C353/8R	24879	334286	657	5496	2.3	122	56	34	3555	41	4.6	1.4	119	2.4	1.9	19
13.5	C353/8S	20483	334286	757	8968	2.5	159	102	62	3646	17	4.9	2.0	555	9.0	1.6	20
16	C353/8T	17608	334286	809	7224	3.0	173	119	73	3921	21	5.5	1.8	451	10.8	1.6	23
18	C353/8U	20322	334286	858	8157	2.4	209	126	77	4250	27	6.7	2.3	320	11.2	2.0	23
20	C353/8V	20846	334286	904	19720	2.8	259	110	67	4684	42	10.3	1.7	351	9.5	1.7	18
25	C353/8W	15412	334286	585	9202	6.2	206	184	112	3498	11	5.4	1.4	222	5.0	1.5	20
30	C353/8X	17135	334286	605	6473	2.7	113	148	90	4269	13	4.1	1.4	293	4.5	1.8	26
35	C353/BY	21759	334286	704	11174	7.1	223	96	58	4710	17	5.4	1.4	411	6.4	1.4	19
41	C353/8Z	21589	334286	809	14755	8.7	260	65	40	5069	15	6.2	1.7	310	9.0	1.7	23
41.5	C353/8AA	27205	334286	857	4423	2.8	108	60	37	6957	22	3.7	7.7	161	2.9	2.0	25
46.5	C353/8AB	24807	334286	808	4554	3.0	108	58	35	3579	19	3.1	1.5	100	2.3	2.2	22
51.5	C353/8AC	28166	334286	768	6995	3.9	147	60	37	19845	17	3.6	9.5	363	3.3	1.5	19
56.5	C353/8AD	26875	334286	779	7716	4.9	207	63	38	6859	21	4.0	4.0	161	3.9	1.9	21
61.5	C353/8AE	25478	334286	719	4936	3.1	107	64	39	4492	19	3.0	1.8	110	2.8	1.6	19
66.5	C353/8AF	22979	334286	691	15983	5.0	283	56	34	4947	19	5.2	1.9	129	3.8	1.5	18
71.5	C353/8AG	24313	334286	739	5385	2.8	102	58	35	5545	17	3.6	2.6	138	3.9	1.9	23

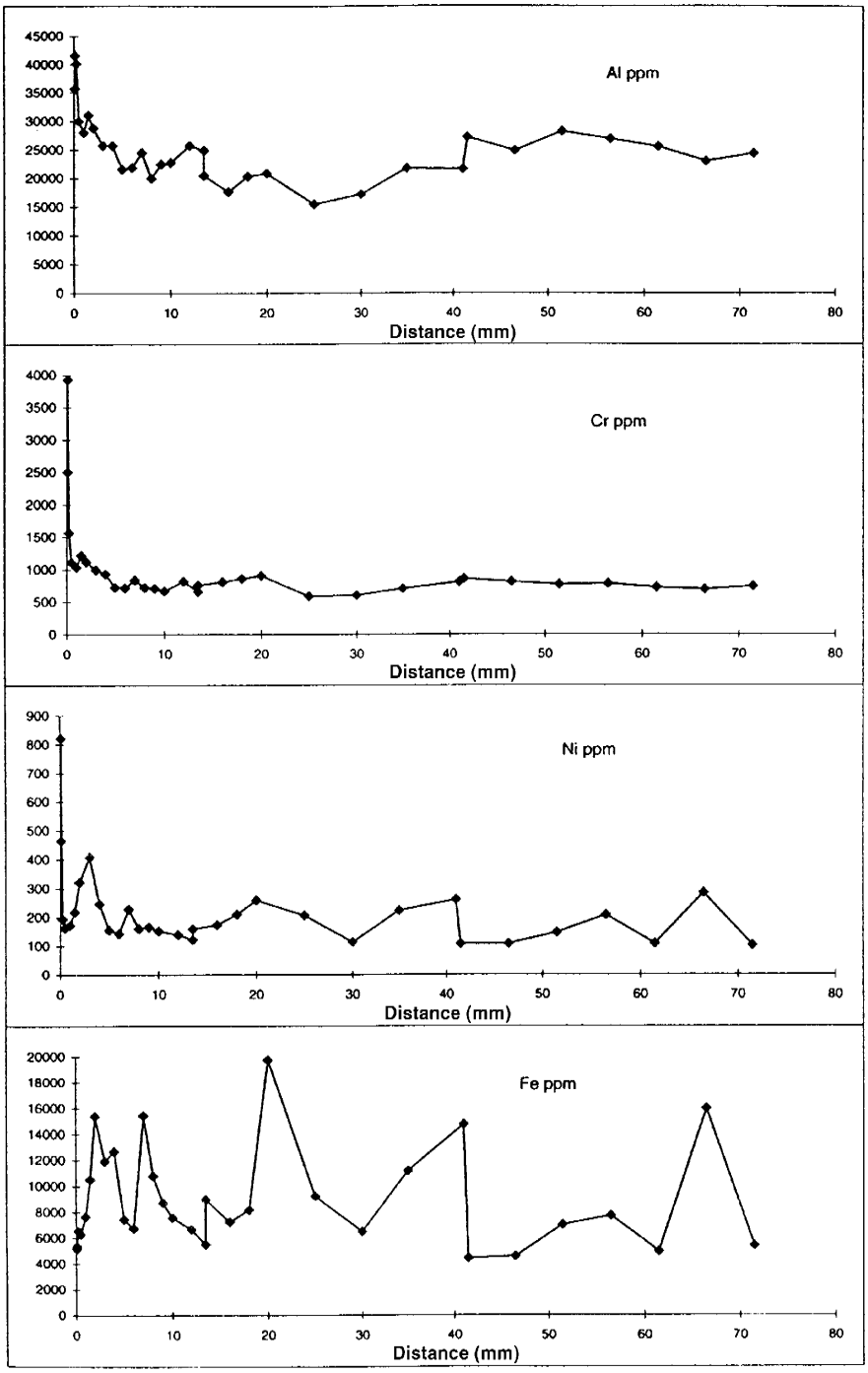
Al ppm
Distance (mm)
Cr ppm
Distance (mm)
Ni ppm
Distance (mm)
Fe ppm
Distance (mm)

Figure J-10

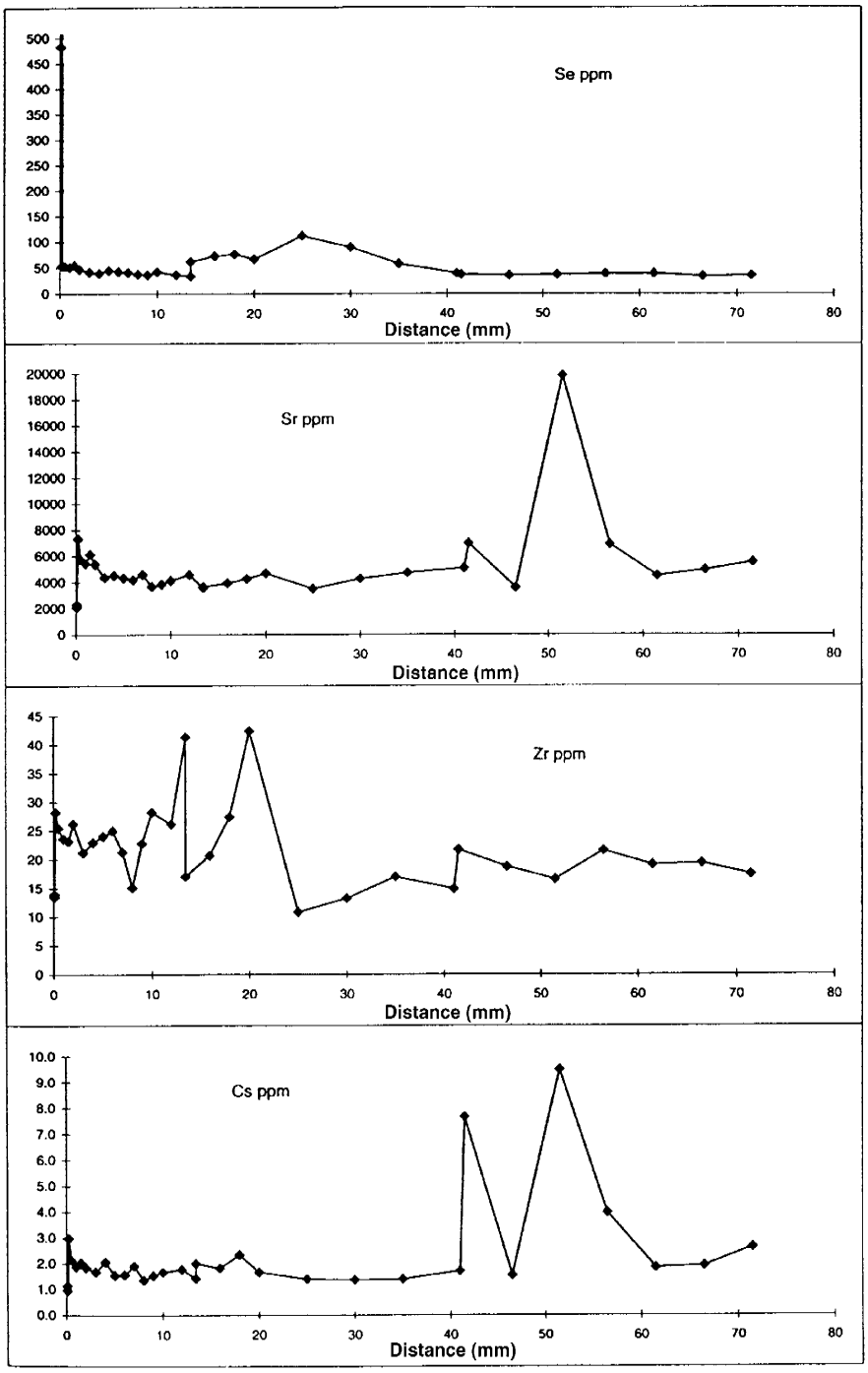
Se ppm
500
450
400
350
300
250
200
150
100
50
0
0 10 20 30 40 50 60 70 80
Distance (mm)
Sr ppm
20000
18000
16000
14000
12000
10000
8000
6000
4000
2000
0
0 10 20 30 40 50 60 70 80
Distance (mm)
Zr ppm
45
40
35
30
25
20
15
10
5
0
0 10 20 30 40 50 60 70 80
Distance (mm)
Cs ppm
10.0
9.0
8.0
7.0
6.0
5.0
4.0
3.0
2.0
1.0
0.0
0 10 20 30 40 50 60 70 80
Distance (mm)

Figure J-11

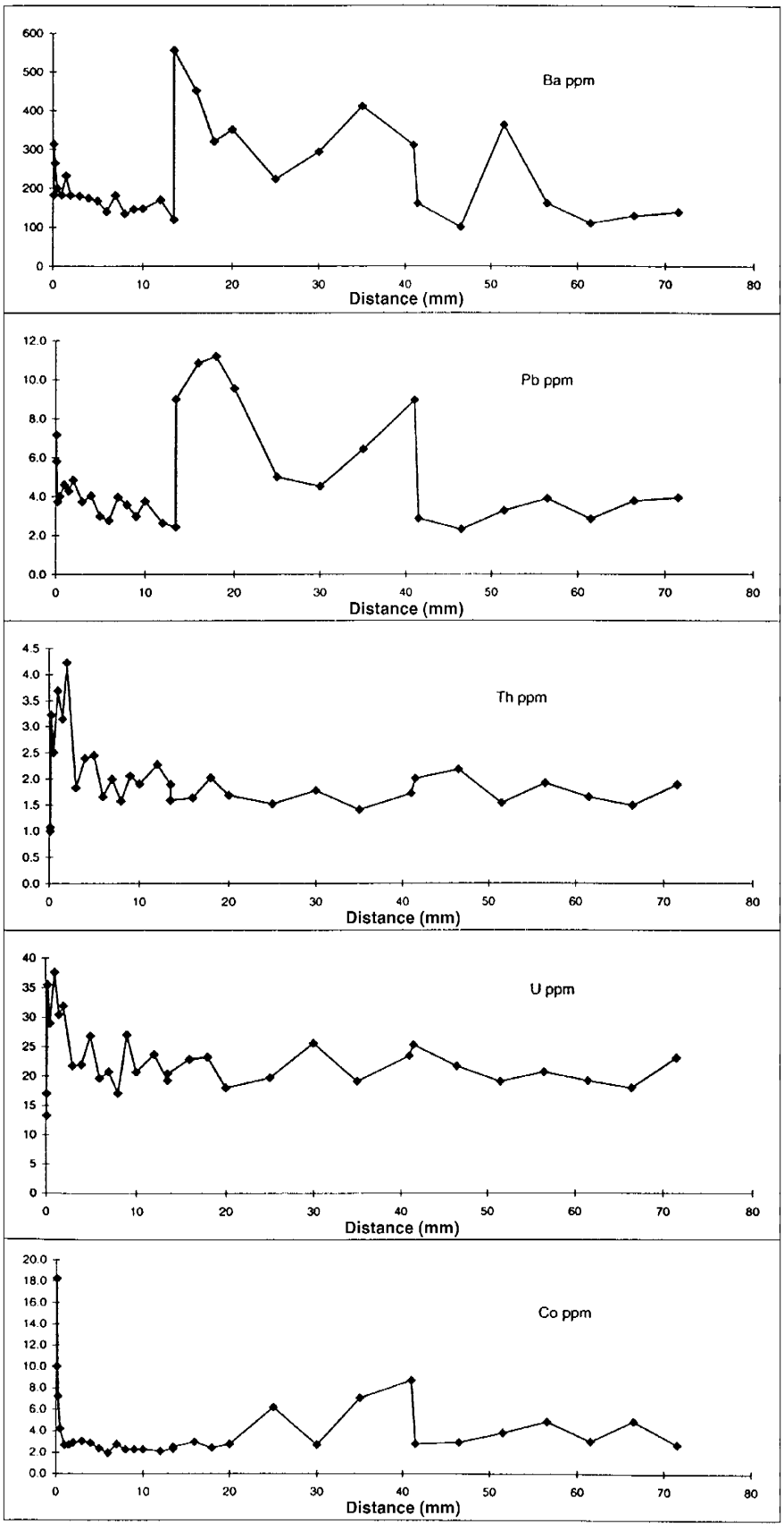
Ba ppm
Distance (mm)
Pb ppm
Distance (mm)
Th ppm
Distance (mm)
U ppm
Distance (mm)
Co ppm
Distance (mm)

Figure J-12

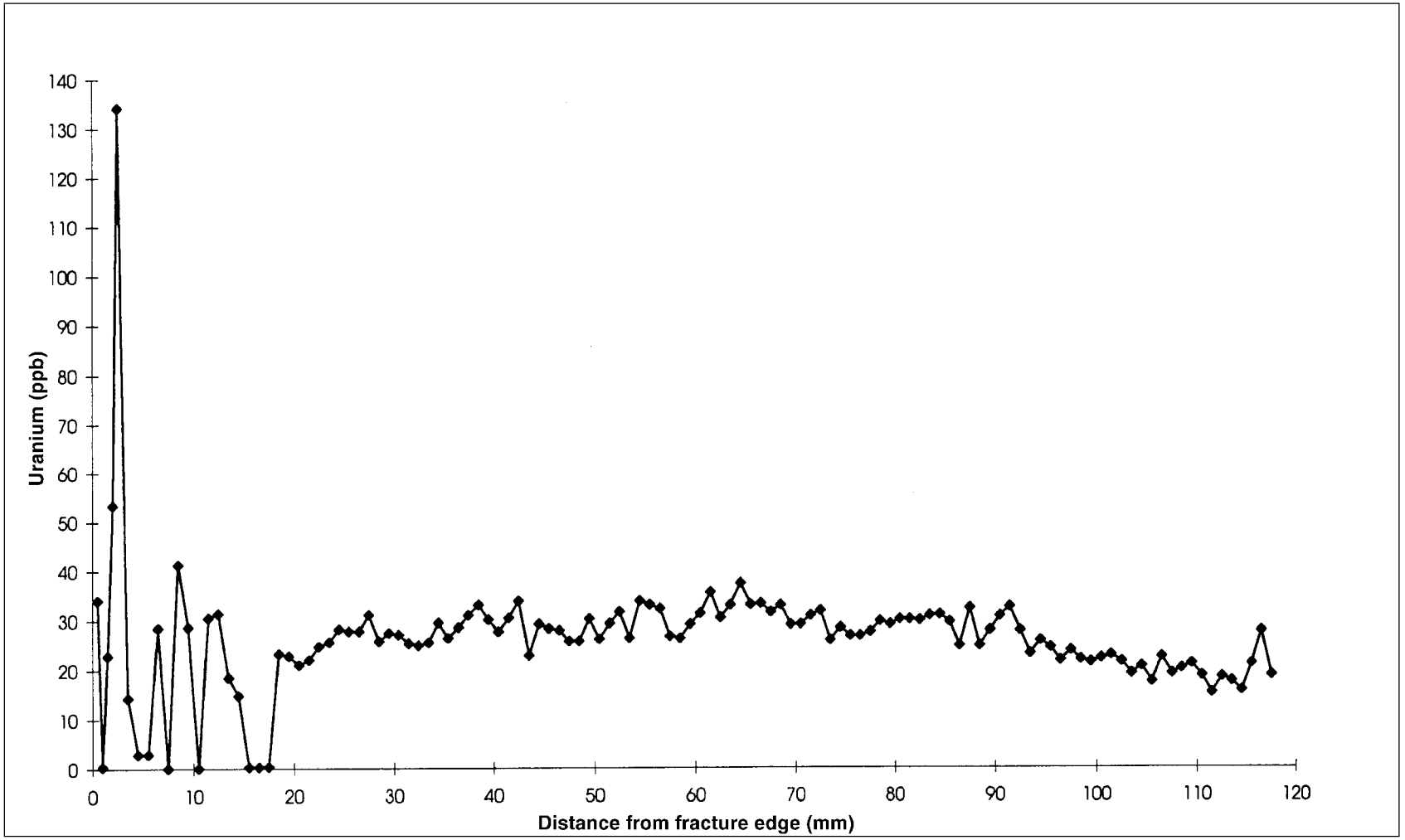

Figure J-13. *Profile C353. Fission Track Registration (FTR) analysis of uranium distribution.*

Table J-3. Profile C353. In situ element analysis of vein material using the Laser Ablation Microprobe (LAMP).

Sample Name Marl	Chromium ^{53}Cr	Iron ^{57}Fe	Cobalt ^{59}Co	Nickel ^{60}Ni	Selenium ^{78}Se	Selenium ^{82}Se	Strontium ^{86}Sr	Zirconium ^{90}Zr	Molybdenum ^{98}Mo	Caesium ^{133}Cs	Barium ^{138}Ba	Lead ^{208}Pb	Thorium ^{232}Th	Uranium ^{238}U
C353/1A	1743	25791	4.8	593	402	377	2683	27	36	1.5	94	6.0	2.2	33
C353/1B	1575	20018	3.8	468	380	262	2244	31	39	1.1	85	5.7	2.3	33
C353/1C	1223	4871	3.0	165	72	76	3525	23	6.3	5.6	119	3.7	2.6	33
C353/1D	952	4242	2.3	144	96	53	3001	24	5.5	4.6	98	2.6	2.6	33
C353/1E	1040	4597	2.2	156	155	73	3813	23	5.2	6.4	151	3.4	2.2	33
C353/1F	1185	4639	2.8	290	426	368	3530	35	6.3	5.6	365	2.7	1.7	33
C353/4A	4598	27165	8.4	826	401	313	8053	101	18	0.7	390	14	10	100
C353/4B	4360	20712	13	991	632	660	7180	93	23	0.8	210	17	11	100
C353/5A	2210	13672	3.5	316	147	154	5279	37	7.5	4.7	2447	4.1	3.2	35
C353/5B	2914	25805	4.5	465	93	170	2299	71	11	0.7	255	7.5	4.5	35
C353/6D	2338	4565	1.9	86	223	193	1007	15	3.6	2.7	856	1.3	1.6	25
C353/8A	6215	13301	25	1152	1449	1198	5175	33	45	2.4	453	18	2.7	33
C353/8B	7617	10002	35	1592	7464	6373	4441	27	37	2.2	608	11	1.9	33
Barite														
C353/2E	43967	1017783	107	14540	577	644	1475	28	92	1.3	672	24	2.1	54
C353/2F	13228	77438	8.5	838	730	895	4816	28	17	1.6	486	45	2.0	54
C353/3A	62111	165282	10	2345	785	630	2619	69	1103	2.1	177	56	2.6	134
C353/3B	38450	324658	12	3679	867	791	5467	103	1499	3.6	316	61	1.1	134
C353/7A	5453	51848	2.8	599	495	448	532	13	125	1.3	595	10	0.3	100
C353/3C	1435	4820	2.7	435	399	311	9292	12	9.3	1.5	127656	3.1	1.0	25
Ettringite														
C353/4C	158	2924	0.9	25	197	192	179	1.8	0.5	0.3	36	1.3	0.1	1
C353/6B	149	3524	0.5	41	43	29	113	1.9	1.9	0.1	13	1.4	0.1	1.0
C353/6C	58	606	0.2	7.3	50	52	36	0.9	0.2	0.1	1.2	0.2	0.1	1.0
C353/8C	95	9857	3	45	6209	5301	1746	1.8	1.1	0.5	39	3.0	0.1	1.0
Calcium silicate														
C353/2C	512	2568	1.3	54	353	411	2111	5.8	4.6	0.6	3854	1.0	0.6	20
C353/3D	2549	5026	4.3	537	426	445	8354	34	11	2.7	123692	4.0	1.2	25
Calcite														
C353/2D	6.9	2940	1.2	9.4	143	96	708	0.8	0.4	0.5	80	1.0	0.1	0.6

Note: Data not subjected to full correction procedure (semi-quantitative only).
Uranium data derived from fission track analysis.

Table J-4. Profile C353. Profiles of U-series data across biomicrite wallrock with increasing distance from fracture edge in sample C353. Error bars represent 1 sigma uncertainties due to counting statistics alone.

Sample	U (ppm)	Th (ppm)	^{226}Ra (mBq/g)	$^{234}U/^{238}U$	$^{230}Th/^{234}U$	$^{228}Th/^{232}Th$	$^{226}Ra/^{238}U$
C353							
0–15 mm	18.7(6)	2.4(2)	224(3)	0.97(3)	1.11(4)	1.0(1)	0.96(3)
15–30 mm	19.8(6)	2.7(2)	–	0.88(3)	1.18(5)	0.7(1)	–
30–45 mm	19.0(6)	2.3(2)	173(2)	0.98(3)	0.98(4)	1.0(1)	0.73(2)
45–60 mm	18.6(5)	2.3(2)	–	0.91(2)	1.06(4)	0.7(1)	–
60–75 mm	18.7(6)	1.8(2)	–	0.89(3)	1.08(4)	1.1(2)	–
75–90 mm	18.5(5)	2.0(2)	236(3)	0.94(3)	1.09(4)	1.1(2)	1.03(3)
C357							
0–10 mm	18.6(5)	2.3(2)	–	0.95(3)	0.99(4)	1.1(2)	–
50–75 mm	19.7(7)	0.9(1)	–	1.02(4)	0.97(4)	1.4(3)	–
C358							
0–15 mm	14.7(5)	1.1(1)	–	1.00(4)	1.06(5)	1.2(2)	–
40–55 mm	17.7(6)	1.0(1)	–	0.96(4)	0.96(4)	1.3(2)	–
C359							
0–10 mm	13.2(4)	3.1(2)	122(2)	0.96(4)	0.96(4)	1.3(1)	0.74(3)
10–17 mm	12.0(3)	2.4(2)	–	0.98(3)	0.97(4)	1.1(2)	–
17–32 mm	12.7(3)	*	137(2)	0.99(3)	1.15(4)	–	0.87(2)
32–48 mm	13.8(4)	*	–	0.94(3)	1.04(5)	–	–
48–63 mm	11.9(4)	2.7(2)	–	0.99(4)	1.08(5)	1.1(1)	–
63–77 mm	12.2(5)	1.3(1)	112(2)	1.02(5)	0.99(5)	0.8(1)	0.74(3)

All errors in parentheses are in least significant place and are 1 sigma uncertainties due to counting statistics alone.

* Results for ^{232}Th for C359 17–32 and 32–48 mm failed laboratory quality assurance (QA).

Average chemical recoveries are C353 (80% U and 77% Th) and C359 (70% U and 71% Th).

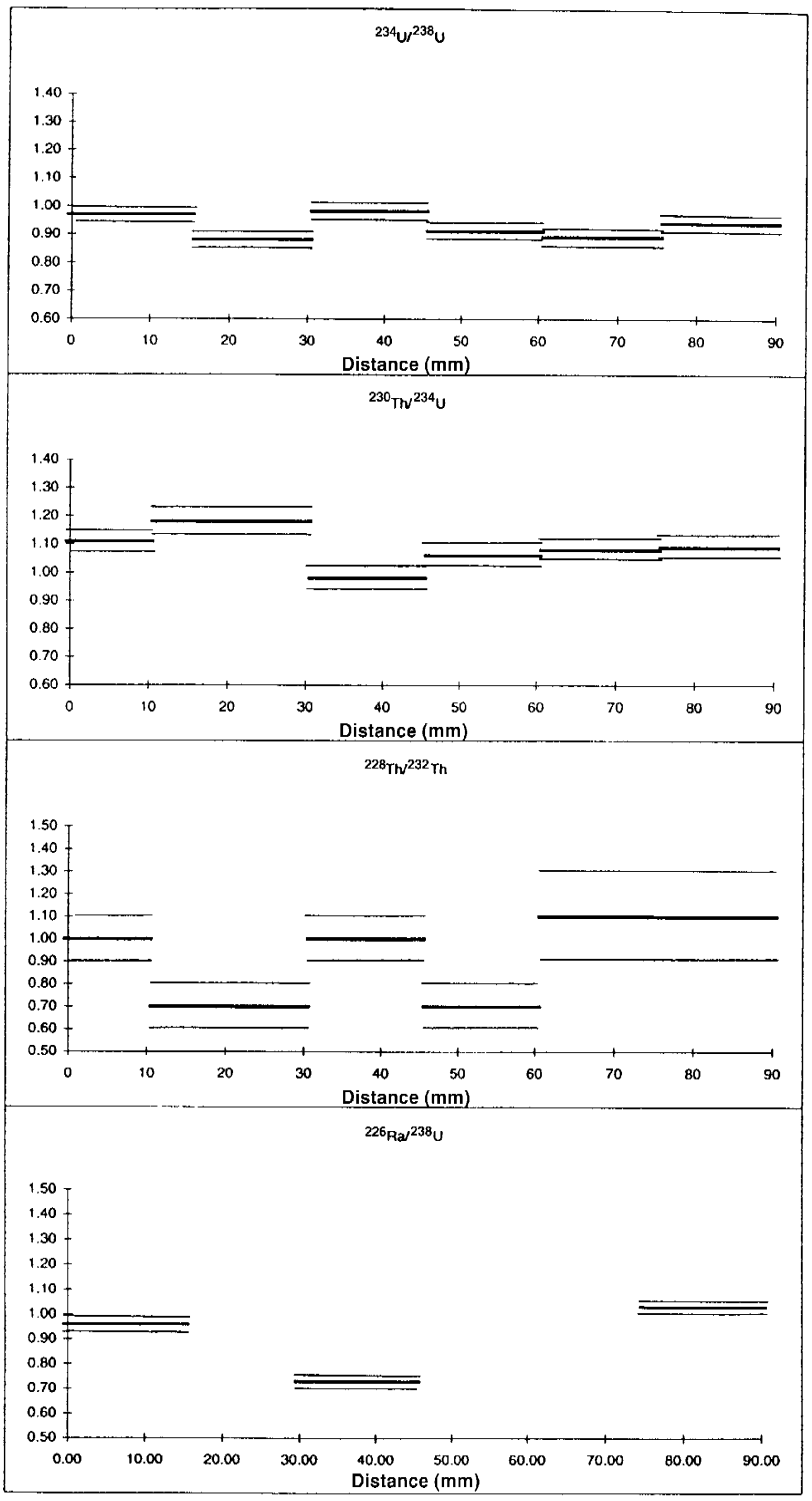

Note: Error bars represent 1 sigma uncertainties due to counting statistics alone.

Figure J-14

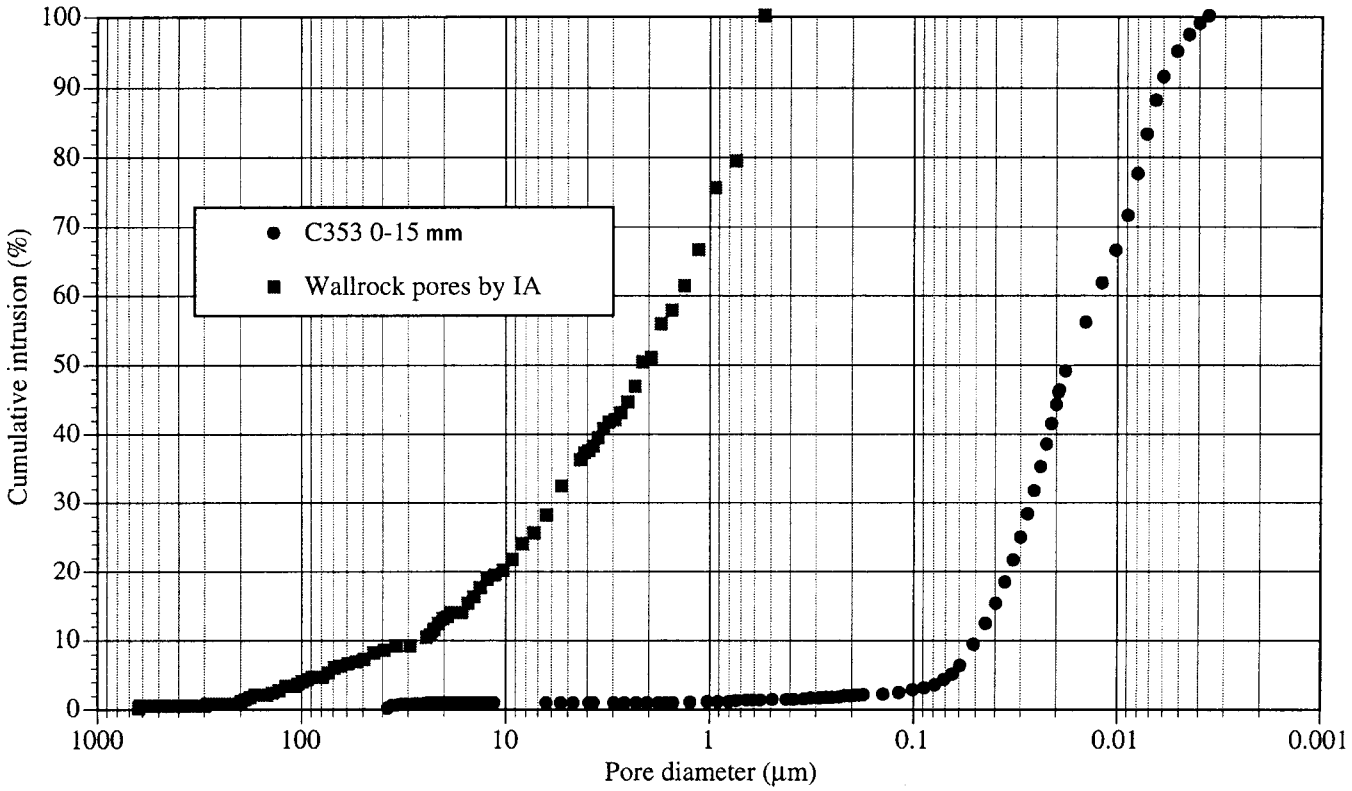

Figure J-15. *Profile C353. Comparison of pore throat diameters determined by liquid resaturation porosimetry and pore areas determined by image analysis from one thin section along profile C353 (0–15 mm).*

PROFILE C357

Figure J-16. *Profile C357. Photograph showing fracture sample C357 in situ in Adit A-6.*

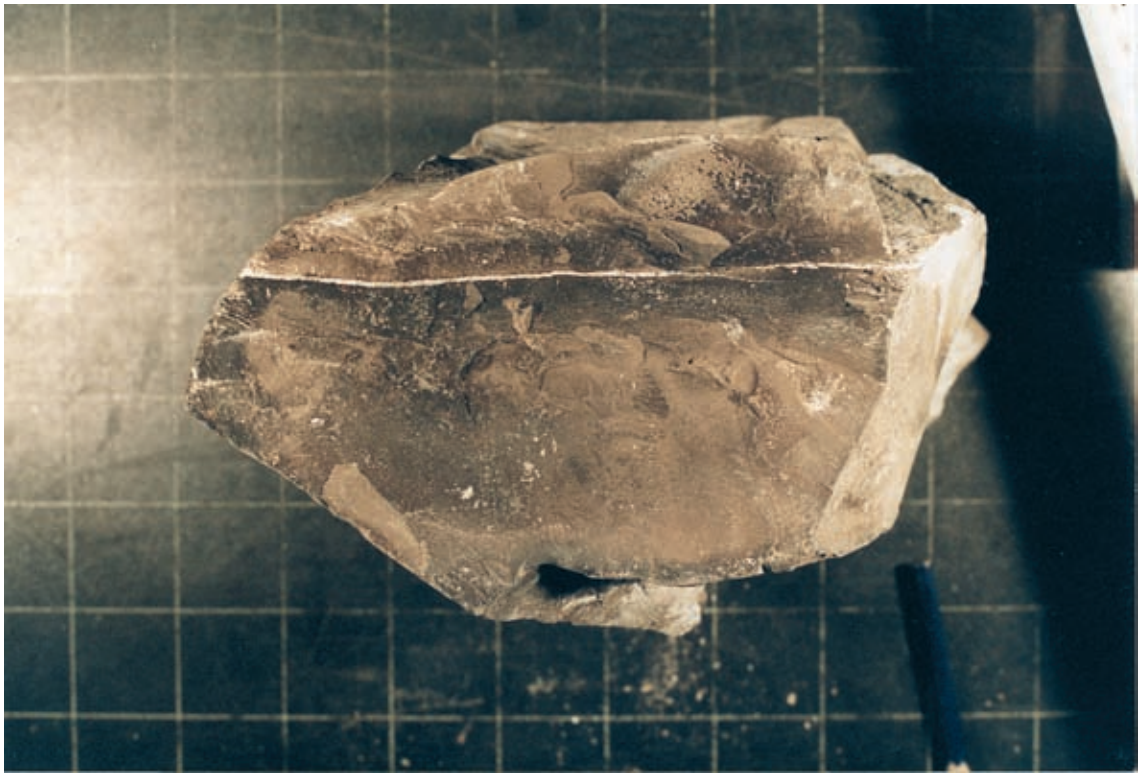

Figure J-17. *Profile C357. Photograph showing sampled vein and wallrock.*

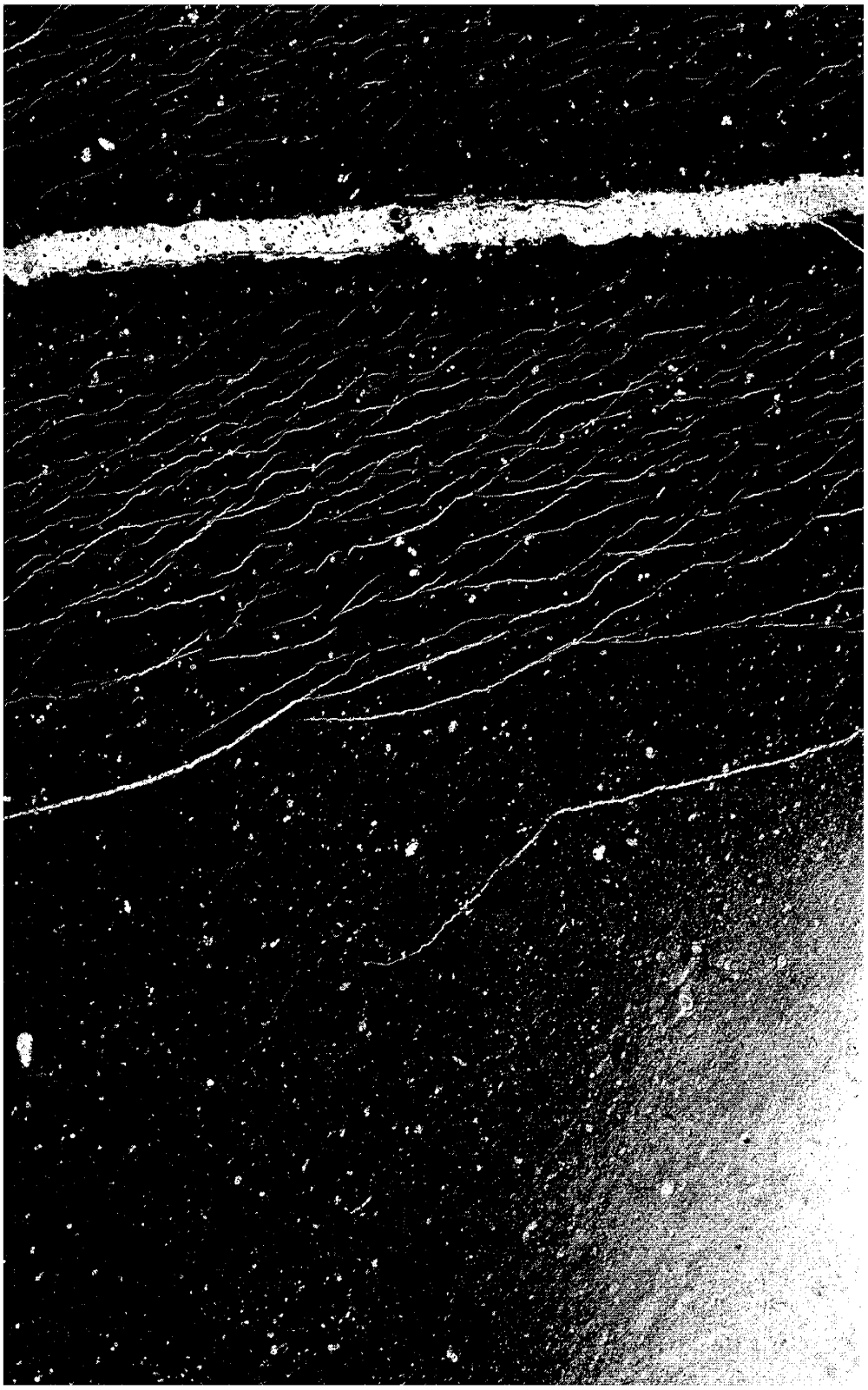

Figure J-18. *Profile C357. Contact print of polished thin section of sample C357 showing main fracture infilled by ettringite and jennite (white band; top), and microfracture network (light) in biomicrite wallrock. Length of polished thin section is 35 mm.*

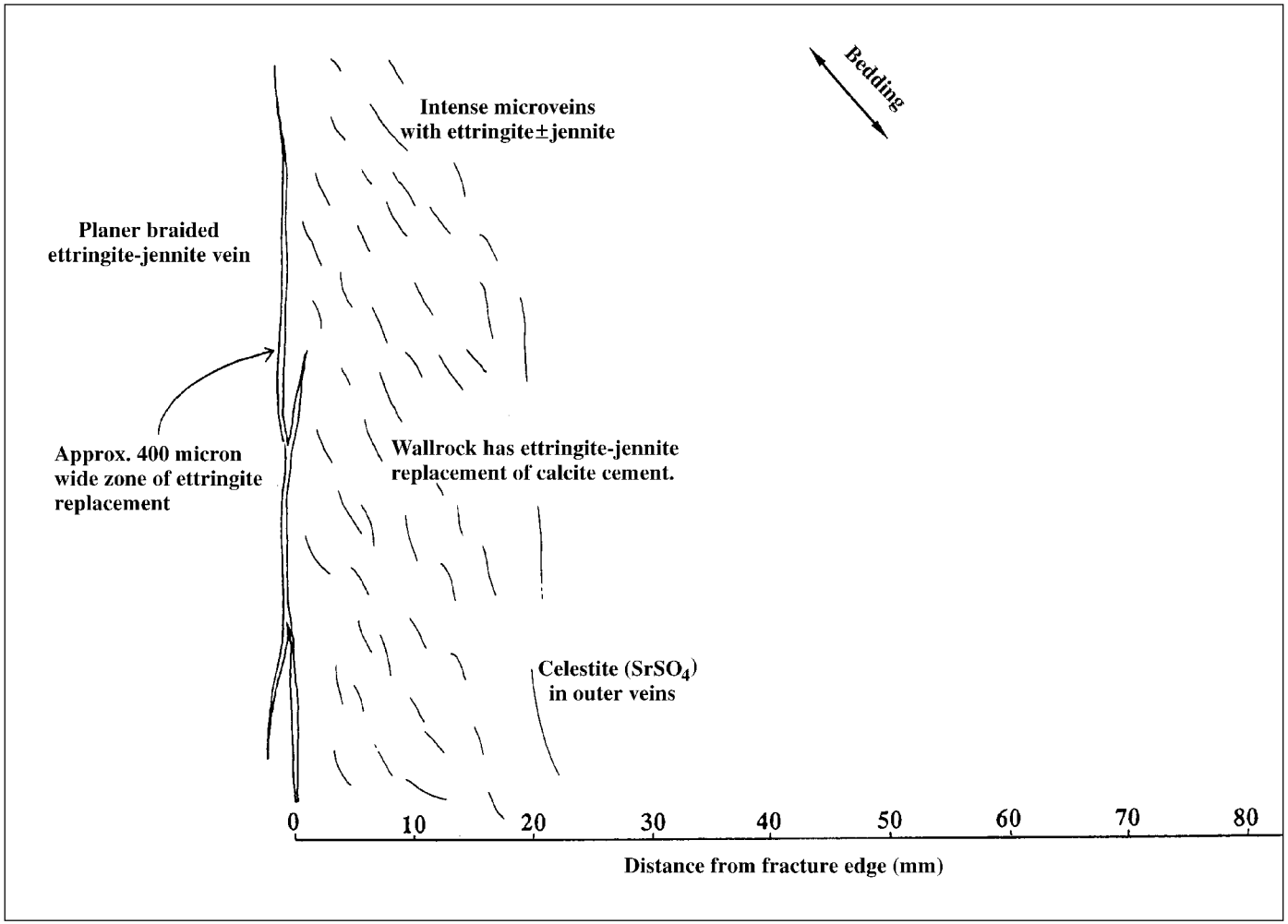

Figure J-19. *Profile C357. Diagrammatic sketch of vein and biomicrite wallrock profile in sample C357.*

Table J-5. Profile C357. Geochemical profiles across biomicrite wallrock with increasing distance from fracture edge in sample C357. [Major elements are expressed as oxide weight per cent; trace elements as parts per million. LOI = Loss On Ignition; Total = total major element oxides including LOI. Total iron is expressed as Fe_2O_3].

Sample	SiO_2 %	TiO_2 %	Al_2O_3 %	Fe_2O_3t %	MnO %	MgO %	CaO %	Na_2O %	K_2O %	P_2O_5 %	LOI %	SO_3 %	Cr_2O_3 %	SrO %	Total %
C353 0–15	9.91	0.17	4.38	2.59	0	0.31	46.28	0.09	0.05	2.23	32.36	0.7	0.09	0.51	99.67
C353 15–30	9.57	0.16	4.51	2.05	0.01	0.27	46.88	0.07	0.06	2.17	32.73	0.6	0.09	0.59	99.76
C353 30–45	9.49	0.16	4.5	1.88	0.01	0.29	46.76	0.07	0.05	2.14	33.08	0.4	0.09	0.58	99.5
C353 45–60	9.64	0.17	4.62	2.03	0.01	0.29	46.78	0.07	0.04	2.16	32.99	0.3	0.08	0.64	99.82
C353 60–75	9.54	0.17	4.58	1.97	0	0.28	46.73	0.08	0.04	2.15	33.2	0.2	0.08	0.7	99.72
C353 75–90	9.29	0.16	4.37	1.92	0.01	0.27	46.81	0.07	0.07	2.12	33.43	0.3	0.08	0.76	99.66
C357 0–10	7.76	0.06	1.89	0.9	0	0.18	43	0.08	0.13	1.65	40.23	3.3	0.04	0.2	99.42
C357 50–75	4.88	0.07	2.01	1.04	0	0.22	42.54	0.11	0.1	1.83	43.33	3.1	0.05	0.26	99.54
C358 0–15	9.02	0.06	3.29	0.95	0	0.2	42.47	0.09	0.12	1.35	40.02	1.8	0.04	0.21	99.62
C358 40–55	5.28	0.07	1.79	1.05	0	0.24	42.52	0.1	0.12	1.51	43.69	2.9	0.05	0.21	99.53
C359 0–10	4.68	0.06	2.17	0.72	0	0.2	46.6	0.06	0.02	1.64	41.03	2.6	0.04	0.17	99.99
C359 10–17	5.48	0.06	2.22	0.67	0	0.18	46.59	0.07	0.02	1.61	40.31	2.4	0.03	0.18	99.82
C359 17–32	4.21	0.06	1.29	0.69	0	0.2	46.94	0.06	0.01	1.74	42.04	2.3	0.04	0.18	99.76
C359 32–48	5.04	0.06	1.15	0.67	0	0.19	46.67	0.07	0.02	1.7	41.17	2.7	0.04	0.18	99.66
C359 48–63	4.64	0.05	1.2	0.65	0	0.19	46.69	0.07	0.02	1.69	41.68	2.6	0.03	0.18	99.7
C359 63–77	3.85	0.06	1.13	0.68	0	0.2	46.88	0.06	0.01	1.72	42.17	2.6	0.04	0.17	99.57

Table J-5 (contd.). Profile C357. Geochemical profiles across biomicrite wallrock with increasing distance from fracture edge in sample C357. [Major elements are expressed as oxide weight per cent; trace elements as parts per million].

Sample	Chromium ppm	Cobalt ppm	Nickel ppm	Selenium ppm	Strontium ppm	Zirconium ppm	Molybdenum ppm	Caesium ppm	Barium ppm	Lead ppm	Thorium ppm	Uranium ppm
C353 (0–30)	564	4.0	264	50	4644	33.5	17.2	1.40	102	<5	2.82	23.4
C353 (15–30)	480	6.7	224	49	5309	27.0	54.0	1.83	118	<5	2.65	23.8
C353 (30–45)	408	7.5	208	42	5516	26.3	5.2	2.10	113	<5	2.51	22.7
C353 (45–60)	437	6.7	194	42	5646	26.2	4.9	2.23	102	<5	2.57	23.0
C353 (60–75)	454	6.7	196	45	6296	28.0	4.8	2.44	95	<5	2.52	22.4
C353 (75–90)	471	6.7	203	43	7208	27.4	5.4	3.00	93	<5	2.48	22.3
C357 (0–10)	318	4.7	162	63	1907	16.3	15.2	1.61	396	<5	1.12	20.1
C357 (50–75)	329	4.5	170	33	2256	16.1	13.8	1.11	106	<5	1.30	22.5
C358 (0–15)	289	2.6	90	33	1794	13.8	10.4	1.33	521	<5	1.03	16.3
C358 (40–55)	325	3.9	151	30	1855	15	13.1	1.17	135	<5	1.17	19.9
C359 (0–10)	250	3.6	127	53	1475	13.1	10.2	0.74	87	<5	0.93	13.0
C359 (10–17)	246	4.0	126	51	1515	13.7	10.5	1.05	109	<5	0.93	13.1
C359 (17–32)	268	3.9	137	49	1532	13.4	9.4	0.95	92	<5	0.95	13.7
C359 (32–48)	253	3.7	138	50	1628	13.2	8.7	1.27	121	<5	0.99	13.5
C359 (48–65)	254	3.9	139	41	1630	13.2	9.2	1.13	122	<5	0.96	13.4
C359 (63–77)	270	4.1	142	47	1529	13.6	10.1	0.89	97	<5	1.07	13.7

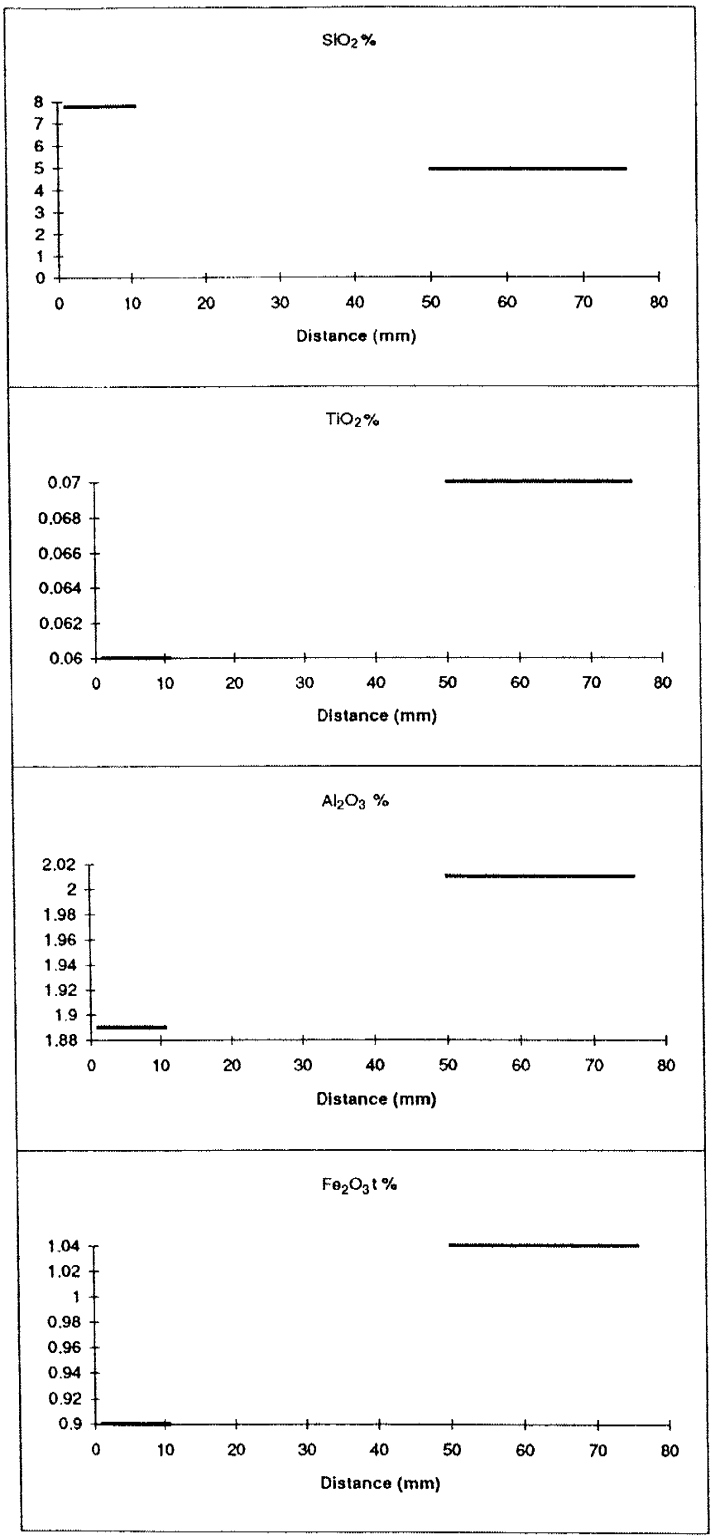
SiO2 %
8
7
6
5
4
3
2
1
0
0 10 20 30 40 50 60 70 80
Distance (mm)
TiO2 %
0.07
0.068
0.066
0.064
0.062
0.06
0 10 20 30 40 50 60 70 80
Distance (mm)
Al2O3 %
2.02
2
1.98
1.96
1.94
1.92
1.9
1.88
0 10 20 30 40 50 60 70 80
Distance (mm)
Fe2O3t %
1.04
1.02
1
0.98
0.96
0.94
0.92
0.9
0 10 20 30 40 50 60 70 80
Distance (mm)

Figure J-20

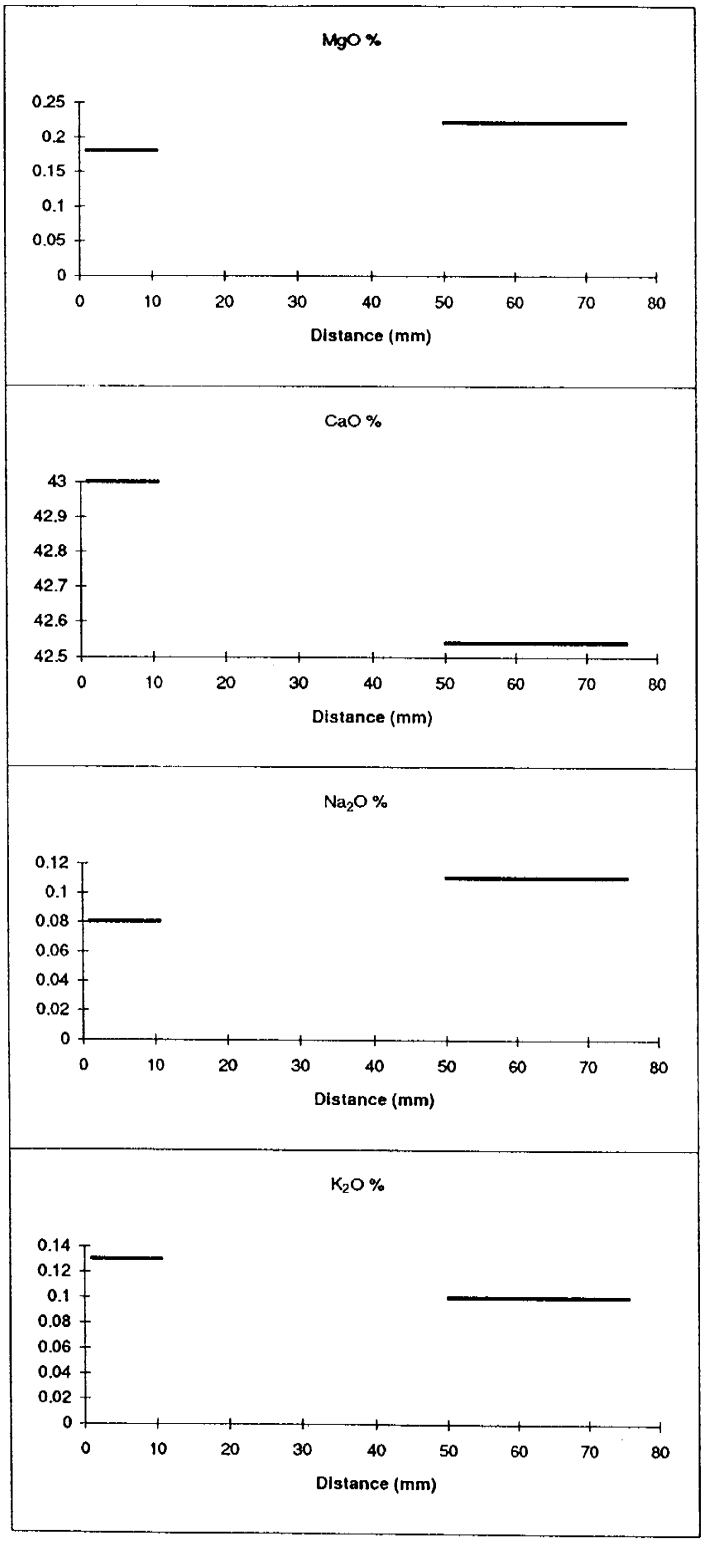
MgO %
0.25
0.2
0.15
0.1
0.05
0
0 10 20 30 40 50 60 70 80
Distance (mm)
CaO %
43
42.9
42.8
42.7
42.6
42.5
0 10 20 30 40 50 60 70 80
Distance (mm)
Na2O %
0.12
0.1
0.08
0.06
0.04
0.02
0
0 10 20 30 40 50 60 70 80
Distance (mm)
K2O %
0.14
0.12
0.1
0.08
0.06
0.04
0.02
0
0 10 20 30 40 50 60 70 80
Distance (mm)

Figure J-21

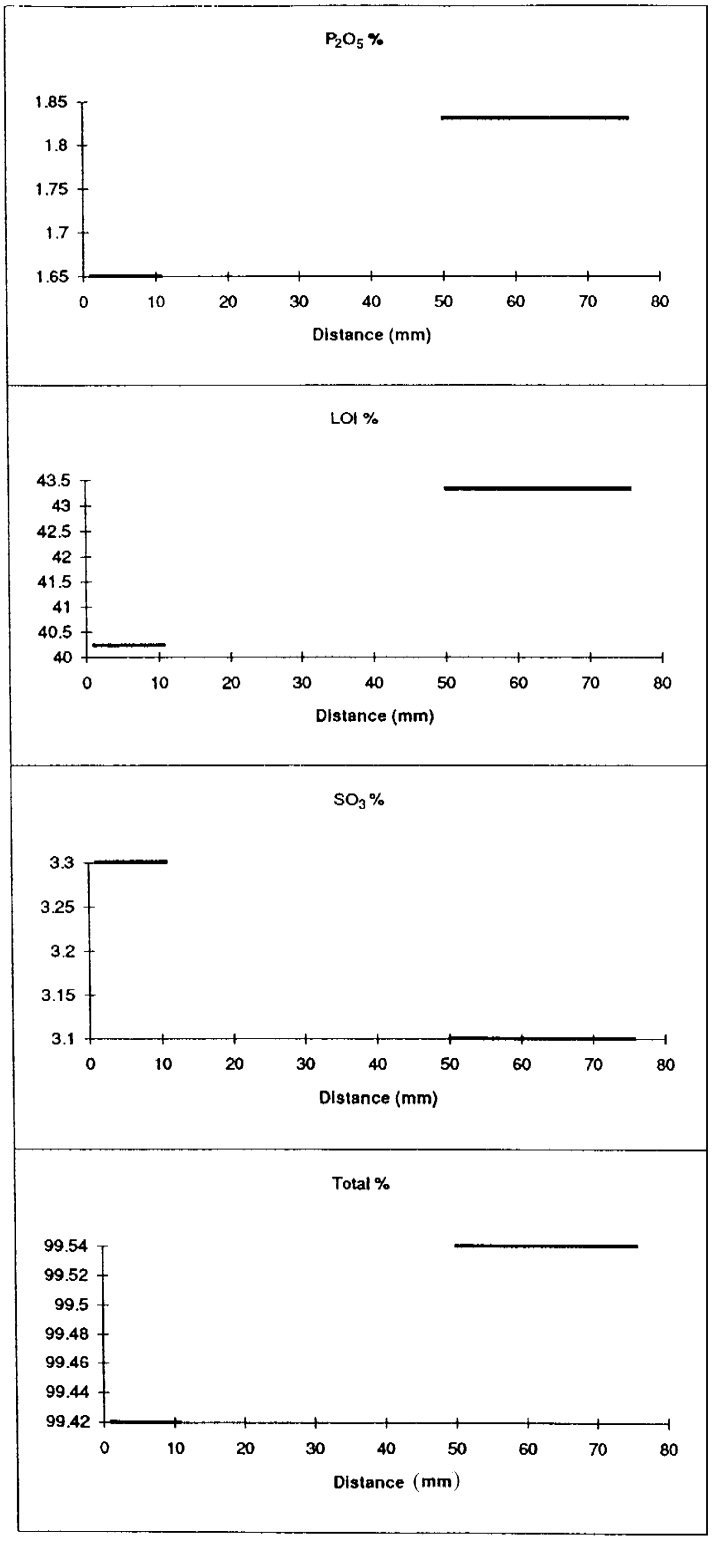
P_2O_5 %
1.85
1.8
1.75
1.7
1.65
0 10 20 30 40 50 60 70 80
Distance (mm)
LOI %
43.5
43
42.5
42
41.5
41
40.5
40
0 10 20 30 40 50 60 70 80
Distance (mm)
SO_3 %
3.3
3.25
3.2
3.15
3.1
0 10 20 30 40 50 60 70 80
Distance (mm)
Total %
99.54
99.52
99.5
99.48
99.46
99.44
99.42
0 10 20 30 40 50 60 70 80
Distance (mm)

Figure J-22

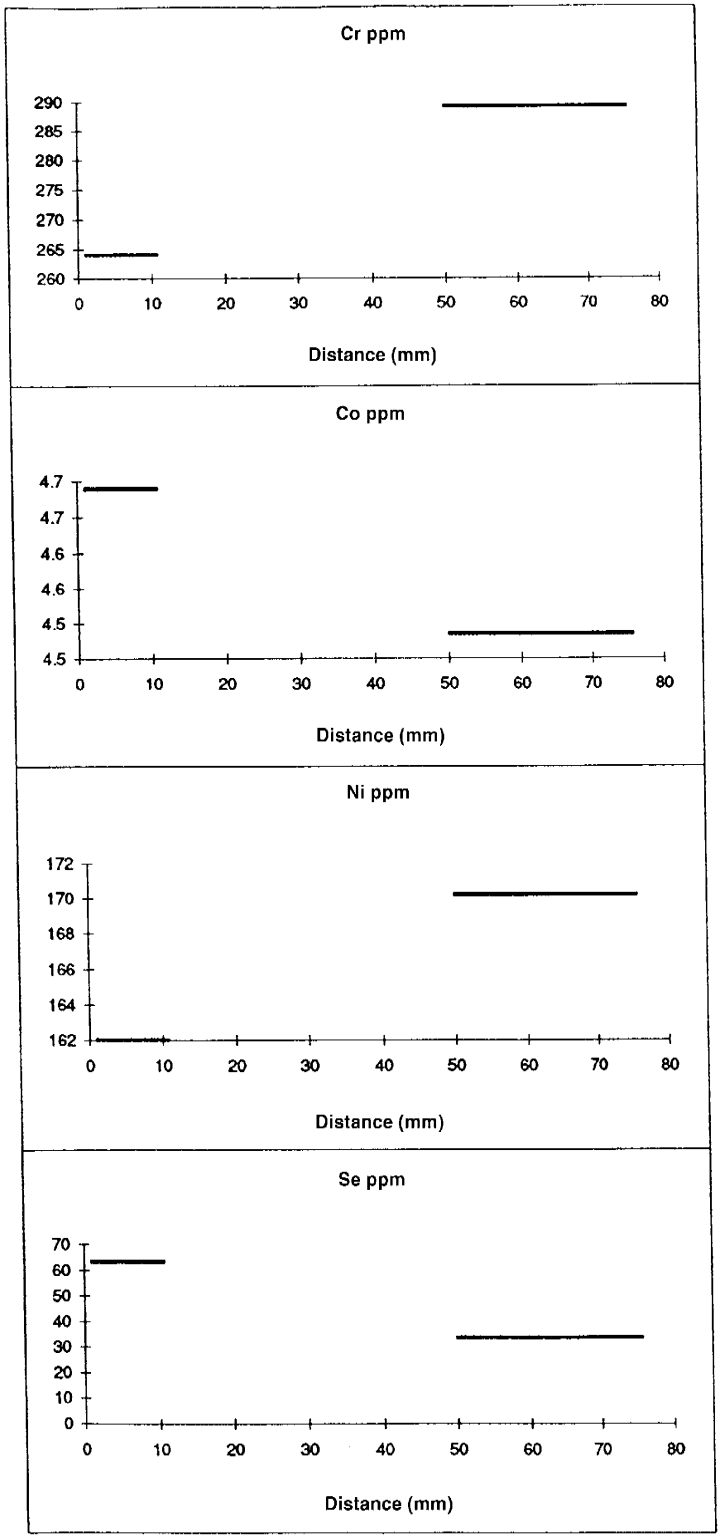
Cr ppm
290
285
280
275
270
265
260
0 10 20 30 40 50 60 70 80
Distance (mm)
Co ppm
4.7
4.7
4.6
4.6
4.5
4.5
0 10 20 30 40 50 60 70 80
Distance (mm)
Ni ppm
172
170
168
166
164
162
0 10 20 30 40 50 60 70 80
Distance (mm)
Se ppm
70
60
50
40
30
20
10
0
0 10 20 30 40 50 60 70 80
Distance (mm)

Figure J-23

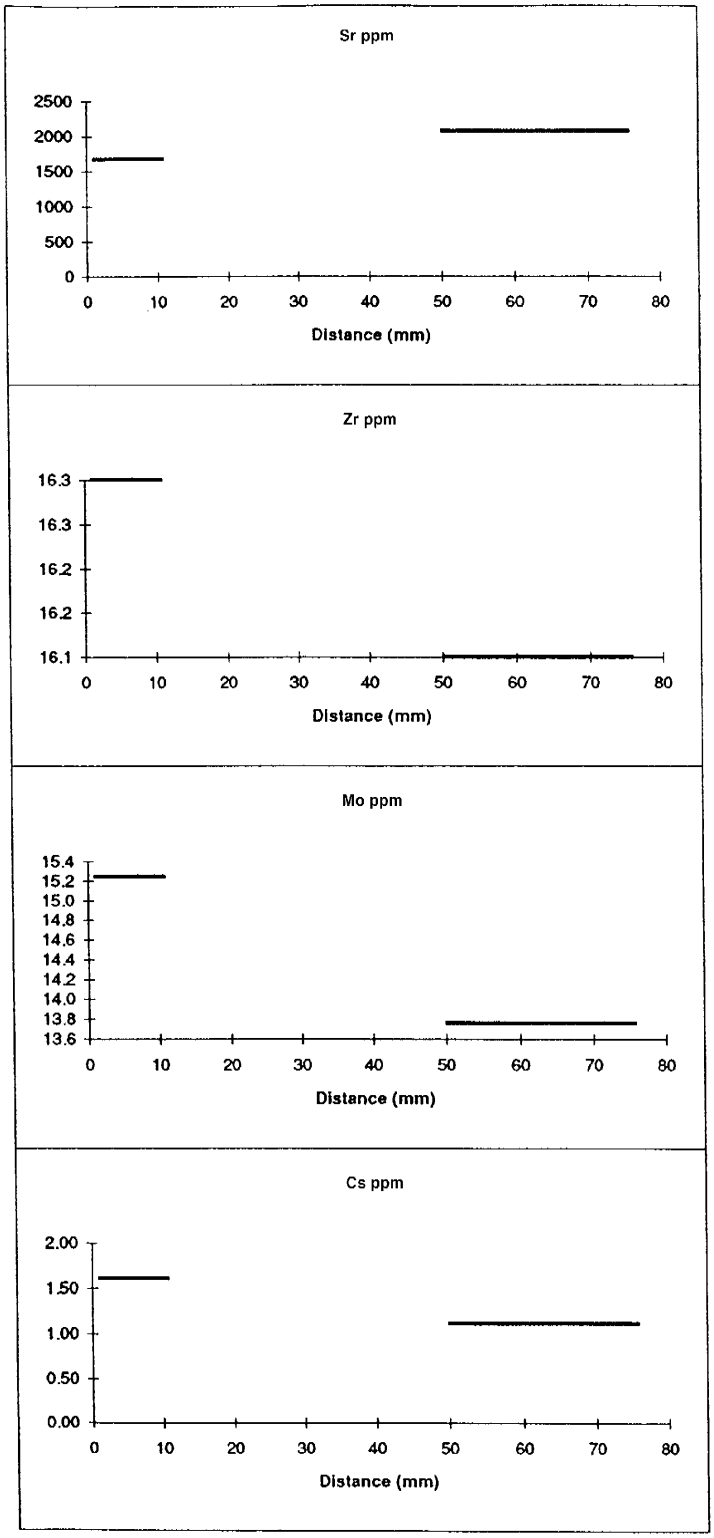
Sr ppm
2500
2000
1500
1000
500
0
0 10 20 30 40 50 60 70 80
Distance (mm)
Zr ppm
16.3
16.3
16.2
16.2
16.1
0 10 20 30 40 50 60 70 80
Distance (mm)
Mo ppm
15.4
15.2
15.0
14.8
14.6
14.4
14.2
14.0
13.8
13.6
0 10 20 30 40 50 60 70 80
Distance (mm)
Cs ppm
2.00
1.50
1.00
0.50
0.00
0 10 20 30 40 50 60 70 80
Distance (mm)

Figure J-24

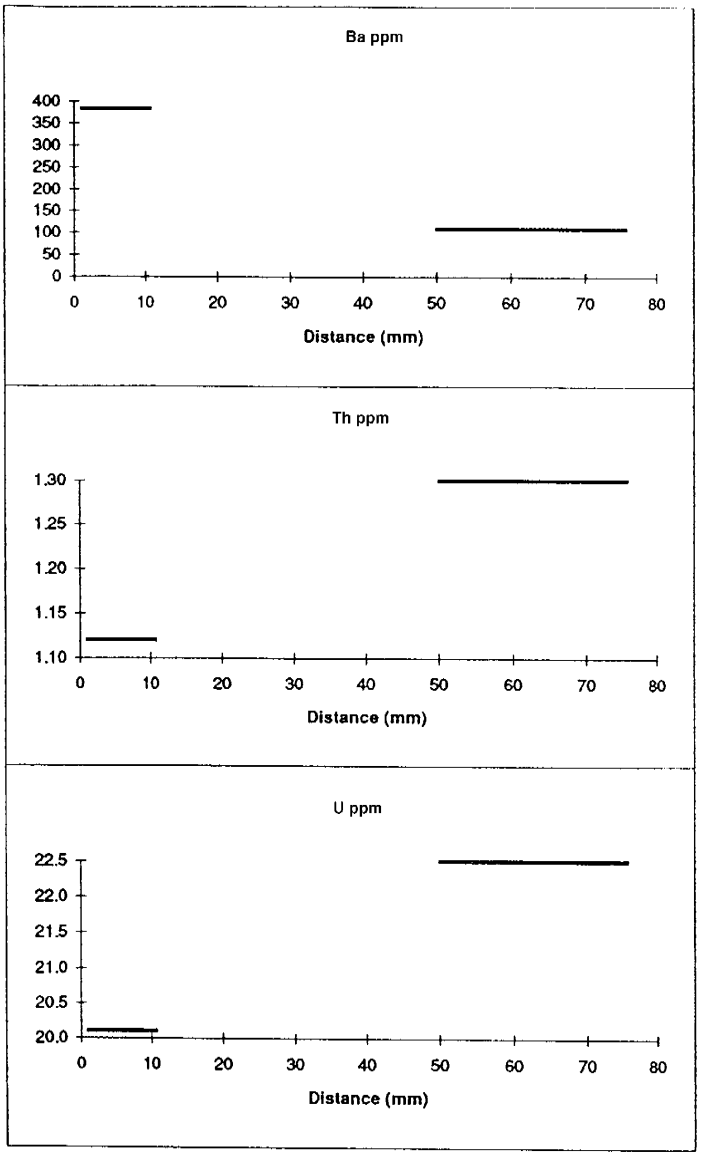
Ba ppm
400
350
300
250
200
150
100
50
0
0 10 20 30 40 50 60 70 80
Distance (mm)
Th ppm
1.30
1.25
1.20
1.15
1.10
0 10 20 30 40 50 60 70 80
Distance (mm)
U ppm
22.5
22.0
21.5
21.0
20.5
20.0
0 10 20 30 40 50 60 70 80
Distance (mm)

Figure J-25

Table J-6. Profile C357. In situ Laser Ablation Microprobe – Inductively Coupled Plasma – Mass Spectrometry (LAMP-ICP-MS) element profiles across biomicrite wallrock with increasing distance from fracture edge in sample C357.

Distance from vein (mm)	Sample	Aluminium ^{27}Al	Calcium ^{44}Ca	Chromium ^{53}Cr	Cobalt ^{59}Co	Selenium ^{78}Se	Selenium ^{82}Se	Strontium ^{86}Sr	Zirconium ^{90}Zr	Molybdenum ^{98}Mo	Caesium ^{133}Cs	Barium ^{138}Ba	Lead ^{208}Pb	Thorium ^{232}Th	Uranium ^{238}U
0	C357A1	28207	305000	6	0.3	72	146	1257	0.4	0.2	0.1	49	2.7	0.1	0.3
-0.5	C357A2	21536	305000	10	0.4	120	149	1488	2.9	0.9	2.7	846	11.8	0.1	1.7
0.5	C357A3	7833	305000	229	1.8	28	47	1796	8.2	10.7	1.6	477	1.4	1.0	20
0.75	C357A4	8175	305000	279	2.2	38	25	1577	10.3	12.8	1.5	416	1.3	1.2	19
1	C357A5	8719	305000	273	2.2	38	30	1467	9.2	10.2	1.7	431	2.3	0.7	15
1.5	C357A6	8108	305000	246	2.9	60	66	1434	8.2	10.3	1.3	383	2.3	0.8	18
2.5	C357A7	7592	305000	231	2.2	30	44	1528	7.4	10.0	1.6	415	1.7	0.7	15
3.5	C357A8	7476	305000	219	2.3	57	81	1498	6.1	10.4	1.4	408	1.5	0.5	11
4.5	C357A9	7636	305000	223	1.5	75	55	1694	9.2	11.6	1.3	410	1.2	0.9	22
5.5	C357A10	7116	305000	247	2.2	51	60	1300	6.7	20.0	1.1	320	1.8	0.6	13
6.5	C357A11	8418	305000	283	1.2	46	28	1626	9.7	12.2	1.2	363	1.1	0.9	18
7.5	C357A12	11244	305000	238	1.3	45	21	1448	9.4	9.6	1.0	263	1.0	0.6	16
8.5	C357A13	7789	305000	333	1.9	36	33	1546	10.1	13.4	1.3	300	1.5	0.7	17
9.5	C357A14	9188	305000	350	1.9	48	28	1585	16.6	18.1	1.3	232	1.7	1.1	21
11.5	C357A15	8797	305000	368	2.3	53	19	1437	12.2	16.3	1.1	169	1.7	1.2	19
13.5	C357A16	8456	305000	352	1.9	46	22	1378	11.9	13.6	1.1	145	6.5	1.1	20
15.5	C357A17	9072	305000	384	1.9	50	9	1410	13.3	15.8	1.1	140	1.5	1.0	18
17.5	C357A18	6430	305000	272	2.3	43	13	1428	9.4	17.2	0.9	154	4.1	1.1	25
19.5	C357A19	4745	305000	237	2.2	40	30	1182	5.3	12.5	0.6	125	1.3	0.4	10
24.5	C357A20	7562	305000	298	1.8	41	11	1456	8.7	17.0	1.0	227	1.1	0.9	19
27.5	C357A21	7180	305000	262	1.6	39	28	1573	7.8	14.5	1.0	207	2.8	0.6	13
27.5	C357B1	9442	305000	329	3.0	67	44	1477	11.5	22.9	1.0	204	4.0	1.1	23
32.5	C357B2	8963	305000	313	2.2	75	22	1666	16.7	14.6	1.0	203	1.1	1.1	22
37.5	C357B3	8634	305000	335	2.8	52	37	1661	11.7	12.6	1.1	169	1.7	1.0	23
42.5	C357B4	8801	305000	314	2.4	46	9	1473	10.8	10.6	1.0	99	1.2	0.7	16
47.5	C357B5	8768	305000	304	2.2	55	25	1440	10.6	11.7	1.0	83	1.4	1.0	23
52.5	C357B6	8714	305000	300	3.2	51	13	1376	9.4	9.9	1.0	76	1.3	1.1	23
57.5	C357B7	6970	305000	263	1.8	46	9	1435	8.6	7.5	0.8	76	1.0	0.8	17
60.5	C357B8	7486	305000	255	2.7	56	11	2937	9.3	7.5	1.0	234	1.4	1.4	20

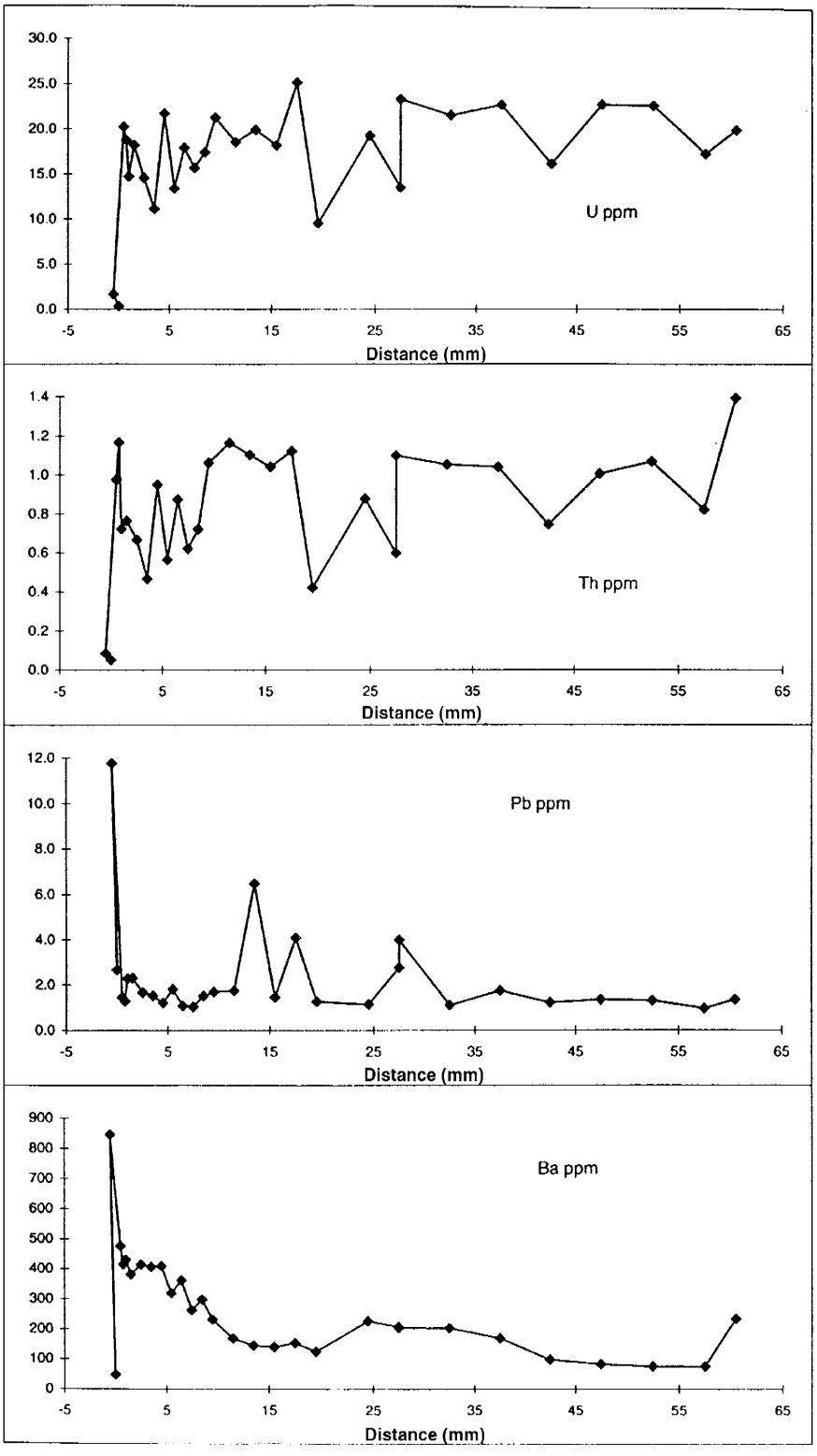
30.0
25.0
20.0
15.0
10.0
5.0
0.0
-5
5
15
25
35
45
55
65
Distance (mm)
U ppm
1.4
1.2
1.0
0.8
0.6
0.4
0.2
0.0
Th ppm
12.0
10.0
8.0
6.0
4.0
2.0
Pb ppm
900
800
700
600
500
400
300
200
100
Ba ppm

Figure J-26

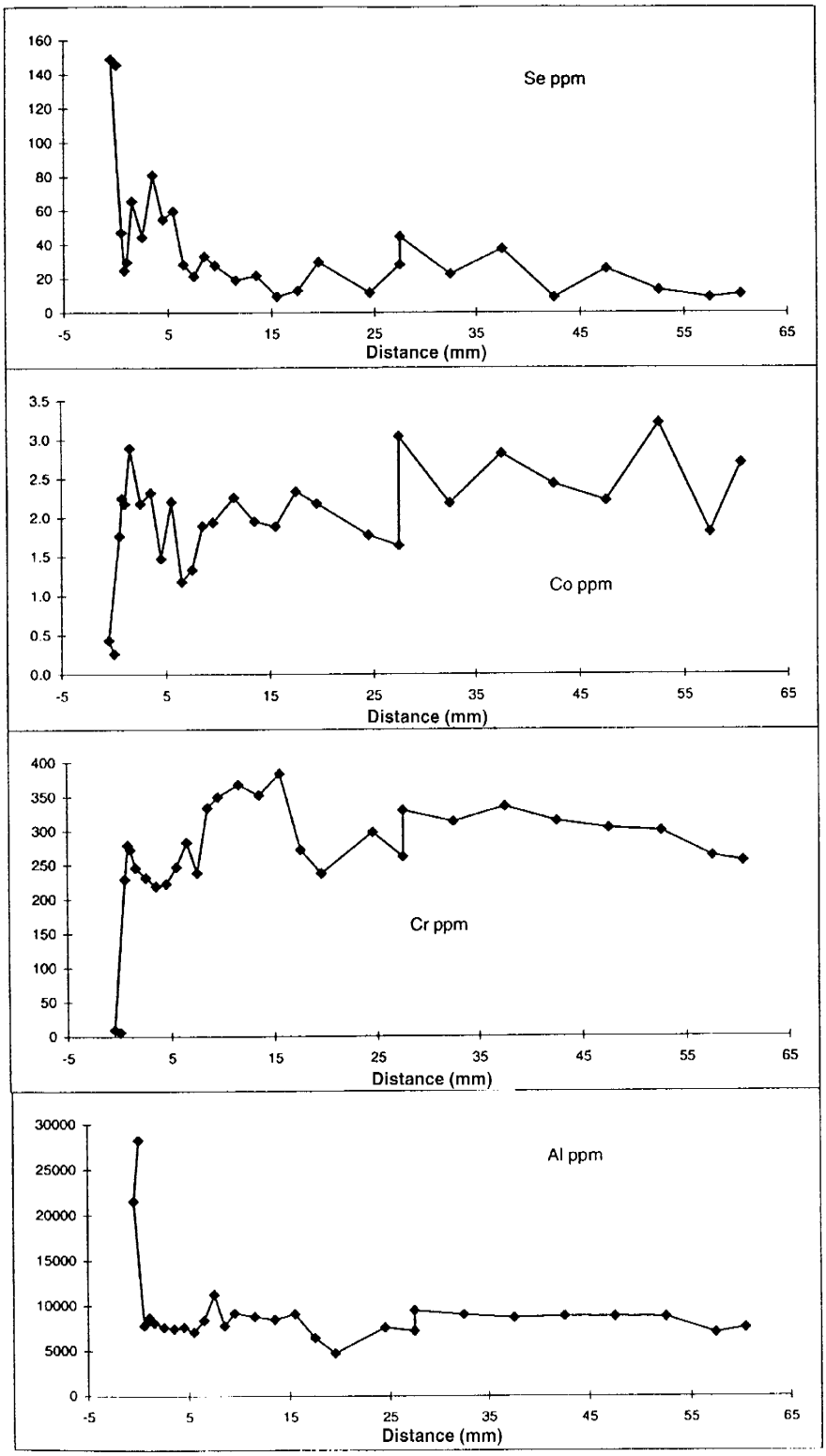
Se ppm
160
140
120
100
80
60
40
20
0
-5
5
15
25
35
45
55
65
Distance (mm)
Co ppm
3.5
3.0
2.5
2.0
1.5
1.0
0.5
0.0
Distance (mm)
Cr ppm
400
350
300
250
200
150
100
50
0
Distance (mm)
Al ppm
30000
25000
20000
15000
10000
5000
0
Distance (mm)

Figure J-27

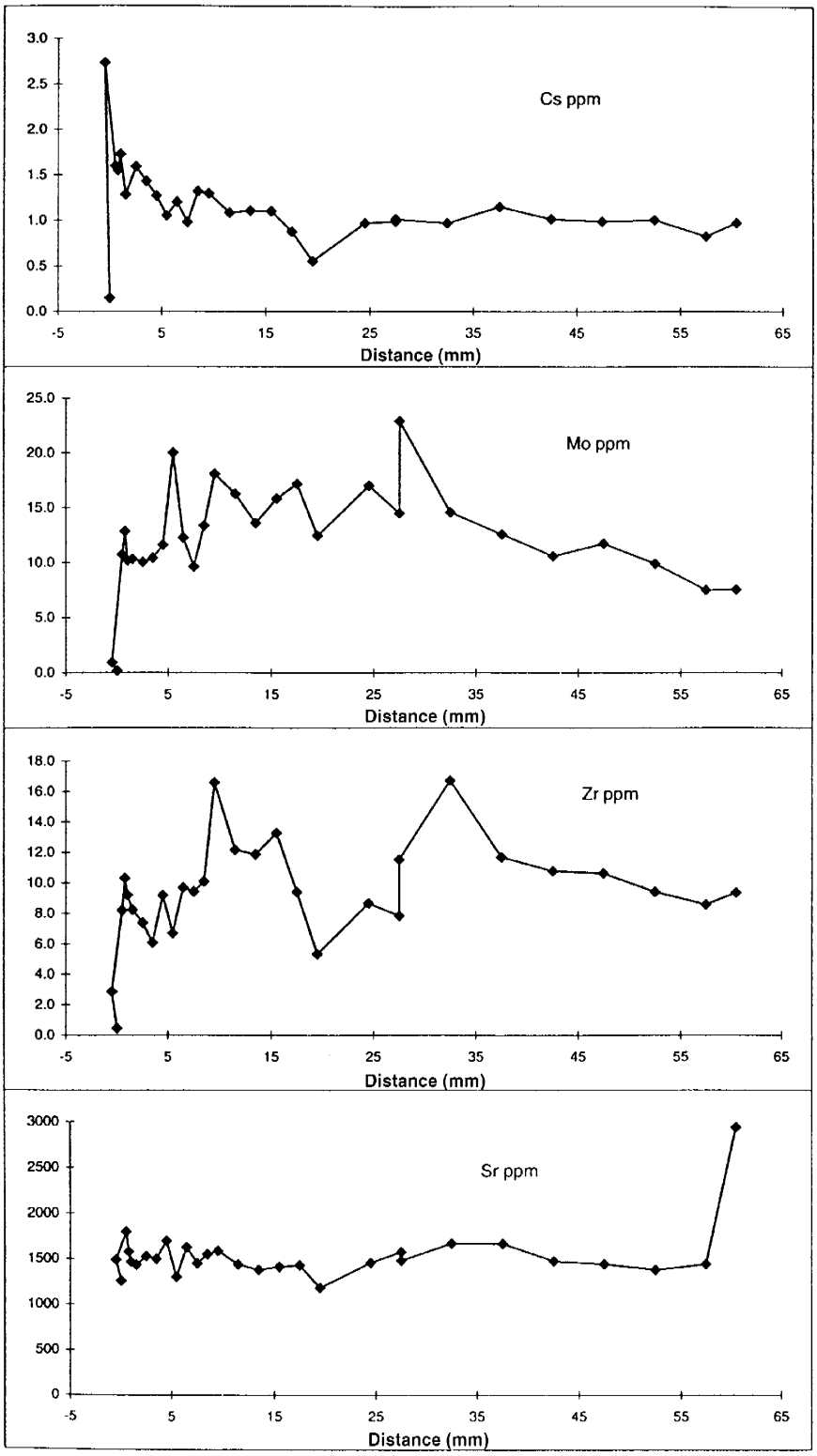
Cs ppm
3.0
2.5
2.0
1.5
1.0
0.5
0.0
-5
5
15
25
35
45
55
65
Distance (mm)
Mo ppm
25.0
20.0
15.0
10.0
5.0
0.0
-5
5
15
25
35
45
55
65
Distance (mm)
Zr ppm
18.0
16.0
14.0
12.0
10.0
8.0
6.0
4.0
2.0
0.0
-5
5
15
25
35
45
55
65
Distance (mm)
Sr ppm
3000
2500
2000
1500
1000
500
0
-5
5
15
25
35
45
55
65
Distance (mm)

Figure J-28

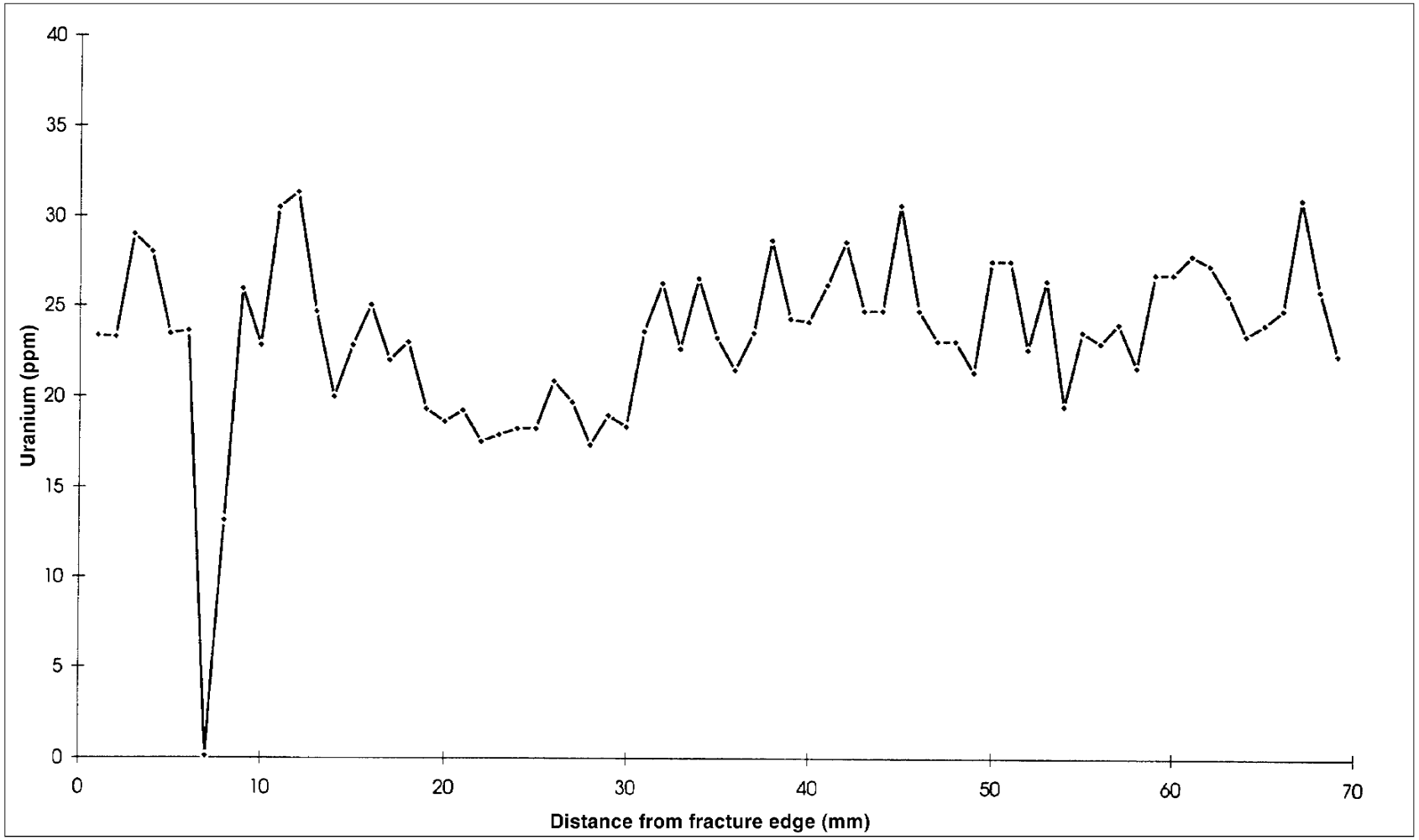

Figure J-29. *Profile C357. Fission Track Registration (FTR) analysis of uranium distribution.*

Table J-7. Profile C357. Profiles of U-series data across biomicrite wallrock with increasing distance from fracture edge in sample C357.

Sample	U (ppm)	Th (ppm)	^{226}Ra (mBq/g)	$^{234}U/^{238}U$	$^{230}Th/^{234}U$	$^{228}Th/^{232}Th$	$^{226}Ra/^{238}U$
C353							
0–15 mm	18.7(6)	2.4(2)	224(3)	0.97(3)	1.11(4)	1.0(1)	0.96(3)
15–30 mm	19.8(6)	2.7(2)	–	0.88(3)	1.18(5)	0.7(1)	–
30–45 mm	19.0(6)	2.3(2)	173(2)	0.98(3)	0.98(4)	1.0(1)	0.73(2)
45–60 mm	18.6(5)	2.3(2)	–	0.91(2)	1.06(4)	0.7(1)	–
60–75 mm	18.7(6)	1.8(2)	–	0.89(3)	1.08(4)	1.1(2)	–
75–90 mm	18.5(5)	2.0(2)	236(3)	0.94(3)	1.09(4)	1.1(2)	1.03(3)
C357							
0–10 mm	18.6(5)	2.3(2)	–	0.95(3)	0.99(4)	1.1(2)	–
50–75 mm	19.7(7)	0.9(1)	–	1.02(4)	0.97(4)	1.4(3)	–
C358							
0–15 mm	14.7(5)	1.1(1)	–	1.00(4)	1.06(5)	1.2(2)	–
40–55 mm	17.7(6)	1.0(1)	–	0.96(4)	0.96(4)	1.3(2)	–
C359							
0–10 mm	13.2(4)	3.1(2)	122(2)	0.96(4)	0.96(4)	1.3(1)	0.74(3)
10–17 mm	12.0(3)	2.4(2)	–	0.98(3)	0.97(4)	1.1(2)	–
17–32 mm	12.7(3)	*	137(2)	0.99(3)	1.15(4)	–	0.87(2)
32–48 mm	13.8(4)	*	–	0.94(3)	1.04(5)	–	–
48–63 mm	11.9(4)	2.7(2)	–	0.99(4)	1.08(5)	1.1(1)	–
63–77 mm	12.2(5)	1.3(1)	112(2)	1.02(5)	0.99(5)	0.8(1)	0.74(3)

All errors in parentheses are in least significant place and are 1 sigma uncertainties due to counting statistics alone.

* Results for ^{232}Th for C359 17–32 and 32–48 mm failed laboratory quality assurance (QA).

Average chemical recoveries are C353 (80% U and 77% Th) and C359 (70% U and 71% Th).

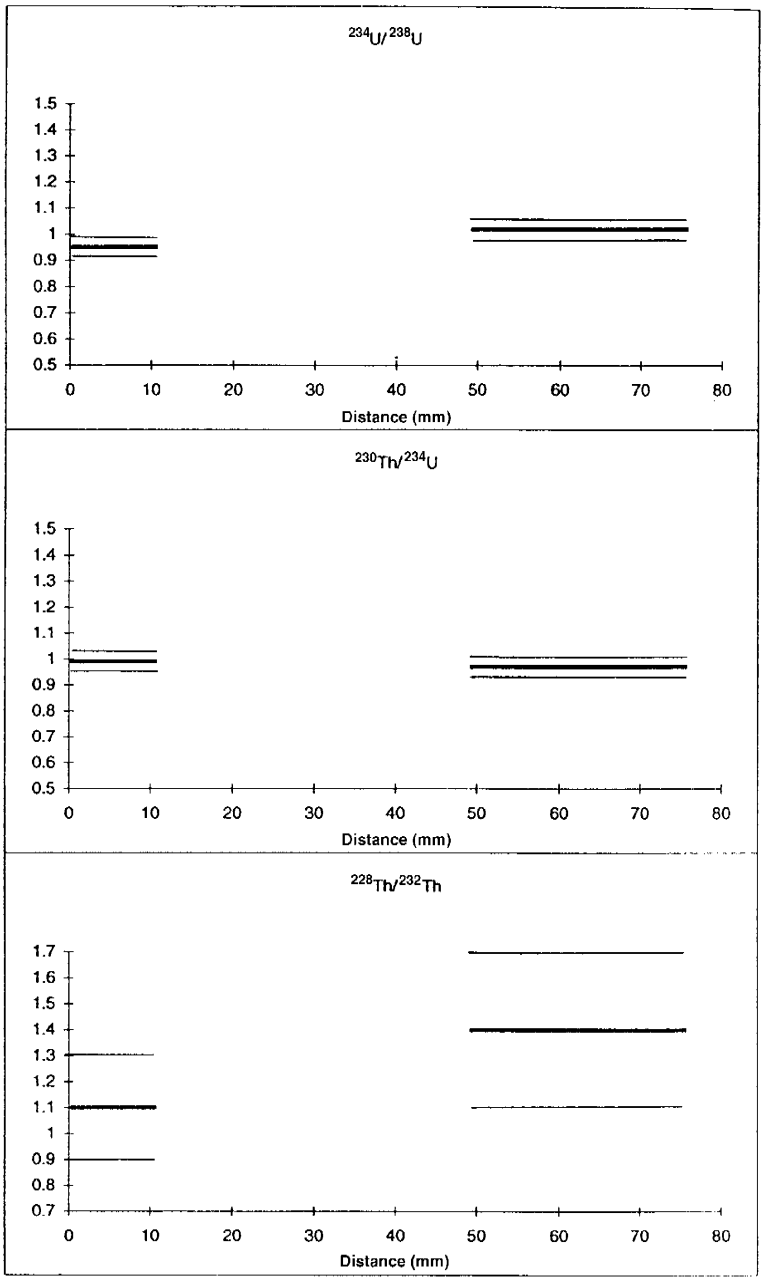

Note: Error bars represent 1 sigma uncertainties due to counting statistics alone.

Figure J-30

PROFILE C358

Figure J-31. *Profile C358. Photograph showing fracture sample C358 in situ in Adit A-6.*

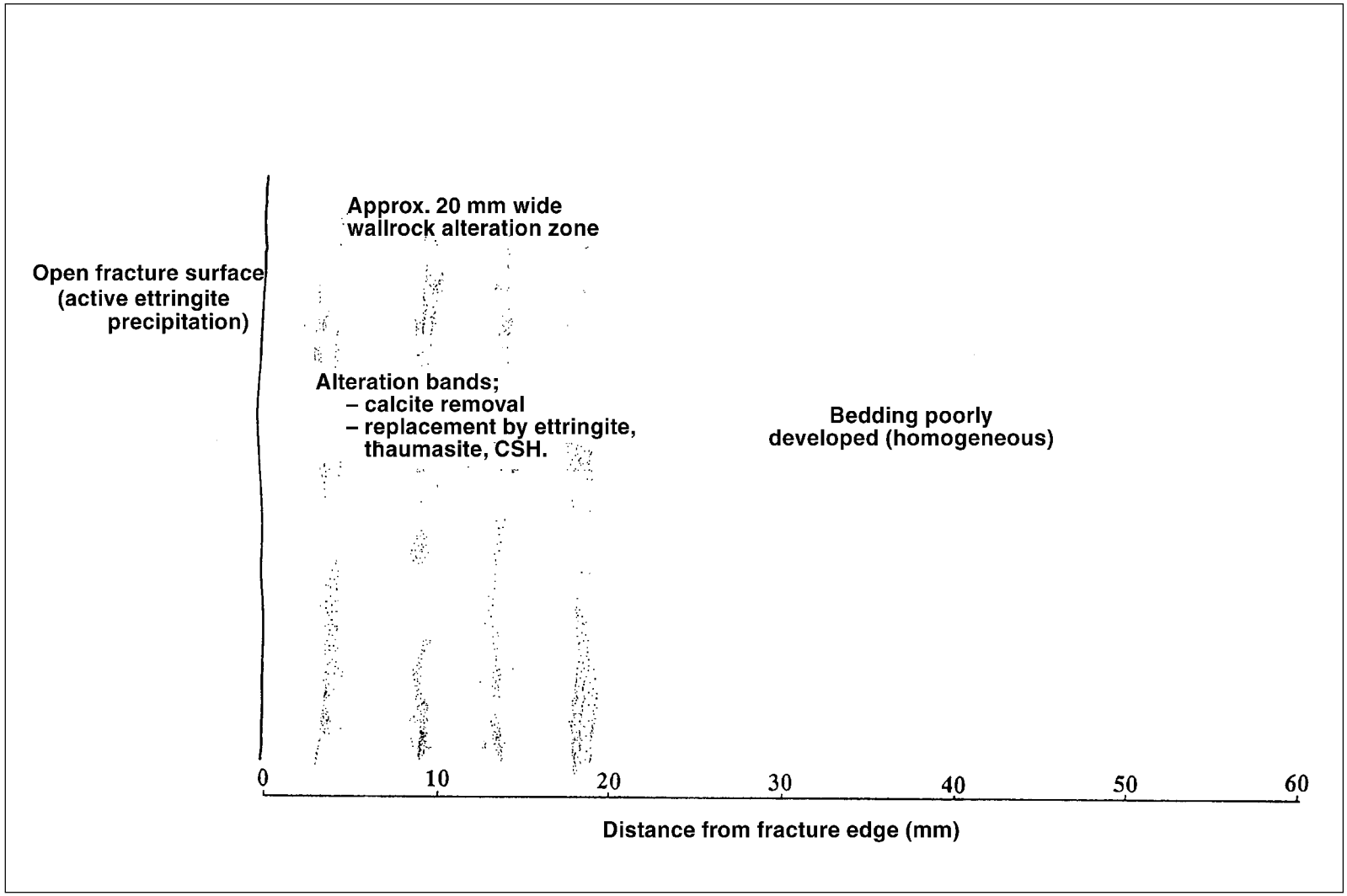

Figure J-32. *Profile C358. Diagrammatic sketch of vein and biomicrite wallrock profile in sample C358.*

Table J-8. Profile C358. Geochemical profiles across biomicrite wallrock with increasing distance from fracture edge in sample C358. [Major elements are expressed as oxide weight per cent; trace elements as parts per million. LOI = Loss On Ignition; Total = total major element oxides including LOI. Total iron is expressed as Fe_2O_3].

Sample	SiO_2 %	TiO_2 %	Al_2O_3 %	Fe_2O_3t %	MnO %	MgO %	CaO %	Na_2O %	K_2O %	P_2O_5 %	LOI %	SO_3 %	Cr_2O_3 %	SrO %	Total %
C353 0–15	9.91	0.17	4.38	2.59	0	0.31	46.28	0.09	0.05	2.23	32.36	0.7	0.09	0.51	99.67
C353 15–30	9.57	0.16	4.51	2.05	0.01	0.27	46.88	0.07	0.06	2.17	32.73	0.6	0.09	0.59	99.76
C353 30–45	9.49	0.16	4.5	1.88	0.01	0.29	46.76	0.07	0.05	2.14	33.08	0.4	0.09	0.58	99.5
C353 45–60	9.64	0.17	4.62	2.03	0.01	0.29	46.78	0.07	0.04	2.16	32.99	0.3	0.08	0.64	99.82
C353 60–75	9.54	0.17	4.58	1.97	0	0.28	46.73	0.08	0.04	2.15	33.2	0.2	0.08	0.7	99.72
C353 75–90	9.29	0.16	4.37	1.92	0.01	0.27	46.81	0.07	0.07	2.12	33.43	0.3	0.08	0.76	99.66
C357 0–10	7.76	0.06	1.89	0.9	0	0.18	43	0.08	0.13	1.65	40.23	3.3	0.04	0.2	99.42
C357 50–75	4.88	0.07	2.01	1.04	0	0.22	42.54	0.11	0.1	1.83	43.33	3.1	0.05	0.26	99.54
C358 0–15	9.02	0.06	3.29	0.95	0	0.2	42.47	0.09	0.12	1.35	40.02	1.8	0.04	0.21	99.62
C358 40–55	5.28	0.07	1.79	1.05	0	0.24	42.52	0.1	0.12	1.51	43.69	2.9	0.05	0.21	99.53
C359 0–10	4.68	0.06	2.17	0.72	0	0.2	46.6	0.06	0.02	1.64	41.03	2.6	0.04	0.17	99.99
C359 10–17	5.48	0.06	2.22	0.67	0	0.18	46.59	0.07	0.02	1.61	40.31	2.4	0.03	0.18	99.82
C359 17–32	4.21	0.06	1.29	0.69	0	0.2	46.94	0.06	0.01	1.74	42.04	2.3	0.04	0.18	99.76
C359 32–48	5.04	0.06	1.15	0.67	0	0.19	46.67	0.07	0.02	1.7	41.17	2.7	0.04	0.18	99.66
C359 48–63	4.64	0.05	1.2	0.65	0	0.19	46.69	0.07	0.02	1.69	41.68	2.6	0.03	0.18	99.7
C359 63–77	3.85	0.06	1.13	0.68	0	0.2	46.88	0.06	0.01	1.72	42.17	2.6	0.04	0.17	99.57

Table J-8 (contd.) Profile C358. Geochemical profiles across biomicrite wallrock with increasing distance from fracture edge in sample C358. [Major elements are expressed as oxide weight per cent; trace elements as parts per million].

Sample	Chromium ppm	Cobalt ppm	Nickel ppm	Selenium ppm	Strontium ppm	Zirconium ppm	Molybdenum ppm	Caesium ppm	Barium ppm	Lead ppm	Thorium ppm	Uranium ppm
C353 (0–30)	564	4.0	264	50	4644	33.5	17.2	1.40	102	<5	2.82	23.4
C353 (15–30)	480	6.7	224	49	5309	27.0	54.0	1.83	118	<5	2.65	23.8
C353 (30–45)	408	7.5	208	42	5516	26.3	5.2	2.10	113	<5	2.51	22.7
C353 (45–60)	437	6.7	194	42	5646	26.2	4.9	2.23	102	<5	2.57	23.0
C353 (60–75)	454	6.7	196	45	6296	28.0	4.8	2.44	95	<5	2.52	22.4
C353 (75–90)	471	6.7	203	43	7208	27.4	5.4	3.00	93	<5	2.48	22.3
C357 (0–10)	318	4.7	162	63	1907	16.3	15.2	1.61	396	<5	1.12	20.1
C357 (50–75)	329	4.5	170	33	2256	16.1	13.8	1.11	106	<5	1.30	22.5
C358 (0–15)	289	2.6	90	33	1794	13.8	10.4	1.33	521	<5	1.03	16.3
C358 (40–55)	325	3.9	151	30	1855	15	13.1	1.17	135	<5	1.17	19.9
C359 (0–10)	250	3.6	127	53	1475	13.1	10.2	0.74	87	<5	0.93	13.0
C359 (10–17)	246	4.0	126	51	1515	13.7	10.5	1.05	109	<5	0.93	13.1
C359 (17–32)	268	3.9	137	49	1532	13.4	9.4	0.95	92	<5	0.95	13.7
C359 (32–48)	253	3.7	138	50	1628	13.2	8.7	1.27	121	<5	0.99	13.5
C359 (48–65)	254	3.9	139	41	1630	13.2	9.2	1.13	122	<5	0.96	13.4
C359 (63–77)	270	4.1	142	47	1529	13.6	10.1	0.89	97	<5	1.07	13.7

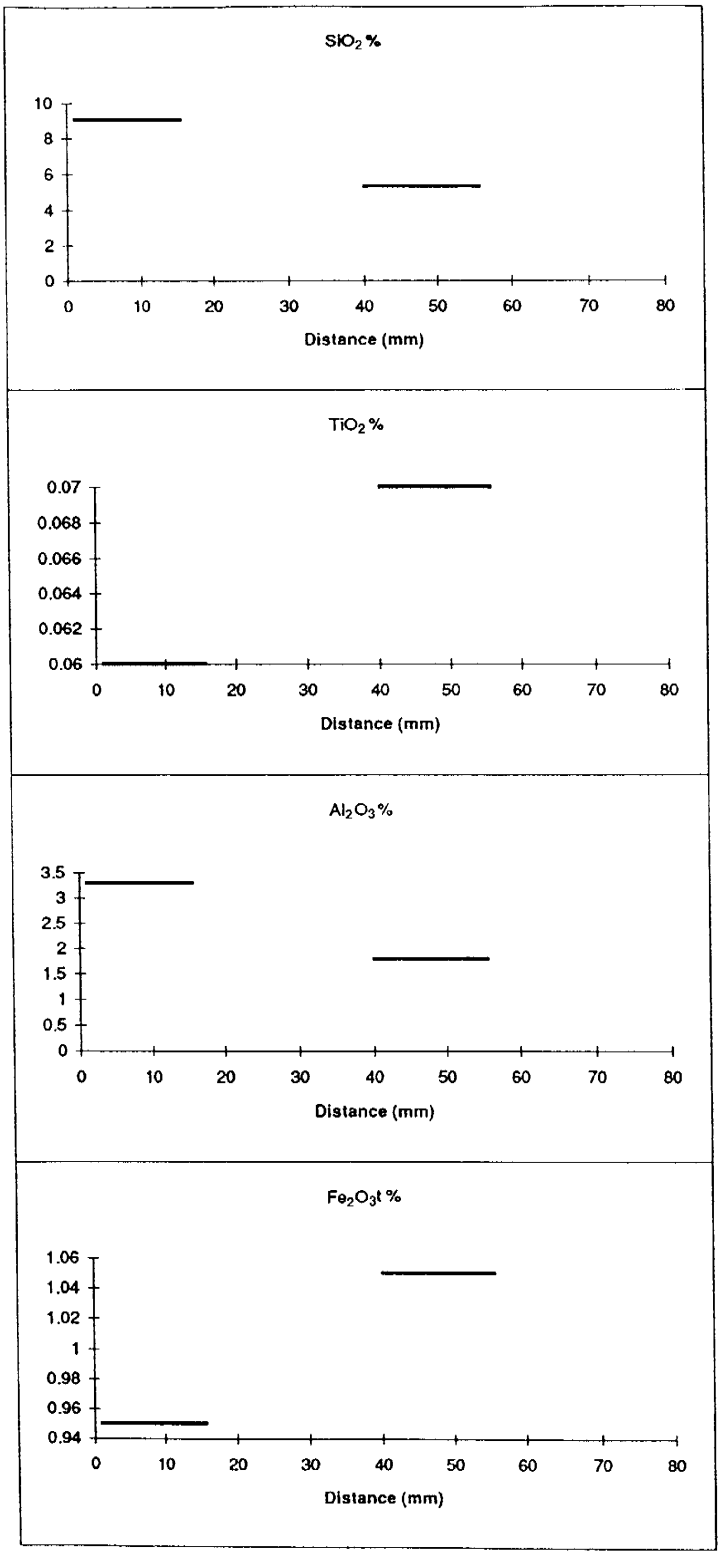
SiO2 %
10
8
6
4
2
0
0 10 20 30 40 50 60 70 80
Distance (mm)
TiO2 %
0.07
0.068
0.066
0.064
0.062
0.06
0 10 20 30 40 50 60 70 80
Distance (mm)
Al2O3 %
3.5
3
2.5
2
1.5
1
0.5
0
0 10 20 30 40 50 60 70 80
Distance (mm)
Fe2O3t %
1.06
1.04
1.02
1
0.98
0.96
0.94
0 10 20 30 40 50 60 70 80
Distance (mm)

Figure J-33

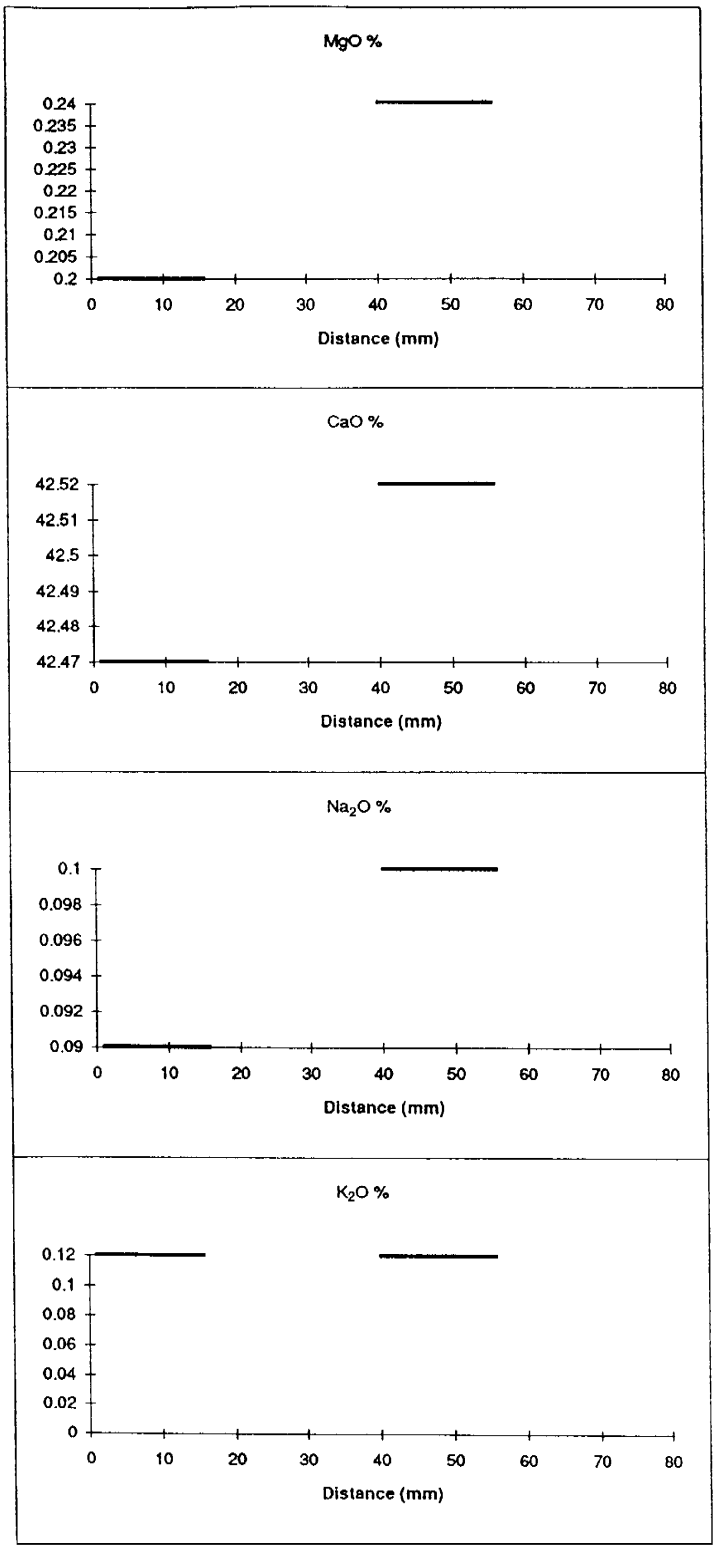
MgO %
0.24
0.235
0.23
0.225
0.22
0.215
0.21
0.205
0.2
0 10 20 30 40 50 60 70 80
Distance (mm)
CaO %
42.52
42.51
42.5
42.49
42.48
42.47
0 10 20 30 40 50 60 70 80
Distance (mm)
Na2O %
0.1
0.098
0.096
0.094
0.092
0.09
0 10 20 30 40 50 60 70 80
Distance (mm)
K2O %
0.12
0.1
0.08
0.06
0.04
0.02
0
0 10 20 30 40 50 60 70 80
Distance (mm)

Figure J-34

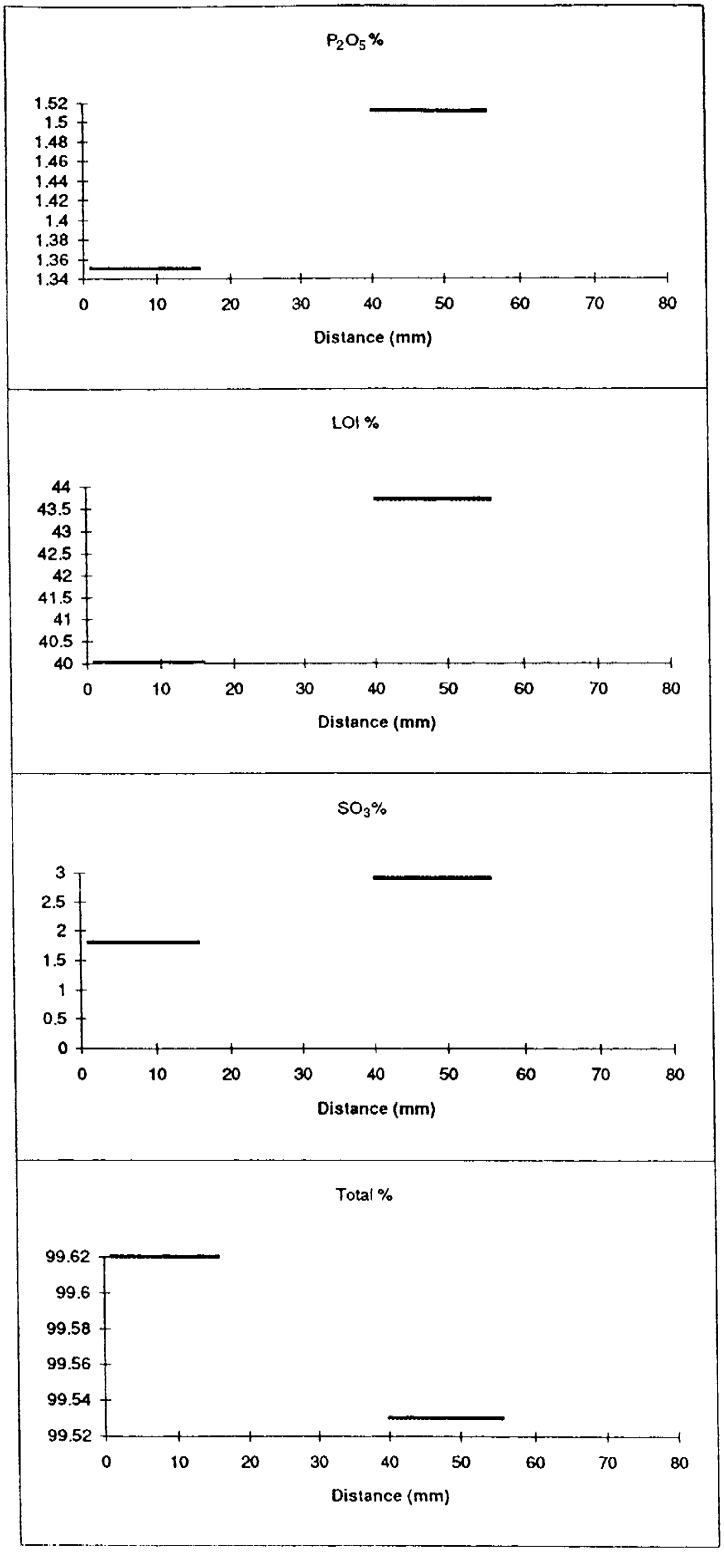
P_2O_5 %
1.52
1.5
1.48
1.46
1.44
1.42
1.4
1.38
1.36
1.34
0 10 20 30 40 50 60 70 80
Distance (mm)
LOI %
44
43.5
43
42.5
42
41.5
41
40.5
40
0 10 20 30 40 50 60 70 80
Distance (mm)
SO_3%
3
2.5
2
1.5
1
0.5
0
0 10 20 30 40 50 60 70 80
Distance (mm)
Total %
99.62
99.6
99.58
99.56
99.54
99.52
0 10 20 30 40 50 60 70 80
Distance (mm)

Figure J-35

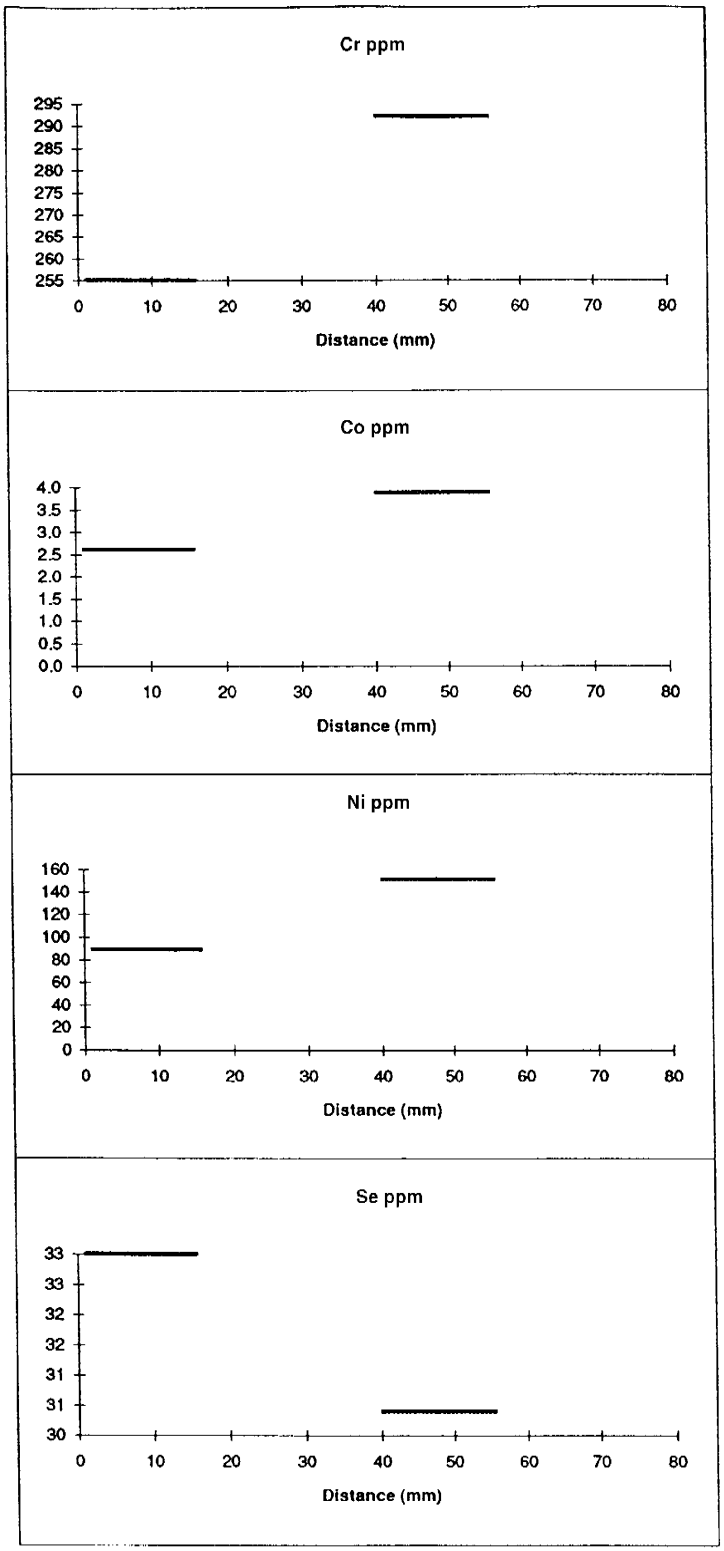
Cr ppm
295
290
285
280
275
270
265
260
255
0 10 20 30 40 50 60 70 80
Distance (mm)
Co ppm
4.0
3.5
3.0
2.5
2.0
1.5
1.0
0.5
0.0
0 10 20 30 40 50 60 70 80
Distance (mm)
Ni ppm
160
140
120
100
80
60
40
20
0
0 10 20 30 40 50 60 70 80
Distance (mm)
Se ppm
33
33
32
32
31
31
30
0 10 20 30 40 50 60 70 80
Distance (mm)

Figure J-36

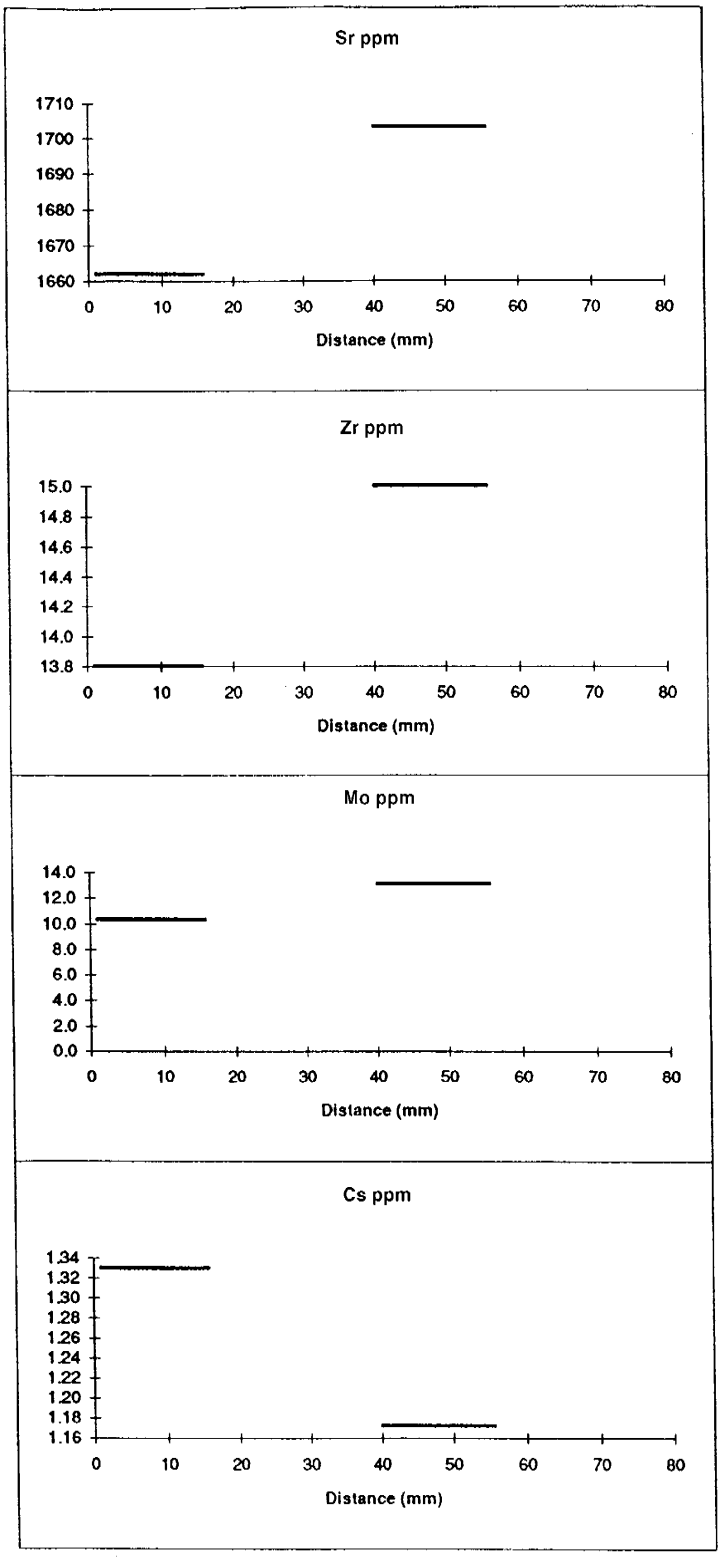
Sr ppm
1710
1700
1690
1680
1670
1660
0 10 20 30 40 50 60 70 80
Distance (mm)
Zr ppm
15.0
14.8
14.6
14.4
14.2
14.0
13.8
0 10 20 30 40 50 60 70 80
Distance (mm)
Mo ppm
14.0
12.0
10.0
8.0
6.0
4.0
2.0
0.0
0 10 20 30 40 50 60 70 80
Distance (mm)
Cs ppm
1.34
1.32
1.30
1.28
1.26
1.24
1.22
1.20
1.18
1.16
0 10 20 30 40 50 60 70 80
Distance (mm)

Figure J-37

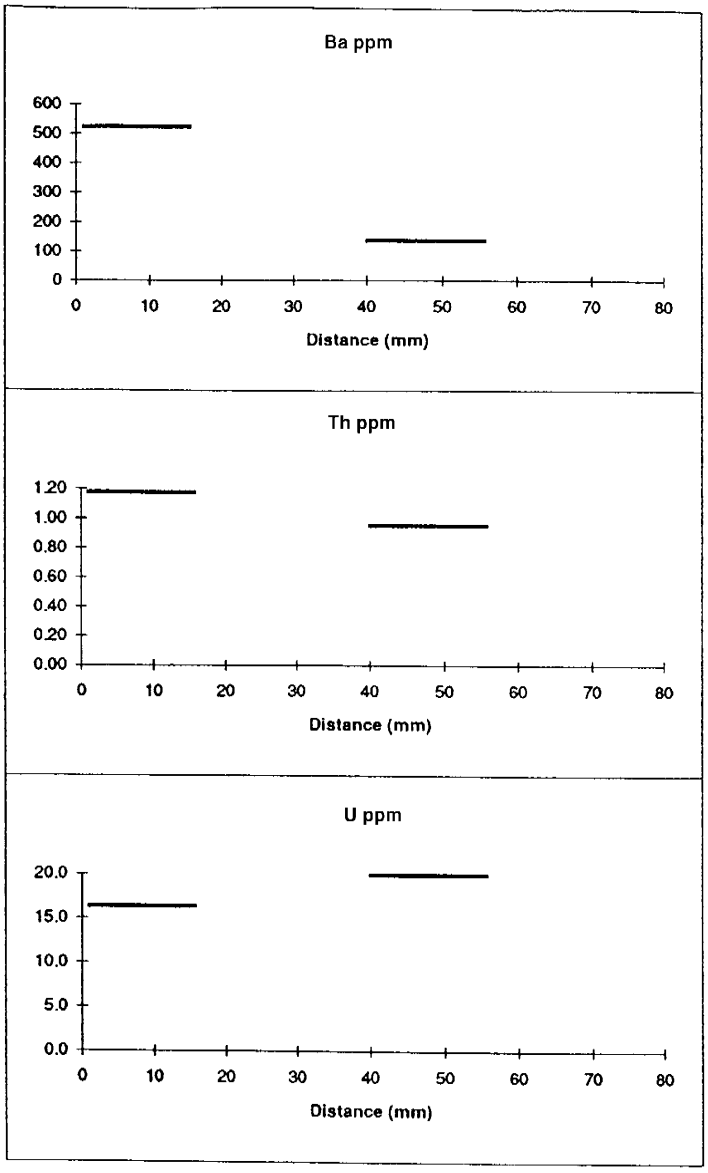
Ba ppm
600
500
400
300
200
100
0
0 10 20 30 40 50 60 70 80
Distance (mm)
Th ppm
1.20
1.00
0.80
0.60
0.40
0.20
0.00
0 10 20 30 40 50 60 70 80
Distance (mm)
U ppm
20.0
15.0
10.0
5.0
0.0
0 10 20 30 40 50 60 70 80
Distance (mm)

Figure J-38

Table J-9. Profile C358. In situ Laser Ablation Microprobe – Inductively Coupled Plasma – Mass Spectrometry (LAMP-ICP-MS) element profiles across biomicrite wallrock with increasing distance from fracture edge in sample C358.

Distance from vein (mm)	Sample	Aluminium ^{27}Al	Calcium ^{44}Ca	Chromium ^{53}Cr	Cobalt ^{59}Co	Selenium ^{78}Se	Selenium ^{82}Se	Strontium ^{86}Sr	Zirconium ^{90}Zr	Molybdenum ^{98}Mo	Caesium ^{133}Cs	Barium ^{138}Ba	Lead ^{208}Pb	Thorium ^{232}Th	Uranium ^{238}U
0	C358A	7315	303714	373	2.1	52	40	1954	15	10.3	1.2	76	1.7	1.4	25.8
0.5	C358B	7371	303714	402	3.8	44	34	2104	15	12.9	1.4	80	1.0	1.3	18.4
1.5	C358C	4019	303714	371	3.2	43	33	1727	12	9.6	1.3	63	1.6	1.1	17.0
2.5	C358D	21851	303714	277	2.5	60	32	2070	10	14.0	1.3	286	34.1	1.0	24.7
3.5	C358E	20967	303714	256	1.5	32	35	1828	17	13.3	1.1	409	15.3	1.1	17.1
4.5	C358F	15219	303714	205	1.6	29	23	1729	23	6.7	1.1	500	4.4	0.5	9.7
5.5	C358G	11398	303714	158	1.2	25	20	2037	24	5.8	1.2	651	3.2	0.4	5.8
6.5	C358H	14113	303714	186	2.0	31	24	1740	4	7.9	1.0	498	13.5	0.4	8.5
7.5	C358I	13984	303714	271	1.6	49	37	1670	10	9.2	1.2	884	7.5	0.7	13.4
8.5	C358J	18770	303714	261	1.2	57	44	1709	7	9.4	0.8	554	1.9	0.9	18.8
9.5	C358K	20246	303714	254	1.1	47	36	1934	22	8.8	0.8	455	1.7	0.6	12.3
10.5	C358L	15910	303714	232	1.0	37	29	1876	8	8.0	1.2	776	2.0	0.9	17.0
12.5	C358M	19032	303714	261	1.0	46	35	1831	9	10.0	1.0	488	1.5	0.7	12.4
14.5	C358N	14278	303714	289	1.1	36	28	1863	6	7.3	0.9	490	4.5	0.7	12.9
16.5	C358O	7684	303714	224	1.9	35	26	1951	7	7.9	1.2	630	1.3	0.7	11.5
18.5	C358P	6608	303714	309	1.6	58	44	1766	19	7.8	1.4	412	1.1	1.4	26.9
20.5	C358Q	5204	303714	309	1.4	58	43	1653	13	6.9	0.9	221	1.3	1.0	17.8
25.5	C358R	5372	303714	303	1.2	53	41	1726	42	7.0	0.8	118	1.1	0.9	17.4
30.5	C358S	6827	303714	333	2.1	56	43	1765	11	8.3	1.1	148	1.5	1.0	17.6
34	C358T	7067	303714	333	2.4	53	41	1754	13	10.2	1.2	144	1.5	1.0	17.6
34	C358U	9339	303714	459	3.1	121	93	1960	19	18.7	1.4	118	3.1	1.7	32.2
39	C358V	9290	303714	429	2.8	56	43	1908	15	12.5	1.4	109	1.7	1.5	27.4
44	C358W	6633	303714	327	2.2	65	50	1835	11	11.4	1.0	176	0.8	0.8	14.5
49	C358X	7314	303714	313	2.5	59	45	1873	10	9.7	1.0	98	1.0	1.0	20.0
54	C358Y	8433	303714	357	1.9	55	42	1968	12	11.3	1.2	95	0.9	1.7	18.2
59	C358Z	11059	303714	398	4.9	53	41	2083	15	11.6	1.3	149	2.7	1.5	31.6
64	C358AA	9066	303714	351	3.0	48	37	1969	12	8.9	1.3	115	1.5	1.2	20.7
66.5	C358AB	9944	303714	378	3.1	65	50	2009	14	11.0	1.3	146	1.9	0.8	15.7

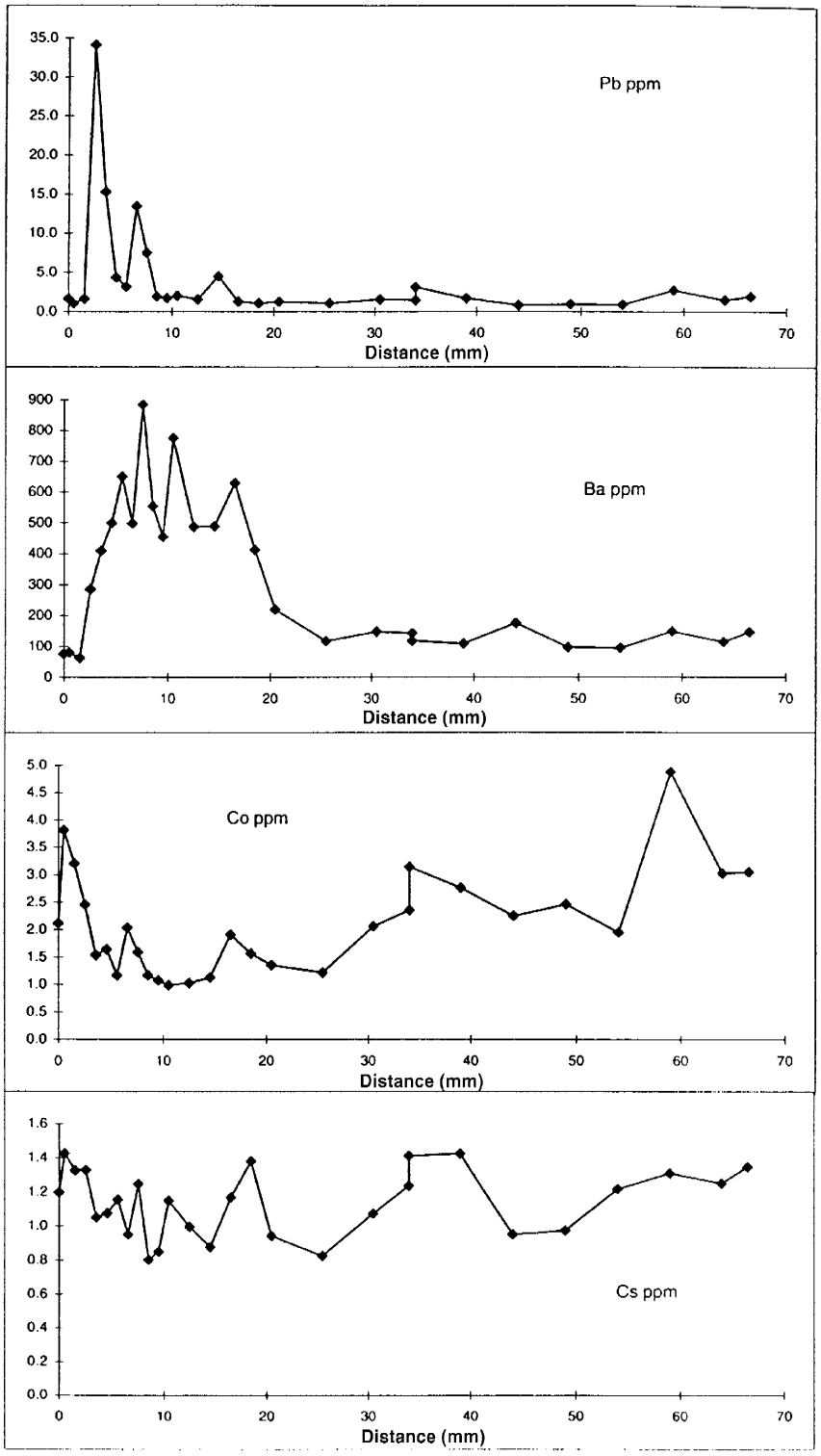
Pb ppm
Distance (mm)
Ba ppm
Distance (mm)
Co ppm
Distance (mm)
Cs ppm
Distance (mm)

Figure J-39

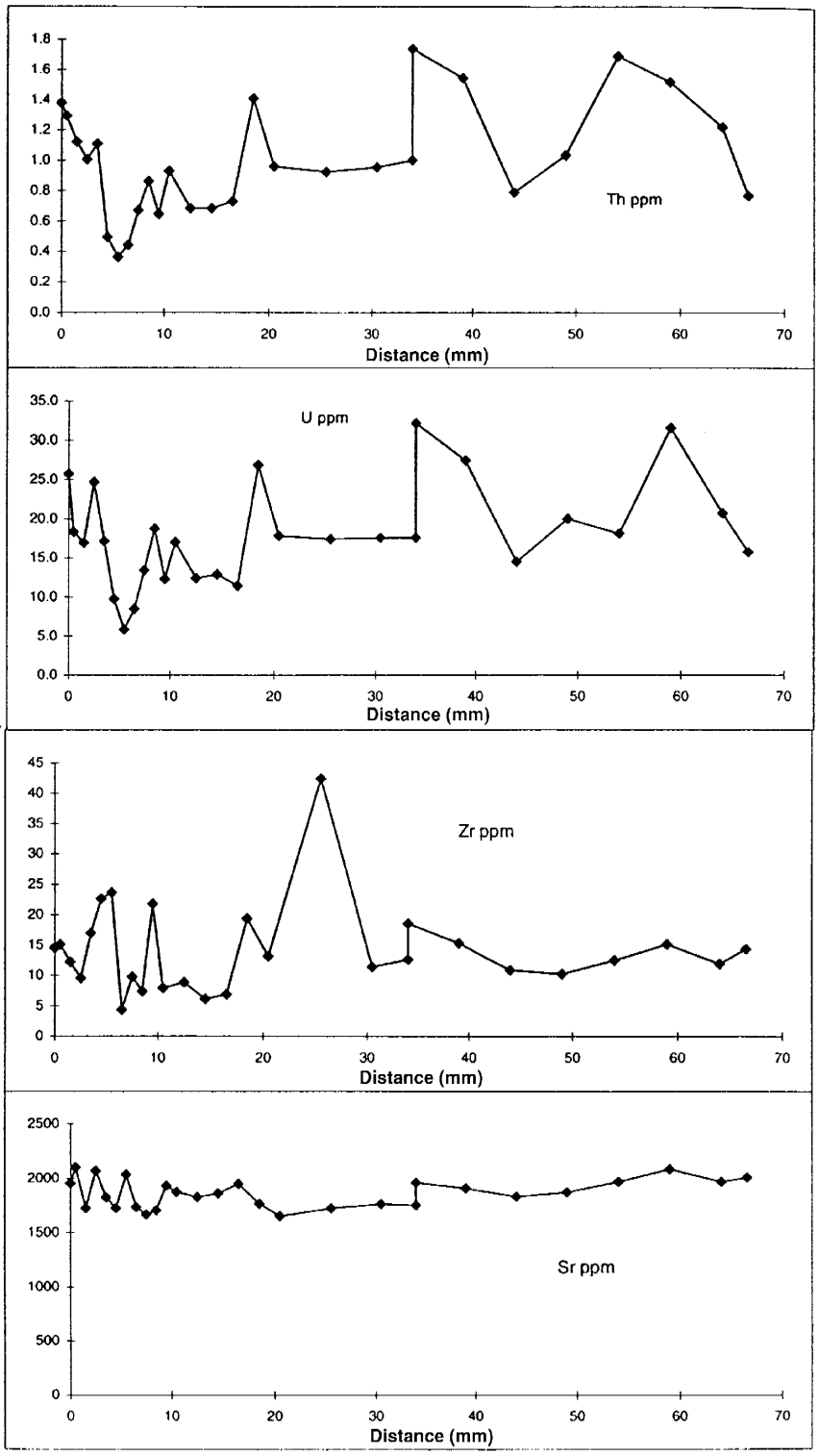
Th ppm
Distance (mm)
U ppm
Distance (mm)
Zr ppm
Distance (mm)
Sr ppm
Distance (mm)

Figure J-40

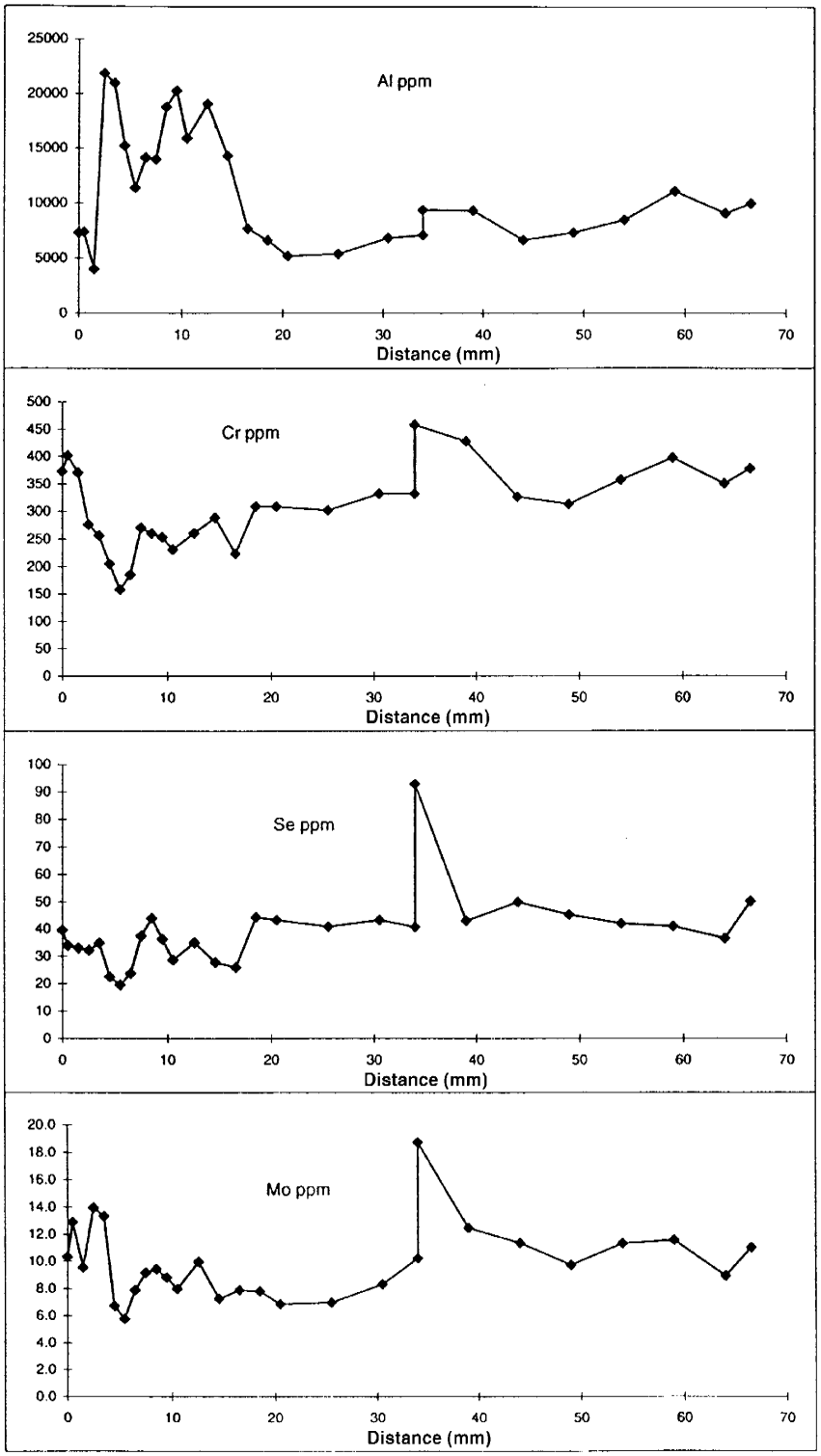
Al ppm
25000
20000
15000
10000
5000
0
0 10 20 30 40 50 60 70
Distance (mm)
Cr ppm
500
450
400
350
300
250
200
150
100
50
0
0 10 20 30 40 50 60 70
Distance (mm)
Se ppm
100
90
80
70
60
50
40
30
20
10
0
0 10 20 30 40 50 60 70
Distance (mm)
Mo ppm
20.0
18.0
16.0
14.0
12.0
10.0
8.0
6.0
4.0
2.0
0.0
0 10 20 30 40 50 60 70
Distance (mm)

Figure J-41

Table J-10. Profile C358. Profiles of U-series data across biomicrite wallrock with increasing distance from fracture edge in sample C358.

Sample	U (ppm)	Th (ppm)	^{226}Ra (mBq/g)	$^{234}U/^{238}U$	$^{230}Th/^{234}U$	$^{228}Th/^{232}Th$	$^{226}Ra/^{238}U$
C353							
0–15 mm	18.7(6)	2.4(2)	224(3)	0.97(3)	1.11(4)	1.0(1)	0.96(3)
15–30 mm	19.8(6)	2.7(2)	–	0.88(3)	1.18(5)	0.7(1)	–
30–45 mm	19.0(6)	2.3(2)	173(2)	0.98(3)	0.98(4)	1.0(1)	0.73(2)
45–60 mm	18.6(5)	2.3(2)	–	0.91(2)	1.06(4)	0.7(1)	–
60–75 mm	18.7(6)	1.8(2)	–	0.89(3)	1.08(4)	1.1(2)	–
75–90 mm	18.5(5)	2.0(2)	236(3)	0.94(3)	1.09(4)	1.1(2)	1.03(3)
C357							
0–10 mm	18.6(5)	2.3(2)	–	0.95(3)	0.99(4)	1.1(2)	–
50–75 mm	19.7(7)	0.9(1)	–	1.02(4)	0.97(4)	1.4(3)	–
C358							
0–15 mm	14.7(5)	1.1(1)	–	1.00(4)	1.06(5)	1.2(2)	–
40–55 mm	17.7(6)	1.0(1)	–	0.96(4)	0.96(4)	1.3(2)	–
C359							
0–10 mm	13.2(4)	3.1(2)	122(2)	0.96(4)	0.96(4)	1.3(1)	0.74(3)
10–17 mm	12.0(3)	2.4(2)	–	0.98(3)	0.97(4)	1.1(2)	–
17–32 mm	12.7(3)	*	137(2)	0.99(3)	1.15(4)	–	0.87(2)
32–48 mm	13.8(4)	*	–	0.94(3)	1.04(5)	–	–
48–63 mm	11.9(4)	2.7(2)	–	0.99(4)	1.08(5)	1.1(1)	–
63–77 mm	12.2(5)	1.3(1)	112(2)	1.02(5)	0.99(5)	0.8(1)	0.74(3)

All errors in parentheses are in least significant place and are 1 sigma uncertainties due to counting statistics alone.

* Results for ^{232}Th for C359 17–32 and 32–48 mm failed laboratory quality assurance (QA).

Average chemical recoveries are C353 (80% U and 77% Th) and C359 (70% U and 71% Th).

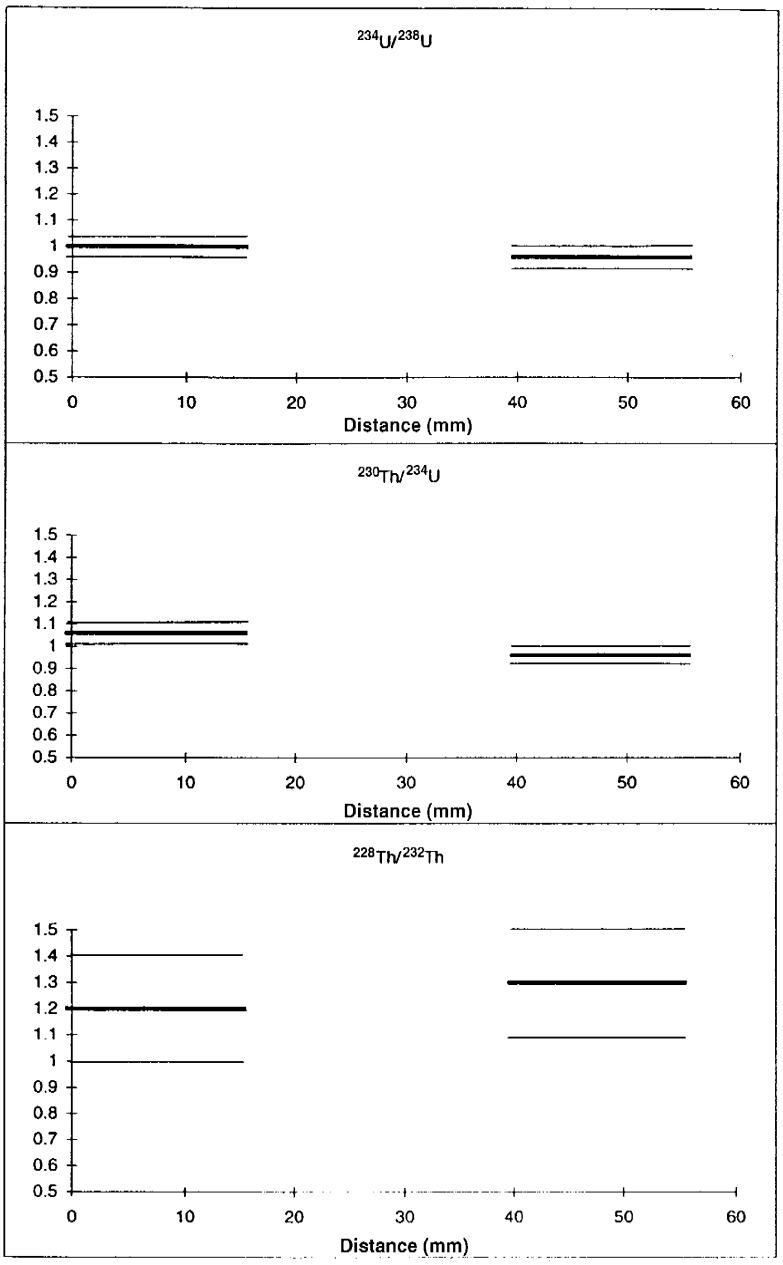

Note: Error bar represents 1 sigma uncertainties due to counting statistics alone.

Figure J-42

PROFILE C359

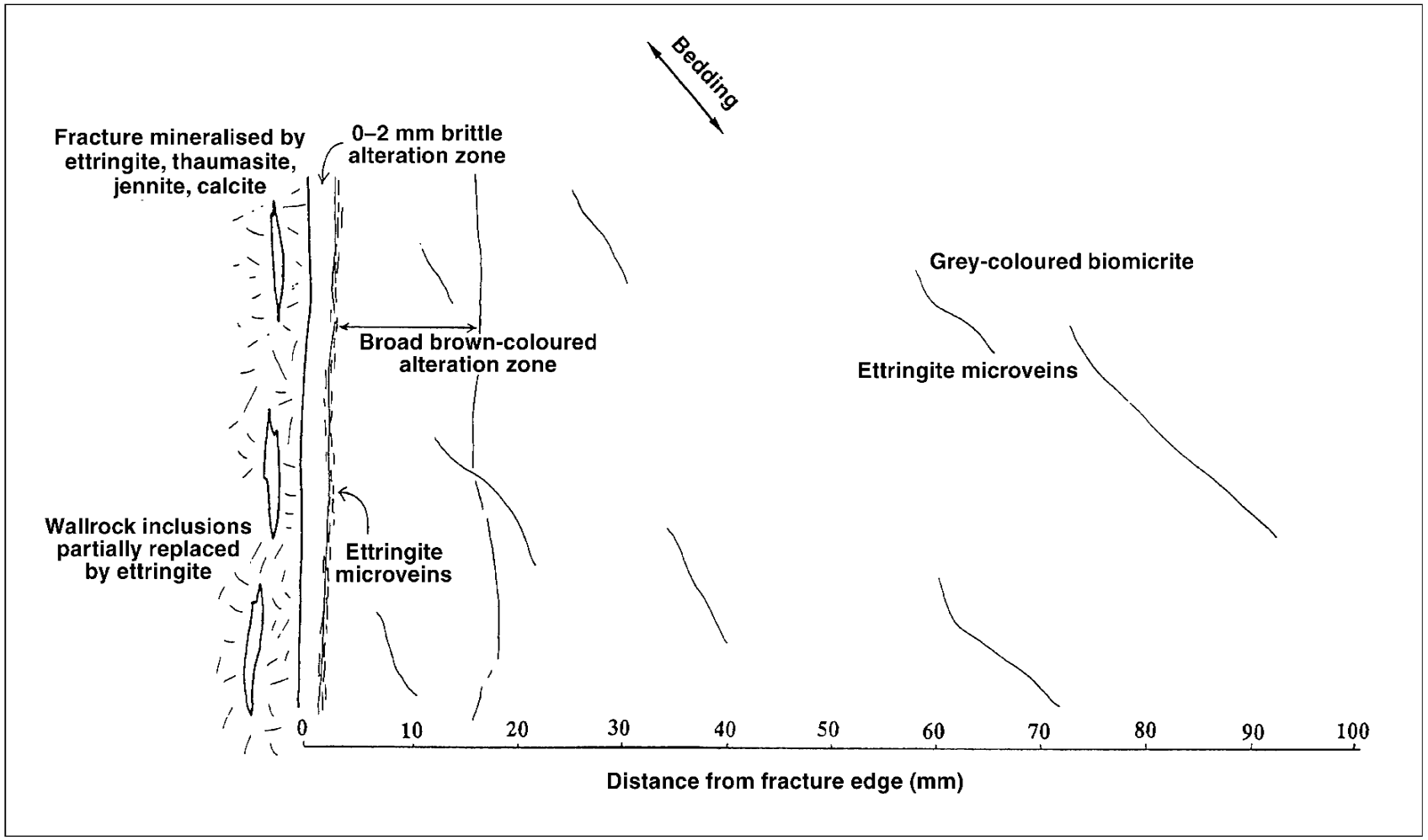

Figure J-43. *Profile C359. Diagrammatic sketch of vein and biomicrite wallrock profile in sample C359.*

Table J-11. Profile C359. Geochemical profiles across biomicrite wallrock with increasing distance from fracture edge in sample C359. [Major elements are expressed as oxide weight per cent; trace elements as parts per million. LOI = Loss On Ignition; Total = total major element oxides including LOI. Total iron is expressed as Fe_2O_3].

Sample	SiO_2 %	TiO_2 %	Al_2O_3 %	Fe_2O_3t %	MnO %	MgO %	CaO %	Na_2O %	K_2O %	P_2O_5 %	LOI %	SO_3 %	Cr_2O_3 %	SrO %	Total %
C353 0–15	9.91	0.17	4.38	2.59	0	0.31	46.28	0.09	0.05	2.23	32.36	0.7	0.09	0.51	99.67
C353 15–30	9.57	0.16	4.51	2.05	0.01	0.27	46.88	0.07	0.06	2.17	32.73	0.6	0.09	0.59	99.76
C353 30–45	9.49	0.16	4.5	1.88	0.01	0.29	46.76	0.07	0.05	2.14	33.08	0.4	0.09	0.58	99.5
C353 45–60	9.64	0.17	4.62	2.03	0.01	0.29	46.78	0.07	0.04	2.16	32.99	0.3	0.08	0.64	99.82
C353 60–75	9.54	0.17	4.58	1.97	0	0.28	46.73	0.08	0.04	2.15	33.2	0.2	0.08	0.7	99.72
C353 75–90	9.29	0.16	4.37	1.92	0.01	0.27	46.81	0.07	0.07	2.12	33.43	0.3	0.08	0.76	99.66
C357 0–10	7.76	0.06	1.89	0.9	0	0.18	43	0.08	0.13	1.65	40.23	3.3	0.04	0.2	99.42
C357 50–75	4.88	0.07	2.01	1.04	0	0.22	42.54	0.11	0.1	1.83	43.33	3.1	0.05	0.26	99.54
C358 0–15	9.02	0.06	3.29	0.95	0	0.2	42.47	0.09	0.12	1.35	40.02	1.8	0.04	0.21	99.62
C358 40–55	5.28	0.07	1.79	1.05	0	0.24	42.52	0.1	0.12	1.51	43.69	2.9	0.05	0.21	99.53
C359 0–10	4.68	0.06	2.17	0.72	0	0.2	46.6	0.06	0.02	1.64	41.03	2.6	0.04	0.17	99.99
C359 10–17	5.48	0.06	2.22	0.67	0	0.18	46.59	0.07	0.02	1.61	40.31	2.4	0.03	0.18	99.82
C359 17–32	4.21	0.06	1.29	0.69	0	0.2	46.94	0.06	0.01	1.74	42.04	2.3	0.04	0.18	99.76
C359 32–48	5.04	0.06	1.15	0.67	0	0.19	46.67	0.07	0.02	1.7	41.17	2.7	0.04	0.18	99.66
C359 48–63	4.64	0.05	1.2	0.65	0	0.19	46.69	0.07	0.02	1.69	41.68	2.6	0.03	0.18	99.7
C359 63–77	3.85	0.06	1.13	0.68	0	0.2	46.88	0.06	0.01	1.72	42.17	2.6	0.04	0.17	99.57

Table J-11 (contd.) Profile C359. Geochemical profiles across biomicrite wallrock with increasing distance from fracture edge in sample C359. [Major elements are expressed as oxide weight per cent; trace elements as parts per million].

Sample	Chromium ppm	Cobalt ppm	Nickel ppm	Selenium ppm	Strontium ppm	Zirconium ppm	Molybdenum ppm	Caesium ppm	Barium ppm	Lead ppm	Thorium ppm	Uranium ppm
C353 (0–30)	564	4.0	264	50	4644	33.5	17.2	1.40	102	<5	2.82	23.4
C353 (15–30)	480	6.7	224	49	5309	27.0	54.0	1.83	118	<5	2.65	23.8
C353 (30–45)	408	7.5	208	42	5516	26.3	5.2	2.10	113	<5	2.51	22.7
C353 (45–60)	437	6.7	194	42	5646	26.2	4.9	2.23	102	<5	2.57	23.0
C353 (60–75)	454	6.7	196	45	6296	28.0	4.8	2.44	95	<5	2.52	22.4
C353 (75–90)	471	6.7	203	43	7208	27.4	5.4	3.00	93	<5	2.48	22.3
C357 (0–10)	318	4.7	162	63	1907	16.3	15.2	1.61	396	<5	1.12	20.1
C357 (50–75)	329	4.5	170	33	2256	16.1	13.8	1.11	106	<5	1.30	22.5
C358 (0–15)	289	2.6	90	33	1794	13.8	10.4	1.33	521	<5	1.03	16.3
C358 (40–55)	325	3.9	151	30	1855	15	13.1	1.17	135	<5	1.17	19.9
C359 (0–10)	250	3.6	127	53	1475	13.1	10.2	0.74	87	<5	0.93	13.0
C359 (10–17)	246	4.0	126	51	1515	13.7	10.5	1.05	109	<5	0.93	13.1
C359 (17–32)	268	3.9	137	49	1532	13.4	9.4	0.95	92	<5	0.95	13.7
C359 (32–48)	253	3.7	138	50	1628	13.2	8.7	1.27	121	<5	0.99	13.5
C359 (48–65)	254	3.9	139	41	1630	13.2	9.2	1.13	122	<5	0.96	13.4
C359 (63–77)	270	4.1	142	47	1529	13.6	10.1	0.89	97	<5	1.07	13.7

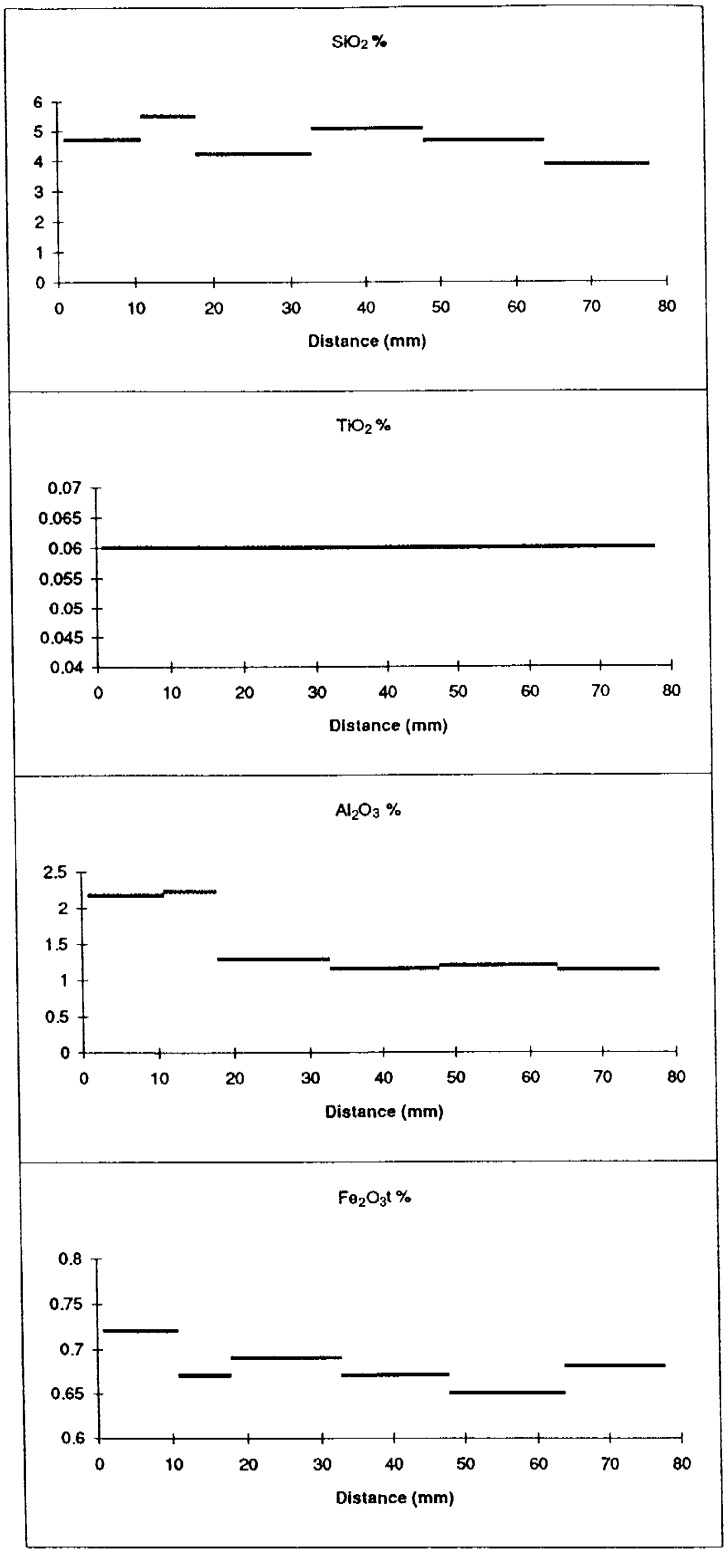
SiO2 %
6
5
4
3
2
1
0
0 10 20 30 40 50 60 70 80
Distance (mm)
TiO2 %
0.07
0.065
0.06
0.055
0.05
0.045
0.04
0 10 20 30 40 50 60 70 80
Distance (mm)
Al2O3 %
2.5
2
1.5
1
0.5
0
0 10 20 30 40 50 60 70 80
Distance (mm)
Fe2O3t %
0.8
0.75
0.7
0.65
0.6
0 10 20 30 40 50 60 70 80
Distance (mm)

Figure J-44

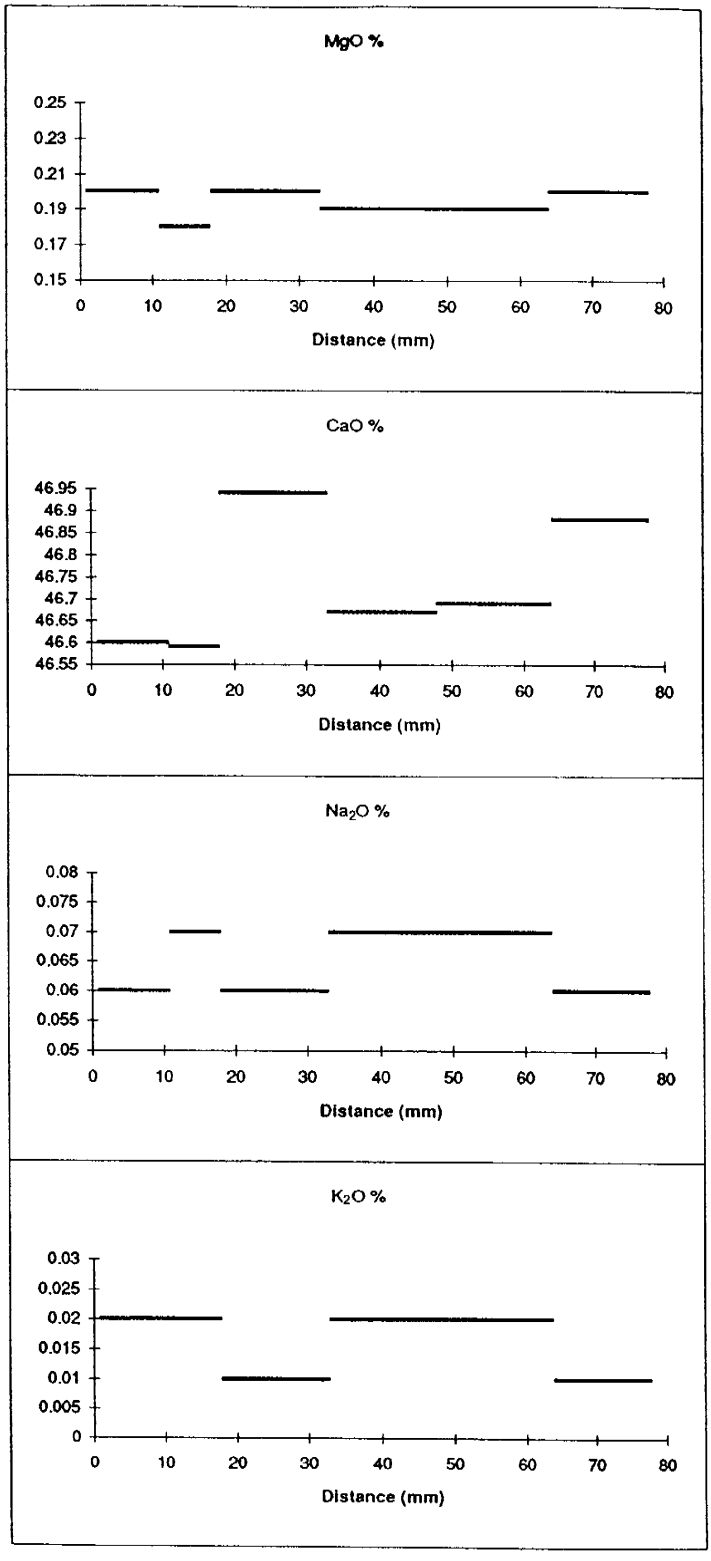
MgO %
0.25
0.23
0.21
0.19
0.17
0.15
0 10 20 30 40 50 60 70 80
Distance (mm)
CaO %
46.95
46.9
46.85
46.8
46.75
46.7
46.65
46.6
46.55
0 10 20 30 40 50 60 70 80
Distance (mm)
Na2O %
0.08
0.075
0.07
0.065
0.06
0.055
0.05
0 10 20 30 40 50 60 70 80
Distance (mm)
K2O %
0.03
0.025
0.02
0.015
0.01
0.005
0
0 10 20 30 40 50 60 70 80
Distance (mm)

Figure J-45

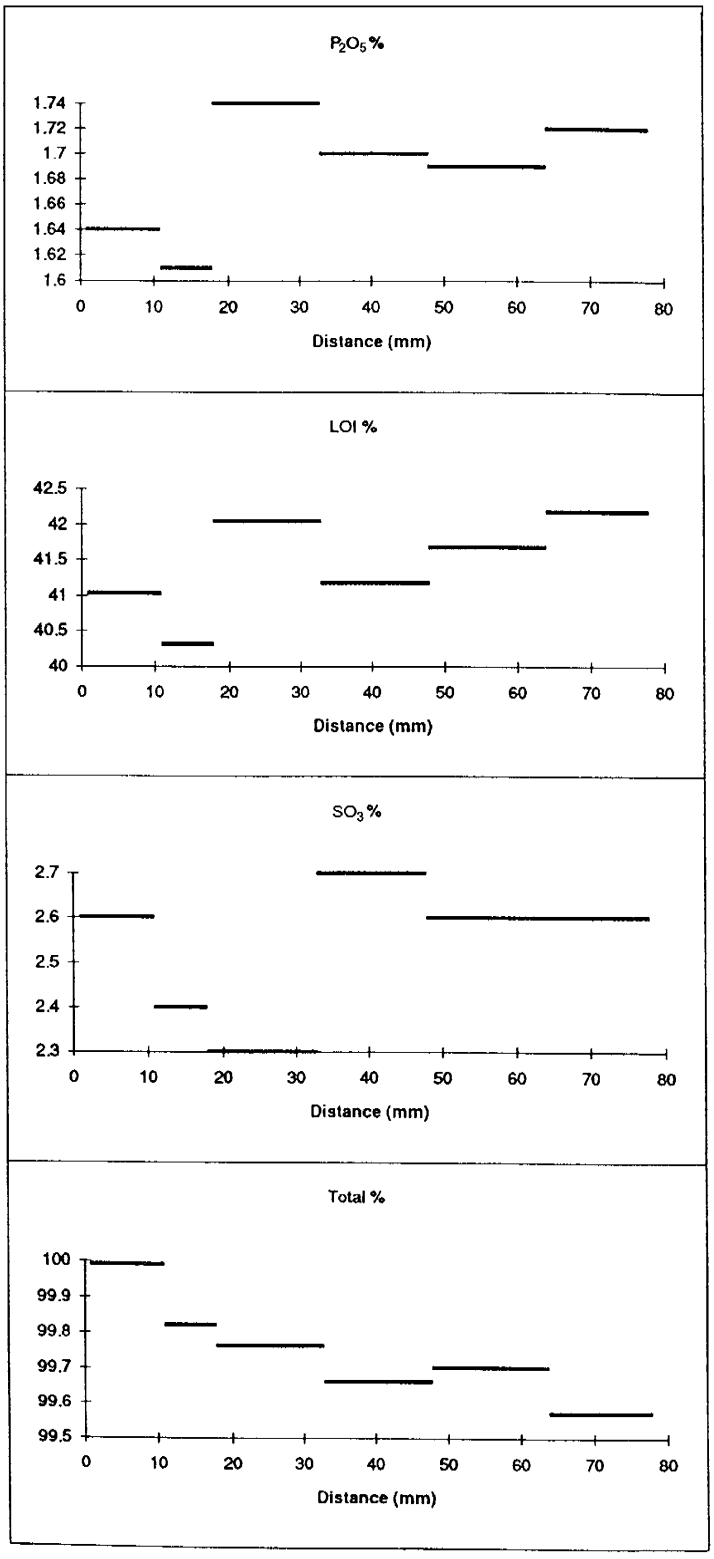
P_2O_5 %
1.74
1.72
1.7
1.68
1.66
1.64
1.62
1.6
0 10 20 30 40 50 60 70 80
Distance (mm)
LOI %
42.5
42
41.5
41
40.5
40
0 10 20 30 40 50 60 70 80
Distance (mm)
SO_3 %
2.7
2.6
2.5
2.4
2.3
0 10 20 30 40 50 60 70 80
Distance (mm)
Total %
100
99.9
99.8
99.7
99.6
99.5
0 10 20 30 40 50 60 70 80
Distance (mm)

Figure J-46

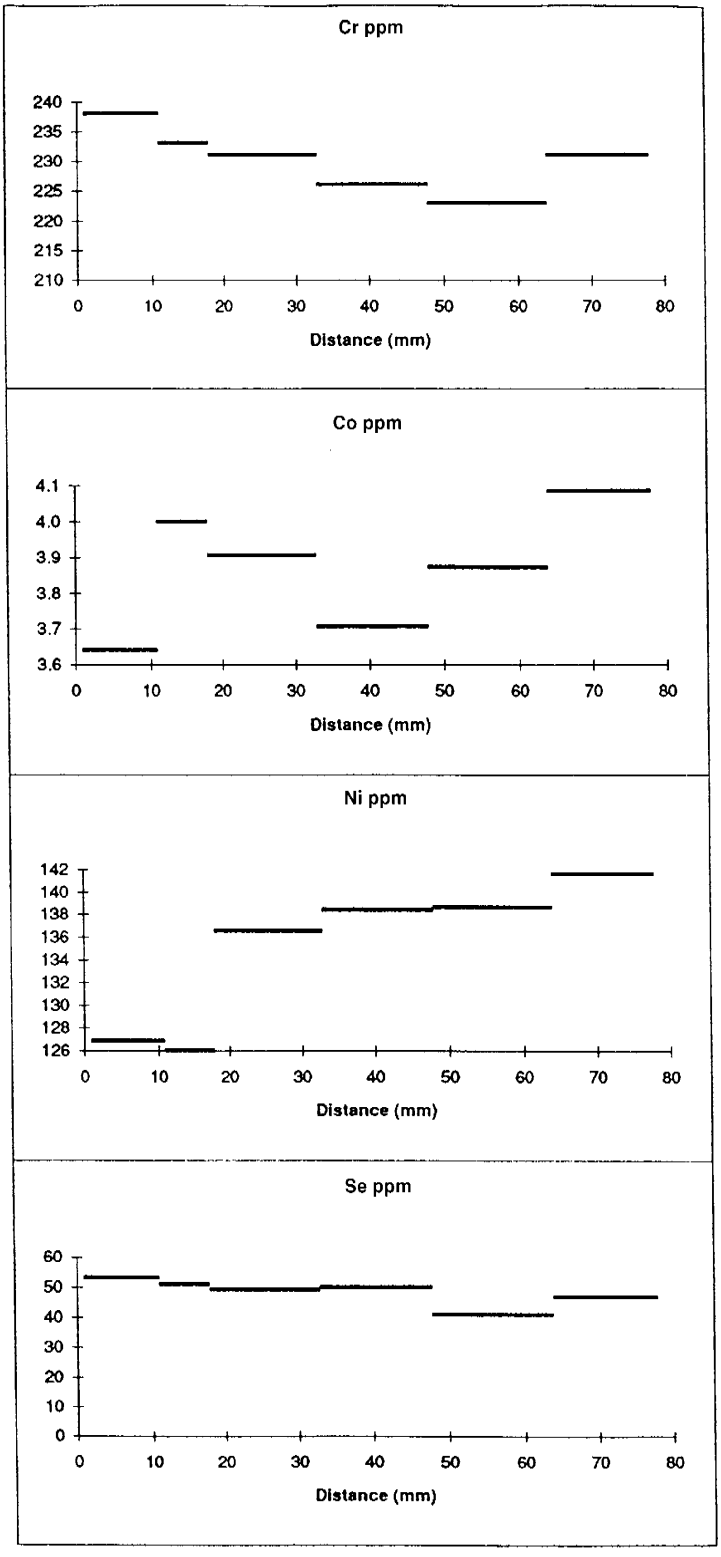
Cr ppm
240
235
230
225
220
215
210
0 10 20 30 40 50 60 70 80
Distance (mm)
Co ppm
4.1
4.0
3.9
3.8
3.7
3.6
0 10 20 30 40 50 60 70 80
Distance (mm)
Ni ppm
142
140
138
136
134
132
130
128
126
0 10 20 30 40 50 60 70 80
Distance (mm)
Se ppm
60
50
40
30
20
10
0
0 10 20 30 40 50 60 70 80
Distance (mm)

Figure J-47

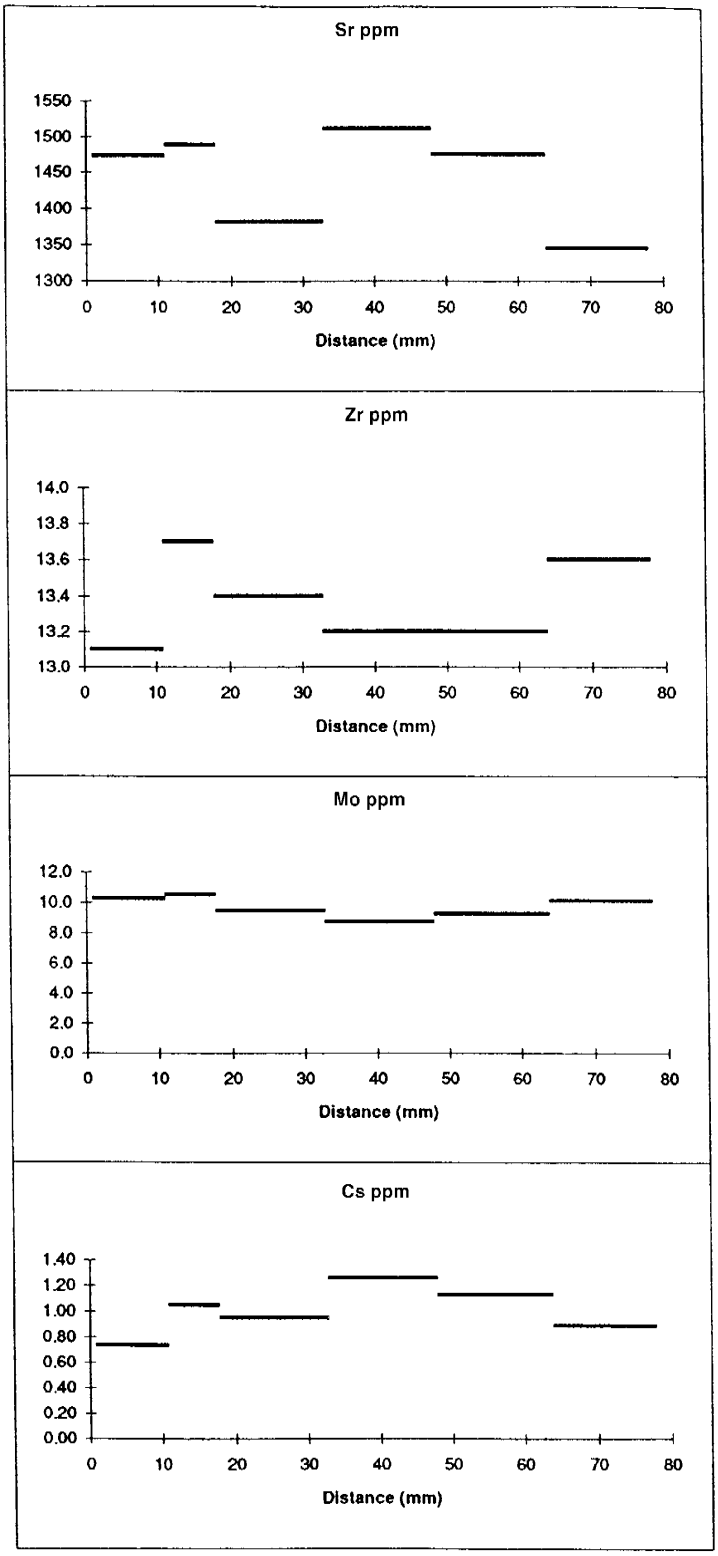
Sr ppm
1550
1500
1450
1400
1350
1300
0 10 20 30 40 50 60 70 80
Distance (mm)
Zr ppm
14.0
13.8
13.6
13.4
13.2
13.0
0 10 20 30 40 50 60 70 80
Distance (mm)
Mo ppm
12.0
10.0
8.0
6.0
4.0
2.0
0.0
0 10 20 30 40 50 60 70 80
Distance (mm)
Cs ppm
1.40
1.20
1.00
0.80
0.60
0.40
0.20
0.00
0 10 20 30 40 50 60 70 80
Distance (mm)

Figure J-48

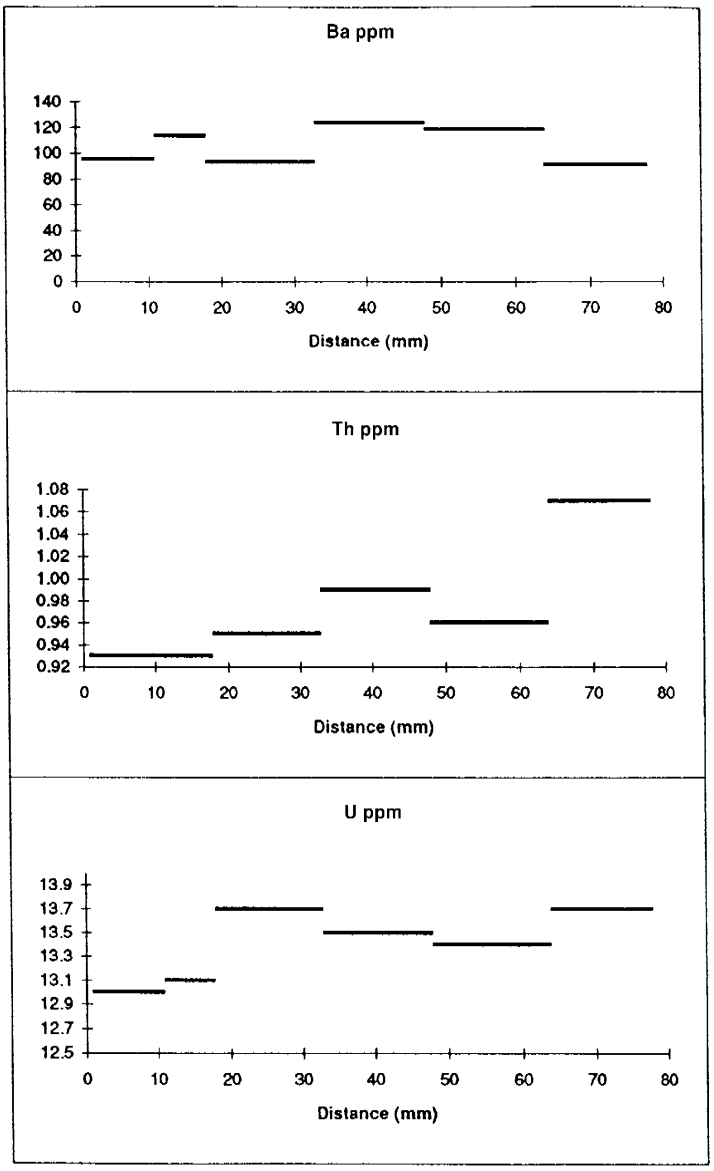
Ba ppm
140
120
100
80
60
40
20
0
0 10 20 30 40 50 60 70 80
Distance (mm)
Th ppm
1.08
1.06
1.04
1.02
1.00
0.98
0.96
0.94
0.92
0 10 20 30 40 50 60 70 80
Distance (mm)
U ppm
13.9
13.7
13.5
13.3
13.1
12.9
12.7
12.5
0 10 20 30 40 50 60 70 80
Distance (mm)

Figure J-49

Table J-12. Profile C359. In situ Laser Ablation Microprobe – Inductively Coupled Plasma – Mass Spectrometry (LAMP-ICP-MS) element profiles across biomicrite wallrock with increasing distance from fracture edge in sample C359.

Distance from vein (mm)	Sample	Aluminium ^{27}Al	Calcium ^{44}Ca	Chromium ^{53}Cr	Cobalt ^{59}Co	Selenium ^{78}Se	Selenium ^{82}Se	Strontium ^{86}Sr	Zirconium ^{90}Zr	Molybdenum ^{98}Mo	Caesium ^{133}Cs	Barium ^{138}Ba	Lead ^{208}Pb	Thorium ^{232}Th	Uranium ^{238}U
-0.75	C359A	20361	333571	10	1.4	109	84	274	3	17	0.7	101	3.3	0.5	0.7
-0.5	C359B	75322	333571	302	1.0	87	67	1198	9	57	0.2	72	5.2	0.8	17.1
-0.25	C359C	25479	333571	39	0.3	122	93	966	1	3	0.2	56	1.4	0.1	1.1
0	C359D	29863	333571	230	1.0	50	39	1735	9	19	1.4	119	3.7	0.5	11.5
0.5	C359E	23204	333571	186	1.0	50	40	1613	7	13	0.9	156	5.8	0.5	11.0
1	C359F	1231	333571	245	2.2	57	44	1472	12	6	0.2	97	2.2	1.1	18.2
2	C359G	4727	333571	245	2.2	60	46	1676	10	4	0.3	113	2.6	0.6	9.7
3	C359H	1329	333571	289	2.0	51	39	1454	14	7	0.4	285	4.2	1.2	17.3
4	C359I	1392	333571	282	2.1	56	43	1535	11	5	0.4	103	1.4	0.8	12.8
5	C359J	2801	333571	344	3.4	59	45	1465	12	9	0.3	238	4.0	0.8	12.5
6	C359K	18466	333571	223	2.2	56	43	1577	8	14	1.2	225	3.6	0.7	12.9
7	C359L	20564	333571	256	1.4	54	41	1583	8	15	1.2	224	2.8	0.7	11.7
8	C359M	2410	333571	284	2.1	58	45	1503	11	10	0.3	104	1.1	0.9	16.1
9	C359N	1641	333571	235	2.0	56	43	1480	9	8	0.3	92	0.9	0.9	12.4
10	C359O	2755	333571	238	1.7	53	41	1365	9	8	0.3	84	1.0	0.8	13.8
12	C359P	17246	333571	276	1.1	53	41	1601	10	13	0.9	200	3.0	0.8	11.9
14	C359Q	17071	333571	235	1.5	49	38	1565	8	12	1.1	197	2.3	0.6	10.6
16	C359R	16371	333571	231	1.6	49	43	1615	11	12	1.2	217	2.7	1.0	16.5
18	C359S	14633	333571	228	1.9	56	43	1513	8	10	1.1	217	2.7	0.5	9.4
20	C359T	14226	333571	312	1.6	52	41	1572	13	13	1.1	212	2.6	0.7	10.0
22	C359U	11059	333571	240	2.0	78	60	1556	12	10	1.1	164	3.0	0.9	12.7
27	C359V	7408	333571	244	1.6	71	43	1814	18	8	0.8	122	1.3	1.0	14.5
32	C359W	7020	333571	250	1.8	78	50	1480	10	8	0.8	175	3.2	0.8	12.1
34.5	C359X	6161	333571	270	1.5	54	41	1548	13	9	0.7	304	5.0	1.0	16.7
34.5	C359Y	5811	333571	276	1.4	56	43	1632	14	9	0.7	84	1.4	1.0	14.3
39.5	C359Z	5715	333571	268	1.8	51	39	1626	9	8	1.0	94	2.0	0.7	9.8
44.5	C359AA	6501	333571	286	1.6	89	44	1646	11	11	1.1	108	1.3	0.9	12.4
49.5	C359AB	5600	333571	313	1.3	52	37	1587	10	9	1.0	123	1.2	0.7	12.3
54.5	C359AC	6650	333571	287	2.8	50	37	1791	12	10	1.5	140	2.0	1.0	13.6
59.5	C359AD	5128	333571	266	1.2	51	42	1405	10	8	1.2	110	0.7	1.4	9.7
64.5	C359AE	6168	333571	260	1.6	51	39	1529	13	9	1.2	115	1.2	1.0	16.2
67.5	C359AF	6642	333571	257	3.5	44	38	1560	9	8	1.1	127	3.3	0.9	12.0

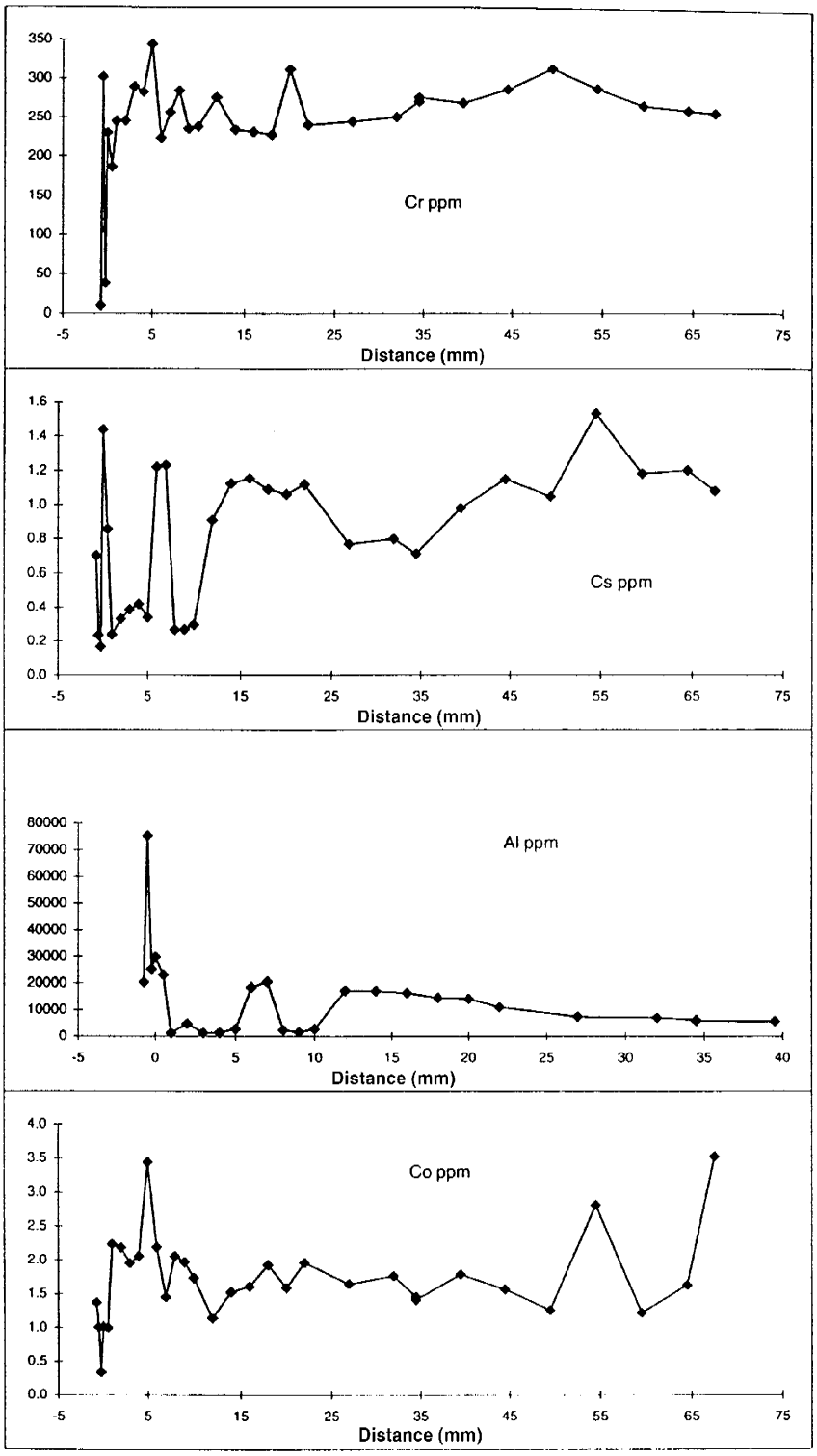
Cr ppm
Distance (mm)
Cs ppm
Distance (mm)
Al ppm
Distance (mm)
Co ppm
Distance (mm)

Figure J-50

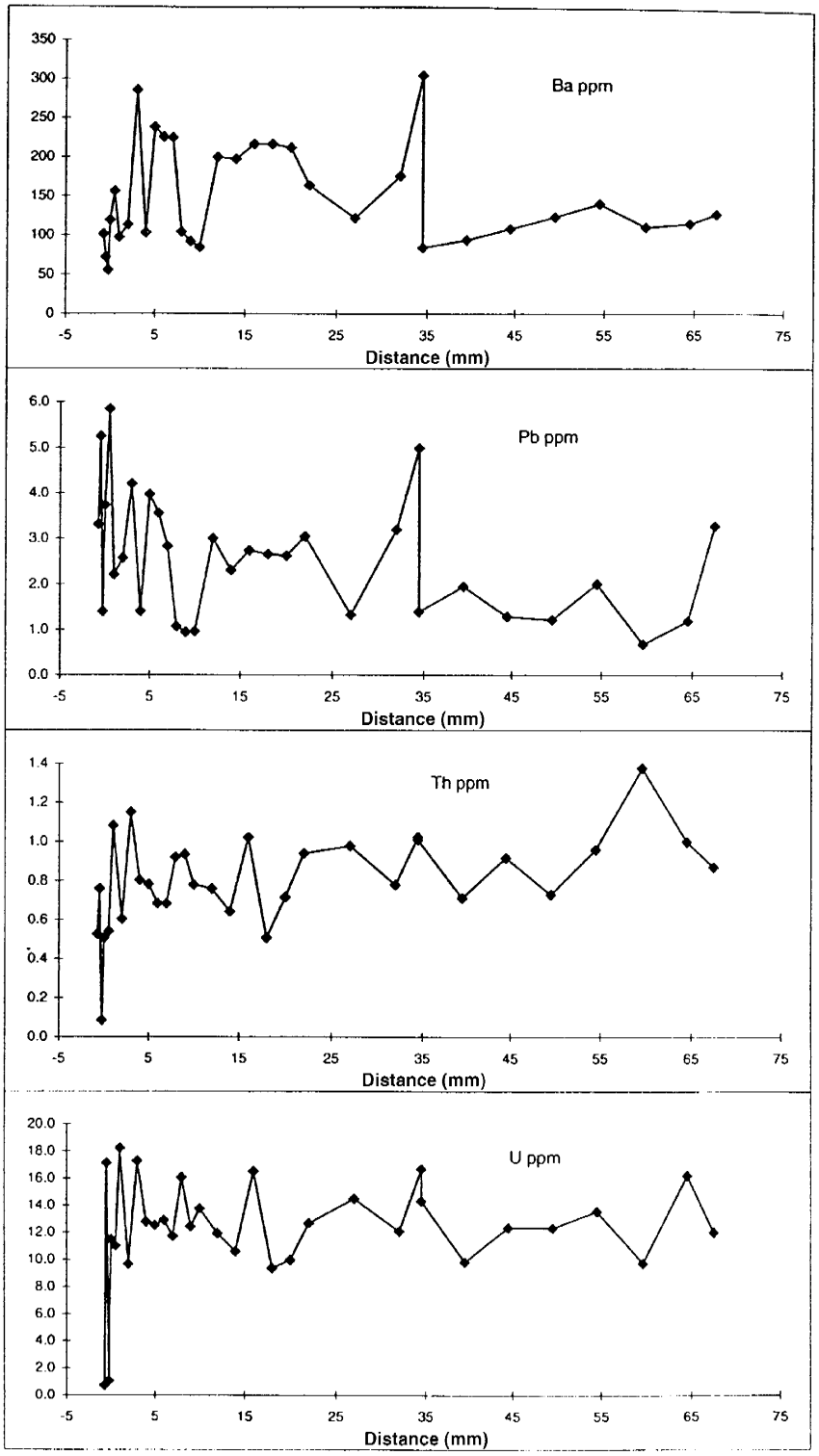
Ba ppm
350
300
250
200
150
100
50
0
-5
5
15
25
35
45
55
65
75
Distance (mm)
Pb ppm
6.0
5.0
4.0
3.0
2.0
1.0
0.0
Distance (mm)
Th ppm
1.4
1.2
1.0
0.8
0.6
0.4
0.2
0.0
Distance (mm)
U ppm
20.0
18.0
16.0
14.0
12.0
10.0
8.0
6.0
4.0
2.0
0.0
Distance (mm)

Figure J-51

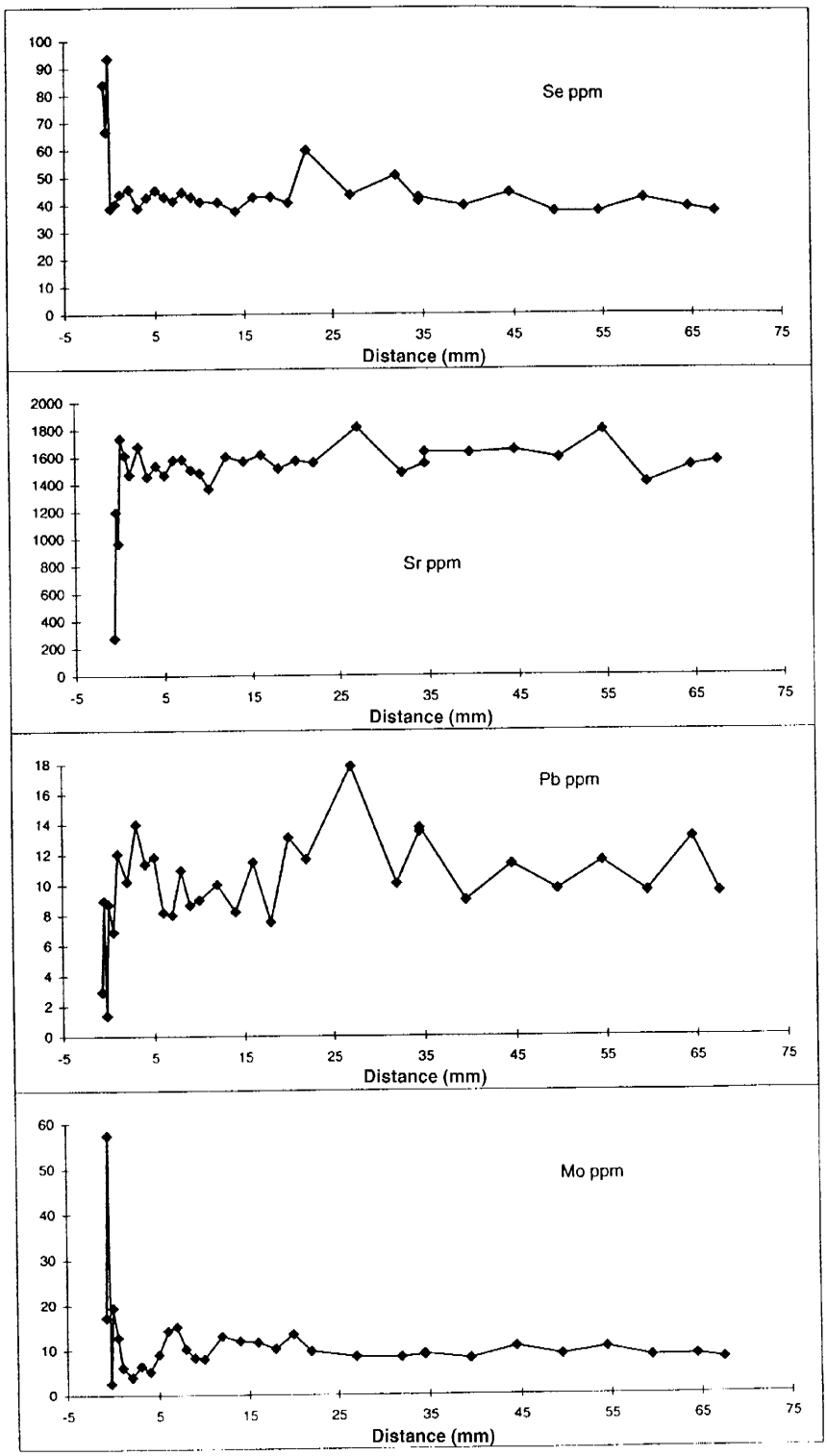
Se ppm
Distance (mm)
Sr ppm
Distance (mm)
Pb ppm
Distance (mm)
Mo ppm
Distance (mm)

Figure J-52

Table J-13. Profile C359. Profiles of U-series data across biomicrite wallrock with increasing distance from fracture edge in sample C359.

Sample	U (ppm)	Th (ppm)	^{226}Ra (mBq/g)	$^{234}U/^{238}U$	$^{230}Th/^{234}U$	$^{228}Th/^{232}Th$	$^{226}Ra/^{238}U$
C353							
0–15 mm	18.7(6)	2.4(2)	224(3)	0.97(3)	1.11(4)	1.0(1)	0.96(3)
15–30 mm	19.8(6)	2.7(2)	–	0.88(3)	1.18(5)	0.7(1)	–
30–45 mm	19.0(6)	2.3(2)	173(2)	0.98(3)	0.98(4)	1.0(1)	0.73(2)
45–60 mm	18.6(5)	2.3(2)	–	0.91(2)	1.06(4)	0.7(1)	–
60–75 mm	18.7(6)	1.8(2)	–	0.89(3)	1.08(4)	1.1(2)	–
75–90 mm	18.5(5)	2.0(2)	236(3)	0.94(3)	1.09(4)	1.1(2)	1.03(3)
C357							
0–10 mm	18.6(5)	2.3(2)	–	0.95(3)	0.99(4)	1.1(2)	–
50–75 mm	19.7(7)	0.9(1)	–	1.02(4)	0.97(4)	1.4(3)	–
C358							
0–15 mm	14.7(5)	1.1(1)	–	1.00(4)	1.06(5)	1.2(2)	–
40–55 mm	17.7(6)	1.0(1)	–	0.96(4)	0.96(4)	1.3(2)	–
C359							
0–10 mm	13.2(4)	3.1(2)	122(2)	0.96(4)	0.96(4)	1.3(1)	0.74(3)
10–17 mm	12.0(3)	2.4(2)	–	0.98(3)	0.97(4)	1.1(2)	–
17–32 mm	12.7(3)	*	137(2)	0.99(3)	1.15(4)	–	0.87(2)
32–48 mm	13.8(4)	*	–	0.94(3)	1.04(5)	–	–
48–63 mm	11.9(4)	2.7(2)	–	0.99(4)	1.08(5)	1.1(1)	–
63–77 mm	12.2(5)	1.3(1)	112(2)	1.02(5)	0.99(5)	0.8(1)	0.74(3)

All errors in parentheses are in least significant place and are 1 sigma uncertainties due to counting statistics alone.

* Results for ^{232}Th for C359 17–32 and 32–48 mm failed laboratory quality assurance (QA).

Average chemical recoveries are C353 (80% U and 77% Th) and C359 (70% U and 71% Th).

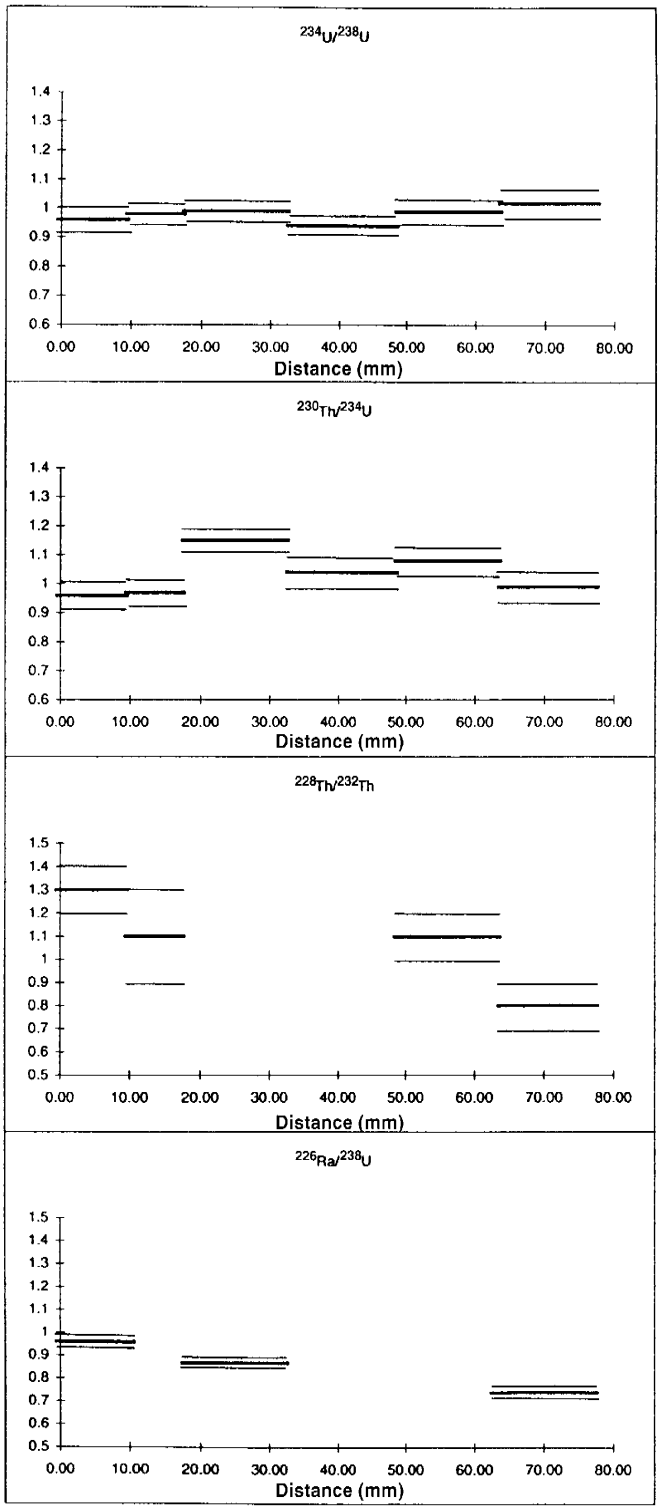

Note: Error bars represent 1 sigma uncertainties due to counting statistics alone.

Figure J-53

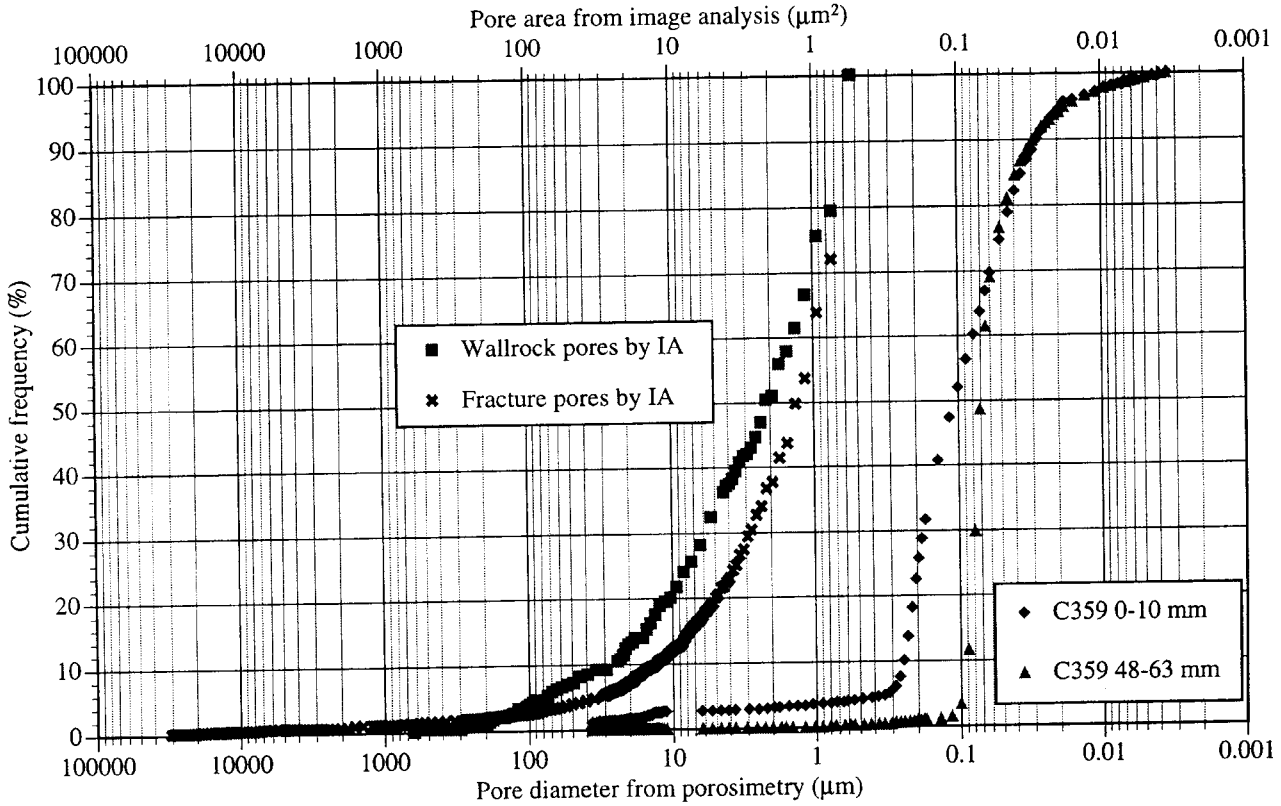

Figure J-54. *Profile C359. Comparison of pore throat diameters determined by liquid resaturation porosimetry and pore areas determined by image analysis from two thin sections along profile C359 (0–10 mm and 48–63 mm).*

APPENDIX K

Regional Groundwater Analyses

(Compiled by E. Salameh)

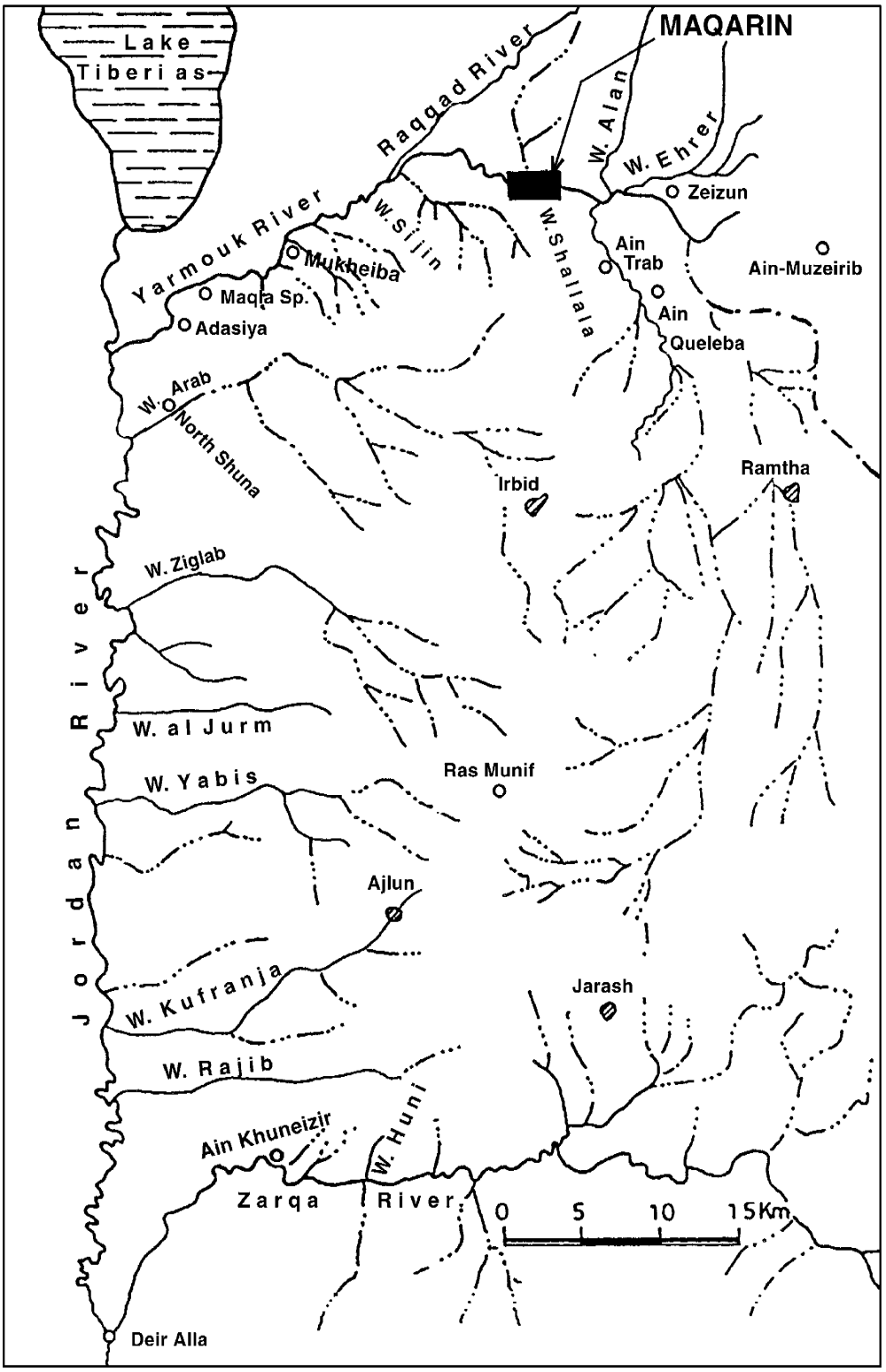

Figure K-1. *Drainage map of NW Jordan showing locations to some of the sampling areas referred to in the tables.*

Table K-1. Regional Groundwater Analyses.

Location	Date Sampled	^{18}O (‰) (±0.2)	^{2}H (‰) (±1.3)	^{3}H (TU) (±1)	^{14}C (pmc)	^{13}C (‰)	EC (µS/cm)	TDS (ppm)	pH	Ca (meq/L)	Mg (meq/L)	Na (meq/L)	K (meq/L)	Cl (meq/L)	SO_4 (meq/L)	HCO_3 (meq/L)	NO_3 (ppm)	SiO_2 (ppm)
R. Farhan 1	19-07-89	-6.4	-31.8	7.01			630	403	7.7	3.6	2.1	0.8	0.1	1.2	0.2	4.6	33.6	
Nuaimeh 2	09-08-89	-5.8	-32.3	10.5			610	390	7.3	3.3	1.8	0.9	0.1	1.0	0.3	4.2	36.0	
Nuaimeh 2	19-08-89	-6.4	-32.1	7.8			610	390	8.0	3.3	2.0	0.8	0.1	1.1	0.1	4.6	35.6	
Nuaimeh 2	11-02-91	-6.3	-29.7	6.4			630	403	7.3	3.5	2.0	1.0	0.1	1.2	0.2	4.5	47.8	
Nuaimeh 2	20-10-92	-6.2	-30.0	5.2			610	390	7.4	3.3	1.9	0.9	0.0	1.1	0.1	4.3	33.2	
Nuaimeh 2	30-12-92	-6.4	-30.4	7.0			690	435	7.4	4.0	2.2	1.0	0.1	1.4	0.3	4.6	52.0	
Nuaimeh 1	11-01-87	-5.5	–	6.2			560	358	7.3	3.3	1.5	0.8	0.1	1.0	0.0	4.4	20.2	
Nuaimek 1	10-03-87	-5.5	–	6.0			540	346	7.3	3.2	1.5	–	–	0.9	0.2	4.4	20.9	
Nuaimeh 1	13-02-88	-7.0	-29.9	6.6	59.6 ± 0.7	-10.9	550	352	7.4	3.1	1.7	0.8	0.1	0.9	0.1	4.3	20.1	
Nuaimeh 1	09-08-88	-5.4	-32.5	8.4			540	346	7.4	3.0	1.6	0.6	0.1	0.9	0.1	3.9	23.0	
Nuaimeh 1	03-05-89	-5.9	-31.5	7.0			530	339	7.5	3.1	2.0	–	–	1.0	0.0	4.3	20.2	
Nuaimeh 1	22-05-89	-5.9	-30.8	5.5			540	346	7.5	3.0	1.4	–	–	0.9	0.9	4.1	20.1	
Nuaimeh 1	19-07-89	-6.1	-30.8	6.9			540	346	7.5	3.3	1.6	0.8	0.1	0.9	0.0	4.4	20.1	
Nuaimeh 1	02-10-89	-5.7	-31.2	5.3			560	353	7.5	3.3	1.5	0.8	0.1	0.9	0.3	4.2	20.0	
Nuaimeh 1	11-02-91	-6.0	-28.2	5.2			550	352	7.4	3.2	1.7	0.8	0.0	0.9	0.0	4.4	19.6	
Nuaimeh 1	03-12-92	-6.0	-29.3	4.5			560	353	7.5	3.1	2.0	0.9	0.0	1.1	0.1	4.2	24.7	
H. Farhan	13-02-88	-7.2	-29.2	9.2	63.1 ± 0.7	-11.3	590	378	7.3	3.4	2.0	0.7	0.0	1.0	0.0	4.7	24.5	
H. Farhan	09-08-88	-5.6	-32.7	10.1			570	365	7.4	3.2	1.7	0.7	0.1	0.9	0.1	4.3	23.2	
H. Farhan	17-07-91	-6.3	-29.9	6.0			620	397	7.2	3.6	1.8	0.8	0.1	1.0	0.0	4.8	27.3	
H. Farhan	20-10-92	-6.2	-30.4	7.2			600	378	7.5	3.5	1.7	0.8	0.0	1.0	0.0	4.6	24.3	
H. Farhan	30-12-92	-6.2	-29.0	2.3			620	391	7.6	3.5	1.8	0.9	0.0	1.0	0.4	4.5	25.3	
Yarm. Uni	11-02-91	-5.9	-28.5	7.1			620	397	7.4	3.7	1.8	0.9	0.0	1.1	0.3	4.7	27.5	
Side Wadies Wells																		
Kufr Ubah	09-11-88	-5.7	-29.5	4.5			490	314	6.7	2.9	1.5	0.8	0.1	0.7	0.1	4.1	22.9	
Kufr Ubah	19-07-89	-5.7	-25.5	4.1			490	314	7.8	2.9	1.8	0.6	0.1	0.7	0.3	4.0	22.8	
Kufr Ubah	08-04-91	-5.6	-18.5	4.0			520	333	7.6	3.0	1.6	0.5	0.0	0.7	0.1	4.1	22.0	
Kufr Assad	16-09-92	-4.3	-19.0	6.3			1 290	826	6.9	9.5	2.1	2.6	0.1	3.1	3.6	6.7	50.1	
Kufr Assad	23-05-91	-4.6	-20.0	4.2			1 380	883	7.0	9.6	2.4	2.8	0.1	3.3	4.0	6.9	56.4	
Deir Yusef 3	06-04-88	-6.4	-28.8	9.9			430	275	7.8	2.9	1.1	0.4	0.1	0.4	0.1	3.7	26.8	
Juhfieh 1	22-05-89	-6.1	-28.5	6.0			540	346	7.6	3.3	1.0	–	–	0.8	0.9	4.2	26.4	
Juhfieh 1	19-07-89	-6.4	-28.8	6.1			540	346	7.6	3.5	1.8	0.6	0.1	0.7	0.3	4.5	26.2	
Juhfieh 1	02-10-89	-6.0	-29.8	5.1			550	352	7.5	3.5	1.7	0.5	0.1	0.7	0.7	4.5	26.0	
Juhfieh 1	13-05-90	-6.0	-28.0	6.4			560	353	7.6	3.6	1.6	0.6	0.1	0.8	0.1	4.5	27.7	
Juhfieh 1	08-04-91	-6.4	-20.9	2.9			600	384	7.6	3.7	1.6	0.6	0.1	0.8	0.0	4.6	28.6	

Table K-1 (contd.). Regional Groundwater Analyses.

Location	Date Sampled	^{18}O (‰) (±0.2)	^{2}H (‰) (±1.3)	^{3}H (TU) (±1)	^{14}C (pmc)	^{13}C (‰)	EC (µS/cm)	TDS (ppm)	pH	Ca (meq/L)	Mg (meq/L)	Na (meq/L)	K (meq/L)	Cl (meq/L)	SO_4 (meq/L)	HCO_3 (meq/L)	NO_3 (ppm)	SiO_2 (ppm)
Side Wadies Wells (contd.)																		
Abu Said 2	14-01-87	-5.7	–	3.5			800	512	8.2	6.1	2.0	1.0	0.2	1.0	0.7	7.4	4.8	
Abu Said 2	07-08-88	-5.3	-30.1	4.6			820	525	6.9	6.1	1.9	0.8	0.1	1.1	0.8	6.9	6.6	
Abu Said 2	08-04-91	-5.6	-24.1	4.1			840	538	7.2	5.8	2.1	0.7	0.1	1.0	0.6	7.0	13.6	
Abu Said 2	20-10-92	-5.6	-24.7	4.2			870	557	7.0	6.5	2.0	0.8	0.0	1.2	0.8	7.1	10.3	
Abu Said 1	21-03-87	-5.9	–	5.5			850	544	7.0	6.1	2.3	–	–	1.0	0.7	6.9	12.8	
Abu Said 1	17-02-88	-6.6	-26.2	4.6			840	538	6.8	6.2	2.4	1.0	0.1	1.1	0.9	7.3	17.5	
Abu Said 1	07-08-88	-5.5	-29.7	0.4			820	525	6.9	5.4	2.4	1.0	0.1	1.1	0.7	6.8	17.0	
Abu Said 1	08-04-91	-6.0	-27.3	4.1			820	525	7.3	4.9	2.6	0.9	0.1	1.0	0.4	6.8	20.7	
Abu Said 1	20-10-92	-6.0	-26.3	3.7			1 020	653	6.9	7.6	2.4	1.0	0.1	1.5	1.8	7.6	18.3	
Wadi Arab 1	11-01-87	-4.9	–	0.0			880	563	7.0	5.5	3.2	1.0	0.1	1.1	1.6	7.2	0.8	
Wadi Arab 1	10-03-87	-4.8	–	0.0			910	582	7.2	5.8	3.3	–	–	1.1	1.4	7.7	3.1	
Wadi Arab 1	15-02-88	-5.7	-23.6	0.0			880	563	7.1	5.3	3.3	1.1	0.1	1.1	1.6	6.9	0.8	
Wadi Arab 1	07-08-88	-4.7	-25.2	1.7			900	576	7.0	5.5	3.2	0.9	0.1	1.1	1.4	7.1	0.5	
Wadi Arab 1	13-05-90	-5.5	-21.3	0.6			900	567	7.1	5.4	3.3	0.9	0.0	1.1	1.6	7.0	0.5	
Wadi Arab 1	22-05-91	-5.1	-22.9	0.0			890	561	7.5	5.6	3.0	1.0	0.0	1.1	1.5	7.0	0.4	
Wadi Arab 1	16-09-92	-5.5	-23.6	–			860	550	7.1	5.5	3.0	1.0	0.1	1.1	1.3	7.0	0.4	
Wadi Arab 1	15-10-92	-5.4	-23.3	–	11.6 ± 0.8	-13.1	860	550	7.0	5.1	3.3	0.9	0.0	1.0	1.4	7.0	0.5	
Wadi Arab 2	11-01-87	-4.7	–	0.0			870	556	7.0	5.6	3.0	1.0	0.1	1.1	1.6	7.2	1.2	
Wadi Arab 2	10-03-87	-4.6	–	2.4			850	544	6.9	5.5	2.8	–	–	1.0	1.3	7.4	0.6	
Wadi Arab 2	15-02-88	-5.6	-24.2	0.2			850	544	7.1	5.3	2.9	1.1	0.1	1.0	1.2	7.1	1.1	
Wadi Arab 2	13-05-90	-5.2	-22.8	0.0			850	536	7.1	5.5	3.0	0.9	0.1	1.1	1.4	6.9	0.7	
Wadi Arab 2	16-09-92	-5.5	-21.8	–			840	538	7.1	5.3	3.1	0.9	0.1	1.1	1.3	6.9	0.8	
Wadi Arab 2	17-10-92	-5.4	-22.1	–	11.0 ± 0.9	-13.5	850	544	7.1	5.4	2.8	0.9	0.1	1.1	1.5	6.7	0.7	
Wadi Arab 3	15-02-88	-5.6	-22.6	0.6	16.7 ± 0.6	-10.5	840	538	7.2	5.4	2.8	1.0	0.1	1.0	1.1	7.0	1.2	
Wadi Arab 3	07-08-88	-4.6	-25.1	0.8			860	550	7.0	5.5	2.8	1.1	0.0	1.1	1.3	6.9	0.8	
Wadi Arab 3	13-05-90	-5.3	-22.6	0.2			840	529	7.2	5.3	3.0	0.8	0.1	1.0	1.4	6.7	1.0	
Wadi Arab 3	23-05-91	-5.3	-22.8	0.0			830	531	7.4	5.6	2.6	0.9	0.1	1.0	1.5	6.7	0.7	
Wadi Arab 3	01-08-91	-5.2	-22.7	–			820	517	7.0	5.4	2.7	0.9	0.1	1.0	1.3	6.7	1.2	
Wadi Arab 3	16-09-92	-5.5	-22.8	–			800	512	7.0	5.3	2.6	0.6	0.1	1.0	1.1	6.7	1.0	
Wadi Arab 3	15-10-92	-5.3	-22.8	–			820	525	7.0	5.2	2.7	0.8	0.1	1.0	1.2	6.7	1.2	
Wadi Arab 4	15-02-88	-5.8	-24.6	0.2	11.9 ± 0.6	-9.6	980	627	7.0	6.0	3.2	1.9	0.1	1.2	2.9	7.1	1.1	
Wadi Arab 4	07-08-88	-4.8	-25.4	0.0			990	634	7.0	5.8	3.4	1.8	0.1	1.2	2.6	7.2	0.7	
Wadi Arab 4	13-05-90	-5.1	-22.9	0.4			960	605	7.1	5.8	3.4	1.3	0.1	1.2	2.3	7.2	0.5	
Wadi Arab 4	08-11-90	-4.9	-22.3	0.0			930	586	7.3	5.7	3.4	1.4	0.1	1.2	2.3	7.0	0.5	
Wadi Arab 4	23-05-91	-5.0	-22.7	0.0			950	608	7.2	5.7	3.3	1.4	0.1	1.1	2.4	7.1	0.4	

Table K-1 (contd.). Regional Groundwater Analyses.

Location	Date Sampled	^{18}O (‰) (±0.2)	^{2}H (‰) (±1.3)	^{3}H (TU) (±1)	^{14}C (pmc)	^{13}C (‰)	EC (µS/cm)	TDS (ppm)	pH	Ca (meq/L)	Mg (meq/L)	Na (meq/L)	K (meq/L)	Cl (meq/L)	SO_4 (meq/L)	HCO_3 (meq/L)	NO_3 (ppm)	SiO_2 (ppm)
Side Wadies Wells (contd.)																		
Wadi Arab 4	01-08-91	-5.3	-22.4	–			940	592	6.9	5.9	3.5	1.4	0.1	1.2	2.4	7.2	0.7	–
Wadi Arab 4	15-10-92	-5.2	-24.8	–			930	595	7.0	5.4	3.3	1.4	0.1	1.1	2.0	7.2	0.7	–
Wadi Arab 5	14-02-88	-5.9	-24.4	0.6	35.3 ± 0.7	-13.0	760	486	7.1	4.6	2.7	0.9	0.1	1.1	0.5	6.5	12.9	–
Wadi Arab 5	07-08-88	-5.1	-27.3	0.0			780	499	7.1	4.7	2.8	0.9	0.1	1.1	0.6	6.4	12.8	–
Wadi Arab 5	13-05-90	-5.2	-24.1	0.0			800	504	7.7	4.8	2.9	0.7	0.1	1.2	0.7	6.4	12.5	–
Wadi Arab 5	23-05-91	-5.4	-24.5	0.0			780	499	7.3	4.9	2.7	0.8	0.1	1.2	0.7	6.4	13.2	–
Wadi Arab 5	01-08-91	-5.4	-24.8	–			770	485	7.0	4.8	2.8	0.8	0.1	1.1	0.6	6.5	12.8	–
Wadi Arab 5	24-03-92	-5.8	-24.8	0.0			800	504	7.1	4.8	2.7	0.8	0.1	1.3	0.5	6.6	13.2	–
Wadi Arab 5	16-09-92	-5.5	-23.9	–			760	486	7.0	5.0	2.3	0.8	0.1	1.2	0.5	6.5	13.4	–
Jdcita Well	14-02-88	-6.4	-26.0	8.1			750	480	7.6	5.2	1.6	0.9	0.1	1.0	0.3	6.1	15.2	–
Jdcita Well	07-08-88	-5.1	-28.4	5.6			710	454	7.2	4.1	2.3	1.1	0.1	1.2	0.3	5.5	26.0	–
Jdcita Well	17-05-90	-5.7	-25.7	6.7			720	454	7.3	4.4	2.4	–	–	1.2	0.5	5.6	27.3	–
Jdcita Well	17-05-90	-5.7	-25.7	6.7			720	454	7.3	4.4	2.4	–	–	1.2	0.5	5.6	27.3	–
Jdcita Well	08-04-91	-6.0	-27.5	6.3			780	499	7.5	4.9	2.1	0.8	0.1	1.1	0.5	6.2	19.0	–
Jdcita Well	19-10-92	-6.2	-26.8	5.2			750	480	7.0	4.6	2.4	0.9	0.1	1.1	0.2	6.1	18.9	–
Jdcita Well	30-03-93	–	–	6.9	73.4 ± 1.7	-13.3												
R. Hazaimeh	19-07-89	-5.2	-22.3	0.5			630	403	7.6	3.6	2.2	0.8	0.1	0.9	0.0	5.2	27.0	–
Waled Khazar	19-10-92	-5.8	–	–			870	548	7.1	5.1	3.0	1.3	0.0	1.4	0.7	7.2	0.9	–
Waled Khazar	06-04-88	-6.0	-25.6	0.0			999	634	7.0	5.5	3.3	1.8	0.1	1.8	1.5	7.1	4.5	–
Waled Khazar	40-03-93	–	–	0.0	11.7 ± 0.7	-12.9												
M. Abdel Wal	06-04-88	-5.6	-22.5	0.0			910	582	7.0	6.1	2.2	1.6	0.1	1.4	1.6	6.8	1.8	–
M. Abdel Wal	25-09-90	-5.3	-23.7	0.1			960	605	7.0	6.2	2.8	1.5	0.1	1.6	1.7	7.2	0.9	–
Adasiya 4	12-11-91	-3.4	-16.5	7.9			2 640	1 690	7.3	7.4	6.4	13.1	0.5	15.7	5.5	5.8	24.3	25.1
Adasiya 4	12-11-91	-3.5	-15.9	8.3			2 640	1 663	7.3	7.4	6.4	13.1	0.5	15.7	5.5	5.8	24.3	25.1
Adasiya 4	12-11-91	-3.6	–	9.1														
Adasiya 5	24-03-92	-3.2	–	10.7			3 900	2 457	7.2	10.2	16.8	12.4	0.6	28.7	7.4	3.7	2.2	–
Adasiya 5	18-07-91	-3.5	-16.2	9.0			3 500	2 240	7.3	9.5	15.7	10.5	0.6	26.3	6.5	3.4	3.9	26.0
Adasiya 6	08-03-92	-3.7	–	5.3			6 100	3 843	7.7	8.4	28.2	24.8	1.5	53.0	5.7	3.4	2.3	17.5
Adasiya B	06-07-91	-4.7	-23.6	0.0			3 600	2 304	7.9	1.8	9.2	22.6	1.4	28.7	2.8	3.8	1.2	24.9
Adasiya 1B	18-03-92	-3.7	–	2.6			13 800	8 832	8.3	10.0	4.3	128.0	1.5	141	0.4	0.7	13.2	–
A.S.	07-08-88	-4.1	-24.8	1.8			1 680	1 075	7.1	4.8	4.9	7.8	0.2	7.6	3.1	6.5	21.8	–
A.S.	08-03-92	-4.9	–	2.6			2 690	1 695	7.4	7.8	8.3	11.3	0.6	12.8	6.0	7.3	102.5	26.0

Table K-1 (contd.). Regional Groundwater Analyses.

Location	Date Sampled	^{18}O (‰) (±0.2)	^{2}H (‰) (±1.3)	^{3}H (TU) (±1)	^{14}C (pmc)	^{13}C (‰)	EC (µS/cm)	TDS (ppm)	pH	Ca (meq/L)	Mg (meq/L)	Na (meq/L)	K (meq/L)	Cl (meq/L)	SO_4 (meq/L)	HCO_3 (meq/L)	NO_3 (ppm)	SiO_2 (ppm)
Ramtha area																		
Rahub	22-03-90	-4.1	-19.0	1.6			590	372	7.5	3.3	0.8	1.7	0.0	1.6	0.3	3.5	24.2	
Ali Samara	13-01-87	-6.4	–	0.1			1 290	826	7.0	6.1	4.2	3.9	0.1	3.4	3.4	7.3	4.8	
Ali Samara	16-02-88	-6.9	-34.9	0.0	6.4 ± 0.3		1 320	845	6.8	6.2	4.3	3.9	0.1	3.5	3.5	7.4	1.7	
Ali Samara	16-05-90	-6.2	-33.6	0.0			1 410	888	7.0	5.7	3.9	–	–	3.3	2.9	7.2	0.9	
Ali Samara	18-03-87	-6.1	–	0.0			1 290	825	7.1	5.8	4.6	–	–	3.0	3.0	7.0	2.9	
K. Tabah 2	07-06-88	-6.5	-36.2	0.0			1 080	691	7.0	5.1	3.6	3.2	0.0	2.9	2.3	6.7	1.0	
K. Tabah 2	16-05-90	-6.4	-34.4	0.4			1 110	699	7.2	4.8	3.3	–	–	2.8	1.9	6.5	1.1	
K. Tabah 2	04-07-89	-6.6	-34.5	1.6	1.2 ± 0.5	-11.5	1 110	710	7.1	5.4	3.5	3.0	0.0	2.9	2.3	6.7	1.0	
M.A. Haji	16-02-88	-5.2	-27.0	0.7	9.8 ± 0.4		1 080	691	7.2	4.1	3.2	3.9	0.1	4.5	1.1	5.4	1.5	
M.A. Haji	16-05-90	-4.7	-25.9	0.9			1 200	756	7.7	4.2	2.6	–	–	4.8	1.3	5.4	1.4	
M.A. Haji	17-07-91	-4.6	-23.3	0.0			1 140	730	7.5	4.3	3.0	3.6	0.1	4.6	1.1	5.4	1.6	
M.A. Haji	19-10-92	-4.3	-24.6	–			1 080	691	7.5	3.9	3.2	3.8	0.1	4.7	1.2	5.2	1.7	
M. Samata	07-06-88	-6.4	-33.7	0.0			1 290	826	6.8	5.8	4.3	4.0	0.1	3.5	3.3	7.4	1.0	
Ahmad Fares	14-02-88	-4.1	-21.4	2.9			1 410	902	7.4	4.0	2.3	7.3	0.1	7.1	1.7	4.0	55.5	
Ahmad Fares	07-04-88	-4.4	-23.1	2.9			1 170	749	7.4	3.5	1.9	6.0	0.1	5.9	1.3	3.5	50.2	
Ahmad Fares	09-08-88	-3.3	-23.0	2.0			1 260	806	7.4	3.5	2.3	6.3	0.1	6.4	1.4	3.6	56.2	
Ahmad Fares	14-02-89	-4.1	-21.4	–			1 410	902	7.4	4.0	2.3	7.3	0.1	7.1	1.7	4.0	55.5	
Ahmad Fares	17-04-89	-4.1	-22.0	1.0			1 350	864	7.6	4.0	2.4	–	–	7.0	1.5	4.1	55.8	
Ahmad Fares	17-07-91	-4.2	-21.9	1.0			1 680	1 075	7.1	4.7	2.5	9.0	0.2	8.9	1.5	4.8	60.6	
Mahasi 4	14-02-88	-6.0	-31.7	4.8			820	525	8.1	1.3	1.1	4.9	0.3	4.8	0.5	2.2	10.7	
Mahasi 4	07-04-88	-5.2	-26.5	9.4			1 350	864	7.7	5.1	2.3	5.4	0.4	6.6	1.4	3.3	124.0	
Nahlawi	22-03-90	-5.1	-28.2	1.4			900	567	7.6	3.2	2.4	3.3	0.1	3.8	0.9	3.7	27.3	
Kur	22-03-90	-4.8	-25.0	2.5			1 200	756	7.5	3.8	2.8	5.3	0.1	5.9	1.7	3.5	46.0	
Mahasi 1	14-02-88	-4.4	-21.7	–			2 310	1 502	7.4	6.4	4.6	10.1	0.8	11.6	2.1	4.2	264.0	
Mahasi 1	14-02-89	-4.2	-21.7	–			2 310	1 502	7.4	6.4	4.6	10.0	0.8	11.6	2.1	4.2	264.0	

Table K-1 (contd.). Regional Groundwater Analyses.

Location	Date Sampled	^{18}O (‰) (±0.2)	^{2}H (‰) (±1.3)	^{3}H (TU) (±1)	^{14}C (pmc)	^{13}C (‰)	EC (µS/cm)	TDS (ppm)	pH	Ca (meq/L)	Mg (meq/L)	Na (meq/L)	K (meq/L)	Cl (meq/L)	SO_4 (meq/L)	HCO_3 (meq/L)	NO_3 (ppm)	SiO_2 (ppm)
North-East desert area																		
Yusef Hmeidi	07-06-88	-5.7	-32.4	0.3			1 020	653	7.2	3.5	3.3	3.1	0.0	4.5	0.9	4.1	28.4	19.0
Taleb Masri	18-03-87	-6.0	–	0.0			940	602	7.4	2.8	2.7	–	–	3.6	1.0	4.7	2.7	
Taleb Masri	08-06-88	-6.4	-32.4	0.0			950	608	7.3	2.8	2.2	4.2	0.2	3.7	0.7	4.8	0.5	
Taleb Masri	04-07-89	-6.4	-32.2	0.0	3.3 ± 0.7	-9.1	970	621	7.4	2.8	2.8	4.2	0.2	3.8	1.0	5.4	0.2	
Taleb Masri	13-01-87	-6.2	–	0.0			950	608	7.4	2.9	2.4	4.0	0.1	3.7	0.4	5.1	1.2	
Swelmeh	07-06-88	-6.0	-35.7	0.2			830	531	7.2	3.1	2.3	3.0	0.1	2.9	0.7	4.8	0.1	
Swelmeh	15-07-91	-5.2	-30.4	0.0			830	531	7.2	3.6	2.0	2.7	0.2	2.8	0.7	4.9	0.3	
Swelmeh	21-10-92	-5.8	-33.6	0.0			840	538	7.3	3.3	2.0	2.8	0.1	2.9	0.6	4.9	0.4	
Qream Saket	08-06-88	-6.1	-30.7	0.3		–	–	–	–	–	–	–	–	–	–	–	–	
Qream Saket	23-05-90	-6.0	-29.9	2.9			780	491	8.1	1.2	1.8	4.4	0.2	3.4	1.1	2.7	13.6	
Qream Saket	15-07-91	-5.7	-26.8	0.5			810	518	7.8	1.3	1.7	4.3	0.2	3.7	1.0	2.8	14.1	
Qream Saket	20-10-92	-6.0	-29.3	0.0			840	538	8.1	1.1	2.0	4.8	0.2	3.8	1.3	2.9	13.9	
Qasem Awjan	07-06-88	-6.2	-31.6	1.5			760	486	7.7	1.5	1.9	4.0	0.1	3.0	1.0	3.3	9.6	
Qasem Awjan	15-07-91	-6.3	-29.9	0.0			750	480	7.7	1.6	1.8	3.6	0.2	2.9	1.1	3.1	10.6	
M. Jalad	08-06-88	-6.1	-30.3	0.0			850	544	8.1	1.1	2.2	4.7	0.1	4.0	1.4	2.4	19.6	
M. Jalad	17-07-91	-6.1	-29.9	0.0			910	582	7.9	1.4	2.3	4.4	0.2	4.3	1.5	2.4	19.9	
M. Bachtian	23-05-90	-6.0	-30.8	0.0			720	454	8.0	1.0	1.8	3.9	0.1	2.8	1.0	2.9	12.9	
Ali Khashman	23-05-90	-5.9	-32.0	0.3			960	605	8.1	3.2	1.5	3.8	0.2	3.3	1.0	5.0	0.0	
Moh. Arjani	21-10-92	-6.5	-32.6	0.0			670	429	7.6	2.3	2.1	2.1	0.1	2.0	0.8	4.0	0.3	
M. Jahmani	07-06-88	-6.1	-34.4	0.0			770	493	7.6	1.7	2.0	3.9	0.1	2.9	1.2	3.5	1.9	
M. Jahmani	15-07-91	-6.2	-28.5	0.0			790	506	8.1	2.1	1.9	3.6	0.2	2.9	1.2	3.7	1.9	
M. Jahmani	21-10-92	-6.2	-29.9	0.0			780	499	7.8	1.8	2.0	3.7	0.2	2.9	1.1	3.8	1.5	
Ali Ajian	07-06-88	-6.5	-29.6	1.1			890	570	7.8	1.3	1.9	5.0	0.1	4.3	1.1	3.0	10.9	
Ali Ajian	23-05-90	-6.1	-30.2	0.7			850	536	8.1	1.4	1.9	5.3	0.2	4.3	1.2	3.0	10.3	
Ali Ajian	15-07-91	-6.3	-30.5	0.6			920	589	8.0	1.6	1.9	4.9	0.3	4.3	1.3	3.0	10.7	
Abdelhamid Z.	08-06-88	-6.1	-32.2	0.0			890	570	7.9	1.2	2.5	4.7	0.1	4.5	1.3	2.5	19.8	
Abdelhamid Z.	21-10-92	-6.1	-31.5	0.0			1 020	653	7.8	1.3	3.0	5.1	0.2	5.4	1.4	2.6	20.9	
Musa Samara	21-10-92	-5.9	-31.7	0.0			790	506	8.0	3.0	2.0	2.8	0.1	2.7	0.5	4.7	0.4	

Table K-1 (contd.). Regional Groundwater Analyses.

Location	Date Sampled	^{18}O (‰) (±0.2)	^{2}H (‰) (±1.3)	^{3}H (TU) (±1)	^{14}C (pmc)	^{13}C (‰)	EC (µS/cm)	TDS (ppm)	pH	Ca (meq/L)	Mg (meq/L)	Na (meq/L)	K (meq/L)	Cl (meq/L)	SO_4 (meq/L)	HCO_3 (meq/L)	NO_3 (ppm)	SiO_2 (ppm)
Thermal Water																		
Balsam Sp.	11-01-87	-5.7	–	0.0			1 000	640	7.0	5.0	2.7	2.8	0.2	2.7	2.0	6.0	0.5	–
Balsam Sp.	10-03-87	-5.4	–	1.5			980	627	7.0	5.1	2.5	–	–	2.8	1.6	5.9	0.5	–
Balsam Sp	05-07-87	-5.5	-26.9	1.6			1 000	640	7.1	5.3	1.8	2.8	0.2	2.8	1.8	5.5	0.4	–
Balsam Sp.	09-02-88	-7.1	-28.7	1.6			1 020	653	7.1	4.7	2.6	3.9	0.2	3.8	1.9	5.6	0.4	31.5
Balsam Sp.	17-02-08	-6.4	-29.3	1.3			980	627	7.0	4.3	3.1	3.9	0.1	3.8	2.0	5.6	0.4	–
Balsam Sp.	19-07-89	-6.0	-30.3	1.6			1 020	653	7.1	5.0	2.8	2.9	0.2	2.9	2.0	5.9	0.5	–
Balsam Sp.	20-05-90	-5.8	-29.0	1.4			1 050	662	7.2	5.2	2.8	–	–	2.8	2.0	5.8	0.5	–
Balsam Sp.	31-07-91	-6.1	-28.3	–			–	–	–	–	–	–	–	–	–	–	–	–
Balsam Sp.	29-11-92	-5.9	-28.0	–			1 020	653	7.1	5.2	2.6	2.7	0.2	3.0	1.6	6.0	0.6	19.9
Maqla Sp.	11-01-87	-6.1	–	0.0			1 380	883	7.0	5.8	2.9	5.2	0.0	5.6	2.9	5.5	3.2	–
Maqla Sp.	10-03-87	-5.9	–	0.0			1 370	874	7.1	6.0	2.6	–	–	5.4	3.2	5.4	3.9	–
Maqla Sp.	05-07-87	-6.0	-28.9	0.8			1 410	902	7.2	5.8	2.5	5.3	0.4	5.5	3.5	5.1	3.5	–
Maqla Sp.	09-02-88	-7.4	-30.7	0.8			1 380	883	7.1	5.6	2.7	5.3	0.4	5.7	3.2	5.2	6.2	19.0
Maqla Sp.	17-02-88	-6.9	-31.5	0.9			1 350	864	7.1	5.6	2.6	5.2	0.4	5.5	3.2	5.2	3.0	–
Maqla Sp.	19-07-89	-6.4	-32.9	1.5			1 410	902	7.3	5.9	3.0	5.4	0.4	5.6	3.5	5.5	3.4	33.5
Maqla Sp.	20-05-90	-6.2	-31.7	1.6			1 500	945	7.3	6.2	2.8	–	–	5.7	3.4	5.6	3.5	–
Maqla Sp.	31-07-91	–	–	–	16.6 ± 0.9	-9.6	1 410	902	6.9	6.0	2.9	5.2	0.4	5.7	3.4	5.5	3.4	26.9
Maqla Sp.	29-11-92	-6.4	-30.9	–			1 410	902	7.4	6.2	2.8	5.4	0.4	5.9	3.4	5.5	3.8	33.5
JRV I	11-01-87	-6.1	–	1.0			1 470	940	7.2	6.0	3.6	5.5	0.3	4.7	4.5	5.9	3.1	–
JRV I	21-03-87	-6.1	–	0.4			1 410	902	7.2	5.9	3.6	–	–	4.9	4.5	5.7	19.0	–
JRV I	07-04-88	-5.9	-26.7	–			1 500	960	7.0	6.1	3.5	5.7	0.3	5.5	4.5	5.5	3.5	13.6
JRV I	07-04-88	-6.6	-32.3	0.4	22.9 ± 0.6		1 500	960	7.0	6.1	3.5	5.7	0.3	5.5	4.5	5.5	3.5	–
JRV I	19-07-89	-6.6	-32.4	1.5	5.36 ± 0.5	-9.4	1 500	960	7.1	6.3	3.8	6.0	0.3	5.8	4.8	5.7	2.7	–
JRV I	20-05-90	-6.4	-32.1	0.0			1 620	1 021	7.4	6.6	3.6	–	–	5.7	5.1	5.3	0.6	–
JRV I	27-11-90	-6.7	-29.5	0.0			1 620	1 021	7.5	6.7	3.7	6.1	0.5	6.0	5.3	5.4	2.8	–
JRV I	23-05-91	-6.4	-32.1	0.0			1 590	1 018	7.6	6.5	3.6	5.8	0.4	6.6	5.0	4.9	0.3	–
JRV I	17-09-92	-6.6	-31.9	–			1 560	998	7.1	6.5	3.5	5.8	0.4	6.2	4.5	5.3	1.0	–
JRV I	29-11-92	-6.8	-33.2	–			1 650	1 056	7.1	7.0	3.8	6.9	0.4	6.3	6.1	5.5	0.4	28.9
Mukheiba 1	14-01-87	-5.5	–	2.1			830	531	7.1	4.4	2.5	2.0	0.2	1.6	1.3	6.2	1.0	–
Mukheiba 1	21-03-87	-5.6	–	0.5			800	512	7.2	4.5	2.4	–	–	1.6	1.0	6.2	0.0	–
Mukheiba 1	20-07-89	-5.7	-27.8	1.7	16.8 ± 0.6	-12.9	820	525	7.4	7.9	2.6	1.8	0.1	1.7	1.3	6.2	0.7	–
Mukheiba 1	20-05-90	-5.7	-27.8	2.1			860	542	7.3	4.7	2.7	–	–	1.6	0.9	6.2	0.3	–
Mukheiba 1	27-11-91	-5.8	-26.9	0.3			810	510	7.3	4.6	2.8	1.6	0.1	1.7	1.3	6.2	0.6	–
Mukheiba 1	23-05-91	-6.1	-27.1	0.6			860	550	7.5	4.6	2.6	1.7	0.1	1.6	1.3	6.1	0.2	–

Table K-1 (contd.). Regional Groundwater Analyses.

Location	Date Sampled	^{18}O (‰) (±0.2)	^{2}H (‰) (±1.3)	^{3}H (TU) (±1)	^{14}C (pmc)	^{13}C (‰)	EC (µS/cm)	TDS (ppm)	pH	Ca (meq/L)	Mg (meq/L)	Na (meq/L)	K (meq/L)	Cl (meq/L)	SO_4 (meq/L)	HCO_3 (meq/L)	NO_3 (ppm)	SiO_2 (ppm)
Thermal Water (contd.)																		
Mukheiba 1	17-09-92	-5.8	-27.2	–			830	531	7.0	4.7	2.5	1.7	0.1	1.7	1.0	6.3	0.4	–
Mukheiba 1	29-11-92	-5.9	-27.1	–			840	538	7.3	4.6	2.7	1.8	0.1	1.8	1.0	6.3	0.6	15.1
Mukheiba 2	23-05-91	-6.1	-27.3	1.1			830	531	7.3	4.4	2.7	1.7	0.1	1.5	1.3	6.0	0.1	–
Mukheiba 2	31-07-91	–	–	–			820	525	7.2	4.3	2.7	1.9	0.1	1.7	1.2	6.0	0.4	14.6
Mukheiba 2	08-08-91	–	–	–	18.0 ± 0.9	-11.6	820	517	7.2	4.3	2.7	1.9	0.1	1.7	1.2	6.0	0.4	14.6
Mukheiba 2	17-09-92	-6.0	-27.4	–			800	512	7.2	4.4	2.3	1.8	0.1	1.7	0.9	6.0	0.4	–
Mukheiba 2	29-11-92	-5.9	-27.4	–			820	525	7.4	4.5	2.6	1.8	0.1	1.7	0.9	6.2	2.6	16.4
Mukheiba 3	23-05-91	-6.1	-27.1	0.1			860	550	7.3	4.7	2.6	1.8	0.1	1.7	1.2	6.3	0.0	–
Mukheiba 3	17-09-92	-5.7	-27.3	–			830	531	7.2	4.6	2.6	1.8	0.1	1.8	1.1	6.1	0.4	–
Mukheiba 3	29-11-92	-5.8	-27.0	–			850	544	7.3	4.6	2.7	1.7	0.1	1.7	1.0	6.3	1.7	15.7
Mukheiba 3	08-08-91	-6.0	-27.0	–			830	531	7.2	4.6	2.6	1.9	0.1	1.8	1.2	6.1	0.2	14.3
Mukheiba 4	20-07-89	-6.1	-27.7	1.1			780	499	7.7	3.9	2.6	2.1	0.1	1.8	1.1	5.5	3.2	13.2
Mukheiba 4	23-05-91	-5.5	-27.4	0.0			840	538	7.4	4.5	2.7	1.7	0.1	1.6	1.4	6.1	0.2	–
Mukheiba 4	17-09-92	-5.8	-27.5	–			790	506	7.2	4.1	2.4	1.8	0.1	1.6	1.0	5.8	0.4	–
Mukheiba 4	29-11-92	-5.7	-26.5	–			840	538	7.4	4.6	2.7	1.8	0.1	1.7	1.1	6.2	1.4	16.4
Mukheiba 4	31-07-91	–	–	–			820	525	7.2	4.5	2.6	1.8	0.1	1.7	1.1	6.1	0.4	14.2

Table K-2. Isotope data and deuterium excess of precipitation (Ref. Water Authority of Jordan: Open Files).

Location	Date Sampled	^{3}H (TU) (±1)	^{18}O (‰) (±0.15)	^{2}H (‰) (±1.0)	Precipitation (mm)	^{2}H excess (‰)
Ras Munif	10-87	8.6	-3.7	-11.2	15.3	18.4
Ras Munif	11-87	–	-5.9	-15.9	18.8	31.3
Ras Munif	12-87	7.2	-8.1	-36.4	184.1	28.3
Ras Munif	01-88	9.5	-9.1	-45.3	163.7	27.4
Ras Munif	02-88	9.1	-8.0	-40.3	187.8	24.0
Ras Munif	03-88	8.3	-5.3	-21.4	108.1	21.2
Ras Munif	04-88	12.9	-5.7	-27.6	21.7	17.6
Ras Munif	11-88	7.0	-6.9	-33.3	44.2	21.7
Ras Munif	12-88	6.7	-6.9	-28.8	195.6	26.1
Ras Munif	01-89	6.9	-7.2	-32.0	53.4	25.3
Ras Munif	06-89	–	-4.2	-22.3	52.4	11.5
Ras Munif	02-89	10.7	-5.7	-15.7	53.3	30.0
Ras Munif	03-89	16.0	-7.4	-41.1	88.8	17.9
Ras Munif	10-89	–	-4.9	-15.5	13.9	23.5
Ras Munif	11-89	5.8	-6.9	-32.4	80.0	22.6
Ras Munif	12-89	4.4	-7.6	-39.9	81.3	21.1
Ras Munif	01-90	4.7	-7.6	-36.5	149.1	24.2
Ras Munif	02-90	6.5	-6.4	-29.6	73.9	21.7
Ras Munif	03-90	8.1	-6.4	-27.7	107.7	23.7
Ras Munif	04-90	13.3	-7.2	-39.4	27.9	17.8
Ras Munif	10-90	4.3	-4.8	-15.3	6.6	23.4
Ras Munif	12-90	4.9	-4.1	-4.0	28.8	29.0
Ras Munif	01-91	4.7	-7.9	-38.9	169.5	24.5
Ras Munif	02-91	4.9	-6.4	-22.3	82.5	29.0
Ras Munif	03-91	6.2	-8.0	-40.8	133.6	23.1
Ras Munif	04-91	6.1	-5.7	-26.9	39.1	19.0
Irbid	10-87	–	-5.2	-36.8	15.6	4.8
Irbid	11-87	6.8	-5.9	-16.3	8.4	31.0
Irbid	12-87	5.3	-7.9	-37.9	126.6	25.2
Irbid	01-88	8.1	-7.8	-36.4	120.0	25.7
Irbid	02-88	8.5	-8.7	-43.0	147.3	26.4
Irbid	03-88	9.9	-4.3	-13.4	115.2	21.1
Irbid	04-88	21.7	-4.3	-17.9	16.7	16.6
Irbid	10-88	–	-4.2	-11.1	6.4	22.5
Irbid	11-88	8.1	-7.6	-36.8	35.1	23.9
Irbid	12-88	6.4	-5.9	-20.9	106.5	26.1
Irbid	06-89	11.9	-2.1	-13.9	48.2	3.2
Irbid	01-89	7.7	-6.3	-25.4	30.3	25.0
Irbid	02-89	8.8	-5.1	-13.3	46.9	27.6
Irbid	03-89	11.1	-6.5	-33.8	54.0	18.4
Irbid	10-89	–	-4.9	-18.1	2.5	20.9
Irbid	11-89	5.6	-6.5	-33.3	45.0	19.0
Irbid	12-89	5.5	-5.9	-29.0	50.3	18.3
Irbid	01-90	6.4	-7.5	-41.2	152.0	18.6
Irbid	02-90	6.9	-6.6	-34.5	67.5	18.5
Irbid	03-90	7.9	-4.9	-18.6	97.7	20.8
Irbid	04-90	10.4	-8.3	-44.6	29.7	22.0
Irbid	10-90	–	0.5	17.0	4.2	12.9
Irbid	11-90	3.8	-5.4	-12.0	22.9	31.1
Irbid	12-90	4.7	-3.8	-2.6	30.3	28.1
Irbid	01-91	4.9	-7.2	-34.8	165.7	23.0
Irbid	02-91	6.3	-7.3	-36.0	48.4	22.2
Irbid	03-91	7.9	-3.1	-10.8	116.5	14.1
Irbid	04-91	6.9	-5.2	-19.8	43.6	21.9

Table K-2 (contd.). Isotope data and deuterium excess of precipitation (Ref. Water Authority of Jordan: Open Files).

Location	Date Sampled	^{3}H (TU) (±1)	^{18}O (‰) (±0.15)	^{2}H (‰) (±1.0)	Precipitation (mm)	^{2}H excess (‰)
Deir Alla	12-87	8.9	-4.8	-19.1	82.5	19.4
Deir Alla	01-88	12.6	-6.0	-26.8	63.9	21.6
Deir Alla	02-88	9.0	-6.2	-27.8	130.4	21.8
Deir Alla	03-88	15.8	0.4	15.2	24.7	12.3
Deir Alla	10-88	–	-0.2	8.7	2.0	10.3
Deir Alla	11-88	7.1	-4.6	-21.9	21.3	15.2
Deir Alla	12-88	8.7	-3.0	-8.3	45.0	15.8
Deir Alla	01-89	11.5	-3.1	-7.5	44.0	17.0
Deir Alla	02-89	11.7	-1.5	5.1	37.3	17.1
Deir Alla	10-89	–	-1.1	6.0	9.1	15.0
Deir Alla	11-89	6.0	-3.3	-8.2	64.4	18.2
Deir Alla	12-89	5.0	-3.3	-8.5	62.6	18.0
Deir Alla	01-90	6.7	-4.9	-28.3	79.2	11.1
Deir Alla	02-90	6.8	-2.0	-0.6	31.9	15.2
Deir Alla	03-90	13.4	-3.3	-13.3	45.1	12.9
Deir Alla	01-91	5.4	-3.8	-15.9	93.0	14.5
Deir Alla	02-91	7.2	-5.2	-29.7	121.3	11.8
Deir Alla	03-91	7.9	-8.6	-53.7	113.2	15.4
Deir Alla	04-91	8.7	-1.2	-0.5	10.0	8.8

Table K-3. Composition of Rijam Formation water (Ref. Abdul-Jaber, K., 1989. Hydrochemische, geochemische und petrographische Untersuchungen im Maqarin – Gebiet Nord Jordanien. Diss. Westfälischen Wilhelms-Universität, Münster, Germany).

Sample	Date	pH	EC (µS/cm)	TDS (mg/L)	Ca^{2+} (mg/L)	Ca^{2+} (meq/L)	Mg^{2+} (mg/L)	Mg^{2+} (meq/L)	Na^{+} (mg/L)	Na^{+} (meq/L)	K^{+} (mg/L)	K^{+} (meq/L)	HCO_3^{-} (mg/L)	HCO_3^{-} (meq/L)	SO_4 (mg/L)	SO_4 (meq/L)	Cl^{-} (mg/L)	Cl^{-} (meq/L)	No^{-} (mg/L)
Ain Quelbe	03.08.72	–	–	233.5	70.5	3.52	4.4	0.37	10.4	0.45	2.4	0.06	211.1	3.46	19.7	0.41	20.6	0.59	–
Ain Quelbe	14.12.77	–	–	229.3	68.1	3.40	6.1	0.51	18.4	0.80	1.2	0.03	211.1	3.46	1.9	0.04	28.0	0.80	–
Ain Quelbe	07.05.80	–	–	253.1	70.5	3.51	4.7	0.39	13.8	0.60	0.4	0.01	205.0	3.36	5.8	0.12	22.0	0.63	33.5
Ain Quelbe	10.11.80	–	–	258.7	68.1	3.40	7.3	0.68	15.2	0.66	2.4	0.06	207.5	3.40	14.4	0.30	22.7	0.69	24.9
Ain Quelbe	07.05.84	7.28	448	282.3	79.6	3.98	6.0	0.50	14.7	0.64	1.6	0.04	244.7	4.01	9.8	0.20	24.8	0.71	24.2
Ain Quelbe	04.06.84	7.56	445	283.5	72.1	3.60	9.7	0.81	14.5	0.63	1.6	0.04	244.7	4.01	10.1	0.21	20.9	0.60	32.3
Ain Quelbe	14.10.85	6.99	458	263.3	76.2	3.81	6.6	0.55	16.3	0.71	1.6	0.04	219.7	3.60	6.7	0.14	21.3	0.61	24.8
Ain ct-Trab	08.09.80	6.8	–	263.5	68.1	3.40	7.3	0.68	23.0	1.00	0.8	0.02	225.8	3.70	6.5	0.14	22.7	0.69	22.3
Ain ct-Trab	18.05.84	7.44	440	259.2	76.2	3.81	6.0	0.50	14.3	0.62	0.4	0.01	216.0	3.54	7.8	0.16	27.0	0.77	21.7
Ain ct-Trab	11.07.84	–	–	278.6	77.7	3.88	10.0	0.83	14.0	0.61	0.4	0.01	219.7	3.60	12.0	0.25	39.4	1.13	19.2
Ain Abda	11.07.84	–	–	250.6	71.9	3.59	2.3	0.19	27.6	1.20	1.6	0.04	238.6	3.91	6.2	0.13	22.0	0.63	19.2
Ain Ba'boul	06.09.80	6.8	–	606.4	128.3	6.41	41.3	3.44	41.4	1.80	2.4	0.06	390.5	6.40	62.7	1.31	79.4	2.27	6.4
Ain Sombol	06.09.80	6.8	–	444.3	110.2	5.51	20.7	1.75	22.1	0.96	3.1	0.08	372.2	6.10	111.9	2.33	61.9	1.77	11.5
Ain Shalaq	20.07.80	–	–	362.5	66.1	3.30	14.6	1.22	42.8	1.86	3.1	0.08	223.3	3.66	28.8	0.60	61.4	1.75	46.5
W. Shallala-1	18.05.84	7.68	706	445.4	113.4	5.67	19.5	1.62	23.9	1.04	1.6	0.04	388.7	6.37	38.9	0.81	43.6	1.25	11.2
W. Shallala-1	15.10.85	8.16	639	362.9	80.2	4.01	22.4	1.87	26.2	1.14	1.2	0.03	268.5	4.40	37.0	0.77	45.0	1.29	16.7
W. Shallala-2	15.10.85	7.09	739	427.8	108.2	5.41	20.6	1.71	23.9	1.04	1.6	0.04	353.9	5.80	37.0	0.77	47.9	1.37	11.8
W. Shallala-3	15.10.85	6.99	789	480.5	116.2	5.81	23.4	1.95	26.7	1.16	2.0	0.05	414.9	6.80	49.5	1.03	43.6	1.25	11.8

Table K-4. Jordan Himma, Maqla (Ref. Salameh, E., University of Jordan, Dept. of Geology).

Measurement	Minimum	Maximum	Mean	Std. Dev.
Eh-value	10.1	12.1	11.45	0.78
Temp (°C)	33.5	47.1	41.40	3.18
pH	6.75	8.10	7.125	0.334
EC (µS/cm)	1 283	1 400	1 336.5	41.5
Na (meq/L)	3.82	7.14	5.869	0.853
Mg (meq/L)	0.20	1.33	0.435	0.289
Ca (meq/L)	2.18	4.09	2.699	0.500
Cl (meq/L)	5.72	6.93	6.208	0.378
NO_3 (meq/L)	0.01	0.11	0.049	0.032
SO_4 (meq/L)	2.16	5.21	3.447	0.866
HCO_3 (meq/L)	5.15	6.10	5.539	0.247
CO_2 (mg/L)	25.00	152.87	78.663	44.013
F (mg/L)	0.732	0.880	0.8060	0.1046
Br (mg/L)	2.003	3.940	3.1313	0.7264
I (mg/L)	0.038	0.140	0.0971	0.0402
TDS (mg/L)	883.7	1 233.1	1 117.25	87.17
TOC (meq/L)	13.10	16.70	15.200	1.017
Fe (mg/L)	0.050	0.800	0.1830	0.2357
Mn (mg/L)	0.000	0.030	0.0086	0.0114
Cd (mg/L)	0.000	0.005	0.0027	0.0015
Zn (mg/L)	0.000	0.111	0.0185	0.0329
Pb (mg/L)	0.003	0.070	0.0294	0.0208
Cu (mg/L)	0.000	0.004	0.0004	0.0012
Sr (mg/L)	2.292	3.275	2.8494	0.3119
SI-calcite	0.06	1.40	0.423	0.329
SI-dolomite	-0.03	2.62	0.685	0.655
SI-gypsum	-1.39	-1.01	-1.189	0.101
SI-halite	-0.40	-0.60	-5.736	1.620
Rn (C/10 m)	18	2 289	1 398.1	-25.2
pH-equil	7.01	7.10	7.051	0.022
pCO_2	0.349	7.979	3.8992	1.8391
NH_4 (mg/L)	0.50	8.00	2.616	2.694
H_2S (mg/L)	3.50	17.50	9.500	7.211

Averages

TDS (mg/L)	**1 117.26**	**CO_2 free (mg/L)**	**78.66**
Temp. (°C)	**41.40**	**H_2S (mg/L)**	**9.50**
pH	**7.13**	**Radon (nCi/L)**	**31.459**
Br (mg/L)	**3.31**	**NH_4 (mg/L)**	**2.62**

Element	mg/L	meq/L	meq%
Na	135.01	5.87	38.6
K	17.20	0.44	2.9
Mg	32.82	2.70	17.7
Ca	124.45	6.21	40.8
Cl	213.76	6.03	40.0
NO_3	3.10	0.05	0.3
SO_4	165.60	3.45	22.9
HCO_3	338.05	5.54	36.8

Table K-5. North Shuhnab Thermal Well (Ref. Salameh, E., University of Jordan, Dept. of Geology).

Measurement	Minimum	Maximum	Mean	Std. Dev.
Eh-value	11.2	14.1	12.31	1.36
Temp (°C)	47.0	54.5	52.69	2.48
pH	6.77	7.36	7.060	0.162
EC (µS/cm)	940	1 016	981.3	23.4
Na (meq/L)	1.85	4.36	3.305	0.636
K (meq/L)	0.06	0.33	0.115	0.073
Mg (meq/L)	3.40	4.20	3.664	0.269
Ca (meq/L)	3.54	4.65	4.076	0.311
Cl (meq/L)	2.35	3.06	2.813	0.193
NO_3 (meq/L)	0.00	0.09	0.024	0.016
SO_4 (meq/L)	1.04	2.00	1.757	0.288
HCO_3 (meq/L)	5.35	6.83	6.376	0.382
CO_2 (mg/L)	40.30	77.50	59.181	13.768
F (mg/L)	0.380	1.383	0.9063	0.5302
Br (mg/L)	0.213	1.383	0.9063	0.5302
I (mg/L)	0.028	0.072	0.0491	0.0217
TDS (mg/L)	812.9	908.5	863.20	32.39
TOC (meq/L)	10.00	11.90	11.027	0.578
Fe (mg/L)	0.038	0.300	0.1264	0.0972
Mn (mg/L)	0.000	0.030	0.0072	0.0109
Cd (mg/L)	0.000	0.008	0.0024	0.0025
Zn (mg/L)	0.000	0.010	0.0023	0.0041
Pb (mg/L)	0.006	0.060	0.0308	0.0175
Cu (mg/L)	0.000	0.000	0.0000	0.0000
Sr (mg/L)	0.970	1.422	1.1277	0.1396
SI-calcite	0.09	0.70	0.378	0.173
SI-dolomite	0.50	1.62	0.990	0.321
SI-gypsum	-1.81	-1.32	-1.558	0.118
SI-halite	-7.01	-5.39	-6.679	0.416
Rn (C/10 m)	156	1 187	453.5	390.9
pH-equil	7.07	7.29	7.135	0.058
pCO_2	2.731	10.899	5.6983	2.3818
NH_4 (mg/L)	0.50	1.60	1.150	0.437
H_2S (mg/L)	1.50	12.50	5.833	5.859

Averages

TDS (mg/L)	**1 117.26**	**CO_2 free (mg/L)**	**78.66**
Temp. (°C)	**41.40**	**H_2S (mg/L)**	**9.50**
pH	**7.13**	**Radon (nCi/L)**	**31.459**
Br (mg/L)	**3.31**	**NH_4 (mg/L)**	**2.62**

Element	mg/L	meq/L	meq%
Na	76.13	3.31	29.6
K	4.69	0.12	1.1
Mg	44.49	3.66	32.8
Ca	81.76	4.08	36.5
Cl	99.61	2.81	25.6
NO_3	1.24	0.02	0.2
SO_4	84.48	1.76	16.0
HCO_3	389.31	6.38	58.2

Table K-6. North-Shuna Well (Ref. Salameh, E., University of Jordan, Dept. of Geology).

	3/89	5.89	1.91
EC (µS/cm)	1 036	990	1 050
TDS (mg/L)	536	755	
Temp (°C)	49.5	55	50.1
pH	5.44	6.5	7.36
Ca (meq/L)	4.4	3.63	4.32
Mg (meq/L)	3.6	4.02	3.49
Na (meq/L)	3.55	3.55	3.48
K (meq/L)	0.135	0.153	0.125
Cl (meq/L)	3.05	2.96	2.94
SO_4 (meq/L)	4.11	2.37	0.97
HCO_3 (meq/L)	5.92	6.27	6.52
NO_3 (meq/L)	0.004	0.113	0.01
I (mg/L)	0.0041	–	–
Br (mg/L)	1.67	–	–
F (mg/L)	1.035	–	–
PO_4 (mg/L)	0.004	0.021	0.02
Li (mg/L)	0.11	0.10	0.11
SiO_2 (mg/L)	26.95	–	–
TOC (mg/L)	–	–	6.40
COD (mg/L)	–	–	10.2

Table K-7. Wadi Arab Wells (Ref. Salameh, E., University of Jordan, Dept. of Geology).

	1 1989	1 1990	2 1989	2 1990	3 1989	3 1990/10	4 1989	4 1990	5 1989	5 1990
EC (µS/cm)	866	874	826	–	872	853	990	928	7.59	792
TDS	–	–	–	–	–	–	–	–	–	–
Temp (°C)	26.7	30.4	26.2	–	25.6	27.4	26.6	–	23.6	25.3
pH	6.77	7.08	5.74	–	6.35	6.97	6.24	7.11	7.64	7.08
Ca (meq/L)	5.50	5.55	5.50	4.2	4.2	5.65	6.00	4.96	4.9	4.83
Mg (meq/L)	3.20	3.18	3.20	2.9	2.9	2.88	3.30	3.2	3.3	2.88
Na (meq/L)	0.85	1.11	0.46	0.85	0.85	1.01	1.37	1.55	0.46	0.80
K (meq/L)	0.11	0.05	0.11	0.11	0.11	0.07	0.135	0.10	0.11	0.07
Cl (meq/L)	1.30	1.04	1.2	1.15	1.15	1.0	1.25	1.13	1.25	1.04
SO_4 (meq/L)	0.373	1.86	2.210	1.612	1.612	1.84	2.865	1.38	0.847	0.805
HCO_3 (meq/L)	6.552	7.17	6.461	5.733	5.733	7.35	6.532	7.35	6.00	6.58
NO_3 (meq/L)	0.002	0.001	0.007	0.003	0.003	0.004	0.003	0.001	0.18	0.15
I (mg/L)	0.0021	–	0.002	–	0.002	–	0.0022	–	0.0022	–
Br (mg/L)	0.52	–	0.498	–	0.513	–	0.61	–	0.161	–
F (mg/L)	0.652	0.930	0.764	–	0.774	1.24	0.915	1.505	0.667	1.12
TOC (mg/L)	5.567	10.63	5.567	–	4.00	12.35	5.567	3.73	2.148	3.73
Li (mg/L)	0.11	0.12	0.11	–	0.11	0.006	0.11	0.15	0.11	0.10
COD (mg/L)	–	151.9	–	–	–	49.0	–	–	–	10.05
PO_4 (mg/L)	–	0.016	–	–	–	0.006	–	–	–	0.052

Table K-8. Basalt Springs (Syria) (Ref. Salameh, E., University of Jordan, Dept. of Geology).

	Taley Kaum	Qcini	Qurei	Uion
EC (µS/cm)	350	159.2	360	346
TDS	240	90	240	220
Temp (°C)	19.6	18.1	18.6	17.4
pH	7.78	7.78	7.63	7.54
Ca (meq/L)	1.2	0.8	1.5	1.7
Mg (meq/L)	1.3	0.4	1.0	1.1
Na (meq/L)	0.896	0.30	0.798	0.598
K (meq/L)	0.127	0.032	0.119	0.065
Cl (meq/L)	0.71	0.41	0.816	0.071
SO_4 (meq/L)	0.145	0.08	0.253	0.264
HCO_3 (meq/L)	2.56	0.886	2.16	1.87
NO_3 (meq/L)	0.229	0.175	0.260	0.160
I (mg/L)	0.001	0.001	0.001	0.001
Br (mg/L)	0.008	0.002	0.002	0.002
F (mg/L)	0.01	0.006	0.009	0.008
TOC (mg/L)	1.38	0.61	0.77	123
Li (mg/L)	0.01	0.01	0.02	0.02
COD (mg/L)	0.0	0.0	0.00	0.0
PO_4 (mg/L)	0.52	0.19	0.30	0.30
SiO_2 (mg/L)	25.89	24.22	27.57	27.57
DO (mg/L)	9.0	9.7	7.8	7.9

Table K-9. Diversion tunnel Unity Dam (Ref. Harza Company: Maqarin Dam Project (1988), Update of Maqarin Dam Study of 1982. Jordan Valley Authority, Amman, Jordan).

	Spring 1 10/89	Spring 2 10/89
EC (µS/cm)	960	820
TDS	630	–
Temp (°C)	27.6	28.4
pH	7.01	7.03
Ca (meq/L)	5.02	4.04
Mg (meq/L)	2.86	2.56
Na (meq/L)	3.25	2.37
K (meq/L)	0.15	0.13
Cl (meq/L)	3.35	1.85
SO_4 (meq/L)	1.02	1.02
HCO_3 (meq/L)	6.51	5.46
NO_3 (meq/L)	0.06	0.06
Br (mg/L)	0.074	0.024
I (mg/L)	0.0021	0.0021
F (mg/L)	0.396	0.286
TOC (mg/L)	8.05	1.19
COD (mg/L)	48.72	0.0?
Li (mg/L)	0.14	0.12
PO_4 (mg/L)	0.043	0.021
SiO_2 (mg/L)	11.39	11.16
NH_4 (mg/L)	0.2	0.0
HS (mg/L)	3.0	3

Table K-10. Yarmouk River at Maqarin (Ref. Salameh, E., University of Jordan, Dept. of Geology).

	Western Springs	
	12/89	**12/89**
EC (µS/cm)	810	7.46
TDS	–	–
Temp (°C)	19.1	18.1
pH	8.51	8.29
Ca (meq/L)	2.1	1.7
Mg (meq/L)	2.2	2.5
Na (meq/L)	3.79	3.75
K (meq/L)	0.13	0.13
Cl (meq/L)	2.8	2.6
SO_4 (meq/L)	1.56	1.44
HCO_3 (meq/L)	3.38	3.22
NO_3 (meq/L)	0.36	0.35
Br (mg/L)	0.050	0.047
I (mg/L)	0.033	0.032
F (mg/L)	0.048	0.046
Li (mg/L)	0.10	0.05
PO_4 (mg/L)	0.09	0.158
SiO_2 (mg/L)	10.92	8.39

Table K-11. Yarmouk River at Mukheiba (Ref. Salameh, E., University of Jordan, Dept. of Geology).

	2/89	**5/89**	**10/89**	**1/90**	**3/90**	**8/90**	**2/91**
EC (µS/cm)	809	830	840	870	813	915	866
TDS	–	–	–	–	–	–	–
Temp (°C)	18	28	27	19.1	–	29.5	18.2
pH	8.24	8.82	7.93	8.35	7.98	8.15	8.56
Ca (meq/L)	2.10	2.616	2.66	2.5	2.36	2.60	2.40
Mg (meq/L)	2.3	1.666	2.86	2.1	2.37	2.40	2.40
Na (meq/L)	3.29	3.431	4.15	3.67	4.0	4.25	4.17
K (meq/L)	0.14	0.143	0.153	0.21	0.08	0.14	0.13
Cl (meq/L)	2.7	2.856	3.43	3.05	2.95	3.99	3.05
SO_4 (meq/L)	1.38	1.789	1.77	1.58	1.36	1.84	1.04
HCO_3 (meq/L)	3.17	3.332	3.26	3.15	3.38	3.64	3.75
NO_3 (meq/L)	0.161	0.19	0.30	0.32	0.30	0.14	0.25
Br (mg/L)	1.15	–	0.101	0.368	1.62	1.05	–
I (mg/L)	0.021	–	0.006	0.026	0.02	0.001	–
F (mg/L)	0.456	–	0.079	0.381	0.702	0.605	–
Li (mg/L)	0.112	0.135	0.12	0.13	0.19	0.12	0.09
PO_4 (mg/L)	0.154	0.11	0.042	0.274	0.18	0.24	0.49
SiO_2 (mg/L)	–	4.46	33.36	9.35	11.04	–	–
COD (mg/L)	–	24.11	–	–	57.0	–	25.25

Table K-12a. Composition of Rijam Formation water (Ref. Salameh, E., University of Jordan, Dept. of Geology).

	Trab		SL	El
	2/74	8/77	9/80	5/84
EC (µS/cm)	450	460	–	440
TDS (mg/L)	288	299	263.5	259.2
Temp (°C)	–	–	–	–
pH	7.45	7.50	6.8	7.44
Ca (meq/L)	3.34	3.24	68.1	76.2
Mg (meq/L)	0.32	0.56	7.3	6.0
Na (meq/L)	0.75	0.65	23.0	14.3
K (meq/L)	0.01	0.02	0.8	0.4
C (meq/L)	0.79	0.70	22.7	27.0
SO_4 (meq/L)	0.14	0.04	6.5	7.8
HCO_3 (meq/L)	3.5	3.28	225	216.0
NO_3 (mg/L)	–	–	22.3	21.7
Cd (mg/L)	–	–	0.1	0.1
Co (mg/L)	–	–	0.3	0.5
Cr (mg/L)	–	–	23	–
Cu (mg/L)	–	–	1.3	1.5
Fe (mg/L)	–	–	10.6	5.7
Mn (mg/L)	–	–	0.3	0.1
Ni (mg/L)	–	–	3.8	2.8
Zn (mg/L)	–	–	17	47.0

Table K-12b. Composition of Rijam Formation Water.

	Shallala 1					Shallala 2	Shallala 3
	6/74	2/78	5/84	10/85		10/85	10/85
EC (µS/cm)	600	500	706	639	–	739	789
TDS (mg/L)	3.84	326	445.4	362.9	–	427.8	480.5
Temp (°C)	–	–	–	–	–	–	–
pH	7.45	7.95	7.68	8.16	–	7.09	6.99
Ca (meq/L)	3.41	5.1	5.67	4.01	–	5.41	5.81
Mg (meq/L)	0.77	1.04	1.62	1.87	–	1.72	1.17
Na (meq/L)	1.2	1.80	1.04	1.014	–	1.04	1.15
K (meq/L)	0.52	0.03	0.04	0.03	–	0.04	0.05
Cl (meq/L)	1.45	1.5	1.25	1.29	–	1.37	1.25
SO_4 (meq/L)	0.67	0.50	0.81	0.77	–	0.77	1.03
HCO_3 (meq/L)	3.66	3.06	6.37	4.40	–	5.80	6.80
NO_3 (mg/L)	–	–	11.2	16.7	–	11.8	11.8
Cd (mg/L)	–	–	–	0.1	0.3	0.7	0.3
Co (mg/L)	–	–	–	0.1	–	–	–
Cr (mg/L)	–	–	–	12	28	31.0	22.0
Cu (mg/L)	–	–	–	1.0	1.1	0.6	–
Fe (mg/L)	–	–	–	7.4	–	–	–
Mn (mg/L)	–	–	–	0.6	0.50	0.2	0.5
Ni (mg/L)	–	–	–	12.0	12.4	17.0	13.0
Pb (mg/L)	–	–	–	0.3	0.2	0.5	0.9
Zn (mg/L)	–	–	–	27.0	9.0	79.0	80

Table K-12c. Composition of Rijam Formation Water.

	Habis		Ba'boul	Sombol	Shalaq
	9/23	3/78	9/80	9/80	7/80
EC (µS/cm)	600	590	–	–	–
TDS (mg/L)	384	378	606.4	444.3	362.5
Temp (°C)	–	–	–	–	–
pH	7.65	7.35	6.8	6.8	
Ca (meq/L)	3.04	3.32	6.415	5.51	3.31
Mg (meq/L)	1.26	0.92	3.45	1.72	1.22
Na (meq/L)	1.75	1.50	1.80	0.96	1.86
K (meq/L)	0.08	0.03	0.06	0.078	0.078
Cl (meq/L)	1.4	1.47	2.27	1.77	1.75
SO_4 (meq/L)	1.0	0.60	1.31	2.50	0.60
HCO_3 (meq/L)	3.76	3.80	6.40	4.46	3.66
NO_3 (mg/L)	–	–	6.4	11.5	46.5

Table K-12d. Composition of Rijam Formation Water.

	Abda		
	12/1969	7/76	7/84
EC (µS/cm)	460	500	–
TDS (mg/L)	294	320	250.6
Temp (°C)	–	–	–
pH	8.05	7.45	–
Ca (meq/L)	2.52	3.10	3.60
Mg (meq/L)	1.16	0.7	0.185
Na (meq/L)	0.8	1.15	1.20
K (meq/L)	0.08	0.04	0.04
Cl (meq/L)	0.79	1.15	0.62
SO_4 (meq/L)	0.40	0.20	0.13
HCO_3 (meq/L)	3.26	3.34	3.91
NO_3 (mg/L)	–	–	19.2
Cd (mg/L)	–	–	0.2
Co (mg/L)	–	–	0.7
Cu (mg/L)	–	–	2.1
Fe (mg/L)	–	–	16.5
Mn (mg/L)	–	–	7.4
Ni (mg/L)	–	–	2.4
Zn (mg/L)	–	–	21.0

Table K-12e. Composition of Rijam Formation Water.

	Barashta		Quelba					
	2/1972	2/78	11/72	7/76	5/80	11/80	6/84	10/85
EC (µS/cm)	400	465	450	445	–	–	445	458
TDS (mg/L)	256	298	288	285	253.1	258.7	283.5	263.3
Temp (°C)	–	–	–	–	–	–	–	–
pH	7.95	7.5	7.7	7.85			7.56	6.99
Ca (meq/L)	2.93	3.4	3.5	3.31	3.52	3.41	3.61	3.81
Mg (meq/L)	0.32	0.50	0.5	0.64	4.7	0.61	0.81	0.50
Na (meq/L)	0.75	0.60	0.48	0.48	0.60	0.66	0.64	0.71
K (meq/L)	0.03	0.01	0.02	0.04	0.01	0.06	0.04	0.04
Cl (meq/L)	0.68	0.73	1.77	0.67	0.63	6.49	0.60	0.61
SO_4 (meq/L)	0.6	0.16	0.1	0.14	0.12	0.30	0.210	0.140
HCO_3 (meq/L)	2.68	3.56	3.65	3.41	3.36	3.40	4.01	3.60
NO_3 (mg/L)	–	–	–	–	33.5	24.9	32.3	24.8
Cd (mg/L)	–	–	–	–	–	–	0.1	0.2
Co (mg/L)	–	–	–	–	–	–	0.6	–
Cr (mg/L)	–	–	–	–	–	–	–	21.0
Cu (mg/L)	–	–	–	–	–	–	1.6	–
Fe (mg/L)	–	–	–	–	–	–	18	–
Mn (mg/L)	–	–	–	–	–	–	2.0	–
Ni (mg/L)	–	–	–	–	–	–	1.9	2.5
Pb (mg/L)	–	–	–	–	–	–	0.7	0.1
Zn (mg/L)	–	–	–	–	–	–	6.0	9.0

Table K-12f. Composition of Rijam Formation Water.

	Um Queis			Tasa		
	5/68	3/78	92	6/74	2/78	92
EC (µs/cm)	750	850	842	700	540	693
TDS (mg/L)	480	544	440	448	346	4.30
Temp (°C)	–	–	22.8	–	–	22.4
pH	8.5	7.25	8.12	7.20	7.88	8.27
Ca (meq/L)	3.7	4.30	4.90	5.79	3.09	5.8
Mg (meq/L)	2.40	2.54	2.60	0.77	0.98	1.5
Na (meq/L)	1.92	1.90	1.60	0.55	1.40	0.35
K (meq/L)	–	0.05	0.06	0.03	0.02	0.03
Cl (meq/L)	2.40	2.10	2.10	0.8	1.18	0.7
SO_4 (meq/L)	1.12	1.36	1.11	0.3	0.32	0.27
HCO_3 (meq/L)	3.80	5.40	5.10	5.95	3.60	5.91
NO_3 (mg/L)	–	–	25.8	–	–	13.8
I (mg/L)	–	–	0.033	–	–	0.024
Br (mg/L)	–	–	1.51	–	–	0.49
F (mg/L)	–	–	0.21	–	–	0.3
COD (mg/L)	–	–	19.6	–	–	88.2
PO_4 (mg/L)	–	–	0.006	–	–	0.044
Li (mg/L)	–	–	0.14	–	–	0.11
TOC (mg/L)	–	–	–	–	–	4.3

APPENDIX L

Geochemistry and Mineralogy of Rocks from the Maqarin Area

(Compiled by H.N. Khoury)

List of Tables (Rocks and minerals)

GEOCHEMISTRY AND MINERALOGY OF ROCKS FROM THE MAQARIN AREA

F – Miscellaneous

Table L-23	Expected primary altered Bituminous Marl minerals (Reference C)
Table L-24	Expected secondary minerals in the altered Bituminous Marl (Reference C)
Table L-25	Uranium/thorium series isotope determinations (Reference B, Phase I).
Table L-26	Uranium, thorium and radium radiometric isotope determinations for fracture mineralisation and altered wallrock in bituminous clay biomicrites from Adit A-6 (Reference B, Phase II).
Table L-27	Stable isotopes for carbonate samples (Reference B, Phase I).

References cited in the following Tables:

Reference A: Khoury, H.N. and Nassir, S., 1982. High temperature mineralisation in the bituminous limestone in the Maqarin area – northern Jordan. N. Jb. Miner. Abh., 144:2, 197–213.

Reference B:

Maqarin Phase I Study — Alexander, W.R. (Ed.), 1992. A natural analogue study of the Maqarin hyperalkaline groundwaters. I: Source term description and thermodynamic database testing. Nagra Tech. Rep. (NTB 91-10), Nagra, Wettingen, Switzerland.

Maqarin Phase II Study — Linklater, C.M. (Ed.), 1998. A natural analogue study of cement-buffered, hyperalkaline groundwaters and their interaction with a repository host rock: Phase II. Nirex Science Report, S/98/003, Nirex, Harwell. U.K.

Maqarin Phase III Study — This study.

Reference C: Unpublished reports by Khoury, H.N. and Salameh, E., University of Jordan, Dept. of Geology, Amman.

Table L-1. Mineralogy of travertines and recent precipitates. (Ref. A and B).

Mineral phase	General formula	Modal anal.
Calcite	$CaCO_3$	Dominant
Aragonite	$CaCO_3$	Major
Quartz	SiO_2	Trace
Portlandite	$Ca(OH)_2$	Trace
Geochemistry	See Tables L-2 and L-3.	

Table L-2. Chemical composition of some travertines and secondary precipitates (Ref. B, Phase I).

Element	Sample						
	MQ1.1P A-6	MQ1.2P A-6	MQ2.1P A-6	MQ5P Tr.	MQ6.2P G-Tr.	MQ7.2P Y-Tr.	MQ9P RC
Weight%							
SiO_2	0.66	0.16	0.43	2.73	5.59	0.18	0.37
Al_2O_3	0.21	0.04	0.03	0.39	0.80	0.06	0.08
Fe_2O_3	0.07	0.01	0.01	0.18	0.36	0.02	0.03
MgO	0.05	0.00	0.00	1.68	1.82	0.02	0.03
CaO	51.34	52.52	51.26	48.05	46.54	48.46	51.93
Na_2O	0.03	0.02	0.02	0.08	0.11	0.03	0.04
K_2O	0.01	0.01	0.01	0.08	0.27	0.01	0.00
P_2O_5(XRF)	0.14	0.01	0.02	0.09	0.76	0.03	0.03
P_2O_5(ICPOES)	0.14	0.07	0.06	0.10	0.41	0.06	0.07
ppm							
Li	15	14	14	16	24	13	16
Sr	1 945	2 151	11 378	2 716	2 669	1 870	2 412
Ba	27	21	21	349	306	26	30
Mn	5	1	2	35	64	3	5
Ti	58	34	25	212	428	52	68
Co	7	7	7	8	8	7	7
Cu	18	9	6	4	8	3	4
Ni	11	1	2	9	23	2	<1
Zn	79	58	60	19	69	25	43
Pb	<5	<5	<5	<5	<5	<5	<5
Cd	<1	<1	<1	<1	<1	<1	<1
Ag	<1	<1	<1	<1	<1	<1	<1
Mo	<25	<25	<25	<25	<25	<25	<25
Cr	21	4	4	14	111	13	52
V	11	6	6	14	26	6	8
As	<1	<1	<1	<1	<1	<1	<3
Sn	<2	<2	3	<2	<2	<2	<2
Sc	2	1	1	2	2	1	1
Zr(XRF)	16	11	11	19	32	11	11
ZR(ICPOES)	<1	1	1	3	7	<1	<1
Nb	2	2	2	1	1	2	2
Th	1	<1	4	<1	<1	<1	<1
U	3	<1	<1	<1	<1	<1	<1
Cl	<6	<6	<6	9	36	<6	25
F	281	700	642	632	876	583	447
S	11 299	7 356	7 983	5 530	15 763	11 000	14 691
Se	<2	<2	<2	<2	10	2	2
Y	1.40	0.10	0.10	1.40	7.90	0.20	0.20
La	0.90	0.20	0.21	1.69	4.88	0.38	0.54
Ce	2.38	1.18	0.69	4.45	6.89	1.25	2.47
Pr	0.29	0.22	0.25	0.21	1.06	0.32	0.35
Nd	1.70	1.60	1.10	3.50	4.70	1.50	2.70
Sm	0.02	0.09	0.12	0.11	0.69	0.12	0.11
Eu	0.05	0.00	0.00	0.06	0.18	0.01	0.01
Gd	0.35	0.14	0.06	0.49	0.93	0.21	0.33
Dy	0.17	0.02	0.01	0.26	0.91	0.03	0.05
Ho	0.06	0.02	0.01	0.07	0.20	0.02	0.04
Er	0.05	0.08	0.06	0.21	0.62	0.06	0.06
Yb	0.10	0.01	0.01	0.13	0.56	0.01	0.03
Lu	0.04	0.02	0.02	0.04	0.10	0.02	0.03
ppb							
Pd	<1	<1	<1	<1	n.d.	<1	n.d.

A-6: Adit A-6.
G-Tr: Green precipitates – Western Springs.
Y-Tr: Yellow precipitates – Western Springs.
RC: Maqarin Station Railway Cutting.
n.d. not detected.

Table L-3. Chemical composition of some travertines (Ref. C).

Element	Sample				
	A-6	Tr-1	Tr-2	Tr-3	Tr.W.Sh
Weight %					
SiO_2	– –	–	–	–	
CaO	59.54	60.94	59.54	64.36	60.31
MgO	0.21	0.01	0.03	0.03	0.56
Al_2O_3	1.58	0.51	0.51	0.42	0.79
Fe_2O_3	0.24	0.08	0.06	0.10	0.19
Na_2O	0.63	0.48	0.48	0.49	0.90
K_2O	0.21	0.13	0.13	0.13	0.40
P_2O_5	0.09	0.04	0.04	0.04	0.66
SO_3	1.14	1.61	1.46	2.35	–
$CaCO_3$	93.00	94.00	94.30	93.70	–
ppm					
Cd	3	3	3	3	–
Co	39	35	36	36	–
Cr	28	64	22	98	–
Cu	16	11	10	10	–
Mn	27	8	12	50	–
Ni	43	38	36	43	–
Pb	166	93	96	90	–
Zn	82	–	60	68	–

A-6	Adit A-6.
Tr-1	Maqarin Station Railway Cutting.
Tr-2	– ” –
Tr-3	– ” –
Tr.W.Sh.	Travertine, Wadi Shallala.

Table L-4. Mineralogy of the Pleistocene basalts (Ref. C).

Mineral phase	General formula	Modal analysis J 147	J 149
Orthoclase	$KAlSi_3O_8$	6.8	6.6
Albite	$NaAlSi_3O_8$	9.8	20.5
Anorthite	$CaAl_2Si_2O_8$	26.4	22.6
Nepheline	$(Na,K)AlSiO_4$	4.1	7.2
Diopside	$CaFeSi_2O_6$	23.8	13.1
Olivine	$Fe,MgSiO_4$	17.6	21.5
Magnetite	Fe_3O_4	2.2	1.6
Ilmenite	$FeTiO_3$	4.3	4.1
Apatite	$Ca_5(PO_4)_3F$	1.8	1.8

General

J 147	: Alkali basalt
J 149	: Basanite
Alteration	: Amorphous Ca-K-Na Zeolites
Age	: <1 Ma; K/Ar method

Geochemistry See Table L-5

Table L-5. Chemical composition of Pleistocene basalts.

	Sample	
Element	**J 147**	**J 149**
Weight %		
SiO_2	43.28	46.39
CaO	12.15	8.86
MgO	9.35	9.17
Al_2O_3	14.22	16.11
Fe_2O_3	3.74	1.09
Na_2O	2.04	4.02
K_2O	1.0	1.11
P_2O_5	0.76	0.77
L.O.I.	3.14	0.65
FeO	7.80	9.51
ppm		
U	0.73	0.53
Th	2.6	2.7
Hr	3.8	3.9
Zr	198.0	183.0
Ta	2.4	2.5
Ba	285	361
Sr	804	840
Cs	0.1	0.1
Rb	12	14
Sb	0.1	0.1
Cr	194	200
Co	53	55
Ni	182	190
Sc	23	23
La	27	27
Eu	2.1	2.1
Tb	0.71	0.73

Table L-6. Primary metamorphic minerals in the Metamorphic Unit (Cement Zone).

Mineral phase	General formula	Reference
Fluorapatite	$Ca_{10}(PO_4)_6F_2$	**A + B**
Francolite	$Ca_{10-x-y}(Na,K)_xMg_x(PO_4)_{6-z}(CO_3)_zF_{0.4z}F_2$	**A**
Ellestadite	$Ca_{10}(SiO_4)_3(SO_4)_3O_{24}(Cl,OH,F)_2$	**B**
Spurrite	$Ca_5(SiO_4)_2(CO_3)$	**A + B**
Urarovite	$Ca_3Cr_2(SiO_4)_2$	**C**
Wollastonite	$CaSiO_3$	**A**
Larnite	Ca_2SiO_4	**B**
Diopside-hedenbergite	$Ca(Al,Fe)Si_2O_6$	**A**
Anorthite	$CaAl_2Si_2O_8$	**A**
Brownmillerite	$Ca_2(Al,Fe)_2O_5$	**A + B**
Ca-ferrite	$CaFe_2O_3$	**B**
(?) ferrites	undefined Ba, Cr, Al, Ti, Mg, Zn, Mn-bearing	**B**
Hematite or ferric oxide	Fe_2O_3	**B**
Ca-aluminate	undefined	**B**
Calcite	$CaCO_3$	**A + B**
Graphite	C	**A**
Lime	CaO	**B**
Ba, Ca, S-silicate	undefined	**B**
Ba, Ca, Zr, Mo, silicate	undefined	**B**
Oldhamite	CaS to $CaS_{0.9}Se_{0.1}$	**B**
Cu, K, Na-selenide	$Cu_{10.2}K_3Na_{0.2}Se_{7.7}S_{2.3}$(approx)	**B**
UCa-oxycarbonate (?)	Ca: U = 2	**B**

Modal anal.: Variable from one sample to another.

Reference B = B: Phase I.

Table L-7. Secondary minerals in the Metamorphic Unit (Cement Zone).

Mineral phase	General formula	Reference
Jourauskite	$Ca_3Mn(CO_3)(SO_4)(OH)_6 \cdot 12H_2O$	**B + C**
Hydrotalcite	$Mg\ Al_2(CO_3)(OH)_{16} \cdot 4H_2O$	**B + C**
Calcite	$CaCO_3$	**A + B**
Aragonite	$CaCO_3$	**B**
Vaterite	$CaCO_3$	**A + B**
Kutnahorite	$Ca_{0.75}(Mn,Mg)_{0.26}CO_3$	**A**
Ankerite	$Ca(FeMg)(CO_3)_2$	**C**
Strontianite	$SrCO_3$	**B**
Hematite	Fe_2O_3	**A + B**
Maghemite	Fe_2O_3	**A**
Gibbsite	$Al(OH)_3$	**A + B**
Brucite	$Mg(OH)_2$	**A**
Portlandite	$Ca(OH)_2$	**A + B**
Quartz	SiO_2	**A + B**
Opal-CT	SiO_2	**A**
Opal-A	$SiO_2 \cdot nH_2O$	**A**
Baryte	$BaSO_4$	**A + B**
Barytocelestite	$(SrBa)SO_4$	**B**
Calcian barytocelestite	$(SrBaCa)SO_4$	**B**
Hashemite	$BaCrO_4$ to $BaSO_4$ complete solid solution	**B**
Cd-sulphate	undefined	**B**
Pb-sulphate	undefined	**B**
Gypsum	$CaSO_4$	**A + B**
Bassanite	$CaSO_4 \cdot 0.5H_2O$	**A**
Anhydrite	$CaSO_4$	**C**
Ettringite	$Ca_6Al_2(SO_4)_3(OH)_{12} \cdot 25H_2O$	**A + B**
Thaumasite	$Ca_6Si_2(SO_4)(CO_3)_2(OH)_{12} \cdot 24H_2O$	**A + B**
Cu, Zn-sulphate	undefined	**B**
Hydroxyapatite	$Ca_{10}(PO_4)6(OH)_2$	**A**
Fluorapatite	$Ca_{10}(PO_4)_6F_2$	**A + B**
Francolite	$Ca_{10-x-y}(Na,K)_xMg_x(PO_4)_{6-z}(CO_3)_zF_{0.4z}F_2$	**A**
Ellestadite	$Ca_{10}(SiO_4)_3(PO_4)_3O_{24}(Cl, OH, F)_2$	**A + B**
Afwillite	$Ca_3Si_2O_4(OH)_6$	**A + B**
Tobermorites	$Ca_5Si_6O_{16}(OH)_2 \cdot 2\text{-}8H_2O$	**A + B**
Jennite	??? $Ca_7H_2Si_6O_{18}(OH)_8 \cdot 6H_2O$	**A + B**
Apophyllite	$KCa_4Si_8O_{20}(OH,F)8H_2O$	**A + B**
Birunite	$Ca_{15}(CO_3)_{5.5}(SiO_3)_{8.5}SO_4 \cdot 15H_2O$	**B**

Table L-7 (contd.). Secondary minerals in the Metamorphic Unit (Cement Zone).

Mineral phase	General formula	Reference
CSH gel	amorphous, undefined	**B**
CASH gel	amorphous	**B + C**
U, Ca-silicate	unidentified	**B**
Ca-Cr-Si-gel	unidentified	**C**
Tacharanite	$Ca_{12}Al_2Si_{18}O_{15}(OH)_2 \cdot 3H_2O$	**B**
Mordenite	$CaNa_2K_2Al_2Si_{10}O_{24} \cdot 7H_2O$	**B**
Dachiardite	$(CaNa_2K_2)_5Al_{10}Si_{38}O_{96} \cdot 25H_2O$	**B**
Henlandite	$(CaNa_2)Al_2Si_7O_{18} \cdot 6H_2O$	**B**
Epistilbite	$Ca_3Al_6Si_{18}O_{48} \cdot 16H_2O$	**B**
Yugarawaralite	$Ca_2Al_4Si_{12}O_{32} \cdot 8H_2O$	**B**
Laumontite	$Ca_4Al_8Si_{16}O_{49} \cdot 16H_2O$	**B**
Wairakite	$Ca_8Al_{16}Si_{32}O_{96} \cdot 16H_2O$	**B**
Leonhardite	$Ca_4(Al_8Si_{16}O_{48}) \cdot 14H_2O$	**B**

Reference B = B: Phase I

Geochemistry: see Tables L-8, L-9, L-10 for whole-rock and Tables L-11 and L-12 for mineral phases.

Table L-8. Chemical composition of the Metamorphic Unit (altered Bituminous Marls)* (Ref. C).

	Sample									
Element	**2**	**6**	**7**	**8.2**	**10**	**11**	**11.1**	**13**	**14**	**17.1**
Weight %										
SiO_2	n.d.	n.d.	n.d.	n.d.	n.d.	n.d.	n.d.	n.d.	n.d.	n.d.
CaO	57.05	48.66	49.12	53.48	51.95	58.29	51.61	37.47	39.95	49.12
MgO	0.34	1.74	2.42	1.12	0.74	0.71	0.17	1.78	4.95	2.20
Al_2O_3	1.34	2.25	1.52	2.20	1.20	1.41	1.59	2.14	2.12	2.19
Fe_2O_3	0.66	1.34	1.58	1.45	1.20	0.77	0.95	1.92	3.02	1.96
Na_2O	1.35	0.64	0.52	0.84	0.68	0.71	0.49	0.52	0.85	0.66
K_2O	0.24	0.22	0.13	0.26	0.35	0.29	0.18	0.35	0.40	0.21
P_2O_5	1.94	1.54	n.d.	0.79	0.74	0.75	0.36	1.88	2.06	1.27
SO_3	0.06	0.00	1.47	0.00	0.00	0.00	0.00	0.00	0.00	2.80
$CaCO_3$	90.00	77.00	80.00	85.40	81.90	91.70	81.10	63.90	71.50	75.00
ppm										
Cd	4	4	3	4	2	3	4	2	3	2
Co	40	35	36	43	38	41	40	26	34	36
Cr	202	200	112	64	76	46	52	116	106	156
Cu	45	49	35	31	33	23	29	50	22	25
Mn	34	89	308	940	66	275	47	173	378	876
Ni	132	54	101	120	77	51	63	77	120	84
Pb	72	65	64	76	85	93	85	49	56	52
Zn	157	136	87	113	14	36	65	66	77	101

* Samples are from outcrops along the road to Adit A-6.
** n.d. = not detected.

Table L-8 (contd.). Chemical composition of the Metamorphic Unit (altered Bituminous Marls)* (Ref. C).

	Sample									
Element	**17.4**	**18**	**22**	**8.3**	**9**	**20**	**21**	**M-1**	**M-2**	**M-3**
Weight %										
SiO_2	n.d.	n.d.	n.d.	n.d.	n.d.	n.d.	n.d.	n.d.	n.d.	n.d.
CaO	50.37	59.54	44.15	45.63	48.19	55.65	49.12	47.10	43.37	47.88
MgO	1.52	0.68	4.0	3.78	0.43	0.69	3.85	2.03	3.14	1.45
Al_2O_3	2.83	0.99	n.d.	2.07	2.21	1.66	1.39	2.04	3.59	2.22
Fe_2O_3	2.11	0.34	3.96	2.04	2.21	1.24	1.51	2.31	3.39	2.31
Na_2O	0.91	1.01	0.39	0.78	1.48	0.68	0.68	0.72	0.83	0.31
K_2O	0.54	0.17	0.29	0.22	0.35	0.38	0.36	0.45	0.53	0.47
P_2O_5	1.65	2.39	1.83	1.26	1.38	0.68	0.69	n.d.	1.78	1.06
SO_3	0.00	0.87	0.00	0.00	0.00	0.00	0.15	0.00	0.55	0.00
$CaCO_3$	83.30	94.00	72.00	71.90	76.40	88.50	84.00	79.80	73.00	78.00
ppm										
Cd	3	5	3	2	4	3	3	3	7	3
Co	37	39	46	39	44	44	38	30	35	33
Cr	8	110	78	65	132	58	65	98	126	92
Cu	26	28	36	37	58	23	25	25	36	24
Mn	1 542	59	2 542	350	80	1 460	253	854	2 228	1 050
Ni	101	85	77	114	137	46	79	85	183	96
Pb	91	78	85	60	66	99	87	81	73	81
Zn	90	528	121	74	170	81	61	242	198	200

* Samples from outcrop along Adit A-6.
** n.d. = not detected.

Table L-8 (contd.). Chemical composition of the Metamorphic Unit (altered Bituminous Marls)* (Ref. C).

	Sample									
Element	**A-3**	**D-2**	**AM-6**	**A-1**	**A-4**	**A-5**	**B-2**	**AM-7**	**MZ-5**	**B-1**
Weight %										
SiO_2	n.d.	n.d.	n.d.	n.d.	n.d.	n.d.	n.d.	n.d.	n.d.	n.d.
CaO	50.06	46.95	46.33	53.63	46.17	39.63	47.88	51.61	61.87	45.39
MgO	0.44	0.71	4.12	0.39	0.34	0.32	0.34	0.36	0.47	0.39
Al_2O_3	1.96	1.79	3.28	1.86	1.54	0.92	1.71	1.62	1.69	1.01
Fe_2O_3	1.04	0.77	2.63	1.35	0.70	0.56	0.77	1.05	1.19	0.37
Na_2O	0.95	0.97	1.04	0.86	0.80	0.51	0.48	1.04	0.72	0.64
K_2O	0.16	0.16	0.30	0.43	0.22	0.09	0.13	0.25	0.29	0.16
P_2O_5	6.89	3.89	6.60	6.31	6.39	3.39	3.60	6.53	0.53	3.66
SO_3	–	–	5.69	7.12	–	9.10	7.43	5.82	6.98	12.60
$CaCO_3$	81.00	80.00	81.50	87.00	76.00	62.30	72.80	90.00	90.10	70.30
ppm										
Cd	n.d.	n.d.	n.d.	n.d.	n.d.	n.d.	n.d.	n.d.	5	n.d.
Co	28	28	36	36	32	22	24	36	41	30
Cr	546	526	560	510	410	408	448	448	542	212
Cu	74	64	44	60	46	76	70	52	68	42
Mn	34	30	58	34	36	18	26	36	30	38
Ni	218	64	202	216	150	166	164	218	225	144
Pb	n.d.	n.d.	n.d.	n.d.	n.d.	n.d.	n.d.	n.d.	94	n.d.
Zn	504	296	656	688	450	456	434	352	389	204

* Samples from Adit A-7.
** n.d. = not detected.

Table L-8 (contd.). Chemical composition of the Metamorphic Unit (altered Bituminous Marls)* (Ref. C).

	Sample									
Element	**D-3**	**NR-1**	**AM-S**	**QA-15**	**QA-25**	**TM-2**	**C-2**	**C-3**	**D-1**	**E-2**
Weight %										
SiO_2	n.d.	n.d.	n.d.	n.d.	n.d.	n.d.	n.d.	n.d.	n.d.	n.d.
CaO	35.29	46.79	87.47	53.63	57.98	48.33	46.95	46.01	36.37	47.41
MgO	0.83	0.63	0.32	1.20	0.43	3.40	0.42	0.38	17.71	0.43
Al_2O_3	0.59	2.09	1.08	2.59	1.54	1.22	1.74	1.55	0.87	1.43
Fe_2O_3	0.22	0.93	0.76	2.06	0.70	0.52	1.48	2.05	0.32	0.88
Na_2O	0.74	0.74	0.59	0.83	0.77	0.88	0.80	0.65	0.83	0.85
K_2O	0.23	0.19	0.16	0.19	0.18	0.26	0.19	0.16	0.21	0.15
P_2O_5	0.34	2.73	4.05	1.27	15.43	1.38	7.68	6.53	0.70	6.67
SO_3	1.82	5.32	11.51	0.42	7.13	0.44	10.50	7.43	4.62	6.79
$CaCO_3$	96.00	8.23	56.80	78.90	80.90	93.50	78.00	71.00	94.00	78.50
ppm										
Cd	n.d.	n.d.	n.d.	3	4	4	n.d.	n.d.	n.d.	n.d.
Co	22	34.0	n.d.	42	36	33	30	30	14	28
Cr	32	2 028	n.d.	120	94	76	448	412	10	554
Cu	10	112	n.d.	44	54	19	68	70	16	84
Mn	38	40	n.d.	234	95	57	30	24	74	26
Ni	42	226	n.d.	105	148	58	188	190	62	238
Pb	n.d.	n.d.	n.d.	86	83	86	n.d.	n.d.	n.d.	n.d.
Zn	198	678	n.d.	98	352	380	400	n.d.	214	422

* Drillcore samples.
** n.d. = not detected.

Table L-8 (contd.). Chemical composition of the Metamorphic Unit (altered Bituminous Marls)* (Ref. C).

	Sample									
Element	**E-3**	**F-1**	**G-1**	**VN**	**AM-1**	**AM-2**	**AM-3**	**AM-4**	**AM-8**	**CO-2**
Weight %										
SiO_2	n.d.	n.d.	n.d.	n.d.	n.d.	n.d.	n.d.	n.d.	n.d.	n.d.
CaO	39.02	49.11	46.01	41.97	41.51	35.99	34.97	46.95	48.81	45.39
MgO	0.26	0.33	0.32	0.18	0.32	0.65	0.48	0.31	0.34	0.57
Al_2O_3	0.42	1.87	2.32	1.03	0.52	1.81	1.55	1.89	1.10	0.94
Fe_2O_3	0.18	1.27	1.67	0.72	0.37	1.62	1.50	0.65	1.14	0.26
Na_2O	0.47	–	0.67	0.59	0.91	0.68	0.69	1.07	0.97	1.05
K_2O	0.10	0.03	0.81	0.28	0.21	0.17	0.16	0.23	0.20	0.28
P_2O_5	0.88	3.84	3.60	1.54	15.47	11.30	6.60	3.98	6.96	2.83
SO_3	9.86	9.24	7.64	5.11	9.10	9.29	10.19	4.03	3.92	5.28
$CaCO_3$	61.80	81.50	69.80	71.00	66.30	40.80	45.00	81.00	81.50	72.30
ppm										
Cd	n.d.	n.d.	n.d.	n.d.	n.d.	n.d.	n.d.	n.d.	n.d.	n.d.
Co	18	34	26	28	32	30	30	34	34	28
Cr	118	694	516	480	354	534	600	362	402	398
Cu	24	114	78	56	68	124	104	76	28	36
Mn	20	30	36	18	64	38	28	26	30	36
Ni	58	33	152	172	164	184	322	144	134	248
Pb	n.d.	n.d.	n.d.	n.d.	n.d.	n.d.	n.d.	n.d.	n.d.	n.d.
Zn	8 000	574	434	2 128	174	448	514	434	164	3 580

* Adit A-7 and drillcore samples.
** n.d. = not detected.

Table L-8 (contd.). Chemical composition of the Metamorphic Unit (altered Bituminous Marls)* (Ref. C).

	Sample									
Element	**CO-3**	**CO-5**	**CO-6**	**CO-7**	**CO-8**	**CO-9**	**CO-11**	**CO-12**	**CO-13**	**QA-26**
Weight %										
SiO_2	n.d.	n.d.	n.d.	n.d.	n.d.	n.d.	n.d.	n.d.	n.d.	n.d.
CaO	47.27	30.31	43.22	45.39	47.88	55.03	33.11	43.99	45.55	n.d.
MgO	0.49	6.2	0.40	0.38	0.80	0.45	0.22	0.61	0.62	0.67
Al_2O_3	2.33	10.40	0.67	1.41	3.10	1.17	0.39	2.17	1.41	1.57
Fe_2O_3	3.25	8.45	1.06	1.04	4.23	0.49	0.44	2.90	0.74	0.34
Na_2O	0.93	0.76	0.72	0.77	1.03	1.11	n.d.	0.78	0.55	0.51
K_2O	0.22	0.21	0.67	0.14	0.28	1.80	0.04	0.16	0.14	0.08
P_2O_5	0.70	8.04	0.68	3.23	2.73	1.72	0.35	n.d.	0.70	5.56
SO_3	47.50	7.28	1.44	5.93	3.88	6.25	19.19	8.90	5.52	10.54
$CaCO_3$	79.30	33.30	76.30	67.30	70.50	87.50	14.30	56.80	71.80	69.80
ppm										
Cd	n.d.	n.d.	n.d.	n.d.	n.d.	n.d.	n.d.	n.d.	n.d.	7
Co	42	60	22	28	42	38	26	58	26	33
Cr	190	290	126	458	156	322	138	486	108	1 220
Cu	100	34	64	88	116	60	42	64	12	57
Mn	86	1 056	38	36	82	22	18	240	250	17
Ni	246	382	130	334	400	294	112	446	66	140
Pb	n.d.	n.d.	n.d.	n.d.	n.d.	n.d.	n.d.	n.d.	n.d.	35
Zn	650	1 788	130	546	1 012	1 300	412	394	20	260

* Drillcore samples.
** n.d. = not detected.

Table L-8 (contd.). Chemical composition of the Metamorphic Unit (altered Bituminous Marls)* (Ref. C).

	Sample				
Element	**QA-26**	**QA-27**	**QA-28**	**QA-29**	**QA-30**
Weight %					
SiO_2	n.d.	n.d.	n.d.	n.d.	n.d.
CaO	32.65	42.75	54.72	43.32	50.21
MgO	0.17	0.25	0.23	1.58	0.20
Al_2O_3	0.35	0.17	3.06	5.55	2.20
Fe_2O_3	0.09	0.39	1.75	4.08	1.75
Na_2O	0.36	0.64	0.85	0.76	0.81
K_2O	0.08	0.16	0.26	0.20	0.13
P_2O_5	0.11	2.27	n.d.	3.18	1.88
SO_3	14.39	13.96	8.62	5.34	7.73
$CaCO_3$	n.d.	64.3	80.9	59.4	72.1
ppm					
Cd	2	38	4	3	3
Co	24	82	38	39	37
Cr	54	452	446	64	452
Cu	12	63	38	34	52
Mn	00	11	40	2 232	16
Ni	18	135	130	203	143
Pb	64	64	64	1 120	84
Zn	12	248	143	121	99

* Samples from outcrops along the road to Adit A-6.
** n.d. = not detected.

Table L-8 (contd.). Chemical composition of the Metamorphic Unit (altered Bituminous Marls)* (Ref. C).

	Sample								
Element	**AM-10**	**MZ-3**	**TM-1**	**CO-14**	**CO-4**	**CO-10**	**TM-3**	**E-1**	**A-6cr****
Weight %									
SiO_2	n.d.	n.d.	n.d.	n.d.	n.d.	n.d.	n.d.	n.d.	3.00
CaO	47.27	54.56	56.27	48.35	43.22	46.48	57.36	43.06	0.56
MgO	0.39	1.03	0.39	0.38	0.39	1.65	0.40	0.17	0.34
Al_2O_3	0.80	2.03	1.22	1.59	5.72	1.74	1.60	1.16	0.56
Fe_2O_3	0.35	1.50	0.60	1.06	5.21	1.66	1.05	0.85	0.12
Na_2O	0.77	0.74	0.55	0.92	0.45	0.71	0.90	0.66	0.04
K_2O	1.54	0.12	0.14	1.80	0.13	1.80	0.24	0.18	0.01
P_2O_5	1.11	3.66	2.44	3.05	6.10	1.04	11.66	2.37	0.20
SO_3	0.62	7.07	4.38	7.78	7.28	0.71	7.42	2.71	–
$CaCO_3$	77.3	75.5	82.9	80.0	28.3	88.3	77.5	68.5	–
ppm									
Cd	n.d.	4	97	n.d.	n.d.	n.d.	3.5	n.d.	–
Co	20	34	34	28	36	30	37	28	–
Cr	190	768	614	572	488	610	846	208	2 900
Cu	42	78	84	102	70	82	72	56	–
Mn	34	36	14	30	74	78	11	38	–
Ni	124	225	231	242	260	156	135	170	–
Pb	n.d.	108	57	n.d.	n.d.	n.d.	65	n.d.	–
Zn	–	918	954	854	438	278	248	1 704	–

* Samples from drillcores.
** A-6cr: a chromium-rich sample analysed by Clay Tech. (Lund, Sweden).
*** n.d. = not detected.

Table L-9. Chemical composition of the Cement Zone (Ref. B, Phase I).

	Sample					
Element	**M2P2***	**M3P**	**M4P2**	**M15P**	**M18P**	**M28P**
Weight %						
SiO_2	n.d.	10.27	n.d.	8.64	n.d.	10.80
Al_2O_3	0.02	1.22	0.64	2.73	0.17	1.10
Fe_2O_3	0.01	0.25	0.16	0.74	0.02	0.45
MgO	0.44	0.35	0.30	0.53	0.00	0.35
CaO	54.62	50.55	43.30	52.27	31.80	48.65
Na_2O	0.02	0.03	0.03	0.22	0.02	0.07
K_2O	0.01	0.01	0.00	0.02	0.01	0.00
P_2O_5(XRF)	n.d.	1.82	n.d.	10.60	n.d.	1.37
P_2O_2(ICPOES)	0.07	1.09	2.00	6.32	0.06	0.81
ppm						
Li	12	14	13	20	11	12
Sr	293	1 100	1 407	1 638	643	769
Ba	18	231	43	341	10	30
Mn	11	19	22	39	2	20
Ti	11	336	187	517	6	282
Co	7	8	7	8	7	9
Cu	3	78	202	76	5	71
Ni	1	168	98	188	3	220
Zn	4	568	2 530	435	10	592
Pb	<5	<5	<5	5	5	23
Cd	<1	108	<1	<1	<1	<1
Ag	<1	<1	<1	<1	<1	1
Mo	<25	43	45	<25	<25	62
Cr	3	329	275	506	1 468	231
V	10	618	192	227	8	309
As	n.d.	<1	n.d.	<1	n.d.	23
Sn	n.d.	<2	n.d.	<2	n.d.	4
Sc	1	4	3	5	1	4
Zr(XRF)	n.d.	44	n.d.	39	n.d.	35
Zr(ICPOES)	1	1	<1	1	2	12
Nb	3	2	2	2	1	2
Th	n.d.	<1	n.d.	<1	n.d.	1
U	n.d.	19	10	28	<1	2
Cl	n.d.	163	n.d.	1 074	n.d.	230
F	n.d.	847	n.d.	5 227	n.d.	1 139
S	n.d.	21 026	n.d.	52 590	n.d.	85 655
Se	n.d.	39	n.d.	116	n.d.	20

Table L-9 (contd.). Chemical composition of the Cement Zone (Ref. B, Phase I).

	Sample					
Element	**M2P2***	**M3P**	**M4P2**	**M15P**	**M18P**	**M28P**
ppm (contd.)						
Y	0.80	25.10	18.50	67.80	0.20	24.40
La	0.50	9.63	6.70	25.60	0.22	10.25
Ce	0.63	9.61	6.09	16.68	0.54	5.08
Pr	0.21	2.39	1.82	4.03	0.11	2.16
Nd	1.50	10.40	7.40	17.40	0.90	9.50
Sm	0.10	1.44	0.87	3.03	0.09	1.60
Eu	0.05	0.45	0.29	0.82	0.01	0.46
Gd	0.20	2.34	1.17	4.34	0.07	1.90
Dy	0.12	2.27	1.54	4.91	0.02	2.29
Ho	0.08	0.54	0.38	1.17	0.00	0.52
Er	0.13	1.61	1.36	4.00	0.05	1.63
Yb	0.10	1.57	1.26	3.64	0.01	1.58
Lu	0.02	0.25	0.21	0.57	0.01	0.25
ppb						
Pd	n.d.	n.d.	n.d.	13	n.d.	n.d.

* = vein material.
n.d. = not detected.
XRF = X-ray Fluorescence.
ICPOES = Inductively Coupled Plasma Atomic Emission Spectrometry.

Table L-10. Composition of minerals present in unaltered Bituminous Marls (Ref. B, Phase II).

Mineral phase	A 961	A 962	A1
Calcite [$CaCO_3$]	74.4	74.8	67.9
Dolomite [$CaMgCO_3$]	1.1	1.1	1.3
Apatite [$Ca_5(PO_4)_3F$]	3.5	4.6	5.1
Albite [$NaAlSi_3O_8$]	1.0	0.7	n.d.
Illite [$K_{0.8}(Al_{0.8}S_{3.2})Al_2O_{10}(OH_2)$]	1.1	2.1	n.d.
Kaolinite [$Al_2Si_2O_5(OH)_4$]	1.9	5.3	n.d.
Pyrite [FeS_2]	0.9	0.5	2.0
Fe-oxides [Fe_2O_3]	0.06	1.8	n.d.
Quartz/opal [SiO_2]	1.7	5.2	7.0
Total clay	–	–	5.0
Organic matter	–	–	14.8
Others*	–	–	–

General
Λ 961 and Λ 962 – Λdit Λ-6
A1 – Average whole-rock composition
Bituminous marl: Muwaqqar/Bituminous Marl Formation (B_3)

***Others:** (Minor constituents)
Ankerite
Pyrite/sphalerite/galena/NiSe/Ag Se Ag - Cu - Ni - Fe - Zn - Cd - S - Se - Zn - Cu - Fe - Ni - S, Zn - Cu - Fe - Ni - Se
Native Se

Collophane
Glauconite
Barite
Gypsum
Se-rich gypsum

Geochemistry	See Table L-11

Table L-11. Chemical composition of unaltered Bituminous Marls (Ref. C).

	Sample				
Element	**19**	**24**	**31**	**32**	**33**
Weight %					
SiO_2	–	–	–	–	–
CaO	53.32	54.10	58.12	35.76	33.63
MgO	0.89	0.39	0.18	0.56	3.14
Al_2O_3	2.46	2.31	1.59	5.79	0.82
Fe_2O_3	1.36	1.44	1.29	4.54	0.30
Na_2O	0.67	0.88	0.88	0.74	1.02
K_2O	0.36	0.41	0.33	0.42	0.16
P_2O_5	11.66	2.83	1.06	3.95	39.76
SO_3	0.17	0.68	3.83	12.89	56.00
$CaCO_3$	75.50	84.80	89.00	56.00	32.90
ppm					
Cd	–	4	4	2	16
Co	–	36	36	34	25
Cr	–	2 194	178	496	106
Cu	–	46	44	80	31
Mn	–	49	27	40	5
Ni	–	126	102	186	91
Pb	–	76	96	57	32
Zn	–	251	185	438	408

Table L-12. Normative mineralogical composition for altered bituminous clay biomicrite matrix in sample A 960 (Adit A-6) calculated from broad defocussed beam EMPA* analyses (Ref. B, Phase II).

	Distance from fracture (mm)							
Mineral	**1.30**	**1.15**	**0.93**	**0.69**	**0.50**	**0.38**	**0.26**	**0.17**
Calcite [$CaCO_3$]	69.2	67.1	64.2	58.6	27.9	0.0	0.0	41.0
Apatite [$Ca_5(OH)(PO_4)_3$]	10.3	11.4	14.7	8.6	6.1	13.1	8.2	13.9
Gypsum [$CaSO_4 \cdot 2H_2O$]	1.6	1.3	1.2	1.2	3.6	3.9	2.1	2.0
"CASH" [Ca:Si:Al = 23:22:5]	14.5	15.7	15.3	26.2	52.6	70.5	84.0	29.5
Talc [$Mg_3Si_4O_{10}(OH)_2$]	1.2	1.0	1.3	1.1	1.4	2.3	1.9	2.3
Goethite [FeO(OH)]	1.1	1.1	0.9	0.8	0.7	2.3	0.5	0.8
Gibbsite $Al(OH)_3$	2.1	2.4	2.4	3.5	7.7	7.9	3.3	10.5
Others**	–	–	–	–	–	–	–	–
Porosity	29.4	24.3	21.0	22.1	37.6	70.0	43.1	50.3

General

Paragenesis in Adit A-6 – High pH-effect:

Upstream = 140 m.
Aragonite – ettringite – thaumasite – CSH gel – zeolites.

Intermediate alteration zone
No zeolites, tobermorite 11 Å and 14 Å.

Downstream away from alkaline seepages (40–55 m from Adit A-6 entrance)
Aragonite – ettringite-thaumasite – CSH ??

* = Electron Microprobe Analysis.
** = Others: Low temperature minerals, see Table L-7.

Geochemistry	See Tables L-13, L-14 and L-15 for whole-rock and Tables L-18, L-19 and L-20 for mineral phases.

Table L-13-a. EMPA* and ATEM results for the altered Bituminous Marls (M81). (Ref. B, Phase II supplementary).**

	SAMPLE							REFERENCE							
Element	**M81001**	**M81002**	**M81003**	**M81004**	**M81005**	**M81006**	**M81007**	**M81008**	**M81009**	**M81010**	**M81011**	**M81012**	**M81013**	**M81014**	**M81015**
Fe	0.00	0.00	0.00	0.00	0.00	0.00	0.00	0.34	0.45	0.29	0.00	0.00	0.00	0.22	0.00
Na	0.00	0.00	0.00	0.00	0.00	0.00	0.00	0.00	0.00	0.00	0.00	0.00	0.00	0.00	0.00
K	0.00	0.00	0.00	0.00	0.00	0.00	0.22	0.00	0.14	0.17	0.18	0.15	0.12	0.17	0.23
Mg	0.00	0.00	0.00	0.00	0.00	0.00	0.00	0.00	0.00	0.00	0.00	0.29	0.00	0.18	0.00
Ca	42.53	43.39	45.20	43.21	4292	42.95	41.76	39.17	38.01	38.00	36.56	36.31	34.19	37.84	43.00
Al	8.02	10.73	7.82	10.71	10.05	7.94	0.72	1.99	2.56	3.60	7.78	7.41	7.85	2.81	0.51
S	9.32	6.60	3.32	4.70	4.41	3.45	0.60	2.09	3.05	5.67	12.52	12.71	14.08	3.48	0.21
Si	0.99	1.21	6.41	3.55	4.66	7.63	17.97	16.70	15.67	11.80	1.28	1.33	0.97	15.07	17.79

* = Electron Microprobe Analysis.
** = Analytical Transmission Electron Microscopy.

Table L-13-b. ATEM* results for the altered Bituminous Marls (M85). (Ref. B, Phase II supplementary).

	SAMPLE								REFERENCE								
Element	**M85001**	**M85002**	**M85003**	**M85004**	**M85005**	**M85006**	**M85007**	**M85008**	**M85009**	**M85010**	**M85011**	**M85012**	**M85013**	**M85014**	**M85015**	**M85016**	**M85017**
Si	11.53	5.61	10.40	3.04	7.43	7.91	10.36	13.32	7.50	11.85	12.78	11.75	1.68	11.15	13.11	13.32	10.99
Al	0.40	3.31	1.69	0.00	0.00	2.20	1.04	0.45	0.44	0.86	0.92	0.40	0.00	0.00	0.36	0.65	4.64
Fe	0.00	2.55	0.00	0.00	0.00	0.00	0.00	0.00	0.00	0.00	0.00	0.00	0.00	0.00	0.00	0.00	0.00
Mg	0.00	0.00	0.00	0.00	0.00	0.00	0.00	0.00	0.00	0.00	0.00	0.00	0.00	0.00	0.00	0.00	0.00
Ca	43.99	34.79	42.11	51.34	38.08	40.69	40.49	44.61	37.54	42.01	44.10	46.28	48.06	40.31	46.77	46.27	41.83
Na	0.00	0.00	0.00	0.00	0.00	0.00	0.00	0.00	0.00	0.00	0.00	0.00	0.00	0.00	0.00	0.00	0.00
K	0.00	0.00	0.00	0.00	0.00	0.00	0.00	0.00	0.00	0.00	0.00	0.00	0.00	0.00	0.00	0.00	0.00
S	5.23	11.80	6.27	8.69	12.36	8.83	7.71	3.30	12.26	5.71	3.70	0.75	11.71	7.92	2.34	2.22	3.69

* = Analytical Transmission Electron Microscopy.

Table L-14. EMPA* and ATEM results for the altered Bituminous Marls (M93). (Ref. B, Phase II).**

	SAMPLE REFERENCE															
Element	**M93005**	**M93006**	**M93007**	**M93008**	**M93009**	**M93010**	**M93011**	**M93012**	**M93013**	**M93014**	**M93015**	**M93016**	**M93017**	**M93018**	**M93019**	**M93020**
Fe	0.70	1.87	5.53	6.86	0.65	0.89	0.72	2.74	1.38	17.87	28.39	0.00	3.26	4.24	4.78	0.26
Na	0.00	0.00	1.56	0.69	0.00	0.00	0.00	0.56	0.85	0.00	0.00	0.00	0.00	0.00	0.00	0.00
K	0.83	0.83	0.83	0.83	0.83	0.83	0.83	0.83	0.83	0.83	0.83	0.83	0.83	0.83	0.83	0.83
Mg	0.00	0.00	1.71	1.43	0.00	0.19	0.00	1.06	0.65	0.00	0.00	0.00	0.00	0.49	0.00	0.42
Ca	62.71	30.96	7.06	5.77	23.70	22.18	22.52	3.86	2.27	21.89	8.17	66.22	14.70	5.45	13.64	1.34
Al	0.81	5.72	13.41	11.61	6.19	7.34	6.15	17.86	20.65	5.60	7.00	0.34	9.41	18.05	11.31	24.19
S	0.00	0.00	0.00	0.00	0.00	0.00	0.00	0.00	0.00	0.00	0.00	0.00	0.24	0.00	0.00	0.00
Si	3.58	16.94	18.63	20.56	21.27	20.74	21.86	19.34	18.83	12.01	11.97	2.70	21.28	20.00	20.04	20.53

* = Electron Microprobe Analysis.
** = Analytical Transmission Electron Microscopy.

Table L-15. Whole-rock chemical analyses of unaltered and altered Bituminous Marls (Ref. B, Phase II).

Element	Sample Reference							
	MQ10.5P altered	A6.1P altered	A62.P altered	A6.3P altered	A6.4P2.1 altered	A6.4P2.2 altered	A6.7P unaltered	A6.9P unaltered
Weight %								
SiO_2	8.84	13.46	11.55	7.65	12.02	n.d.	9.53	10.07
Al_2O_3	2.72	4.29	3.32	1.53	4.02	2.99	2.33	2.77
Fe_2O_3	1.30	1.46	1.02	0.65	1.64	0.84	1.04	1.00
MgO	0.20	0.28	0.18	0.19	0.22	0.37	0.19	0.26
CaO	47.02	43.37	44.17	48.08	41.83	37.12	43.24	40.20
Na_2O	0.05	0.09	0.05	0.03	0.04	0.04	0.07	0.10
K_2O	0.14	0.58	0.17	0.00	0.01	0.00	0.81	0.18
P_2O_5(XRF)	2.80	2.45	2.49	2.11	2.38	n.d.	3.68	2.94
P_2O_5(ICPOES)	1.49	1.31	1.32	1.10	1.44	0.95	1.78	1.42
ppm								
Li	21	52	17	15	15	15	32	24
Sr	1 259	2 942	1 320	991	914	820	2 263	1 770
Ba	216	177	64	95	62	54	174	103
Mn	35	42	27	30	32	20	42	25
Ti	561	876	608	318	751	499	461	519
Co	10	11	9	9	10	8	9	9
Cu	68	47	51	63	47	33	66	49
Ni	154	153	122	137	136	80	159	133
Zn	233	311	198	160	325	178	364	230
Pb	<5	13	10	<5	<5	<5	12	7
Cd	<1	3	<1	<1	<1	<1	3	4
Ag	<1	<1	<1	<1	<1	<1	<1	<1
Mo	<25	<25	<25	<25	35	33	<25	<25
Cr	218	457	363	178	320	485	313	354
V	97	93	101	72	98	64	91	105
As	9	12	5	<1	12	n.d.	6	7
Sn	<2	<2	<2	5	3	n.d.	3	2
Sc	5	6	5	4	6	4	5	4
Zr(XRF)	31	34	19	24	36	n.d.	25	32
Zr(ICPOES)	15	16	13	11	17	11	12	12
Nb	<1	1	<1	1	<1	<1	<1	<1
Th	<1	<1	<1	<1	1	n.d.	<1	<1
U	16	15	13	15	14	5	19	17
Cl	36	59	46	<6	26	n.d.	157	698
F	1 881	1 520	1 569	886	1 139	n.d.	1 988	1 881
S	73 697	10 826	22 841	60 629	94 493	n.d.	8 616	62 082
Se	23	26	40	13	17	n.d.	148	262
Y	28.70	25.10	21.80	23.20	23.80	15.20	27.60	26.30
La	13.93	15.70	9.66	10.27	13.56	9.43	14.10	13.16
Ce	14.94	26.80	20.90	13.60	20.07	13.34	15.65	16.21
Pr	2.16	3.40	2.90	2.69	3.57	2.31	3.55	3.51
Nd	11.50	16.90	14.60	11.60	15.40	9.90	15.00	14.00
Sm	2.08	2.36	1.94	1.65	2.15	1.47	2.26	1.92
Eu	0.55	0.65	0.57	0.51	0.66	0.43	0.66	0.57

Table L-15 (contd.). Whole-rock chemical analyses of unaltered and altered Bituminous Marls (Ref. B, Phase II).

	Sample Reference							
Element	**MQ10.5P[1]**	**A6.1P**	**A62.P[2]**	**A6.3P**	**A6.4P2.1[3]**	**A6.4P2.2[3]**	**A6.7P**	**A6.9P**
ppm (contd.)								
Gd	2.67	2.31	2.54	2.15	3.08	1.91	3.23	2.48
Dy	2.81	2.91	2.44	2.41	2.71	1.74	2.99	2.60
Ho	0.61	0.64	0.55	0.53	0.59	0.37	0.65	0.60
Er	2.04	1.80	1.53	1.57	1.63	0.88	1.66	1.70
Yb	1.85	1.67	1.46	1.52	1.57	1.00	1.80	1.61
Lu	0.33	0.25	0.28	0.24	0.25	0.18	0.32	0.31
ppb								
Pd	n.d.	n.d.	3	4	n.d.	n.d.	5	n.d.

n.d. = not detected.
[1] = "baked" variety.
[2] = "cherty" variety.
[3] = "mottled" variety.

XRF = X-ray Fluorescence.
ICPOES = Inductively Coupled Plasma Atomic Emission Spectrometry.

Table L-16. Chemical composition of secondary minerals in altered Bituminous Marls (M81). (Ref. B, Phase I supplementary).

	SAMPLE TYPE					
Element	**Wall rock alteration**	**Amorphous CSH**	**Gibbsite in W.R.**	**Ellastidite**	**CSH (Dull)**	**Jennite**	**Ettringite**
F	0.14	0.15	0.84	0.67	0.02	0.03	0.37
Cl	0.50	0.53	0.11	0.28	0.58	0.16	0.70
Fe	0.46	0.31	0.06	0.32	0.02	0.02	0.02
Na	0.07	0.06	0.11	0.11	0.05	0.01	0.06
K	0.02	0.03	0.00	0.05	0.03	0.00	0.01
Mn	0.01	0.00	0.00	0.01	0.01	0.01	0.01
Mg	0.26	0.32	0.21	0.21	0.05	0.02	0.17
Ca	22.94	21.70	6.33	30.37	17.85	32.51	16.60
Cr	0.09	0.11	0.00	0.24	0.02	0.07	0.13
Al	1.71	0.91	39.20	0.64	0.76	0.35	3.59
S	1.04	0.68	0.29	2.37	0.09	0.22	4.42
Si	5.10	6.03	0.68	6.13	9.99	14.52	2.71
P	0.49	0.46	0.06	2.35	0.03	0.04	0.04
Ti	0.09	0.06	0.00	0.07	0.00	0.00	0.00

Table L-17. Chemical composition of secondary minerals in altered Bituminous Marls (M86). (Ref. B, Phase I supplementary).

	SAMPLE TYPE						
Element	**Mg-rich vein**	**Quartz alteration**	**Quartz alteration**	**CSH late**	**Ropey CSH**	**Fibrous CSH**	**Massive CSH**
F	0.14	0.53	0.40	0.25	0.20	0.09	0.13
Cl	0.04	0.06	0.05	0.03	0.17	1.02	0.08
Fe	0.07	0.01	0.02	0.01	0.01	0.01	0.01
Na	0.06	0.15	0.19	0.14	0.10	0.05	0.08
K	0.01	0.02	0.04	0.02	0.03	0.00	0.01
Mn	0.01	0.01	0.01	0.00	0.01	0.01	0.01
Mg	22.90	0.01	0.01	0.00	3.93	0.01	3.48
Ca	0.55	19.63	40.45	19.65	17.24	18.24	16.62
Cr	0.01	0.01	0.02	0.00	0.01	0.01	0.00
Al	0.44	0.04	0.06	0.04	0.04	0.70	0.03
S	0.56	0.07	0.12	0.09	0.17	0.04	0.07
Si	16.60	19.73	44.13	19.90	18.78	22.78	19.67
P	0.13	0.02	0.06	0.03	0.04	0.03	0.02
Ti	0.00	0.00	0.00	0.00	0.00	0.00	0.00

Table L-18. Chemical composition of secondary minerals in the altered Bituminous Marls (M91). (Ref. B, Phase II).

Element	Fracture filling	Amorphous CSH	CSH-replacing calcite	Ettringite and gypsum	Ettringite and gypsum	Acicular CASH	Massine CASH	M93	M93
F	0.19	0.15	0.08	0.62	1.34	0.38	0.10	n.d.	n.d.
Cl	0.72	0.28	0.72	0.36	0.17	0.58	0.02	n.d.	n.d.
Fe	0.24	0.04	0.03	0.00	0.03	0.02	0.00	3.59	4.73
Na	0.04	0.07	0.07	0.02	0.02	0.21	0.08	0.00	0.96
K	0.13	0.37	0.20	0.01	0.01	0.01	0.20	0.83	0.83
Mn	0.00	0.01	0.01	0.00	0.08	0.00	0.00	n.d.	n.d.
Mg	3.53	0.03	0.32	0.01	0.06	0.25	0.01	0.00	0.60
Ca	5.53	9.14	7.40	19.90	27.66	23.22	17.69	44.49	5.56
Cr	0.25	0.02	0.14	0.00	0.00	0.01	0.00	n.d.	n.d.
Al	3.53	6.80	3.64	5.86	5.41	8.44	3.68	4.64	18.16
S	1.48	0.26	0.12	13.72	6.78	7.81	0.02	0.00	0.00
Si	7.53	18.59	12.74	0.10	0.20	4.78	18.23	9.07	18.43
P	0.54	0.06	0.01	0.02	0.04	0.04	0.02	n.d.	n.d.
Ti	0.07	0.00	0.00	0.00	0.01	0.00	0.00	n.d.	n.d.

n.d. = not detected.

Table L-19. EMPA* and LA-ICP-MS** data for selected fracture infilling minerals in the unaltered Bituminous Marls (Ref. B, PhaseII).

Element		SAMPLE								
		Average Jennite	Average Wairakite	Average Ettringite	Average Thaumasite	Average Calcite	Average Aragonite	Average Hydr. CSH	Average Brucite	Average Portlandite
EPMA Data										
	Mg	0.04	0.00	0.05	0.02	0.14	0.64	0.01	42.41	0.00
	Al	0.12	1.19	2.79	1.86	0.79	0.26	0.06	0.00	0.00
	Si	16.22	0.14	0.40	2.95	0.30	0.30	44.13	0.00	0.00
	Ca	34.35	18.97	20.74	21.14	39.82	40.18	40.45	0.00	54.09
	Fe	0.01	0.00	0.02	0.01	0.03	0.16	0.02	0.00	0.00
	P	0.38	0.02	0.12	0.25	0.18	0.19	0.06	0.00	0.00
	S	0.12	10.22	8.63	5.07	0.05	0.09	0.12	0.00	0.00
	Cl	0.04	0.73	0.52	0.52	0.02	0.02	0.05	0.00	0.00
LA-ICP-MS Data										
	Mg	253	5 650	982	567	2 038	5 018	3 032	0	2 275
	Al	888	269 750	32 741	8 693	0	0	0	492	0
	Si	137 201	n/a	38 973	40 671	0	0	0	0	n.d.
	Ca	308 633	190 000	207 573	211 400	0	0	0	0	1
	Cr	191	872	739	112	439	43	48	126	131
	Mn	9	46	6	4	56	16	37	23	n.d.
	Fe	435	6 820	755	526	2 533	2 147	3 400	2 214	4 403
	Co	1	21	1	0	4	7	n.d.	9	19
	Cu	12	542	8	10	73	17	19	17	130
	Zn	250	207	327	99	59	36	300	55	368
	Sr	165	2 352	459	181	941	1 836	1 103	32	4 420
	Ba	8	799	10	3	40	76	205	17	371
	Pb	2	51	7	1	18	21	2 407	428	80
	Th	1	2	0	0	1	1	11	n.d.	1
	U	19	51	3	1	10	1	8	26	15

n.d. = not detected.
* = Electron Microprobe Analysis.
** = Laser Ablation – Inductively Coupled Plasma – Mass Spectrometry.

Table L-20. Fracture minerals acting as sinks for various trace elements (Ref. B, Phase II).

	Element										
Sinks	**Ba**	**Sr**	**Fe**	**Cr**	**Cu**	**Zn**	**Mn**	**Co**	**Pb**	**Th**	**U**
Jennite											●
Zeolite	●	●	●	●	●		●	●	(●)	?	●
("Wairakite" Ettringite											
Thaumasite)				●		●					
Calcite		(●)					●				
Aragonite		●									
Hydrated CSH	●	(●)				●	●		●		(●)
Brucite									(●)		●
Portlandite	●	●			(●)	●	●	●	(●)		(●)

Indication in parenthesis () shown to identify subordinate role as a sink for trace elements.

Table L-21. The mineralogy of the Silicified Limestone Unit, Amman Formation (B_2). (Ref. C).

Mineral phase	**Formula**	**Modal anal.**
Quartz	SiO_2	Major
Calcite	$CaCO_3$	Dominant
Dolomite	$CaMg(CO_3)_2$	Major
Apatite	$Ca_5(PO_4)_3F$	Major
Ankerite	$Ca(FeMg)(CO_3)_2$	Trace

Geochemistry	See Table L-22

Table L-22. Chemistry of the Silicified Limestone Unit, Amman Formation (B_2) (Ref. C).

Constituents	34	35	35*
Weight %			
SiO_2			
CaO	0.23	54.72	–
MgO	2.54	1.83	–
Al_2O_3	0.02	0.65	–
Fe_2O_3	0.00	0.09	–
Na_2O	0.34	0.71	–
K_2O	0.07	0.16	–
P_2O_5	–	5.43	–
SO_3	–	2.15	–
$CaCO_3$	–	81.30	–
ppm			
Cd	–	7	14
Co	–	34	5
Cr	–	128	142
Cu	–	26	155
Mn	–	6	0
Ni	–	74	279
Pb	–	76	41
Zn	–	496	185.7

34 = Chert.
35 = Fossiliferous marl.
* = Acid treated.

Table L-23. Expected primary altered Bituminous Marl minerals (Ref. C).

Mineral	General formula	Association
Periclase	MgO	dolomite
Spinel-hercynite	$(Mg, Fe)Al_2O_4$	melilite, larnite
Majnesioferrite	$MgFe_2O_4$	larnite, melilite, magnesioferrite
Magnetite	Fe_3O_4	andradite, pervoskite, hematite
Titanomegnetite	Fe_2TiO_4	larnite, melilite
Hematite	Fe_2O_3	larnite, calcite
Pervoskite	$CaTiO_3$	gehlenite-larnite
Mayenite	$Ca_{12}Al_{14}O_{33}$	spurrite-larnite
Calcium dialuminate	$CaAl_4O_7$	brownmillerite and mayenite
Monticellite	$CaMgSiO_4$	spurrte-calcite
Merwinite	$B\text{-}Ca_3Mg(SiO_4)_2$	larnite, spinel andradite
Bredigite	$\propto\text{-}Ca_2SiO_4$	rankinite, melilite, pervoskite, andradite
Nagelschmidtite	$\propto\text{-}Ca_2(SiO_4)Ca_{1.5}(PO_4)$	rankinite gehlenite, pervoskite
Grossular	$Ca_3Al_2(SiO_4)_3$	anorthite, diopside
Andradite	$Ca_3(Fe,Ti)_2(SiO_4)_2$	melilite
Tricalcuim silicate	$Ca_3\ O/SiO_4$	larnite, brownmillerite meyenite
Rankinite	$Ca_3Si_2O_7$	larnite, nagelschmidtite, gehlenite, pseudowollastonite
Kilchoanite	$Ca_3(Si_2O_7)$	melilite-rankinite, cuspidine and wollastonite
Gehlenite	$Ca_2Al(Si, Al)_2O_7$	rankinite, pseudowollastonite
Akermanite	$Ca_2MgSi_2O_7$	larnite, gehlenite, merwinite, spinel
Cuspidine	$Ca_4(F, OH)_2Si_2O_7$	gehlenite, nagelschmidtite
Vesuvianite	$Ca_{10}(Mg>Fe_2)Al_4(OH)_4(SiO_4)_5Si_2O_7$	anorthite, hedenbergite
Fassaite	$Ca(Mg, Fe^{3+}, Al)(SiAl)_2O_6$	anorthite wollastonite gehlenite
Aegirine-augite	$(Na, Ca)(Fe^{3+}Fe^{2+}, Mg, Al)Si_2O_6$	hornfels
Pseudowollastonite	$\propto\text{-}CaSiO_3$	rankinite, gehlenite. larnite
Xanthophyllite	$Ca(Mg, Al)_3Al_2Si_2O_{10}(OH)_2$	vesuvianite, garnet, spinel, melilite, rankinite

Table L-24. Expected secondary minerals in the altered Bituminous Marl (Ref. C).

Mineral	General formula	Association
Native sulphur	S	gypsum
Greigite	Fe_3S_4	organic matter, chlorite
Halite	NaCl	efflorescent, filling cavities
Pyrolusite	MnO_2	marls
Bayerite	∝-$Al(OH)_3$	calcite, gypsum, tobermorite lizardite (cavity fillings)
Boehmite	ΛlOOH	gibbsite
Goethite	∝-FeO-OH	Fe-gehlenite
Dicalcium aluminate hydrate	$Ca_2Al_2O_5 \cdot nH_2O$	portlandite
Tetracalcium aluminate hydrate	$Ca_4Al_2O_7 \cdot nH_2O$	DΛH, calcite, aragonite, vaterite, ettringite, portlandite
Hydrocalumite	$Ca_{16}Al_{18}(OH)_{54} \cdot CO_3 \cdot 21H_2O$	in cavities
Chromium oxide hydrate	$Cr_2O_3 \cdot nH_2O$	gypsum and zeolites
Siderite	$FeCO_3$	lizardite
Veatchite	$Sr_3B_{16}O_{27} \cdot 5H_2O$	tobermorite
Hydromagnesite	$Mg_5[OH(CO_3)_2]_2 \cdot 4H_2O$	weathering crust of melilite
Calcium aluminate tricarbonate hydrate	$3CaO \cdot Al_2O_3 3 \cdot CaCO_3 \cdot 32H_2O$	ettringite
Chromatite	$CaCrO_4$	calcite, aragonite portlandite, gypsum
Meta-autunite	$Ca[(UO_2)(PO_4)]_2 \cdot 2\text{-}6H_2O$	efflorescence
Meta-tyuyamunite	$Ca[(UO_2)(PO_4)]_2 3\text{-}5H_2O$	efflorescence
Hydrogarnet	$Ca_3Al_2(OH)_{12}\text{-}Ca_3Al_2(SiO_4)_3$	zeolitic-calcitic marl
Bultfonteinite	$Ca_2[F/SiO_3 \cdot OH] \cdot H_2O$	tobermorite, afwillite
Pumpellyite	$Ca_2(Mg, Fe, Mn, Al)(Al, Fe, Ti)_2 (OH,H_2O)_2 SiO_4Si_2O_7$?	calcite, ettringite
Prehnite	$Ca_2Al_2(OH)_2Si_3O_{10}$	zeolites
Okenite	$CaH_2(Si_2O_6) \cdot H_2O$	Ca-silicates
Xonotlite	$Ca_6(OH)_2Si_6O_{17}$	jennite, tobermorite, truscottite
Foshagite	$Ca_4(OH)_2Si_3O_9$	cavities
Hillebrandite	$Ca_2(SiO_4) \cdot H_2O$	tobermorite
Plombierite	$Ca_5H_2(Si_3O_9)_2\ 6H_2O$	ettringite, gypsum
Tobermorites	$Ca_5H_2(Si_3O_9)_2 \cdot 2\text{-}4H_2O$	ettringite, (11.3–11.7 Å, 10Å, 9.3Å)
Gyrolite	$Ca_2(Si_4O_{10})4H_2O$	truscottite, afwillite, tobermorite, ettringite
Truscottite	$Ca_2Si_4O_{10} \cdot H_2O$	Ca-silicates
Dicalcium silicate-hydrate	∝-$Ca_2(HSiO_4)OH$	cavity filling
Pyrophyllite	$Al_2Si_4O_{10}(OH)_2$	voids
Chlorite	$(Fe, Mg, Al)_6(SiAl)_4O_{10}(OH)_8$	zeolites

Table L-24 (contd.). Expected secondary minerals in the altered Bituminous Marl (Ref. C).

Mineral	General formula	Association
Illite	$K_{0.5-0.75}$ (Al, Fe, Mg)$_2$(SiAl)$_4$O$_{10}$(OH)$_2$	marl
Montmorillonite	K0.3 (Al$_{1.7}$Mg$_{0.3}$Si$_4$O$_{10}$(OH)$_2$ · nH$_2$O	marl
Saponite	X$_{0.3}$ Mg$_3$(Al$_{0.3}$Si$_{3.7}$)O$_{10}$(OH)$_2$	marl
Nontronite	K$_{0.3}$(Fe, Al)$_2$(FeSi)$_4$O$_{10}$(OH)$_2$	marl
Volkonskoite	1.06^{M+}(Si$_{7.39}$Al$_{0.61}$) (Cr$_{2-20}$Mg$_{2.52}$O$_{20}$(OH)$_4$	marl
Sepiolite	Mg$_4$Si$_6$O$_{15}$(OH)$_2$ · 6H$_2$O	marl
Lizardite	Mg$_6$Si$_4$O$_{10}$(OH)$_8$	dolomite
Poorly crystalline serpentine	Mg$_6$Si$_4$O$_{10}$(OH)$_8$	dolomite
Al-serpentine	(Si$_{4-x}$Al$_x$)(Mg$_{6-x}$Al$_x$)O$_{10}$(OH)$_8$	altered marble
Allophane	nAl$_2$O$_3$ · mSiO$_2$ · nH$_2$O	clays
Analcite	NaAlSi$_2$O$_6$ · H$_2$O	cristobalite, thomsonite and phillipsite
Scolecite	CaAl$_2$Si$_3$O$_{10}$ · 3H$_2$O	phillipsite and thomsonite
Mesolite	Na$_2$Ca$_2$(Al$_2$Si$_3$O$_{10}$)$_3$ · 8H$_2$O	thomsonite
Thomsonite	NaCa$_2$[Al$_2$(AlSi)Si$_2$O$_{10}$]$_2$ · 6H$_2$O	phillipsite
Heulandite	CaAl$_2$Si$_7$O$_{18}$ · 6H$_2$O	thomsonite
Epistilbite	CaAl$_2$Si$_6$O$_{16}$ · 5H$_2$O	apophyllite
Gismondite	CaAl$_2$Si$_2$O$_8$ · 4H$_2$O	phillipsite, thomsonite
Phillipsite	KCa(Al$_3$Si$_5$O$_{16}$) · 6H$_2$O	thomsonite
Harmotome	BaAl$_2$Si$_6$O$_{16}$ · 6H$_2$O	barite
Chalsuzite	(Ca, Na$_2$) Al$_2$Si$_4$O$_{12}$ · 6H$_2$O	phillipsite, thomsonite
Levyne	CaAl$_2$Si$_4$O$_{12}$ · 6H$_2$O	gismondite
Gmelinte	(Na$_2$Ca)(Al$_2$Si$_4$O$_{12}$) · 6H$_2$O	gypsum, calcite

Table L-25. Uranium/thorium series isotope determinations (Ref. B, Phase I).

(a) Analysis by ANSTO[1]

Sample code	M28P	M3P	M15P	A6.7P
Rock type	**Highly altered Bit. Marl (leached)**	**Altered bit. Marl (leached)**	**Largely altered Bit. Marl**	**Unaltered Bit. Marl**
Isotope (Bq/kg)				
^{238}U	31.08 ± 1.00	310.7 ± 9.0	504.7 ± 13.7	483.5 ± 12.7
^{234}U	31.43 ± 1.02	304.7 ± 9.0	460.5 ± 12.5	454.3 ± 12.0
^{232}Th	5.095 ± 0.683	4.155 ± 0.677	6.338 ± 0.985	6.400 ± 0.683
^{230}Th	137.4 ± 5.3	230.2 ± 7.8	462.3 ± 16.5	456.0 ± 11.2
^{228}Th	32.33 ± 2.35	6.458 ± 0.937	4.157 ± 0.877	5.278 ± 0.700
^{226}Ra	164.9 ± 0.184	270.8 ± 4.5	428.5 ± 7.7	434.8 ± 7.83
$^{234}U/^{238}U$	1.01	0.98	0.91	0.94
$^{230}Th/^{234}U$	4.37	0.76	1.00	1.00
$^{226}Ra/^{230}Th$	1.20	1.18	0.93	0.95
$^{228}Th/^{232}Th$	6.35	1.55	0.66	0.82

[1](Australian Nuclear Science and Technology Organisation.

Table L-25 (contd.). Uranium/thorium series isotope determinations (Ref. B, Phase 1).

(b) Analysis by SURRC[2]

Sample code	M28P	M3P	M15P	A6.7P	MQ2.1P	MQ6.2P
Rock type	**Highly altered Bit. Marl (leached)**	**Altered Bit. Marl (leached)**	**Largely altered Bit. Marl**	**Unaltered Bit. Marl**	**Travertine precipitate**	**Travertine precipitate**
Isotope (Bq/kg)						
^{238}U	51/50.6*	44/305.9*	2052/204.8*	83/82.7*	47	24/56.6*
^{226}Ra	176/-	298/-	521/-	231/-	122	66/-
$^{234}U/^{238}U$	1.03/1.03*	0.91/1.04*	0.91/0.91*	0.97/0.97*	1.16	1.20/1.16*
$^{230}Th/^{234}U$	-/3.73	-/0.87	2.9	-/3.77	-/1.52	–
$^{226}Ra/^{230}Th$	-/0.90	-/1.07	0.10	-/0.76	-/1.30	–
$^{210}Pb/^{226}Ra$	0.82/1.03*	0.08/0.82*	0.90	1.40/1.37*	0.82	1.30/1.33*

[2](Scottish Universities Reactor Research Centre.

* indicates duplicate analyses.

Table L-26. Uranium, thorium and radium radiometric isotope determinations for fracture mineralisation and altered wallrock in bituminous clay biomicrites from Adit A-6 (Ref. B, Phase II).

(a) RADIONUCLIDE CONCENTRATIONS (Bq/kg)

Sample	Description	^{238}U	^{234}U	^{230}Th	^{226}Ra	^{232}Th
A960CD1	Pre-hyperalkaline groundwater interaction calcite vein fill (diagenetic)	26.1 ± 0.8	30.9 ± 0.9	29.0 ± 1.4	25 ± 3	3.4 ± 0.4
A960CD2	Zeolitic alteration- and ettringite-thaumasite-CSH wallrock alteration	381 ± 10	520 ± 12	410 ± 10	429 ± 20	23.8 ± 1.4
A962CD1	Pure tobermorite vein-fill (monomineralic)	78 ± 2	144 ± 3	82 ± 3	699 ± 50	10.5 ± 0.7
A962CD2	Wallrock 3 cm distant from tobermorite vein contains minor ettringite-filled cracks	254 ± 4	242 ± 4	290 ± 8	196 ± 10	39.9 ± 2.1
A962CD3	Wallrock immediately adjacent to tobermorite vein (0–1 cm)	280 ± 4	268 ± 4	287 ± 6	240 ± 17	12.2 ± 0.8
A965CD1	Jennite vein-fill with minor ettringite-thaumasite	280 ± 5	570 ± 9	303 ± 8	207 ± 14	18.1 ± 1.1
A965CD2	Wallrock adjacent to jennite vein fill. Contains ettringite veinlets	146 ± 3	149 ± 3	148 ± 3	150 ± 10	8.7 ± 0.5

(b) ACTIVITY RATIOS

Sample	$^{234}U/^{238}U$	$^{230}Th/^{234}U$	$^{226}Ra/^{230}Th$
A960CD1	1.18 ± 0.05	0.94 ± 0.05	0.86 ± 0.11
A960CD2	1.36 ± 0.05	0.79 ± 0.03	1.05 ± 0.05
A962CD1	1.84 ± 0.06	0.57 ± 0.02	8.50 ± 0.70
A962CD2	0.95 ± 0.02	1.20 ± 0.04	0.67 ± 0.04
A962CD3	0.95 ± 0.02	1.07 ± 0.03	0.84 ± 0.06
A965CD1	2.04 ± 0.05	0.53 ± 0.02	0.68 ± 0.05
A965CD2	1.02 ± 0.03	0.99 ± 0.03	1.01 ± 0.07

Table L-27. Stable isotopes for carbonate samples (Reference B, Phase I).

		^{18}O (PDB ‰)	^{13}C (PDB ‰)
Precipitates from hyperalkaline waters			
MQ-1.1P	Pool sediment	-20.02	-22.92
MQ-1.2P	Pool rim	-20.60	-23.29
MQ-2.1P	Drip straws	-21.62	-25.37
MQ-4P	Crust by He sample	-21.40	-25.73
MQ-5P	Vent at river	-05.15	-11.05
MQ-5/6.1P	Seepage crust	-11.00	-21.92
MQ-5/6.2P	Seepage crust	-12.63	-22.23
MQ-5/6.4P	Colluvium matrix	-11.76	-17.30
MQ-6.1P	Vent crust	-04.46	-11.26
A6-2 (89)	Stalactite	-20.87	-30.75
A6-12 (89)	White wall crust	-21.08	-23.54
RS-3 (i)	Railway cut stalagmite/tites	-16.86	-30.08
RS-3 (iii)	– " –	-18.32	-28.32
RS-3 (vi)	– " –	-18.77	-29.48
RS-3 (viii)	– " –	-18.48	-29.82
RS-3 (ix)	– " –	-18.24	-29.04
Spontaneous combustion Cement Zone samples			
MQ-10.2Pa	Bituminous	-4.23	-0.37
MQ-10.2Pb	Light, non-bit., fractured	-4.81	-0.54
MQ-10.2Pc	Friable altered lmst. ext.	-7.31	-2.35
MQ-10.3Pa	Darker, free lmst. bit.	-6.80	-0.83
MQ-10.3Pb	Lighter rim of altered lmst.	-8.67	-1.80
MQ-10.3Pc	Friable coating, altered lmst.	-9.53	-3.63
MQ-10.4P	Buff, highly altered lmst. soft	-7.47	-3.59
MQ-10.5Pa	Darker, free lmst. bit.	-5.33	-0.33
MQ-10.5Pb	Lighter rim of altered lmst.	-6.22	-2.16
MQ-10.5Pc	Friable coating, altered lmst.	-7.77	-4.95
MQ-10.7P	Unaltered bitum. lmst., free bit.	-4.82	0.72
Host altered limestone from road cut			
MQ-11.1	Altered lmst. (white)	-5.05	-1.33
MQ-11.2	Altered lmst. (red)	-5.40	-1.48

Table L-27 (contd.). Stable isotopes for carbonate samples (Ref. B, Phase I).

		^{18}O (PDB ‰)	^{13}C (PDB ‰)
Adit A-6 wall sample			
A6.1Pa	230 m secondary crust on fracture	-17.60	-29.17
A6.1Pb	230 m altered lmst. (buff)	-06.71	-03.23
A6.2P	210 m bit. lmst.	-04.41	-03.26
A6.3Pa	180 m fracture cal., micro-cx	-14.74	-24.74
A6.3Pb	180 m fracture cal., crs-cx	-14.95	-24.40
A6.3Pc	180 m altered lmst.	-16.04	-19.67
A6.4Pa	175 m open fracture surface	-16.97	-22.61
A6.4Pc	175 m altered lmst.	-14.33	-25.82
A6.5P	160 m altered lmst.	-14.99	-19.16
A6.6P	120 m altered lmst.	-14.09	-20.74
A6.8Pa	2 m laminated white calcite	-15.37	-28.75
A6.8Pb	2 m altered host lmst.	-05.60	-01.96
A6-3A (89)	2 m unaltered bit. lmst.	-05.36	-00.92
KZ-10a	Host red marble	-12.17	-15.52
KZ-10b	Pale red, along fracture	-12.55	-15.23
KZ-10c	White fracture surface coating	-01.10	-19.94
KZ-11a	Host maroon marble	-09.24	-17.30
KZ-11b	Buff dusting on 11a	-06.06	-09.89
KZ-11c	Laminated, crs-cx (recx?)	-09.00	-11.69
KZ-11d	Powdery lams of cal.	-07.79	-14.80
KZ-12a	Red marble clast in white	-10.43	-17.11
KZ-12b	Green clast/mottle	-10.43	-15.74
KZ-12c	White calcite vug lining	-08.00	-09.81
KZ-13a	Dark buff/grey host lmst.	-10.07	-14.47
KZ-13b	White crpt cx cal. fract. lining	-06.75	-05.19
KZ-13c	Crs cx cal. in middle of fract.	-09.88	-07.04
Cement zone with low temperature mineralisation			
M1	–	-11.4895	-24.51
M2	Calcite, qtz, thaumasite	-08.07485	-18.22
M3	–	-14.1668	-15.44
M4	Calcite, thaumasite	-11.0917	-14.58
M5	Calcite, thaumasite, tobermorite, wollastonite	-14.4966	-16.21
M6	Calcite, thaumasite, apatite, wollastonite	-13.0319	-15.36
M7	Calcite, thaumasite, apatite	-09.11281	-17.59
M8	Thaumasite, calcite, apatite	-12.4692	-19.39
M8a	Thaumasite, calcite, apatite	-10.9559	-17.85
M9	– " –	-11.1693	-15.37
M10	– " –	-10.6649	-19.22

Table L-27 (contd.). Stable isotopes for carbonate samples (Ref. B, Phase I).

		^{18}O (PDB ‰)	^{13}C (PDB ‰)
M11	Calcite, spurrite, apatite?	-14.5937	-19.11
M12	Calcite thaumasite, portlandite, apatite	-13.6430	-16.89
M14	No carbonate	–	–
M15	–	-13.2647	-14.00
M24	Calcite, apatite, spurrite	-14.8459	-18.94
M26	Calcite, portlandite, apatite	-14.0892	-18.31

Note: lmst. = limestone.
bit. = bituminous.
cal. = calcite.
cx. = crystalline.
recx. = recrystalline.

APPENDIX M

Hydrogeochemical Modelling: Groundwater Chemical Data Set

(Compiled by H.N. Waber)

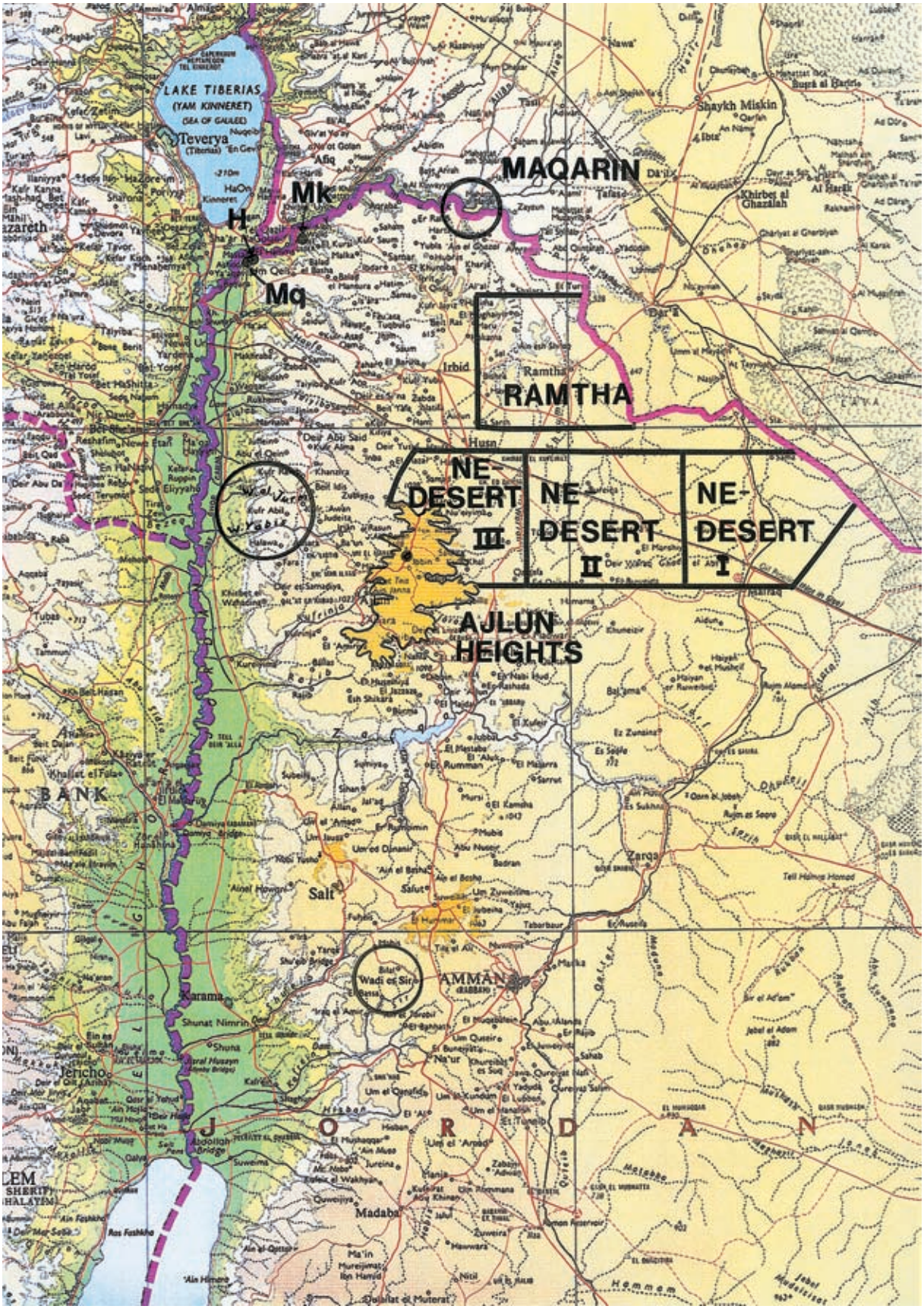

Figure M-1. *Regional topographic setting of the Maqarin Project area. Marked are key regions and some place names referred to in the text (H = El Hamma; Mq = Maqla; Mk = Mukheiba).*

(© Bartholomew 1995. Reproduced with kind permission).

Table M-1. Average chemical composition of groundwater from the Kurnub-Aquifer (data from E. Salameh, pers. comm. 1996; El-Nasser, 1991).

		El-Hamma Spring			S-90 borehole		
		Average	*Stdev*	*n*	*Average*	*Stdev*	*n*
pH		6.38	0.06	3	6.3	0	2
Eh (mV)		–	–		–	–	
T (°C)		27.7	1.2	3	20.0	0.0	2
Cond (µS/cm)		3273.3	136.5	3	3750.0	70.7	2
TDS (calc.)	mg/L	2214.7	61.2	3	2962.1	14.3	2
Na	mg/L	369.9	28.5	3	302.3	1.6	2
K	mg/L	48.5	5.0	3	150.5	2.8	2
Mg	mg/L	52.2	3.3	3	44.4	0.9	2
Ca	mg/L	292.6	28.1	3	526.5	5.7	2
F	mg/L	1.1	0.1	3	–	–	
Cl	mg/L	495.4	2.9	3	166.6	5.0	2
Br	mg/L	5.8	0.3	3	–	–	
I	mg/L	0.1	0.0	3	–	–	
SO_4	mg/L	683.6	29.2	3	1385.7	10.2	2
NO_3	mg/L	0.8	0.0	3	2.1	0.2	2
HCO_3	mg/L	517.3	21.0	3	781.1	17.3	2
SiO_2	mg/L	19.5	0.9	3	–	–	

El-Nasser, H., 1991. Groundwater resources of the deep aquifer systems in NW-Jordan: Hydrology and hydrochemical quasi 3-dimensional modelling. Ph.D. Thesis, University of Würzburg, Germany.

Table M-2. Average saturation state of Kurnub groundwater for measured values and recalculated for calcite equilibrium.

		El-Hamma Spring			S-90 Borehole		
		Average n=3	*Stdev*	*n*	*Average* n=2	*Stdev*	*n*
Measured:							
pH		6.38	0.06	3	6.30	0.06	2
Total C	mol/L	1.46E-02	6.45E-04	3	2.48E-02	5.64E-03	2
Calcite	SI	-0.17	0.10	3	-0.01	0.11	2
log pCO_2	bar	-0.72	0.04	3	-0.51	0.12	2
Adjusted for calcite equilibrium:							
pH		6.55	0.06	3	6.31	0.06	2
Ionic strength		4.46E-02	1.23E-03	3	5.79E-02	1.23E-03	2
Total C	mol/L	1.27E-02	1.01E-03	3	2.45E-02	1.01E-03	2
log pCO_2	bar	-0.88	0.08	3	-0.53	0.08	2
Calcite	SI	0.00	0.00	3	0.00	0.00	2
Dolomite disord.	SI	-0.91	0.02	3	-1.36	0.02	2
Dolomite ord.	SI	-0.38	0.02	3	-0.79	0.02	2
Fluorite	SI	-0.66	0.07	2	–	–	
Gypsum	SI	-0.60	0.05	3	-0.15	0.05	2
Portlandite	SI	-12.07	0.07	3	-12.95	0.07	2
Chalcedony	SI	-1.11	1.97	2	–	–	
Quartz	SI	-0.68	1.96	2	–	–	
Magnesite	SI	-0.95	0.02	3	-1.36	0.02	2

SI = Saturation Index.

Table M-3. Average chemical composition of groundwater from the Wadi es Sir Formation (A_7-Aquifer) in the NE-Desert area and the Side Wadi area (data from E. Salameh, pers. com. 1996)

		Recharge NE Desert I			Discharge Side Wadis		
		Average	*Stdev*	*n*	*Average*	*Stdev*	*n*
pH		7.86	0.18	5	7.53	0.35	8
Eh (mV)		–	–		–	–	
T (°C)		20	0	5	20	0	8
Cond (µS/cm)		834.0	76.4	5	522.5	52.3	8
TDS (calc.)	mg/L	455.2	44.0	5	289.0	27.5	8
Na	mg/L	104.8	16.6	5	13.2	2.7	8
K	mg/L	7.0	3.3	5	3.9	0.0	8
Mg	mg/L	22.9	0.5	5	19.3	2.7	8
Ca	mg/L	29.6	2.6	5	65.1	7.1	8
Cl	mg/L	133.3	26.2	5	24.4	4.4	8
SO_4	mg/L	54.8	5.5	5	11.7	10.7	7
NO_3	mg/L	10.4	0.5	5	25.4	2.5	8
HCO_3	mg/L	187.9	8.0	5	259.3	19.6	8
^{18}O	‰	-6.28	0.15	5	-6.03	0.34	8
^{2}H	‰	-30.36	0.77	5	-26.23	4.28	8
^{3}H	TU	0.8	0.6	5	5.4	2.2	8

Table M-4. Average saturation state of the Wadi es Sir Formation (A_7-Aquifer) groundwater for measured values and recalculated for calcite equilibrium.

		NE Desert			Side Wadis		
		Average	*Stdev*	*n*	*Average*	*Stdev*	*n*
Measured:							
pH		7.86	0.18	5	7.53	0.35	8
Total C	mol/L	3.15E-03	1.71E-04	5	4.64E-03	6.19E-04	8
Calcite	SI	0.03	0.16	5	0.20	0.36	8
log pCO_2	bar	-2.64	0.20	5	-2.16	0.36	8
Adjusted for calcite equilibrium:							
pH		7.83	0.05	5	7.32	0.07	8
Ionic strength		1.03E-02	7.45E-04	5	8.51E-03	7.75E-04	8
Total C	mol/L	3.16E-03	1.44E-04	5	4.69E-03	4.21E-04	8
log pCO_2	bar	-2.61	0.07	5	-1.95	0.10	8
Calcite	SI	0.00	0.00	5	0.00	0.00	8
Dolomite disord.	SI	-0.39	0.05	5	-0.81	0.07	8
Dolomite ord.	SI	0.18	0.05	5	-0.24	0.07	8
Gypsum	SI	-2.24	0.06	5	-2.69	0.35	8
Portlandite	SI	-10.87	0.07	5	-11.52	0.10	8
Magnesite	SI	-0.40	0.05	5	-0.82	0.07	8

SI = Saturation Index.

Table M-5. Average chemical composition of groundwater from the Wadi es Sir – Amman Formation (A_7/B_2-Aquifer) in the NE-Desert area (data from E. Salameh, pers. comm. 1996; Bajjali, 1994).

Average		NE Desert I			NE Desert II			NE Desert III		
		Average	*Stdev*	*n*	*Average*	*Stdev*	*n*	*Average*	*Stdev*	*n*
pH		7.96	0.13	8	7.40	0.26	8	7.44	0.13	9
Eh (mV)		–	–		–	–		–	–	
T (°C)		20.0	0.0	8	20	0	8	20	0	9
Cond (µS/cm)		852.5	90.7	8	887.5	71.5	8	604.4	46.4	9
TDS (calc.)	mg/L	458.7	48.5	8	459.2	45.0	8	317.3	28.3	9
Na	mg/L	104.3	8.4	8	77.8	16.3	7	19.9	2.3	9
K	mg/L	6.4	2.0	8	5.6	2.1	7	2.8	1.0	9
Mg	mg/L	26.3	5.3	8	28.0	3.8	8	23.4	2.2	9
Ca	mg/L	24.0	2.6	8	60.8	5.8	8	69.2	5.9	9
Cl	mg/L	141.4	27.6	8	115.7	16.8	8	38.6	5.7	9
SO_4	mg/L	60.0	9.3	8	33.6	10.3	8	9.1	6.0	9
NO_3	mg/L	16.8	3.5	8	0.7	0.9	8	19.2	7.4	9
HCO_3	mg/L	161.7	12.6	8	299.8	14.4	8	274.5	10.6	9
^{18}O	‰	-6.01	0.14	8	-5.95	0.45	6	-6.38	0.45	9
^{2}H	‰	-30.09	1.63	8	-32.67	1.81	6	-29.56	1.08	9
^{3}H	TU	0.4	1.0	8	0.0	0.1	8	6.6	1.4	8
^{13}C	‰	–	–		-9.1	–	1	-11.10	0.28	2
^{14}C	pmc	–	–		3.3	–	1	61.4	2.5	2

Bajjali, W.T., 1994. Recharge and regional circulation of thermal groundwater in northern Jordan using isotope geochemistry. Ph.D. Thesis, University of Ottawa, Canada.

Table M-6. Average saturation state of the NE-Desert groundwater (A_7/B_2-Aquifer) for measured values and recalculated for calcite equilibrium.

Average		NE Desert I			NE Desert II			NE Desert III		
		Average	*Stdev*	*n*	*Average*	*Stdev*	*n*	*Average*	*Stdev*	*n*
Measured:										
pH		7.96	0.13	8	7.40	0.26	8	7.44	0.13	9
Total C	mol/L	2.69E-03	2.09E-04	8	5.36E-03	3.29E-04	8	4.84E-03	2.26E-04	9
Calcite	SI	-0.03	0.11	8	0.08	0.24	8	0.18	0.13	9
log pCO_2	bar	-2.81	0.13	8	-1.98	0.26	8	-2.05	0.14	9
Adjusted to calcite equilibrium:										
pH		7.99	0.05	8	7.32	0.04	8	7.26	0.05	9
Ionic strength		1.05E-02	1.16E-03	8	1.13E-02	8.46E-04	8	9.25E-03	8.53E-04	9
Total C	mol/L	2.68E-03	2.14E-04	8	5.41E-03	2.69E-04	8	5.01E-03	2.38E-04	9
log pCO_2	bar	-2.84	0.08	8	-1.89	0.05	8	-1.87	0.07	9
Calcite	SI	0.00	0.00	8	0.00	0.00	8	0.00	0.00	
Dolomite (disordered)	SI	-0.25	0.07	8	-0.62	0.09	8	-0.74	0.05	9
Dolomite (ordered)	SI	0.32	0.08	8	-0.05	0.09	8	-0.17	0.04	9
Gypsum	SI	-2.30	0.08	8	-2.19	0.13	8	-2.76	0.35	9
Portlandite	SI	-10.64	0.07	8	-11.58	0.05	8	-11.57	0.10	9
Magnesite	SI	-0.25	0.08	8	-0.63	0.09	8	-0.75	0.04	9

SI = Saturation Index.

Table M-7. Average chemical composition of groundwater from the Amman Formation (B_2-Aquifer) in the Ramtha area (data from E. Salameh, pers. comm. 1996; Bajjali, 1994).

		Ramtha B_2		
		Average	*Stdev*	*n*
pH		7.26	0.30	14
Eh (mV)		–	–	
T (°C)		20.0	0.0	14
Cond (µS/cm)		1003.6	218.6	14
TDS (calc.)	mg/L	561.2	147.3	14
Na	mg/L	73.6	14.3	14
K	mg/L	3.9	0.0	11
Mg	mg/L	38.6	8.5	14
Ca	mg/L	81.5	28.4	14
Cl	mg/L	119.0	25.6	14
SO_4	mg/L	77.2	53.5	14
NO_3	mg/L	1.5	1.0	14
HCO_3	mg/L	336.0	80.5	14
SiO_2	mg/L	21.40	–	1
^{18}O	‰	-5.84	0.74	14
^{2}H	‰	-30.5	3.9	13
^{3}H	TU	0.3	0.5	10
^{13}C	‰	-10.9	0.8	2
^{14}C	pmc	5.1	3.8	4

Bajjali, 1994. See Table M-5 for reference.

Table M-8. Average saturation state of the Amman Formation (B_2-Aquifer) groundwaters in the Ramtha area for measured values and recalculated for calcite equilibrium.

		Ramtha B_2		
		Average	*Stdev*	*n*
Measured:				
pH		7.26	0.30	14
Total C	mol/L	6.36E-03	2.05E-03	14
Calcite	SI	0.06	0.18	14
log pCO_2	bar	-1.81	0.38	14
Adjusted for calcite equilibrium:				
pH		7.21	0.22	14
Ionic strength		1.40E-02	3.56E-03	14
Total C	mol/L	6.38E-03	1.92E-03	14
log pCO_2	bar	-1.75	0.31	14
Calcite	SI	0.00	0.00	14
Dolomite disord.	SI	-0.59	0.07	14
Dolomite ord.	SI	-0.02	0.07	14
Gypsum	SI	-1.86	0.37	14
Portlandite	SI	-11.73	0.31	14
Chalcedony	SI	0.16	–	1
Quartz	SI	0.61	–	1
Magnesite	SI	-0.60	0.07	14

SI = Saturation Index.

Table M-9. Average chemical composition of groundwater from the Wadi es Sir – Amman Formation (A_7/B_2 Aquifer) in the Side Wadi area (data from E. Salameh, pers. comm. 1996; El-Nasser, 1991).

		Wadi Arab			Wadi Jurum, Wadi Yabis		
		Average	*Stdev*	*n*	*Average*	*Stdev*	*n*
pH		7.09	0.13	19	7.19	0.39	13
Eh (mV)		–	–		–	–	
T (°C)		20.0	0.0	19	20	0	13
Cond (µS/cm)		900.5	47.2	19	820.8	75.3	13
TDS (calc.)	mg/L	518.4	41.3	19	452.0	54.7	13
Na	mg/L	26.9	7.1	19	20.9	2.7	12
K	mg/L	3.9	0.0	19	4.3	1.2	12
Mg	mg/L	38.8	2.4	19	26.6	3.3	13
Ca	mg/L	111.0	4.6	19	113.2	18.6	13
Cl	mg/L	39.6	2.1	19	39.3	4.9	13
SO_4	mg/L	86.7	24.8	19	32.1	19.4	13
NO_3	mg/L	0.7	0.2	19	15.4	5.8	13
HCO_3	mg/L	430.4	8.5	19	411.7	36.9	13
^{18}O	‰	-5.23	0.33	17	-5.85	0.47	11
^{2}H	‰	-23.29	1.21	17	-27.01	1.87	11
^{3}H	TU	0.1	0.2	12	4.6	1.8	13
^{13}C	‰	-12.07	2.15	3	–	–	
^{14}C	pmc	11.5	0.5	3	–	–	

El-Nasser, 1991. See Table M-1 for reference.

Table M-10. Average saturation state of the Wadi es Sir – Amman Formation (A_7/B_2-Aquifer) groundwaters in the Side Wadis area (data from E. Salameh, per. comm. 1996; El-Nasser, 1991).

		Wadi Arab			NW Desert Area II		
		Average	*Stdev*	*n*	*Average*	*Stdev*	*n*
Measured:							
pH	7	7.09	0.13	19	7.19	0.39	13
Total C	mol/L	8.28E-03	4.14E-04	19	7.90E-03	1.14E-03	13
Calcite	SI	0.15	0.13	19	0.26	0.38	13
log pCO_2	bar	-1.52	0.14	19	-1.64	0.40	13
Adjusted for calcite equilibrium:							
pH		6.94	0.01	19	6.93	0.09	13
Ionic strength		1.40E-02	8.04E-04	19	1.28E-02	1.33E-03	13
Total C	mol/L	8.74E-03	2.15E-04	19	8.45E-03	1.07E-03	13
log pCO_2	bar	-1.36	0.02	19	-1.38	0.13	13
Calcite	SI	0.00	0.00	19	0.00	0.00	13
Dolomite disord.	SI	-0.74	0.03	19	-0.91	0.10	13
Dolomite ord.	SI	-0.17	0.03	19	-0.33	0.10	13
Gypsum	SI	-1.60	0.12	19	-2.04	0.29	13
Portlandite	SI	-12.11	0.02	19	-12.10	0.13	13
Magnesite	SI	-0.74	0.03	19	-0.91	0.10	13

SI = Saturation Index.

El-Nasser, 1991. See Table M-1 for reference.

Table M-11. Average chemical composition of groundwater from the Rijam (lower Calky Limestone) Formation (B_4-Aquifer) in the Ramtha area (data from E. Salameh, pers. comm. 1996) and the Project sample M4 from Adit A-7 at the Maqarin Eastern Springs site for comparison.

		Ramtha B_4			Project Sample
		Average	*Stdev*	*n*	*M4*
pH		7.51	0.28	9	7.44
Eh (mV)		–	–		275
T (°C)		20	0	9	20
Cond (µS/cm)		1244.4	265.1	9	650
TDS (calc)	mg/L	696.8	156.0	9	516.1
Li	mg/L				0.01
Na	mg/L	140.0	37.9	9	43.2
K	mg/L	6.5	4.4	9	12.1
Mg	mg/L	27	6	9	4.1
Ca	mg/L	73.6	21.5	9	78.2
Sr	mg/L	–	–		1.12
Mn	mg/L	–	–		0.008
Fe_{tot}	mg/L	–	–		0.25
NH_4	mg/L	–	–		0.39
Ba	mg/L	–	–		0.035
Zn	mg/L	–	–		0.022
Cu	mg/L	–	–		0.007
F	mg/L	–	–		0.96
Cl	mg/L	222.5	51.6	9	67
SO_4	mg/L	64.6	19.5	9	85.5
NO_3	mg/L	54.0	30.9	9	34.8
HCO_3	mg/L	221.0	42.3	9	129
Al	mg/L	–	–		0.03
As	mg/L	–	–		3.2
P	mg/L	–	–		0.013
SiO_2	mg/L	–	–		79.0
B	mg/L	–	–		0.572
O_2	mg/L	–	–		4
TOC	mg/L	–	–		42.2
^{18}O	‰	-4.6	0.8	9	-2.8
^{2}H	‰	-24.7	3.5	9	-10
^{3}H	TU	3.4	2.7	8	4.1

Table M-12: Average saturation state of groundwater from the Rijam (lower Chalky Limestone) Formation (B_4-Aquifer) in the Ramtha area (data from E. Salameh, pers. comm. 1996) and the Project sample M4 from Adit A-7 at the Maqarin Eastern Springs site for comparison.

		Ramtha B4			Project Sample
		Average	*Stdev*	*n*	*M4*
Measured:					
pH		7.51	0.28		7.44
Total C	mol/L	3.90E-03	8.87E-04		2.26E-03
Calcite	SI	0.07	0.14		-0.13
log pCO_2	bar	-2.24	0.36		-2.38
Adjusted to calcite equilibrium:					
pH		7.44	0.23	9	7.58
Ionic strength		1.66E-02	3.84E-03	9	9.79E-03
Total C	mol/L	3.93E-03	8.37E-04	9	2.14E-03
log pCO_2	bar	-2.16	0.31	9	-2.54
Calcite	SI	0.00	0.00	9	0.00
Dolomite disord.	SI	-0.70	0.09	9	-1.56
Dolomite ord.	SI	-0.13	0.09	9	-0.99
Fluorite	SI	–	–	–	-0.95
Gypsum	SI	-1.92	0.28	9	-1.63
Portlandite	SI	-11.31	0.31	9	-10.94
Chalcedony	SI	–	–	–	0.73
Quartz	SI	–	–	–	1.17
Barite	SI	–	–	–	-0.08
Celestite	SI	–	–	–	-1.77
Strontianite	SI	–	–	–	-1.36
Magnesite	SI	-0.71	0.09	9	-1.57
$Al(OH)_3$ am.	SI	–	–	–	-1.53
Gibbsite mc	SI	–	–	–	-0.06
Kaolinite	SI	–	–	–	5.56
$Fe(OH)_3$ am.	SI	–	–	–	4.40
Goethite	SI	–	–	–	8.40

Table M-13. Average chemical composition of groundwater from the Wadi Shallala (Chalky Limestone) Formation (B_5-Aquifer) from Wadi Shallala east of the Maqarin area (data from E. Salameh, pers. comm. 1996) and the Project sample M6 from Ain Quelba spring (Wadi Shallala) for comparison.

		Wadi Shallala $B_{4/5}$			Project Sample
		Average	*Stdev*	*n*	*M6*
pH		7.40	0.42	17	7.77
Eh (mV)		–	–		321
T (°C)		20	0	17	20
Cond (µS/cm		592.8	140.4	16	503
TDS (calc.)	mg/L	343.5	88.2	17	302.4
Na	mg/L	20.8	5.6	17	12.4
K	mg/L	3	5	17	3.6
Mg	mg/L	14.1	7.3	17	5.43
Ca	mg/L	87.708	19.475	17	75.3
Sr	mg/L	–	–		0.27
Mn	mg/L	0.001	0.001	4	–
Fe_{tot}	mg/L	0.013	0.007	2	–
Ba	mg/L	–	–		0.349
Zn	mg/L	0.040	0.037	5	–
Cu	mg/L	0.0	0.0	3	–
Ni	mg/L	0.0	0.0	5	–
F	mg/L	–	–		0.34
Cl	mg/L	35.0	12.0	17	20.9
SO_4	mg/L	24.8	16.8	17	9.8
NO_3	mg/L	19.0	7.6	15	25.2
HCO_3	mg/L	288.2	77.7	17	217
Al	mg/L	–	–		0.02
As	mg/L	–	–		0.7
P	mg/L	–	–		0.003
SiO_2	mg/L	–	–		36.98
O_2	mg/L	–	–		5
TOC	mg/L	–	–		4.38
^{18}O	‰	–	–		-4.5
^{2}H	‰	–	–		-21
^{3}H	TU	–	–		3.9
^{34}S	‰	–	–		9.6

Table M-14. Average saturation state of groundwater from the Wadi Shallala (Chalky Limestone) Formation (B_5-Aquifer; data from E. Salameh, pers. comm. 1996) and the Project sample M6 for comparison.

		Wadi Shallala $B_{4/5}$			Project Sample
		Average	*Stdev*	*n*	*M6*
Measured:					
pH		7.40	0.42	17	7.44
Total C	mol/L	5.29E-03	1.56E-03	17	2.26E-03
Calcite	SI	0.22	0.42	17	-0.13
log pCO_2	bar	-2.00	0.45	17	-2.38
Adjusted to calcite equilibrium:					
pH		7.18	0.18	9	7.32
Ionic strength		9.58E-03	2.28E-03	9	7.52E-03
Total C	mol/L	5.51E-03	1.82E-03	9	3.91E-03
log pCO_2	bar	-1.78	0.28	9	-2.02411
Calcite	SI	0.00	0.00	9	0.00
Dolomite disord.	SI	-1.13	0.18	9	-1.42
Dolomite ord.	SI	-0.55	0.18	9	-0.85
Fluorite	SI	–	–	–	-1.83
Gypsum	SI	-2.26	0.39	9	-2.54
Portlandite	SI	-11.70	0.28	9	-11.45
Chalcedony	SI	–	–	–	0.40
Quartz	SI	–	–	–	0.84
Barite	SI	–	–	–	0.06
Celestite	SI	–	–	–	-3.28
Strontianite	SI	–	–	–	-1.97
Magnesite	SI	-1.13	0.18	9	-1.43
$Al(OH)_3$ am.	SI	–	–	–	-1.44
Gibbsite mc	SI	–	–	–	0.03
Kaolinite	SI	–	–	–	5.08
$Fe(OH)_3$ am.	SI	2.98	0.29	–	–
Goethite	SI	6.98	0.29	–	–

SI = Saturation Index.

Table M-15. Average chemical composition of basaltic groundwater from the Jordanian-Syrian border region (B_a-Aquifer; data from E. Salameh, pers. comm. 1996).

		Basalt young waters			Basalt evolved waters		
		Average	*Stdev*	*n*	*Average*	*Stdev*	*n*
pH		7.50	0.47	4	7.5	0	2
Eh (mV)		–	–		–	–	
T (°C)		20.0	0.0	4	20	0	2
Cond (µS/cm)		322.8	113.6	4	792.5	38.9	2
TDS (calc.)	mg/L	201.8	57.2	4	445.2	24.7	2
Li	mg/L	0.013	0.006	3	–	–	0
Na	mg/L	23.2	16.9	4	83.9	4.9	2
K	mg/L	4.1	1.9	4	3.8	0.4	2
Mg	mg/L	12.2	5.2	4	28.0	3.5	2
Ca	mg/L	22.5	6.0	4	48.1	2.8	2
F	mg/L	0.008	0.002	3	–	–	0
Cl	mg/L	28.2	12.3	4	80.4	0.0	2
Br	mg/L	0.004	0.003	3	–	–	0
I	mg/L	0.001	0.000	3	–	–	0
SO_4	mg/L	9.8	5.5	4	87.8	16.4	2
NO_3	mg/L	15.0	3.3	4	14.3	1.9	2
HCO_3	mg/L	123.7	47.6	4	201.4	8.6	2
P	mg/L	0.110	0.055	3	–	–	0
SiO_2	mg/L	33.6	2.2	3	–	–	0
O_2	mg/L	8.8	1.0	3	–	–	0
TOC	mg/L	0.9	0.4	3	–	–	0

Table M-16. Average saturation state of basaltic groundwater from the Jordanian-Syrian border region (B_a-Aquifer; data from E. Salameh, pers. comm. 1996).

		Basalt Young Waters			Basalt Evolved Waters		
		Average	*Stdev*	*n*	*Average*	*Stdev*	*n*
Measured:							
pH		7.50	0.47	4	7.50	0.00	2
Ionic strength		4.75E-03	1.59E-03	4	3.51E-03	1.50E-04	2
Total C	mol/L	2.29E-03	1.03E-03	4	-0.10	0.02	2
log pCO_2	bar	-2.48	0.60	4	-2.25	0.02	2
Adjusted for calcite equil.:							
pH		–	–		7.58	0.01	2
Ionic strength		–	–		1.11E-02	4.97E-04	2
Total C	mol/L	–	–		3.55E-03	1.57E-04	2
log pCO_2	bar	–	–		-2.32	0.01	2
Calcite	SI	-0.59	0.49	4	0.00	0.00	2
Dolomite disord.	SI	-1.76	0.95	4	-0.53	0.08	2
Dolomite ord.	SI	-1.19	0.95	4	0.04	0.08	2
Fluorite	SI	-5.53	0.31	3	–	–	–
Gypsum	SI	-3.04	0.30	4	-1.85	0.05	2
Portlandite	SI	-11.59	0.97	4	-11.16	0.01	2
Chalcedony	SI	0.35	0.03	3	-0.54	0.08	2
Quartz	SI	0.80	0.03	3	–	–	
Magnesite	SI	-1.18	0.48	4	–	–	

SI = Saturation Index.

Table M-17. Average chemical composition of Amman Formation groundwaters in the Maqarin area (B_2-Aquifer; data from E. Salameh, pers. comm. 1996; Abdul Jaber, 1982, 1989).

		Maqarin B_2			Project Sample
		Average	*Stdev*	*n*	*M9*
pH		6.84	0.15	16	7.61
Eh (mV)		–	–		–
T (°C)		20	0.0	16	20
Cond (µS/cm)		–	–		–
TDS (calc.)	mg/L	504.7	102.0	16	540.1
Na	mg/L	62.0	15.0	16	64.1
K	mg/L	6.4	5.9	16	4.5
Mg	mg/L	34.3	8.7	16	28.7
Ca	mg/L	78.0	22.8	16	93.0
Sr	mg/L	–	–		0.870
Mn	mg/L	–	–		0.004
Ba	mg/L	–	–		0.197
Zn	mg/L	–	–		0.034
F	mg/L	–	–		0.620
Cl	mg/L	89.4	31.6	16	108.0
Br	mg/L	–	–		0.340
SO_4	mg/L	76.8	42.6	16	68.8
NO_3	mg/L	1.4	1.1	14	11.6
HCO_3	mg/L	318.5	75.3	16	319.0
Al	mg/L	–	–		0.030
As	mg/L	–	–		1.3
SiO_2	mg/L	–	–		29.78
B	mg/L	–	–		0.629
^{18}O	‰	–	–		-5.1
^{2}H	‰	–	–		-23.9
^{3}H	TU	–	–		1.3
$^{87}Sr/^{86}Sr$					0.707680

Abdul-Jaber, Q., 1982. Hydrochemistry and hydrology of the Maqarin area. M.Sc. Thesis, University of Jordan, Amman, Jordan.

Abdul-Jaber, Q., 1989. Hydrochemische, geochemische und petrographische untersuchungen im Maqarin-Gebiet Nord-Jordanien. Ph.D. Thesis, Westfälische Wilhelms Universität, Munster, Germany.

Table M-18. Average saturation state of Amman Formation groundwaters in the Maqarin area (B_2-Aquifer; data from E. Salameh, pers. comm. 1996; Abdul Jaber, 1982, 1989).

		Maqarin B_2			Project Sample
		Average	*Stdev*	*n*	*M9*
Measured:					
pH		6.84	0.15	16	7.61
Total C	mol/L	6.87E-03	1.72E-03	16	5.46E-03
Calcite	SI	-0.39	0.26	16	0.47
log pCO_2	bar	-1.41	0.20	16	-2.17
Adjusted for calcite equilibrium:					
pH		7.24	0.23	16	7.13
Ionic strength		1.27E-02	2.35E-03	16	1.36E-02
Total C	mol/L	5.97E-03	1.70E-03	16	6.03E-03
log pCO_2	bar	-1.80	0.32	16	-1.69
Calcite	SI	0.00	0.00	16	0.00
Dolomite disord.	SI	-0.63	0.16	16	-0.79
Dolomite ord.	SI	-0.06	0.16	16	-0.22
Fluorite	SI				-1.33
Gypsum	SI	-1.84	0.32	16	-1.73
Portlandite	SI	-11.67	0.32	16	-11.79
Chalcedony	SI	–	–		0.31
Quartz	SI	–	–		0.75
Barite	SI	–	–		0.51
Celestite	SI	–	–		-2.06
Strontianite	SI	–	–		-1.55
Magnesite	SI	-0.63	0.16	16	-0.80

SI = Saturation Index.

Abdul-Jaber, 1982, 1989. See Table M-17 for references.

Table M-19. Average chemical composition of Muwaqqar (Bituminous Marl) Formation groundwaters in the Maqarin area (B_3-Aquitard; data from E. Salameh, pers. comm. 1996; Abdul Jaber, 1982, 1989).

		Maqarin B_3: low mineralised			Maqarin B_3 : high mineralised		
		Average	*Stdev*	*n*	*Average*	*Stdev*	*n*
pH		6.92	0.28	30	6.87	0.12	3
Eh (mV)		–	–		–	–	
T (°C)		20.0	0.0	30	20	0	3
Cond (µS/cm)		893.0	35.8	3	–	–	
TDS (calc.)	mg/L	459.9	64.8	30	1548.7	555.7	3
Na	mg/L	49.0	17.5	30	151.8	76.0	3
K	mg/L	7.4	4.3	30	11.9	9.1	3
Mg	mg/L	27.0	7.8	30	44.9	23.7	3
Ca	mg/L	81.3	20.1	30	309.3	148.1	3
Mn	mg/L	0.035	0.013	3	–	–	
Fe_{tot}	mg/L	0.027	0.004	2	–	–	
Zn	mg/L	0.007	0.005	3	–	–	
Cu	mg/L	0.001	0.000	2	–	–	
Ni	mg/L	0.003	0.002	2	–	–	
Cl	mg/L	63.3	21.5	30	220.3	139.3	3
SO_4	mg/L	73.5	34.9	30	604.7	282.0	3
NO_3	mg/L	1.9	1.4	26	24.9	29.6	3
HCO_3	mg/L	318.9	99.6	30	368.2	144.5	3

Abdul-Jaber, 1982, 1989. See Table M-17 for references.

Table M-20. Average saturation state of Muwaqqar (Bituminous Marl) Formation groundwaters in the Maqarin area (B_3-Aquitard; data from E. Salameh, pers. comm. 1996; Abdul Jaber, 1982, 1989).

Average		Maqarin B_3 : low mineralised			Maqarin B_3 : high mineralised		
		Average	*Stdev*	*n*	*Average*	*Stdev*	*n*
Measured:							
pH		6.92	0.28	30	6.87	0.12	3
Total C	mol/L	6.82E-03	2.26E-03	30	7.76E-03	3.29E-03	3
Calcite	SI	-0.32	0.36	30	0.07	0.28	3
log pCO_2	bar	-1.51	0.45	30	-1.42	0.31	3
Adjusted for calcite equilibrium:							
pH		7.24	0.36	30	6.87	0.12	3
Ionic strength		6.05E-03	2.04E-03	30	3.43E-02	1.08E-02	3
Total C	mol/L	6.05E-03	2.04E-03	30	7.76E-03	3.29E-03	3
log pCO_2	bar	-1.83	0.58	30	-1.42	0.31	3
Calcite	SI	0.00	0.00	33	0.00	0.00	
Dolomite disord.	SI	-0.76	0.21	-1.4	-1.11	0.28	3
Dolomite ord.	SI	-0.19	0.21	-0.8	-0.54	0.28	3
Gypsum	SI	-1.80	0.21	-2.1	-0.62	0.36	3
Portlandite	SI	-11.64	0.58	-12	-12.13	0.59	3
Magnesite	SI	-0.77	0.21	-1.4	-1.12	0.28	3

SI = Saturation Index.

Abdul-Jaber, 1982, 1989. See Table M-17 for references.

APPENDIX N

Zeolite Thermodynamic Data

(Compiled by D. Savage)

N ZEOLITE THERMODYNAMIC DATA

A variety of studies have been carried out to evaluate thermodynamic data for zeolites.

Johnson and co-workers have carried out calorimetric studies to measure thermodynamic properties of the following zeolites: analcime and dehydrated analcime (Johnson et al., 1982); natrolite, mesolite and scolecite (Johnson et al., 1983); heulandite (Johnson et al., 1985); mordenite, dehydrated mordenite and gibbsite (Johnson et al., 1992a). Johnson et al. (1992a) also present revised calorimetric data for analcime, dehydrated analcime, natrolite, scolceite, mesolite and heulandite. Data from Johnson et al., (1992a) are presented in Table N-1.

Hemingway and Robie (1984) made calorimetric measurements on phillipsite and clinoptilolite to determine heat capacities, entropies, enthalpies and Gibbs free energies. These authors note that most zeolites are metastable so that typical equilibrium procedures cannot completely define their thermodynamic properties.

La Iglesia and Aznar (1986) estimated thermodynamic data for a range of zeolites using the method of Tardy and Garrels (1974). These data are presented here in Table N-2.

Chermak and Rimstidt (1989) estimated the thermodynamic properties of a number of minerals, including some zeolites, using a technique summing the so-called 'polyhedral contributions' (Hazen, 1985, 1988). Their data for zeolites are summarised in Table N-3.

Bowers and Burns (1990) compiled available thermodynamic data for zeolites in order to investigate the stability of zeolites at the U.S. potential waste repository site at Yucca Mountain. The thermodynamic data were obtained from Johnson et al. (1982, 1983, 1985), and Hemingway and Robie (1984) and they estimated free energy data for phillipsite using the method of Chen (1975). The thermodynamic data and mineral compositions employed by Bowers and Burns are presented in Table N-4. Bowers and Burns (1990) concluded that clinoptilolite is favoured by aqueous silica activities higher than that buffered by quartz solubility, and the clinoptilolite stability field is broadened by substitution of Ca for Na and K for Ca. In addition, clinoptilolite is not stable at high activities of aqueous aluminium (such as that corresponding to gibbsite saturation). Mesolite stability apparently increases with increasing Al activity, whereas stability fields for clinoptilolite, heulandite, mordenite and phillipsite disappear. At low silica activity, scolecite and albite are stabilised relative to heulandite and mordenite, respectively.

A synthesis of the available thermodynamic data for zeolite solubility is presented in Table N-5. Source references are indicated on this table. The formula weights, densities and molar volumes for these minerals are presented in Table N-6. Where possible, preference has been given to thermodynamic data measured directly, rather than those estimated.

References

Bowers, T.S. and Burns, R.G., 1990. Activity diagrams for clinoptilolite: susceptibility of this zeolite to further diagenetic reactions. Am. Min., 75, 601–619.

Chen, C-H., 1975. A method of estimation of standard free energies of formation of silicate minerals at 298.15 °K. Sci., 275, 801–817.

Chermak, J.A. and Rimstidt, J.D., 1989. Estimating the thermodynamic properties (Agf' and Ahf') of silicate minerals at 298 K from the sum of polyhedral contributions. Am. Min., 74. 1023–1031.

Hazen, R.M., 1985. Comparative crystal chemistry and the polyhedral approach. S.W. Kieffer and A. Navrotsky, In: Microscopic to Macroscopic: Atomic environments to mineral thermodynamics, Min. Soc. Am. Rev. Min., 317–345.

Hazen, R.M., 1988. A useful fiction: Polyhedral modelling of mineral properties. Am. J. Sci., 288-A, 242–269.

Hemingway, B.S. and Robie, R.A., 1984. Thermodynamic properties of zeolites: low-temperature heat capacities and thermodynamic functions for phillipsite and clinoptilolite. Estimates of the thermochemical properties of zeolitic water at low temperature. Am. Min., 69, 692–700.

Johnson, G.K., Flotow, H.E., O'Hare, P.A.G. and Wise, W.S., 1982. Thermodynamic studies of zeolites: analcime and dehydrated analcime. Am. Min., 67, 736–748.

Johnson, G.K., Flotow, H.E., O'Hare, P.A.G. and Wise, W.S., 1983. Thermodynamic studies of zeolites: natrolite, mesolite and scolecite. Am. Min., 68, 1134–1145.

Johnson, G.K., Flotow, H.E., O'Hare, P.A.G. and Wise, W.S., 1985. Thermodynamic studies of zeolites: heulandite. Am. Min., 70, 1065–1071.

Johnson, G.K., Tasker, I.R., Flotow, H.E., O'Hare, P.A.G. and Wise, W.S., 1992a. Thermodynamic studies of mordenite, dehydrated mordenite, and gibbsite. Am. Min., 77, 85–93.

Johnson, J.W., Oelkers, E.H. and Helgeson, H.C., 1992b. SUPCRT92: a software package for calculating the standard molal thermodynamic properties of minerals, gases, aqueous species, and reactions from 1 to 5 000 bar and 0 to 1 000°C. Computers and Geosciences, 18, 899–947.

La Iglesia, A. and Aznar, A.J., 1986. A method of estimating the Gibbs energies of formation of zeolites. Zeolites, 6, 26–29.

Tardy, Y. and Garrels, R.M., 1974. A method estimating the Gibbs energies of formation of layer silicates. Geochim. Cosmochim. Acta, 38, 1101–1116.

Zeng, Y. and Liou, J.G., 1982. Experimental investigation of yugawaralite-wairakite equilibrium. Amer. Min., 67, 937–943.

TABLES

Table N-1. Thermodynamic data for zeolites. From Johnson et al. (1992a).

Mineral	Formula	ΔH_f kJ/mol	ΔG_f kJ/mol
Mordenite	$Ca_{0.289}Na_{0.361}Al_{0.940}Si_{5.060}O_{12} \cdot 3.468H_2O$	-6 756.2	-6 247.6
Dehydrated mordenite	$Ca_{0.289}Na_{0.361}Al_{0.940}Si_{5.060}O_{12}$	-5 661.8	-5 338.6
Analcime	$Na_{0.96}Al_{0.96}Si_{2.04}O_6 \cdot H_2O$	-3 305.8	-3 086.1
Dehydrated analcime	$Na_{0.96}Al_{0.96}Si_{2.04}O_6$	-2 979.1	-2 812.6
Natrolite	$Na_2Al_2Si_3O_{10} \cdot 2H_2O$	-5 732.7	-5 330.7
Scolecite	$CaAl_2Si_3O_{10} \cdot 3H_2O$	-6 063.1	-5 612.0
Mesolite	$Na_{0.676}Ca_{0.657}Al_{1.990}Si_{3.01}O_{10} \cdot 2.647H_2O$	-5 961.2	-5 527.3
Heulandite	$Ba_{0.065}Sr_{0.175}Ca_{0.585}K_{0.132}Na_{3.383}Al_{2.165}Si_{6.835}O_{18} \cdot 6.00H_2O$	-10 622.5	-9 807.0

Table N-2. Thermodynamic data for zeolites estimated by La Iglesia and Aznar (1986).

Mineral	Formula	ΔG_f^0 (k,J/mol)
Wairakite	$CaAl_2Si_4O_{12} \cdot 2H_2O$	-6 210.78
Laumontite	$CaAl_2Si_4O_{12} \cdot 4H_2O$	-6 685.12
Na-phillipsite	$Na_6Al_6Si_{14}O_{40} \cdot 15H_2O$	-22 359.89
K-phillipsite	$K_6Al_6Si_{14}O_{40} \cdot 15H_2O$	-22 536.17
Na-clinoptilolite	$Na_{3.6}Al_{3.6}Si_{14.4}O_{36} \cdot 8.8H_2O$	-18 504.14
K-clinoptilolite	$K_{3.6}Al_{3.6}Si_{14.4}O_{36} \cdot 8.8H_2O$	-18 609.91
Epistilbite	$CaAl_2Si_6O_{16} \cdot 5H_2O$	-8 634.17
Natrolite	$Na_2Al_2Si_3O_{10} \cdot 2H_2O$	-5 315.22
Mesolite	$Na_{0.676}Ca_{0.657}Al_{1.99}Si_{3.01}O_{10} \cdot 2.647H_2O$	-5 526.14
Scolecite	$CaAl_2Si_3O_{10} \cdot 3H_2O$	-5 592.01

Table N-3. Thermodynamic properties of zeolites as estimated by Chermak and Rimstidt (1989).

Mineral	Formula	ΔG_f^0 k,J/mol	ΔH_f^0 k,J/mol
Mesolite	$Na_{0.676}Ca_{0.657}Al_{1.99}Si_{3.01}O_{10} \cdot 2.647H_2O$	-5 530.6	-5 946.6
Natrolite	$Na_2Al_2Si_3O_{10} \cdot 2H_2O$	-5 345.5	-5 716.9
Scolecite	$CaAl_2Si_3O_{10} \cdot 3H_2O$	-5 623.0	-6 062.3
Stilbite	$Na_{0.136}Ca_{1.02}K_{0.006}Al_{2.18}Al_{2.18}Si_{6.82}O_{18} \cdot 7.33H_2O$	-10 132.1	-11 025.2
Erionite	$KAlSi_3O_8 \cdot 3H_2O$	-4 458.7	–
Phillipsite	$K_3Al_3Si_5O_{16} \cdot 6H_2O$	-9 240.6	–
Clinoptilolite	$KAlSi_5O_{12} \cdot 4H_2O$	-6 406.5	–
Mordenite		-6 246.0	-6 765.7
Yugawaralite		-4 212.4	-4 543.8

Table N-4. Thermodynamic data for zeolites compiled by Bowers and Burns (1990).

Mineral	Formula	ΔG_f^o kJ/mol	ΔH_f^o kJ/mol
Na-phillipsite	$Na_2Al_2Si_5O_{14} \cdot 5H_2O$	-7 746.2	-8 382.5
K-phillipsite	$K_2Al_2Si_5O_{14} \cdot 5H_2O$	-7 830.2	-8 474.9
Ca-phillipsite	$CaAl_2Si_5O_{14} \cdot 5H_2O$	-7 784.7	-8 410.1
Phillipsite	$Na_{1.08}K_{0.80}Al_{1.88}Si_{6.12}O_{16} \cdot 6H_2O$	-8 840.2	-9 598.8
Mordenite	$NaAlSi_5O_{12} \cdot 3H_2O$	-6 132.3	–
Epistilbite	$CaAl_2Si_6O_{16} \cdot 5H_2O$	-8 641.0	-9 350.2
Chabazite	$CaAl_2Si_4O_{12} \cdot 6H_2O$	-7 165.7	-7 810.8
Stilbite	$NaCa_2Al_5Si_{13}O_{36} \cdot 14H_2O$	-20 223.7	-21 955.4
Heulandite	$CaAl_2Si_7O_{18} \cdot 6H_2O$	-9 734.4	-10 543.2
Clinoptilolite	$(Na_{0.56}K_{0.98}Ca_{1.5}Mg_{1.23})(Al_{6.7}Fe_{0.3})Si_{29}O_{72} \cdot 22H_2O$	-37 897.8	-41 053.1

Table N-5. ΔG_f^0 and ΔH_f^0 values for zeolites extracted from the literature. Source references are indicated.

Mineral	Formula	ΔG_f^0 (kJ/mol)	ΔH_f^0 (kJ/mol)	Source
Analcime	$Na_{0.96}Al_{0.96}Si_{2.04}O_6 \cdot H_2O$	-3 086.1	-3 305.8	1
Chabazite	$CaAl_2Si_4O_{12} \cdot 6H_2O$	-7 165.7	-7 810.8	2
Clinoptilolite	$KAlSi_5O_{12} \cdot 4H_2O$	-6 406.5	–	3
Epistilbite	$CaAl_2Si_6O_{16} \cdot 5H_2O$	-8 641.0	-9 350.2	2
Erionite	$KAlSi_3O_8 \cdot 3H_2O$	-4 458.7	–	3
Heulandite	$CaAl_2Si_7O_{18} \cdot 6H_2O$	-9 734.4	-10 543.2	2
Laumontite	$CaAl_2Si_4O_{12} \cdot 4H_2O$	-6 681.1	-7 232.7	4
Mesolite	$Na_{0.676}Ca_{0.657}Al_{1.990}Si_{3.01}O_{10} \cdot 2.647H_2O$	-5 527.3	-5 961.2	1
Mordenite	$NaAlSi_5O_{12} \cdot 3H_2O$	-6 132.3	–	2
Natrolite	$Na_2Al_2Si_3O_{10} \cdot 2H_2O$	-5 330.7	-5 732.7	1
Ca-phillipsite	$CaAl_2Si_5O_{14} \cdot 5H_2O$	-7 784.7	-8 410.1	2
Na-phillipsite	$Na_2Al_2Si_5O_{14} \cdot 5H_2O$	-7 746.2	-8 382.5	2
K-phillipsite	$K_2Al_2Si_5O_{14} \cdot 5H_2O$	-7 830.2	-8 474.9	2
Scolecite	$CaAl_2Si_3O_{10} \cdot 3H_2O$	-5 612.0	-6 063.1	1
Stilbite	$NaCa_2Al_5Si_{13}O_{36} \cdot 14H_2O$	-20 223.7	-21 955.4	2
Wairakite	$CaAl_2Si_4O_{12} \cdot 2H_2O$	-6 181.6	-6 607.9	4
Yugawaralite	$Ca_{0.5}AlSi_3O_8 \cdot 2H_2O$	-4 193.9	-4 518.1	5

1 = Johnson et al. (1992a).
2 = Bowers and Burns (1990).
3 = Chermak and Rimstidt (1989).
4 = Johnson et al. (1992b).
5 = Zeng and Liou (1982).

Table N-6. Formula weights, densities and molar volumes of zeolites listed in Table N-5.

Mineral	Formula Wt. (g)	Density ($g\ cm^{-3}$)	V ($cm^3\ mol^{-1}$)
Analcime	219.3	2.24–2.29	96.8
Chabazite	506.5	2.1	241.2
Clinoptilolite	470.5	2.16	217.8
Epistilbite	608.7	2 275	267.6
Erionite	332.4	2.0	166.2
Heulandite	686.72	2.1–2.2	319.4
Laumontite	470.4	2.27	207.55
Mesolite	387.8	2.26	171.6
Mordenite	436.5	2.13	204.9
Natrolite	380.2	2.20–2.26	170.5
Ca-phillipsite	548.6	2.15	255.2
Na-phillipsite	554.5	2.15	257.9
K-phillipsite	586.7	2.15	272.9
Scolecite	387.7	2.25–2.29	170.8
Stilbite	1 431.4	2.1–2.2	665.8
Wairakite	434.4	2.32	186.87
Yugawaralite	295.3	2 239	131.9

APPENDIX O

Colloid Repulsion by the Filter

O COLLOID REPULSION BY THE FILTER

The first stage of the colloid analyses, using the Cambridge S250 SEM, indicated much lower colloid populations (see Table 10-2) than had previously been reported for natural waters. It was therefore decided to check against any possible colloid repulsion by the hyperalkaline-resistant filters using a colloid standard. Unfortunately, it proved too problematic, in the short time scale of the project, to produce a standard solution of cementitious colloids. Consequently, standard solutions for enumeration testing were prepared using 48 nm diameter Polybead Carboxylate Microspheres (2.5% solids in solution) produced by Polysciences Inc. (LOT# 452040). Although it is recognised that these colloids are not directly relevant (due to differences in charge, chemistry etc.), it was nevertheless felt worthwhile to carry on with this initial test to assess any potential major disturbances.

The colloid concentration of this initial solution was calculated to be $3 \cdot 10^{14}$ colloids.mL^{-1}. Two different colloid standard solutions were produced for the tests by dilution of this starting solution, since this was found to have too high a colloid density for realistic enumeration. The first solution was prepared by making up 100 µL of the original standard to 100 mL with ultra-pure water to produce a solution with $3 \cdot 10^{11}$ colloids.mL^{-1}. Initial SEM observations showed the colloid density to be too high for enumeration. The second solution was prepared by making up 100 µL of the original standard to 100 mL with ultra-pure water, pre-filtered through a 0.2 µm membrane (Schleicher & Schuell Lot No. 9108/308). 1 mL of this solution was then made up to 100 mL using filtered ultra-pure water, the final solution produced having a concentration of $3 \cdot 10^{9}$ colloids.mL^{-1}. Pre-filtered water was used as initial SEM observations revealed considerable particulate matter on the filter surfaces.

Two filter types which are marketed as being stable at high pH were used: (i) Amicon 25 mm diameter, 15 nm pore size XM300 (Lot no. ATA211); (ii) Durapore 25 mm diameter, 0.1 µm pore size (Lot No. R6SM 23811). Initial filtrations were performed using 5 mL of the $3 \cdot 10^{11}$ colloids.mL^{-1} solution through each filter type. Corresponding 'blank' filters were prepared using 5 mL of Romil HPLC grade ultra-pure water (Cas. No. 7732-18-5). Filtration was carried out using an Amicon stirred filtration cell with fluid flow under argon top pressure. The stirred filtration cell is used to promote even distribution of particles over the membrane filter surface (see Degueldre et al., 1990). Filters were removed from the cell after drying under argon and sealed into covered petri dishes. A further pair of Amicon filters were prepared, one using 5 mL of the second colloid solution ($3 \cdot 10^{9}$ colloids mL^{-1}), the other 5 mL of 0.2 µm filtered ultra-pure water.

The Durapore 0.1 µm filters showed no evidence of colloid retention, although mineral debris >1 µm in diameter was seen on surfaces of both the blank and colloid solution filters (all data for the filters are given in Table O-1). The initial XM300 filter (15 nm nominal pore size) prepared using a concentration of $3 \cdot 10^{11}$ colloids.mL^{-1} was found to be unsuitable for enumeration due to the excessively high colloid density on the filter surface. Moving from the edge to the centre of the filter, areas were observed where colloids formed dense continuous coatings visible at 200X magnification, whilst other

regions showed relatively low colloid density indicating uneven distribution and possible flocculation of colloids. Mineral debris was observed to be present and was evenly distributed over the surface of the filter. The corresponding 'blank' XM300 filter was also seen to contain a similar volume of mineral debris.

The second XM300 filter prepared with the lower concentration test solution provided images in which the particles could be successfully counted. The uneven distribution of colloids on the filter surface seen in the initial XM300 filter was also observed in this specimen, although to a lesser extent. The number of colloids per image showed an order of magnitude increase moving from the filter edge to the centre. The concentration in solution was calculated for each image and the results averaged to give a value of 8.154 ($\pm$6.877) $\cdot$ 10^8 colloids.mL^{-1} in comparison to the theoretical concentration of 3 $\cdot$ 10^9 colloids.mL^{-1} in the standard solution.

Differences are likely to result from experimental errors in solution dilution, filtering, statistical sampling of unevenly distributed particulates and enumeration. However, the similarity between experimentally determined and theoretical concentrations indicate that colloids are retained and sampled reliably on the Amicon XM300 (15 nm nominal pore size) filters, indicating no significant colloid repulsion. Analysis of the filtrate from the Durapore 0.1 µm filters also showed no evidence that these filters either repel colloids, or retain them through surface interaction.

Examination of the 'blank' filter showed particulate material present, some of which was within the size range of the test colloids. Enumeration of these colloids produced a concentration of 1.505 ($\pm$9.231) $\cdot$ 10^7 colloids.mL^{-1}.

Reference

Degueldre, C,. Longworth, G., Moulin, V. and Vilks, P., 1990. Grimsel colloid exercise: an international intercomparison exercise on the sampling and characterisation of groundwater colloids. Nagra Tech. Rep. (NTB 90-01), Wettingen, Switzerland.

TABLES

Table O-1. Enumeration data for colloid test solution.

	Standard solution			
Image number	97_05501	97_05502	97_05503	97_05504
Colloid count	124	194	484	926
Image X dimension (pixels)	1024	1024	1024	1024
Image Y dimension (pixels)	708	708	708	708
Pixel equivalent (m/pixel)	8.470E-09	8.470E-09	8.470E-09	8.470E-09
Image area (m^2)	5.201E-11	5.201E-11	5.201E-11	5.201E-11
Colloids per m^2 from image	2.384E+12	3.730E+12	9.306E+12	1.780E+13
Total filter area m^2	4.909E-04	4.909E-04	4.909E-04	4.909E-04
Volume filtered m^3	5.000E-06	5.000E-06	5.000E-06	5.000E-06
Colloids /m^3 filtered	2.341E+14	3.662E+14	9.136E+14	1.748E+15
Colloids /mL filtered	2.341E+08	3.662E+08	9.136E+08	1.748E+09
No. of colloids on filter	1170284758	1830929380	4567885670	8739384567
Average colloids/mL	8.154E+08			
Standard deviation	6.877E+08			
Average no. of colloids on filter	4.077E+09			

	Ultra pure filtered water			
Image number	97_05601	97_05602	97_05603	97_05604
Colloid count	17	102	69	131
Image X dimension (pixels)	1024	1024	1024	1024
Image Y dimension (pixels)	708	708	708	708
Pixel equivalent (m/pixel)	8.470E-09	8.470E-09	8.470E-09	8.470E-09
Image area (m^2)	5.201E-11	5.201E-11	5.201E-11	5.201E-11
Colloids per m^2 from image	3.269E+11	1.961E+12	1.327E+12	2.519E+12
Total filter area m^2	4.909E-04	4.909E-04	4.909E-04	4.909E-04
Volume filtered m^3	5.000E-06	5.000E-06	5.000E-06	5.000E-06
Colloids /m^3 filtered	3.209E+13	1.925E+14	1.302E+14	2.473E+14
Colloids /mL filtered	3.209E+07	1.925E+08	1.302E+08	2.473E+08
No. of colloids on filter	1.604E+08	9.627E+08	6.512E+08	1.236E+09
Average colloids/mL	1.505E+08			
Standard deviation	9.231E+07			
Average no. of colloids on filter	7.527E+08			

APPENDIX P

Colloids: Filtrate Chemistry Data Set

Appendix P. Filtrate analysis for the four filter sizes, site M1.

Table P-1. Filtrate chemistry.

		pH	Ca (mg/L)	Na (mg/L)	K (mg/L)	CO_3 (mg/L)	OH (mg/L)	Cl (mg/L)	SO_4 (mg/L)	NO_3 (mg/L)	Cation total (meq/L)	Anion total (meq/L)	Balance (%)	Br (mg/L)	F (mg/L)	TOC (mg/L)	TIC (mg/L)	Total S (mg/L)
A1	1.0 µm	12.5	739	46.2	9.88	26	450	48.8	303	3.56	39.31	35.06	5.72	0.24	0.36	1.00	1.57	99.4
A2	0.1 µm	12.6	748	46.6	9.85	15	462	48.9	303	3.38	39.78	35.44	5.77	0.25	0.38	1.37	1.70	102.0
A4	50 nm	12.6	706	44.4	9.44	17	452	54.8	313	3.75	37.54	35.27	3.13	0.29	0.36	2.04	<1.00	96.5
A3	30 nm	12.6	705	43.6	9.35	30	453	51.0	306	3.19	37.47	35.49	2.71	0.23	0.38	2.77	1.34	94.8
B1	1.0 µm	12.6	693	43.6	9.33	12	462	49.6	306	3.17	36.89	35.42	2.03	0.16	0.36	0.64	1.03	96.1
B2	0.1 µm	12.6	689	43.2	9.19	23	459	49.6	309	3.18	36.67	35.67	1.38	0.2	0.35	1.39	1.33	95.2
B4	50 nm	12.5	705	45.4	9.66	23	452	49.8	306	3.23	37.55	35.22	3.20	0.26	0.37	2.10	1.70	97.3
B3	30 nm	12.6	688	45.1	9.76	13	462	49.8	306	3.13	36.70	35.43	1.76	0.18	0.36	9.36	1.24	96.7
C1	1.0 µm	12.5	683	44.0	9.33	15	459	49.7	303	3.16	36.43	35.30	1.57	0.18	0.36	0.64	1.46	94.9
C2	0.1 µm	12.5	660	41.9	8.91	15	461	50.7	307	3.53	35.16	35.50	-0.48	0.25	0.36	1.35	1.52	91.3
C4	50 nm	12.6	626	40.1	8.43	18	457	51.7	309	3.16	33.33	35.42	-3.03	0.27	0.35	4.24	<1.00	88.2
C3	30 nm	12.6	624	40.2	8.60	12	465	50.8	311	3.24	33.26	35.76	-3.63	0.30	0.35	6.79	1.16	86.6
M1	Phase II	12.67	674	47.2	9.88	37	422	52.4	305	3.28	36.10	33.90	3.04	0.14	0.29	3.20	4.83	–

Table P-1 (contd.). Filtrate chemistry.

		Ba (mg/L)	Sr (mg/L)	Al (mg/L)	Zn (mg/L)	Cr (mg/L)	Mo (mg/L)	Y (µg/L)	Cs (µg/L)	La (µg/L)
A1	1.0 µm	0.034	6.46	0.15	0.098	0.74	0.10	0.06	3.16	0.14
A2	0.1 µm	0.034	6.55	0.32	0.097	0.75	0.10	<.034	2.81	0.12
A4	50 nm	0.032	6.12	0.19	0.092	0.70	0.10	0.05	3.15	0.11
A3	30 nm	0.032	6.08	0.21	0.095	0.71	0.10	0.05	3.09	0.14
B1	1.0 µm	0.031	5.97	0.29	0.092	0.71	0.09	0.05	3.04	0.30
B2	0.1 µm	0.031	5.93	0.41	0.09	0.71	0.09	0.06	3.14	0.24
B4	50 nm	0.034	6.38	0.17	0.094	0.75	0.10	0.05	3.01	0.14
B3	30 nm	0.034	6.16	0.17	0.090	0.73	0.10	0.05	3.10	0.13
C1	1.0 µm	0.033	6.11	0.17	0.098	0.72	0.10	0.08	2.95	0.16
C2	0.1 µm	0.031	5.86	0.18	0.087	0.69	0.09	0.06	2.98	0.15
C4	50 nm	0.030	5.58	0.13	0.840	0.66	0.10	0.04	3.10	0.12
C3	30 nm	0.029	5.58	0.14	0.850	0.65	0.08	0.06	3.05	0.14
M1	Phase II	0.027	–	0.14	0.070	0.75	0.10	–	–	0.17

APPENDIX Q

Western Springs Catchment Area: Chemistry of Near-surface Groundwaters Collected from a Variety of Springs, Domestic Water Sources and Waste Water Disposal Locations

(E. Salameh and H.N. Khoury)

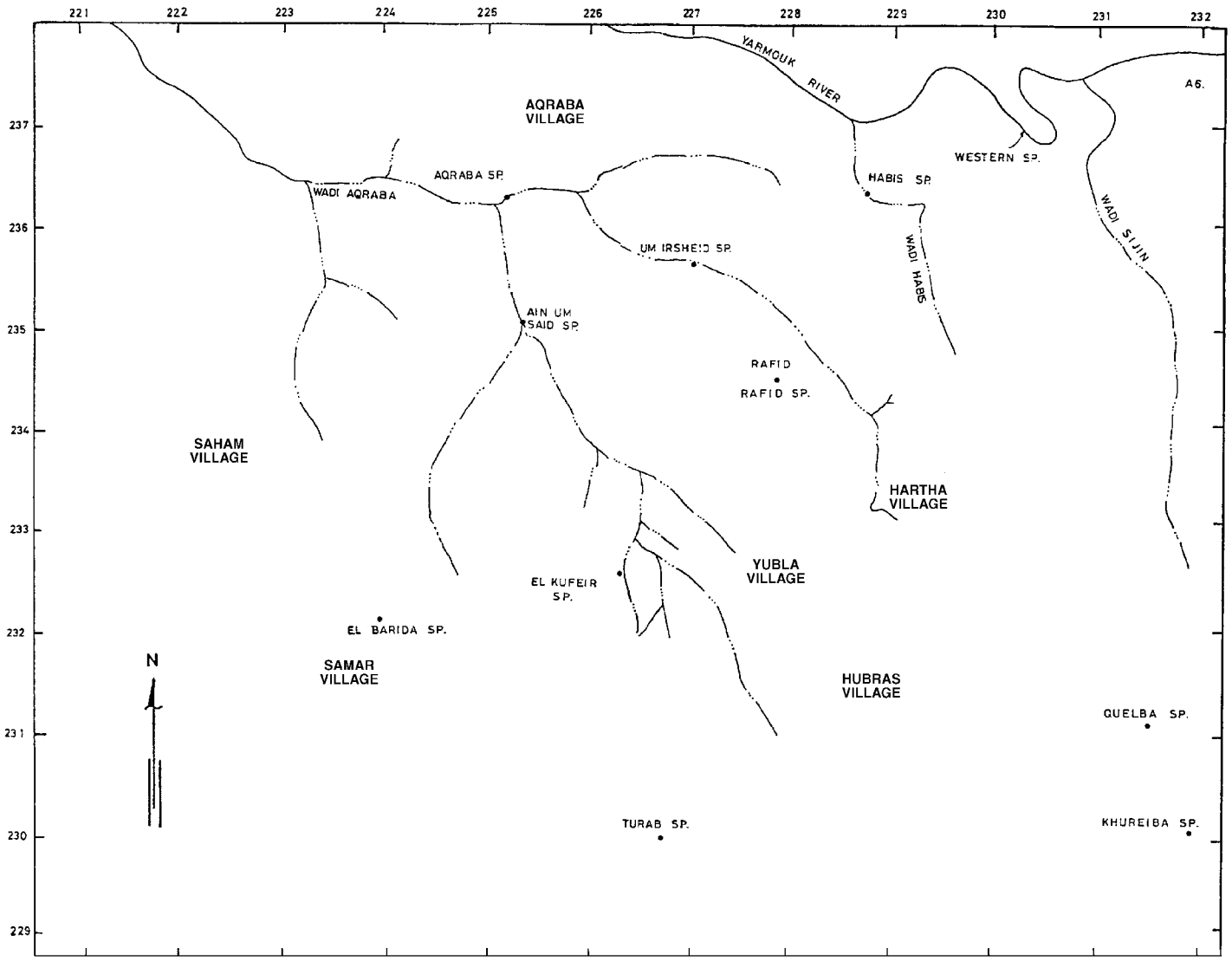

Figure Q-1. *Spring locations west and south of Wadi Sijin.*

Table Q-1. Chemistry of near-surface water samples (University of Jordan, Department of Geology, Amman).

	No	Source	Elect. Cond. (µS/cm)	T.D.S. (mg/L)	pH	Ca^{++} (mg/L)	Mg^{++} (meq/L)	Na^{+} (meq/L)	K^{+} (meq/L)	Cl^{-} (meq/L)	SO_4^{--} (meq/L)	CO_3^{--} (meq/L)	HCO_3^{-} (meq/L)	NO_3^{-} (ppm)	Trace elements (ppm)				
															NH_3	Cr	Ba	Co	Sr
	1	Turab sp.	461	299.60	8.41	3.87	0.64	0.60	0.011	0.70	0.125	0.00	3.77	22.00	0.000	0.020	<0.01	<0.01	0.150
	2	El Barida sp.	586	380.90	6.84	4.05	1.08	0.90	0.180	1.00	0.200	0.00	4.45	36.50	0.000	0.140	<0.01	<0.01	0.280
	3	El Kufeir sp.	924	603.80	6.82	6.23	2.07	1.78	0.220	3.20	0.400	0.00	6.43	36.50	0.000	0.019	<0.01	<0.01	0.780
	4	Um Irsheid sp.	1 217	791.00	7.50	5.61	1.97	2.30	2.170	3.70	0.690	0.00	4.10	200.00	0.000	0.095	<0.01	<0.01	1.230
	5	Quebla sp.	466	302.00	7.80	3.34	0.97	0.43	0.050	0.70	0.150	0.00	3.50	32.10	0.000	0.008	<0.01	<0.01	0.266
	6	Khureiba sp.	551	3.58	7.50	4.13	0.99	0.65	0.092	0.90	0.320	0.00	4.44	21.60	0.000	0.150	<0.01	<0.01	0.225
	7	Rafid sp.	520	338.00	7.60	3.64	0.98	0.76	0.057	1.10	0.260	0.00	3.91	20.40	0.000	0.028	<0.01	<0.01	0.290
*	8	Municipality cistern	275	178.70	10.45	0.30	0.10	0.81	1.060	0.30	0.400	0.42	1.26	1.43	0.000	–	–	–	–
**	9	Private cistern	442	287.00	8.50	3.01	0.99	0.60	0.060	0.82	0.500	0.00	3.15	23.20	0.000	–	–	–	–
***	10	Waste water	2 750	1 787.00	10.50	3.44	4.30	8.60	1.690	9.47	3.590	8.40	11.55	28.70	210.000	–	–	–	–
	11	Habis sp.	591	–	7.90	3.15	1.37	1.41	0.092	1.50	0.410	0.00	3.99	8.00	0.004	0.012	<0.01	<0.01	0.480
	12	Aqraba sp.	838	–	7.80	4.53	1.77	1.73	0.440	2.50	1.200	0.00	4.44	45.00	0.031	0.030	<0.01	<0.01	0.600
	13	Ain um Said sp.	924	604.00	6.82	6.23	2.07	1.78	0.220	3.20	0.400	0.00	6.43	36.50	0.000	0.019	<0.01	<0.01	0.780

Hartha Village:

* Newly cleaned and cemented, therefore the high pH. It collects precipitation water from the roofs of the buildings.

** The water is a mixture of Quelba spring water, precipitation water and Water Authority domestic supply.

*** Cesspit in Hartha.

APPENDIX R

The Nature and Use of Cement in Repository Construction and the Relevance of the Maqarin Analogue Study

(F. Karlsson and B. Lagerblad)

R THE NATURE AND USE OF CEMENT IN REPOSITORY CONSTRUCTION AND THE RELEVANCE OF THE MAQARIN ANALOGUE STUDY

(F. Karlsson and B. Lagerblad)

R.1 Background

Over the timescales required for the safe disposal of radioactive wastes (thousands to hundreds of thousands of years), cementitious materials are expected to undergo various stages of degradation. This long-term degradation was recently conceptualised by Lagerblad and Trägårdh (1994) as:

1. Cementitious materials are susceptible to leaching and this depends on the:

   - permeability of concrete,
   - type of cement,
   - addition of pozzolans,
   - amount of young water (erosion),
   - groundwater composition.

2. Leaching and alteration of cementitious materials in the repository will be influenced by water flux, temperature, pressure and access to atmospheric gases.

3. With time, the hydrous components of the cement paste will successively become more ordered.

4. With time, the cement paste will react with some of the minerals in the surrounding host rock and aggregate.

In an attempt to understand fully the various degradation processes, the long-term influence on a) cement reactions, b) interaction with different host rock-types, and c) stability of the cement hydrous phases, has been studied from the perspective of short-term laboratory experiments (column and leaching experiments), short-term cementitious analogues (e.g. concrete constructions such as dam tunnels, concrete water storage tanks etc.), and long-term effects provided by the Maqarin natural analogue study.

R.2 Cementitious Repository Materials

Irrespective of the type of radioactive waste (high, low to intermediate) and the selected disposal concept, cement will be used to varying degrees in repository construction. In HLW disposal the main use will be limited to stabilise access tunnels during the construction phase (e.g. grouting; shotcrete etc.), and as permanent plugs during final backfilling of tunnels and shafts. Where possible, some concrete will be removed during

closure (e.g. shotcrete flooring etc.). In L/ILW disposal the volumes of concrete, in contrast to HLW, will be enormous, with its possible use for all major forms of construction and containment.

In all disposal construction the major cementitious materials to be considered are mainly injected grout and dense structural concretes.

R.2.1 Different Types of Concrete

Three major types of concrete are envisaged; injection material, porous concrete and dense impermeable concrete. Injection material, in the form of a cement paste, will be used to seal access tunnels and excavated vaults against groundwater incursion. This will be done by injecting cracks, fractures and transmissive zones, and may involve fairly large amounts of material. Dense structural concrete may be used for all the major cementitious components, for example the walls and floors of the vaults, waste containers/moulds etc., and porous concrete will be used to fill up the remaining spaces and voids when the containers have been stacked.

R.2.2 Concrete Properties

Cement

Degerham Standard Portland Cement (DSPC) is an example of a reference cement composition being considered for repository construction. Portland cement is made by heating a mixture of clay and limestone (ratio 1:4) in a rotary kiln to a final temperature of 1 450°C. This produces lime ($CaCO_3$), belite (Ca-silicate), aluminate and ferrite at temperatures up to 800°C; above 1 300°C alite (Ca-silicate) forms at the expense of lime and belite (Taylor, 1990). When cooled, the clinker phases are crystalline, the most important being alite and belite, known as C_3S (tricalcium silicate) and C_2S (dicalcium silicate) respectively. The clinker is finally crushed and mixed with various additives, for example gypsum, to give the product the desired properties.

Cement Paste

Concrete is a mixture of cement, sand, gravel (or crushed rock) and water. More precisely, the mixture is termed *mortar* if only sand is used and *concrete* when it contains coarse aggregates such as gravel or crushed rock. Cement and water forms *cement paste* which sets and hardens due to the hydration reactions of the cement grains. Cement paste with a water to cement ratio (w/c) of about 0.38 should, in principle, be fully hydrated (Taylor, 1990). However, unhydrated cement minerals can be found even in concretes with a higher w/c (Lagerblad, 1996). The hydration products start to grow from the surface of the clinker grains and fill the space between the aggregate grains. The main hydration products are poorly crystalline calcium silicate hydrates and calcium hydroxide (portlandite). The calcium silicate hydrates form a gel in the cement paste, referred to as C-S-H in concrete chemistry nomenclature (Calcium-Silicate-Hydrogel). The wet density of the gel phase C-S-H is 1.85–1.9 g/cm^3 and that of saturated cement paste is 1.9–2.1 g/cm^3 (Taylor, 1990, p 141). In hardened concrete

C-S-H is the principal binding phase which holds the solid grains of cement, sand and gravel together.

Calcium silicate hydrogel, C-S-H, is semicrystalline with a Ca/Si ratio which can vary from 0.8 to 3 with variable amounts of water. The reference concrete, made using DSPC has a Ca/Si ratio in C-S-H of about 1.7 (Lagerblad and Trägårdh, 1994). Calcium silicate hydrate minerals closest in composition to C-S-H in cement are tobermorite ($C_5S_6H_9$ approx.) and jennite ($C_9S_6H_{11}$ approx.). In addition, semicrystalline calcium silicate hydrate exist which are intermediate in structure between these two compounds and C-S-H gel, for example C-S-H(I) and C-S-H(II). They are relatively well defined and close to tobermorite and jennite in composition and structure (Taylor, 1990, p 143).

Investigations of the C-S-H structure in hardened cement paste indicate a layer structure which, together with a pore solution, forms a rigid gel with pores ranging in size from macroscopic (>50 nm) to enlarged interlayer spaces of nanometer dimensions. The C-S-H layers are expected to form subparallel groups, a few layers thick, which enclose pores of dimensions ranging from interlayer spaces and upwards (Feldman-Sereda model, presented in Taylor, 1990, p 252).

Water in Cement Paste

Water in hardened paste is present in different thermodynamic states depending on if, and how, the water molecules interact with the cement phases:

Free water where the water molecules are not directly affected by the forces from the mineral surfaces.

Adsorbed water which consists of about two layers of water absorbed on the cement hydrogel paste.

Absorbed water, gel water, which is largely bound to the C-S-H structure.

Structural water in the minerals such as crystal water and hydroxyl groups (e. g. portlandite).

Several methods have been used to study how water occurs in the cement paste and how it is bound, for example, TG (TermoGravimetry) and DTA (Differential Thermal Analysis). A fully hydrated and saturated Portland cement with a w/c ratio of 0.5 is described by Taylor (Taylor, 1990, p 251) to consist of 21% (weight % of total water) capillary water, 38% gel water and 41% of non-evaporable water (Powers-Brownyard description). Free water, according to the definition above, will be found in the capillary fraction and in parts of the gel (pore spaces). Absorbed water will mainly be in the gel, where it is expected to be the dominating form. Possibly there is also some absorbed water in the non-evaporable part. Structural water is essentially found in the fraction of non-evaporable water.

The water in the gel phase is finely dispersed; most of it is sorbed or in narrow, possibly isolated, pore spaces. Consequently, it has a very low permeability, which is typical for a gel phase, and the hydraulic conductivity of a cement paste is restricted to the fraction of capillary water. The amount of capillary water will, of course, depend very much on the w/c ratio.

Cement pore water is a definition which refers in general to water present in concrete. It can also be seen as an operational definition referring to the water obtained by pressing samples of cement paste or concrete. Dissolved constituents in concrete will be present in the free water but also, to some extent, affected by sorption. However, the influence of sorption is not expected to be strong enough to influence the results of sampling by pressing, so the analysis of pore water samples should be relevant for the conditions in the cement paste.

Cement Pore Water Composition

Alkali hydroxides (NaOH and KOH) in the fresh cement paste will generate a high pH of about 13 and more. If the alkali hydroxides are leached out or consumed by chemical reactions, there is enough portlandite ($Ca(OH)_2$) to keep the pH of cement pore water at about 12.5. The capacity to control the pH at a high level can be estimated from the composition of cement or measured in leaching experiments.

It is reasonable to expect that a major portion of the alkali metals Na and K can be released as NaOH and KOH by leaching. DSPC, with a composition according to Table R-1, has a total alkali oxide content of 0.5% (weight % as Na_2O; Table R-2); for simplicity, it is assumed that all of the alkalis can be released as hydroxides. Concrete contains roughly 350 kg of cement per m^3 which could then release a total of 56 moles of alkali hydroxides per m^3 of concrete.

The same reasoning can hardly be applied to calcium hydroxide because the calcium, originating from calcium silicates (alite and belite) and free lime, will appear both in C-S-H and portlandite in the hydrated cement paste; most of it will be in C-S-H. There will also be some unhydrated clinker left with Ca bound in it. Therefore, it would be exaggerated to assume that all of the CaO in Table R-2 is available as portlandite. Engkvist et al. (1996) leached samples of crushed cement paste until the pH was below 12 and found a weight loss of 20% mostly due to $Ca(OH)_2$. Concrete contains about 350 kg of cement (approx. 420 kg as hydrated cement paste) per m^3 concrete which, combined with the leaching results, implies that 1 m^3 of concrete can release 2 300 moles of hydroxide ions from $Ca(OH)_2$. According to Taylor (Taylor, 1990, p 129) 1.15 moles of portlandite are obtained by the hydration of C_3S in cement. Using Taylor's data and a content of 51% of C_3S according to Table R-1, a portlandite content of 900 moles is obtained. The free lime (see Table R-2) would add another 100 moles to that, thus making a total of 1 000 moles of $Ca(OH)_2$ (2 000 moles of hydroxide ions) in 1 m^3 of concrete which is in reasonable agreement with the previous value. In summary, it can be concluded that between 2 000–2 300 moles of hydroxide ions can be dissolved from $Ca(OH)_2$ in 1 m^3 of concrete.

Leaching of C-S-H will start when there is no portlandite left. The dissolution of C-S-H is incongruent with a higher Ca/Si-ratio in solution than in the solid. The Ca/Si ratio of the remaining C-S-H will decrease to 0.85, when dissolution becomes congruent (Atkins and Glasser, 1992). The pH will successively drop to 11 and remain there during the congruent phase. A model for the dissolution of C-S-H has been developed by Berner (1987). For stoichiometric reasons it is not possible to release more hydroxides from C-S-H dissolution than what remains of the calcium after leaching the portlandite. The total analytical content of CaO is 65.3% (including free lime)

according to Table R-2. Subtracting the portlandite part shows that less than 6 000 moles of hydroxide ions can be released from C-S-H in 1 m^3 of concrete.

R.3 Old Concrete

Modern cement of the Portland type has existed for about 90 years. Although not very old in repository timescales, it is still worthwhile to study samples from early concrete constructions and look for trends of changes, since signs of crystallisation and products from later reactions can be analysed and used to predict future signs of degradation. Old concrete in contact with air gives carbonation to a certain depth due to intrusion of, and reaction with, carbon dioxide. To study the effects of such processes, concrete samples from water saturated environments were selected.

R.3.1 Structure of Old Cement Paste

The cement paste in samples of old concrete from the wall of a water tunnel at the Porjus dam, northern Sweden, were investigated by Grudemo (1982) using X-ray diffraction. The tunnel was built in 1914 but, according to the analysis, no significant change in crystallinity has occurred after 65 years in a water filled inflow tunnel. It was concluded that the C-S-H phases would remain stable for a long time. Rayment (1986) made an electron probe analysis of C-S-H in a 136 year old cement paste and found no major differences compared to modern Portland cement. The C-S-H had remained stable and cement clinker grains were observed still showing no signs of reaction.

Lagerblad (1996) made a comprehensive study of samples from old concrete constructions throughout Sweden. The aim was to find and investigate cases relevant to the deep repository situation and preference was given to samples from water saturated environments. Thin section microscopy, SEM and X-ray diffraction were used. An overview of the study is presented in Table R-4.

The investigations revealed relict grains of unhydrated cement clinker, up to a particle diameter of 0.3 mm, in most of the samples. Cases were also found where the grain had been removed leaving a hollow shell of hydration products behind; leaching could possibly explain this phenomenon. Calcite precipitations were found together with crystals of ettringite/monosulphate and portlandite, all of which tend to grow into voids left in the cement paste. The C-S-H in the good quality old mortars (e.g. the water tank described later) has a composition similar to modern cement paste and it was concluded that C-S-H is very stable if leaching is restricted by, for example, a low hydraulic conductivity. Concrete concrete/mortar with a relatively low w/c ratio (e.g. the inspection tunnel and the water tank) showed a positive maturity development where slowly hydrating clinker grains fill the pore spaces and the concrete gains additional strength by these reactions. The strength of some of the old concrete is greater than what can be produced to-day, at least without superplasticisers. This is due to the relatively coarse-grained cement that has hydrated very slowly *in situ*.

R.3.2 Pore Water Leaching

Another example of long-time contact between concrete/mortar and fresh water is the 90 years old water tank in Uppsala (Lagerblad, 1996). The outermost surface is carbonated by carbonate from the water. There is a general small increase in sulphate ions and the presence of a distinct zone with high sulphate just below the carbonated surface. Below this alteration zone, which is only 2–3 mm thick, there is 20 to 30 mm mortar that is still robust, although it has lost almost between 10 and 20% of its content of calcium oxide. On the outer side of the tank the mortar is protected by steel which shows that the leaching is diffusion controlled from the inner surface.

The portlandite that normally is finely dispersed in the matrix now appears as larger crystals in clusters and in former air voids. The C-S-H gel has also altered, both with regard to texture and chemistry. This shows that the leaching is more complex than earlier assumed and that there will be no distinct pH front accompanying portlandite leaching. As the mortar was only 20 to 30 mm thick in this case, the depth of leaching in real concrete, is still unknown.

The data and observations from the water tank further complicates leaching calculations. Earlier models are based on depletion of portlandite by leaching. Therefore assuming instantaneous release of leachate from the inner surface of the water tank to the fresh water, the following equation (according to Höglund and Bengtsson, 1991) can be used:

$$X=(2D_c c_s t/q_0)^{1/2}$$

where X is the penetration depth (shrinking core model), D_c the effective diffusivity in leached concrete, c_s the solubility of portlandite, t the time and q_o the initial amount of portlandite in the concrete. Parameter values, suggested by Höglund and Bengtsson (1991) and used in performance assessment of repository constructions, are $D_c = 3 \times 10^{-11}$ m^2/s and $c_s = 25$ mol/m^3. According to Table R-3, $q_o = 1\ 150$ mol/m^3 (upper limit).

If it is assumed that all these values are applicable to the water tank, after 90 years the portlandite should be completely leached out to a depth of 6 cm. This is contrary to the observations, which shows that the mortar in the tank is in excellent shape and that a considerable amount of portlandite still exists in the paste. The water tank shows that the performance assessment model is oversimplified, since it does not consider quantitatively the various ageing phenomena, such as hydration of remaining cement grains, precipitation of bicarbonate ions at the surface, and remobilisation.

The observations from the studies of old concrete can be summarised as follows:

- Relicts of unhydrated clinker grains can remain for at least 100 years and possibly much longer in a dense concrete.
- Good quality concrete stored under saturated conditions tends to show an increase in strength with time and a corresponding decrease in hydraulic conductivity provided there is no strong hydraulic gradient driving water through the construction.

- Concrete with a high water/cement ratio and a high water penetration results in hollow spaces and shells which can be later filled with recrystallisation and hydration products.
- Calcite is found as precipitates in the structure (i.e. due to infiltration of carbon dioxide or dissolved carbonates).
- Precipitation of crystals of ettringite and portlandite has been observed; the crystals tend to be formed in voids in the structure.
- No crystallisation of C-S-H is observed and this phase appears to remain stable, at least as long as the pore water composition is controlled by portlandite (high pH and calcium concentration).
- Performance assessment of repository construction concrete cannot be calculated by a simple portlandite depletion model. There are several additional factors to consider and a portlandite depletion model will presumably result in a high leaching rate.

R.4 Natural Analogues

R.4.1 Background

Some of the mineral phases in the cement paste and also the cement pore water composition are not usually found in nature. However, the examples that do exist are of great interest in so far as they can give some insight into the long-term stability of concrete and its influence on the near-field environment. In particular, studies of naturally occurring hyperalkaline springs/seepages have been highly relevant in this respect. Many of these springs/seepages, which are associated with ophiolite formations, can have a pH of up to about 11 and are found, for example, in Cyprus and Oman. The water-mineral reactions giving rise to the high pH are due in part to the alteration of highly reactive ultramafitic (rich in Mg and Fe) rock to serpentinite ($Mg_3Si_2O_5(OH)_4$). The spring waters are generally rich in sodium, potassium, calcium and saturated in magnesium (low concentration due to the high pH). Major anions, in addition to hydroxide, are chloride and sulphate. Sulphide is common which tends to make the water reducing (Eh down to about -0.4 V).

Hyperalkaline springs (pH 11-12) in Oman have been studied as a natural analogue to the influence of cement on radioactive waste (Bath et al., 1987). Trace element concentrations of Se, Pd, Sn, Zr, Ni, U and Th were analysed and compared to calculated values. This was a valuable test of the models and thermodynamic databases, and the general ability to calculate the solubility of radionuclides at high pH in a repository. Bacteria and colloids were also analysed in the spring waters. Alkaliphilic bacteria were found that could survive the high pH; some indications of colloids were also detected, too uncertain for definitive conclusions, but interesting enough to warrant further studies at other sites.

R.4.2 The Maqarin Analogue

The hyperalkaline springs at Maqarin provide an excellent opportunity to study the long-term effects on cement-like material. Maqarin is not unique; there are similar fossil zones of metamorphic cement rock, although they are no longer associated with active hyperalkaline groundwater systems in Israel, Central Jordan, and Syria. According to Kolodny (1979), they form part of the so-called Mottled Zone Complex and many cement minerals have been identified.

R.4.3 Cement Minerals

The ^{230}Th ingrowth method was used to measure a maximum age range of about 0.5 – 2 Ma for the metamorphism of the Bituminous Marl Formation which produced the cement zone at Maqarin (Alexander, 1996). Spontaneous combustion does occur still in the Bituminous Marls due to, for example, exposure of the marl following mechanical excavation. Temperatures of about 450°C have been indicated at such events. The mineral paragenesis, including the cement mineral C_2S (belite/larnite), of the metamorphic cement zone at Maqarin, indicate temperatures in the range 800 – 1 000°C. In Israel, in the "Mottled Zone", which is geologically equivalent to the Maqarin site, the presence of C_3S (hatrurite) indicates a higher temperature. In the manufacture of cement, C_3S (alite) requires temperatures of almost 1 400°C to form. This might indicate differences in the maximum temperature of combustion, but it may indicate also differences in humidity, as C_3S is very reactive. Presumably, the Bituminous Marls were poor in quartz and the major hydration minerals were lime and C_2S. Some of the cement minerals identified at Maqarin and in the "Mottled Zone" of Israel are presented in Table R-6.

R.4.4 Water/rock Interaction of Cement Phases

Cement minerals in a repository environment will initially undergo hydration followed by leaching. At Maqarin, the low-temperature reactions with the cement clinker phases in the cement zone, such as hydration, carbonation and sulphatisation, have created a so-called retrograde assemblage of alteration minerals. These include calcite, apatite, ettringite, thaumasite and portlandite (Table R-7). Locally, and in some veins and dissolution cavities, it was found that gypsum, afwillite, apophyllite, vaterite, birunite and various tobermorites were the major minerals; the veins could be monomineralic. Many of the minerals in the retrograde assemblage in Maqarin are common to cement paste, including portlandite, ettringite and calcium silicate hydrates. Much of the alteration is very fine-grained and the different phases are often intimately intergrown and very hydrous. Larnite (C_2S) and spurrite (C_5S_2-carbonate) are the most readily altered, followed by ellestadite, then brownmillerite, with primary calcite and fluorapatite being the least reactive. Alteration along fractures has caused some degree of expansion and microfracturing. Some primary calcite appears to have been removed.

The latest alteration product appears to have been calcium silicate hydrate with a gel-like morphology which has lined or infilled fractures and other cavities. The Ca/Si-ratio is between 0.8–0.85 which is similar to tobermorite ($C_5S_6H_9$). Ettringite (AFt) is very abundant and may dominate altered lithologies. In most fractures, ettringite is

accompanied by thaumasite; afwillite ($C_3S_2H_3$) seems to have replaced ettringite in some veins (preceded by precipitation of thaumasite).

R.4.5 High pH Water

Two examples of high pH groundwaters from Maqarin are presented in Table R-8 together with pore water pressed from fresh and old (Porjus) Portland concrete for comparison. The Na^+ and K^+ ions are within the range of that obtained from the concrete samples but concentrations of Ca^{2+} and SO_4^{2-} are slightly higher in Maqarin. The pH of Maqarin water is within the range of pore water from old concrete but lower than fresh concrete. The comparison implies that the Maqarin waters, in terms of concrete pore water composition, are slightly more evolved than the old concrete water, i.e. pH is closer to 12.5 and Ca^{2+} starts to dominate over Na^+ and K^+. Another difference, less significant from this point of view, is the higher sulphate content which may be due to the local abundance of pyrite in Maqarin. Concrete, in contrast, is undersaturated with respect to SO_4^{2+}, and will thus not leach this ion to the pore water.

R.4.6 Hyperalkaline Plume

An important task in the Maqarin project is the evaluation of the hyperalkaline groundwater influence on minerals in the surrounding rock (Savage, 1996; Alexander et al., 1996). It has been suggested that alkaline leachates from cement could influence the host rock in the near-field of the repository and thereby change its radionuclide retention properties. This was evaluated from a theoretical point of view. Geochemical calculations were made using the EQ 3 code (Savage, 1996; this report, Chapter 8); important parameters used were pH, Ca^{2+}, dissolved silica and alumina in the plume water. A sequence of minerals was predicted (Fig. R-1) where zeolites are formed first, when pH starts to increase, followed by the precipitation of calcium alumina silicates (CASH) and calcium silicates (CSH). The same sequence of minerals was identified in Maqarin where it was also observed that fractures tend to seal as a result of the secondary minerals formed. Although the open fractures tend to clog, the pore spaces in the rock behind the fractures are still accessible to diffusion so the porosity in the adjacent rock has, apparently, remained open.

R.4.7 Colloids

Colloids, dissolved organic material and bacteria are also being studied in Maqarin. Colloid concentrations are very low in the highly mineralised groundwater which support independent observations of low colloid concentrations in concrete pore water. The Maqarin results also support the conclusion from laboratory studies that colloids are not formed by cement paste. However, it has been argued that colloids could possibly be formed when pH drops at the front of the plume, for example, due to silica supersaturation. This latter phenomenon has not been specifically investigated but, on the other hand, there is no other evidence of colloid formation at Maqarin.

R.4.8 Conclusions

The conclusions from the Maqarin analogue study can be summarised as follows:

- Cement minerals can remain and, to some extent, escape hydration under unsaturated conditions, for timescales in excess of 100 000 years (Milodowski et al., 1998).
- Cement paste minerals, including CSH phases, may remain stable for more than 100 000 years, at least if the hyperalkaline conditions prevail.
- C-S-H gels are found in the mineral assemblages and there is some tendency to a more ordered structure with time (Milodowski et al., 1998).
- The hyperalkaline water has a composition that is similar to solutions leached from mature old concrete.
- The hyperalkaline water reacts with the rock minerals (alumina silicates and silicates) and secondary minerals are formed which tend to clog the fractures and prevent water flow.
- The fracture surfaces are affected but the porosity of the adjacent rock is still open and accessible to diffusion of ions.
- Colloid concentration is very low in the strongly mineralised water and no colloid production is observed.

R.5 References

Alexander, W.R. (Ed.), 1992. A natural analogue study of the Maqarin hyperalkaline groundwaters. I: Source term description and thermodynamic database testing. Nagra Tech. Rep. (NTB 91-10), Nagra, Wettingen, Switzerland.

Alexander, W.R., 1996. Natural cements: How can they help us safely dispose of radioactive waste?. Radwaste Magazine, Sept. Issue, p. 62–69.

Alexander, W.R., Smellie, J.A.T and Crossland, I.G., 1996. Potential effects of hyperalkaline leachates on cementitious repository host rocks: An example from Maqarin, Northern Jordan. In: Chemical containment of wastes in the geosphere. 3-4 September, BGS, Nottingham, U.K. (In press).

Andersson, K., Allard, B. and Bengtsson, M., 1986. Chemical composition of cement pore solutions. Cem. Conc. Res., 19, 327–332.

Atkins, M. and Glasser, F.P., 1992. Application of Portland cement-based materials to radioactive waste immobilisation. Waste Management, 12, 2/3, 105–131.

Bath, A.H., Christofi, N., Neal, C., Philp, J.C., Cave, M.R., McKinley, I.G. and Berner, U., 1987. Trace element and microbial studies of alkaline groundwaters in Oman, Arabian Gulf: A natural analogue for cement pore-waters. Nagra Tech. Rep. (NTB 87-16), Nagra, Wettingen, Sweden.

Berner, U., 1987. Radionuclide speciation in the porewater of hydrated cement. II. The incongruent dissolution of hydrated calcium silicates. Paul Scherrer Institute (PSI) Rep., TM-45-87-10, Würenlingen, Switzerland.

Engkvist, I., Albinsson, Y. and Johansson Engkvist, W., 1996. The long-term stability of cement – Leach tests. SKB Tech. Rep. (TR 96-09), SKB, Stockholm, Sweden.

Gjörv, O.E. and Havdal, J., 1982. Provannanlyser av betongborkjerne (in Norwegian). Rapport STF 65 F82027, FCB, Trondheim, Norway.

Grudemo, Å., 1982. Röntgendiffraktometrisk undersökning av kristallisationstillståndet i bindemedelsfasen av mycket gammal betong (in Swedish). CBI Report No. 8218, Stockholm, Sweden.

Höglund, L.O. and Bengtsson, A., 1991. Some chemical and physical processes related to the long-term performance of the SFR repository. SFR Prog. Rep. (91-06), Stockholm, Sweden.

Kolodny, Y. 1979. Natural cement factory, a geological story. Presented at cement Production and Use, Franklin Pierce College Rindge, New Hampshire, 24-29 June, pp 202–216.

Lagerblad, B. and Trägårdh, J., 1994. Conceptual model for concrete long time degradation in a deep nuclear waste repository. SKB Tech. Rep. (TR 95-21), SKB, Stockholm, Sweden.

Lagerblad, B., 1996. Conceptual model for deterioration of Portland cement concrete in water. SKB Prog. Rep. (AR 96-01), SKB, Stockholm, Sweden.

Milodowski, A.E., Khoury, H.N., Pearce, J.M. and Hyslop, E.K., 1992. Discussion of the mineralogy, petrography and geochemistry of the Maqarin source-term rocks and their secondary alteration products. In: W.R. Alexander (Ed.), A natural analogue study of the Maqarin hyperalkaline groundwaters. I: Source term description and thermodynamic database testing. Nagra Tech. Rep. (NTB 91-10), Nagra, Wettingen, Switzerland, p. 41–51.

Milodowski, A.E., Pearce, J.M., Hyslop, E.K., Hughes, C.R., Ingelthorpe, S.D.J., Strong, G.E., Wheal, N., MacKenzie, A.B., Karnland, O. and Khoury, H.N., 1998. Mineralogy and Petrology. In: C.M. Linklater (Ed.), A natural analogue study of cement-buffered, hyperalkaline groundwaters and their interaction with a repository host rock: Phase II. Nirex Science Report, S/98/003, Nirex, Harwell, U.K., p. 70–145.

Rayment, D.L., 1986. The electron microprobe analysis of the C-S-H in a 136 years old cement paste. Cem. Conc. Res., 16, 341–344.

Savage, D., 1996. Zeolite occurrence, stability and behaviour: A contribution to Phase III of the Jordan natural analogue project. H.M.I.P. Department of the Environment Report, DOE/HMIP/RR/95.020, London, U.K.

Taylor, H.F.W., 1990. Cement chemistry. Academic Press, London, pp 1–475.

TABLES

Table R-1. The phase composition of Degerhamn Standard Portland cement (Lagerblad and Trägårdh, 1994).

Idealised formula	Cement nomenclature	Wt.%
Ca_3SiO_5	C_3S	51
Ca_2SiO_4	C_2S	25
$Ca_3Al_2O_6$	C_3A	1.2
$Ca_2(Al,Fe)_2O_5$	C_4AF	14

Table R-2. Reactants and products for Standard P Degerhamn Portland Cement (amounts in g).

Reactants			Products					
Clinker minerals		H_2O	CH	$C_3S_2H_3$	Al-mon	Fe-mon	C_3AH_6	C_3FH_6
C_3S	51	12.07	24.83	38.25				
C_2S	25	5.23	5.38	24.85				
C_3A	1.2	0.96			2.76			
C_4AF	9.98	4.44				17.22		
C_4AF	4.02	1.49	-1.23				3.13	3.61
CaO-f	0.8	0.26	1.06					
Total		**24.45**	**30.04**	**63.10**	**2.76**	**17.22**	**3.13**	**3.61**

C = CaO, S = SiO_2, A = Al_2O_3, F = Fe_2O_3 and CH = $Ca(OH)_2$. Al-mon and Fe-mon are monosulphate from aluminate and ferrite respectively.

Cement clinker minerals and hydration products of Degerhamn Standard Portland cement. In the calculation all aluminate and the greater part of ferrite are assumed to react with sulphate to form monosulphate. At equilibrium no ettringite will form. The rest of the ferrite is assumed to react to form calcium aluminate hydrate and calcium ferrite hydrate. The composition of the calcium silicate hydrate gel is assumed to be $C_3S_2H_3$.

Table R-3. Release of hydroxides from 1 m^3 of concrete due to leaching.

Leached material/compound	pH	Moles OH^-
1 m^3 of concrete (350 kg of cement)		
NaOH and KOH	13.5–12.5	<56
$Ca(OH)_2$	12.5–12	2000–2300
C-S-H	12–11	<6000

Table R-4. Summary of observations made by Lagerblad (1996).

Name	Age	Environment	Clinker	w/c[a]	New phases and crystals
Sillre/Oxsjön hydropower dam	59 y	Humid	Relict grains	>0.65	Calcite and ettringite
School building in Gävle	100 y	Dry	Relict grains	>0.7	Calcite and/or ettringite
Midskogsforsen hydropower plant	52 y	Saturated	Hydrated	0.5	Ettringite
Rocksta mill	96 y	Wet	Hydrated	>0.7	Ettringite and portlandite
Älvkarleby hydropower plant – inspection tunnel	79 y	Dry	Relict grains	<0.3	N. D.
Älvkarleby hydropower plant – discharge chamber	79 y	Saturated	Some relict grains	0.4–0.6	Ettringite and portlandite
Uppsala Castle water tank	90 y	Saturated	Relict grains	0.4	Calcite, ettringite and portlandite

[a] Estimate of w/c by comparison to modern concrete.

Table R-5. Pore water from samples of the 65 year old Porjus hydropower plant (from the inflow tunnel) compared to pore water from samples of fresh standard Portland cement.

	Fresh std Portland[a]	Old Porjus cement[b]
pH	13.2–13.4	12.4-13
	mmole/L	**mmole/L**
Na^+	60–80	4–150
K^+	140–120	3–130
Ca^{2+}	0.5–2	0.8–10
SO_4^{2-}	1–8	1–7

[a] Andersson et al., 1986
[b] Gjörv and Hovdal (1982).

Table R-6. Identified cement-like minerals from the cement zone in Maqarin and from other locations of the Mottled Zone complex.

Mineral	Ideal formula	Cement	Reference nomenclature
wollastonite[a]	$CaSiO_3$	CS	d,e
rankinite	Ca_3Si_2O	C_3S_2	d
larnite[b]	Ca_2SiO_4	C_2S	d,e
spurrite	$Ca_5(SiO_4)_2CO_3$	C_5S_2-carbonate	d,e
hatrurite[c]	Ca_3SiO_5	C_3S	d
brownmillerite	$Ca_2(Al,Fe)_2O_5$	C_4AF	d,e
merwinite	$Ca_3Mg(SiO_4)_2$	C_3MS_2	d
lime	CaO	C	d,e

[a] Calcium monosilicate (CS) is not really a component of cement which is burnt at normal high temperature (1450 °C).

[b] Larnite is similar to belite in cement (C_2S).

[c] Hatrurite is similar to alite in cement (C_3S).

[d] Kolodny (1979).

[e] Milodowski et al. (1992).

Table R-7. Identified cement-paste-like minerals in the retrograde cement zone assemblage at Maqarin (Milodowski et al., 1992).

Mineral	Ideal formula	Cement nomenclature
calcite[a]	$CaCO_3$	–
gibbsite[b]	$Al(OH)_3$	AH
brucite[c]	$Mg(OH)_2$	MH
portlandite	$Ca(OH)_2$	CH
quartz[d]	SiO_2	S
gypsum	$CaSO_4$	–
ettringite	$Ca_6Al_2(SO_4)_3(OH)_{12}\ 25H_2O$	AFt
thaumasite	$Ca_6Si_2(SO_4)_2(CO_3)_2(OH)_{12}\ 24H_2O$	AFt
afwillite[e]	$Ca_3Si_2O_4(OH)_6$	C_3S_2H
tobermorites[e]	$Ca_5Si_6O_{16}(OH)_2\ \ 2–8H_2O$	C_3S_2H
jennite[e]	$Ca_9H_2Si_6O_{18}(OH)_8\ 6H_2O$	C_5S_6H
C-S-H gel	amorphous	C-S-H

[a] As carbonation product in cement paste.
[b] Not a normal component of Portland cement (occurs in alumiante cement paste).
[c] Present if there is dolomite in the ballast or due to sea water intrusion.
[d] Silica present in the ballast and sometimes used as an additive (e g silica fume).
[e] Calcium silica hydrates present as gel phases, with varying Ca/Si-ratios, in cement paste; (see Chapter 5, subsection 5.2.2).

Table R-8. The MQ-2 (Eastern Springs) samples are taken from Adit A-6 which penetrates the cement zone. Water was collected dripping from a series of stalactites on the wall of the adit. Site MQ-5 (Western Springs) is an artesian spring on the bank of the Yarmouk river, about 10 cm above river level (Alexander, 1992).

Components	MQ-2 water	MQ-5 water
pH	12.34	12.52
Eh	308 mV	127
	mmol/L	**mmol/L**
Ca^{2+}	14.7	26.2
Na^{+}	2.13	5.74
K^{+}	0.3	15.7
Sr^{2+}	0.08	0.18
SO_4^{2-}	2.90	15.4
Cl^{-}	1.59	1.44
F^{-}	0.021	0.049
NO_3^{-}	0.08	0.62
Ionic Strength	41.4	85.9

FIGURE

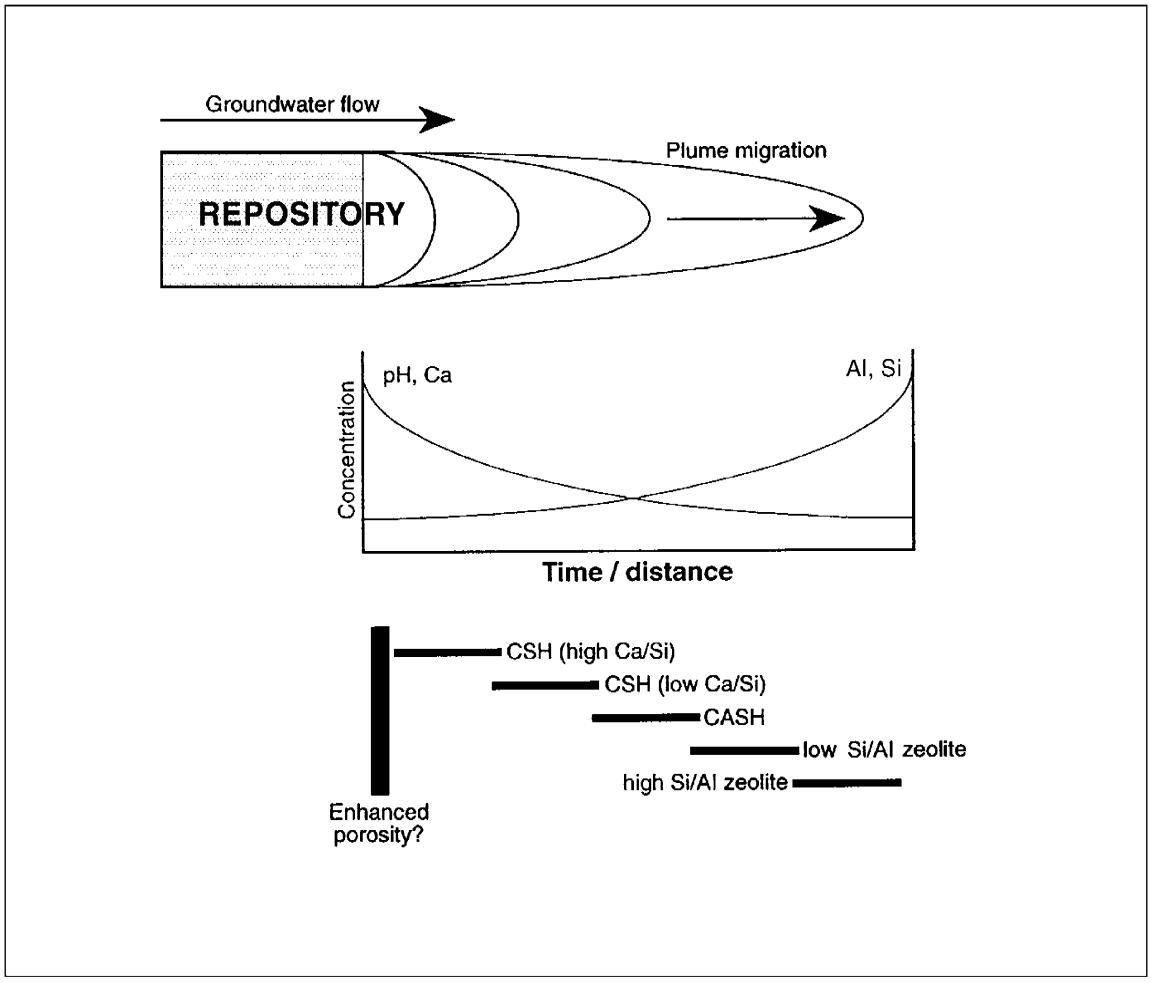

Figure R-1. *Schematic diagram of hyperalkaline plume migration from a cementitious repository for radioactive wastes, showing hypothesised variations in fluid composition and alteration mineralogy in space and time (after Savage, 1996; this report, Chapter 8).*

List of SKB reports

Annual Reports

1977-78
TR 121
KBS Technical Reports 1 – 120
Summaries
Stockholm, May 1979

1979
TR 79-28
The KBS Annual Report 1979
KBS Technical Reports 79-01 – 79-27
Summaries
Stockholm, March 1980

1980
TR 80-26
The KBS Annual Report 1980
KBS Technical Reports 80-01 – 80-25
Summaries
Stockholm, March 1981

1981
TR 81-17
The KBS Annual Report 1981
KBS Technical Reports 81-01 – 81-16
Summaries
Stockholm, April 1982

1982
TR 82-28
The KBS Annual Report 1982
KBS Technical Reports 82-01 – 82-27
Summaries
Stockholm, July 1983

1983
TR 83-77
The KBS Annual Report 1983
KBS Technical Reports 83-01 – 83-76
Summaries
Stockholm, June 1984

1984
TR 85-01
Annual Research and Development Report 1984
Including Summaries of Technical Reports Issued during 1984. (Technical Reports 84-01 – 84-19)
Stockholm, June1985

1985
TR 85-20
Annual Research and Development Report 1985
Including Summaries of Technical Reports Issued during 1985. (Technical Reports 85-01 – 85-19)
Stockholm, May 1986

1986
TR 86-31
SKB Annual Report 1986
Including Summaries of Technical Reports Issued during 1986
Stockholm, May 1987

1987
TR 87-33
SKB Annual Report 1987
Including Summaries of Technical Reports Issued during 1987
Stockholm, May 1988

1988
TR 88-32
SKB Annual Report 1988
Including Summaries of Technical Reports Issued during 1988
Stockholm, May 1989

1989
TR 89-40
SKB Annual Report 1989
Including Summaries of Technical Reports Issued during 1989
Stockholm, May 1990

1990
TR 90-46
SKB Annual Report 1990
Including Summaries of Technical Reports Issued during 1990
Stockholm, May 1991

1991
TR 91-64
SKB Annual Report 1991
Including Summaries of Technical Reports Issued during 1991
Stockholm, April 1992

1992
TR 92-46
SKB Annual Report 1992
Including Summaries of Technical Reports Issued during 1992
Stockholm, May 1993

1993
TR 93-34
SKB Annual Report 1993
Including Summaries of Technical Reports Issued during 1993
Stockholm, May 1994

1994
TR 94-33
SKB Annual Report 1994
Including Summaries of Technical Reports Issued during 1994
Stockholm, May 1995

1995
TR 95-37
SKB Annual Report 1995
Including Summaries of Technical Reports Issued during 1995
Stockholm, May 1996

1996
TR 96-25
SKB Annual Report 1996
Including Summaries of Technical Reports Issued during 1996
Stockholm, May 1997

List of SKB Technical Reports 1998

TR 98-01
Global thermo-mechanical effects from a KBS-3 type repository. Summary report
Eva Hakami, Stig-Olof Olofsson, Hossein Hakami, Jan Israelsson
Itasca Geomekanik AB, Stockholm, Sweden
April 1998

TR 98-02
Parameters of importance to determine during geoscientific site investigation
Johan Andersson[1], Karl-Erik Almén[2], Lars O Ericsson[3], Anders Fredriksson[4], Fred Karlsson[3], Roy Stanfors[5], Anders Ström[3]
[1] QuantiSci AB
[2] KEA GEO-Konsult AB
[3] SKB
[4] ADG Grundteknik KB
[5] Roy Stanfors Consulting AB
June 1998

TR 98-03
Summary of hydrochemical conditions at Aberg, Beberg and Ceberg
Marcus Laaksoharju, Iona Gurban, Christina Skårman
Intera KB
May 1998

ISSN 1404-0344
CM Gruppen AB, Bromma, 1998